

# Starch-based Polymers as Flocculants of Oil Sands Mature Fine Tailings and for Extraction of Bitumen from Oil Sands

by

Bowei Zheng

A thesis  
presented to the University of Waterloo  
in fulfillment of the  
thesis requirement for the degree of  
Doctor of Philosophy  
in  
Chemistry

Waterloo, Ontario, Canada, 2020

© Bowei Zheng 2020

### **Examining Committee Membership**

The following served on the Examining Committee for this thesis. The decision of the Examining Committee is by majority vote.

External Examiner	Joao Soares Professor University of Alberta
Supervisor	Scott Taylor Professor Chemistry
Internal Member	Mario Gauthier Professor Chemistry
Internal Member	Jean Duhamel Professor Chemistry
Internal-external Member	Rajinder Pal Professor Chemical Engineering

## **AUTHOR'S DECLARATION**

I hereby declare that I am the sole author of this thesis. This is a true copy of the thesis, including any required final revisions, as accepted by my examiners.

I understand that my thesis may be made electronically available to the public.

## Abstract

Mature fine tailings (MFT) generated by oil sands extraction operations in Alberta pose significant environmental challenges. Polymeric flocculants are often needed to accelerate the consolidation and dewatering of MFT. A number of starch-based flocculants were synthesized and examined as flocculants for MFT. Thermoresponsive hydroxybutyl (HB) corn starch (HB-CS) and potato starch (HB-PS) were shown to flocculate 2 and 10 wt % MFT and their thermoresponsive behavior was absolutely required for optimal performance in that they were considerably more effective, in terms of initial settling rates (ISR) and supernatant turbidity (ST), for settling tests conducted at temperatures above their lower critical solution temperatures (LCSTs) than below. Cationic corn starch (Cat-CS) and potato starch (Cat-PS) were prepared by incorporating cationic moieties, *N*-(3-chloro-2-hydroxypropyl) trimethyl ammonium chloride (CHPTAC), on CS or PS in basic conditions. It was shown that both Cat-CS and Cat-PS exhibited excellent performance, in terms of ISR and ST, for flocculating 2 wt % MFT. A novel starch-based dual polymer flocculation process was proposed in that the dual polymer flocculants consisting of HB-CS and Cat-CS or HB-PS and Cat-PS were used to flocculate 2 and 10 wt % MFT. The dual polymer flocculants were in all aspects superior to the single polymer flocculant. An ISR as high as 52 m/h and a ST as low as 16 nephelometric turbidity units (NTU) can be achieved with the use of a dual polymer flocculant for the settling of 10 wt % MFT.

Processing aids are generally required to improve the recovery of bitumen from poor processing oil sands ores that contain a relatively high amount of divalent cations and fine and



clay solids. In this thesis, starch-based polymers were examined as processing aids in an aqueous-solvent hybrid bitumen extraction process, in which toluene was added to oil sands slurry to facilitate bitumen liberation. The highest bitumen recovery, at 86 %, was achieved using thermoresponsive starch nanoparticles (TRSNPs) with an LCST of 32 °C at 1 gram per liter of the oil sands slurry and 50 mg of toluene when the extractions were conducted at 45 °C. When the extraction was conducted under the same conditions without the TRSNP, bitumen recovery from the poor processing ores was only 31 %. Moreover, cationic hydrophobically modified SNPs were shown to be a good demulsifier, which significantly enhanced bitumen recovery during the extraction process. The use of the cationic hydrophobically modified SNPs at 1 g/L along with 50 mg of toluene also improved bitumen recovery from aged oil sands ores and a bitumen recovery as high as 81 % was obtained. Without the starch-based polymers, a poor bitumen recovery of 28 % was achieved with 50 mg of toluene for the aged ores.

## Acknowledgements

First, I would like to express my deepest gratitude to my supervisor, Dr. Scott Taylor, who is always kind, supportive, knowledgeable and inspiring to me. I am grateful that I had the opportunity of working with Dr. Taylor. His wisdom, hard-work and dedication to the world of science will always inspire me as a scientist in the years coming. Without his help and guidance, this thesis would not have been possible.

I would like to thank my advisory committee, Dr. Mario Gauthier, Dr. Jean Duhamel and Dr. Rajinder Pal for their fruitful discussions and suggestions during my PhD study. I would like to thank my external examiners, Dr. Joao Soares and Dr. Michael Tam. I would also like to thank Jan Venne for her help with NMR use.

I would like to acknowledge all my current and former lab mates in the Taylor lab (2014-2020). I had the pleasure of working with many great people in the Department of Chemistry at University of Waterloo.

Last but not least, I am grateful to my mother who selflessly give me all the love and support in my whole life, and especially during my PhD study. I am equally grateful to my beloved wife, Sandy, who is always supportive and loving.

## **Dedication**

This dissertation is dedicated to my wife, Sandy and my children, Felicity and Aaron. It is also dedicated to my mother. Their endless support, encouragement and sacrifice have been instrumental in the completion of my education.

## Table of Contents

AUTHOR'S DECLARATION .....	iii
Abstract .....	iv
Acknowledgements.....	vi
Dedication .....	vii
List of Figures .....	xiii
List of Tables .....	xxii
Chapter 1 Introduction .....	1
1.1 Overview of the Thesis .....	1
1.2 Thermoresponsive Polymers .....	4
1.2.1 Critical Solution Temperatures.....	5
1.2.2 Phase Transition Behaviors .....	7
1.2.3 TRP Transmittance Curves.....	10
1.2.4 Factors affecting LCST .....	13
1.2.5 Thermoresponsive Polysaccharides.....	21
1.3 Oil Extraction from Oil Sands.....	27
1.3.1 <i>In situ</i> Extraction Process .....	27
1.3.2 Surface Mining Extraction Process .....	27
1.3.3 Key Aspects in Water-based Bitumen Extraction Process.....	29
1.3.4 Factors Affecting Bitumen Extraction from Oil Sands .....	31
1.3.5 Chemical Aids for Bitumen Extraction of Oil Sands .....	36
1.4 Flocculation of Mature Fine Tailings.....	40
1.4.1 Current Industrial Practices for Tailings Management.....	40
1.4.2 Mature Fine Tailings Composition.....	42
1.4.3 Clay Mineralogy .....	43
1.4.4 Electrical Double Layer.....	44
1.4.5 Colloidal Stability and the DLVO Theory .....	46

1.4.6 Coagulation.....	47
1.4.7 Flocculation .....	48
1.4.8 Previous Studies on Flocculation of Oil Sands Fine Tailings .....	50
1.5 Objectives of the Thesis .....	57
Chapter 2 Thermoresponsive Starch for the Flocculation of Oil Sands Mature Fine Tailings	59
2.1 Introduction .....	59
2.2 Materials and Methods .....	62
2.2.1 Materials .....	62
2.2.2 Preparation of TRS and HMS.....	63
2.2.3 Determination of the Molar Substitution of the Modified Starches .....	63
2.2.4 Determination of LCST by Light Transmittance .....	64
2.2.5 DLS Measurements .....	65
2.2.6 Settling Tests .....	65
2.3 Results and Discussion.....	67
2.3.1 Modified Starches and their Thermoresponsivity .....	67
2.3.2 Settling Tests using HB-CS.....	73
2.3.3 Settling Tests using HB-PS .....	82
2.3.4 Settling Tests using PHE-PS .....	89
2.3.5 Comparison with other Thermoresponsive Polymers .....	94
2.4 Conclusion.....	95
Chapter 3 Cationic Starches for the Flocculation of Oil Sands Mature Fine Tailings .....	96
3.1 Introduction .....	96
3.2 Materials and Methods .....	101
3.2.1 Materials .....	101
3.2.2 Preparation of CS and PS Modified with CHPTAC.....	102
3.2.3 Determination of Molar Substitution of Cationic Starches .....	102
3.2.4 Settling Tests .....	103
3.3 Results and Discussion.....	104

3.3.1 Preparation of Cat-CS and Cat-PS.....	104
3.3.2 Settling Tests of 2 wt % MFT using Cat-CS .....	104
3.3.3 Settling Tests of 2 wt % MFT using Cat-PS .....	110
3.3.4 Settling Tests of 10 wt % MFT using Cat-CS and Cat-PS.....	114
3.4 Comparison with other Polymers.....	115
3.5 Conclusion.....	116
Chapter 4 Dual Functional Starches for the Flocculation of Oil Sands Mature Fine Tailings .....	118
4.1 Introduction .....	118
4.2 Materials and Methods .....	118
4.2.1 Materials .....	118
4.2.2 The preparation of the Dual Functional CS and PS.....	119
4.2.3 Determination of the Molar Substitution of the Dual Functional Starches .....	119
4.2.4 Determination of the LCST by Light Transmittance.....	120
4.2.5 Settling Tests .....	120
4.3 Results and Discussion.....	121
4.3.1 Preparation of the Dual Functional Starches and their Thermoresponsivity .....	121
4.3.2 Settling Tests of 2 wt % MFT using Cat-HB-CS .....	123
4.3.3 Settling Tests of 2 wt % MFT using Cat-HB-PS .....	133
4.4 Comparison with other Dual Functional Polymers.....	139
4.5 Conclusion.....	140
Chapter 5 Flocculation of Oil Sands Mature Fine Tailings by Starch-based Dual Polymer Flocculant System.....	141
5.1 Introduction .....	141
5.2 Materials and Methods .....	142
5.2.1 Materials .....	142
5.2.2 The Preparation of the CS- and PS-based Flocculants .....	142
5.2.3 Settling Tests .....	143

5.3 Results and Discussion.....	144
5.3.1 Determination of the Order of Addition in the Dual Flocculant System.....	144
5.3.2 Dose Effect of HB0.6-CS in a Dual Flocculant System.....	148
5.3.3 Settling Tests of 2 wt % MFT using HB-CS and Cat-CS .....	149
5.3.4 Settling Tests of 2 wt % MFT using HB-PS and Cat-PS .....	165
5.3.5 Settling Tests of 2 wt % MFT using PHE-PS and Cat-PS .....	175
5.3.6 Developing an Economical Flocculant for 2 wt % MFT.....	179
5.3.7 Comparison with other Polymers used to Flocculate 2 wt % MFT.....	181
5.3.8 Conclusion of the Dual Polymer Flocculation for 2 wt % MFT .....	182
5.3.9 Settling Tests of 10 wt % MFT using HB-CS and Cat-CS .....	183
5.3.10 Settling Tests of 10 wt % MFT using HB-PS and Cat-PS .....	184
5.3.11 Effect of Settling Temperatures on the Dual Polymer Flocculation .....	194
5.3.12 Comparison with other Polymers used to Flocculate 10 wt % MFT.....	195
5.3.13 Conclusion of Dual Polymer Flocculation for 10 wt % MFT .....	197
Chapter 6 Preparation and Characterization of Hydrophobically Modified Thermoresponsive Starch .....	199
6.1 Introduction .....	199
6.2 Materials and Methods .....	201
6.2.1 Materials .....	201
6.2.2 Preparation of Hydrophobic Thermoresponsive SNPs.....	201
6.2.3 Determination of Molar Substitution.....	202
6.2.4 Determination of the LCST by Light Transmittance.....	203
6.2.5 DLS Measurements .....	203
6.3 Results and Discussion.....	204
6.3.1 Preparation of Hydrophobic Thermoresponsive SNPs.....	204
6.3.2 Thermoresponsive Properties of PHE-HB-SNPs .....	216
6.4 Conclusion.....	223
Chapter 7 Extraction of Bitumen from Oil Sands using Modified Starch Nanoparticles.....	225

7.1 Introduction .....	225
7.2 Materials and Methods .....	229
7.2.1 Materials .....	229
7.2.2 Preparation of Modified Starch Nanoparticles .....	230
7.2.3 Light Transmittance Studies .....	231
7.2.4 Bitumen Extraction Tests .....	231
7.3 Results and Discussion.....	232
7.3.1 The Stabilization of Thermoresponsive SNPs.....	232
7.3.2 Bitumen Extraction Tests on Fresh Oil Sands Ores .....	233
7.3.3 Bitumen Extraction Tests on Aged Oil Sands Ores .....	245
7.4 Conclusion.....	251
Chapter 8 Summary and Future Directions .....	253
8.1 Summary .....	253
8.2 Future Directions.....	256
8.2.1 Flocculation of Oil Sands MFT .....	256
8.2.2 Extraction of Bitumen from Oil Sands .....	258
Copyright Permissions .....	260
Bibliography .....	277
Appendices.....	293
Appendix A.....	293
Appendix B .....	297
Appendix C .....	299
Appendix D.....	300
Appendix E .....	301



## List of Figures

Figure 1.1. Schematic phase diagrams plotting critical temperatures, $T$ , as a function of polymer volume fraction, $\phi$ , for LCST (A) and UCST (B).....	6
Figure 1.2. Schematic representation of a coil-to-globule transition of a TRP with four thermodynamically stable states from low to high temperature (A), and hydrodynamic radius distributions, $f(Rh)$ , of PNIPAM in a low concentration dispersion at below and above the LCST (B). Both diagrams were adapted from Wu et al. with permission. <sup>17</sup> .....	8
Figure 1.3. A schematic representation of conformational changes of amphiphilic block copolymers in an aqueous dispersion. At low concentration, polymer chains assemble into isolated micelles above LCST; at high concentration, these polymeric micelles further assemble into an ordered gel-like structure. This figure was adapted from Gil et al. with permission. <sup>28</sup> .....	9
Figure 1.4. Schematic representation of two types of micellar structures of PNIPAM grafted block copolymers in an aqueous dispersion: a block copolymer consisting of a hydrophobic block and a thermoresponsive block (A), and a block copolymer containing a hydrophilic block and a thermoresponsive block (B). Both diagrams were adapted from Gil et al. with permission. <sup>28</sup> .....	10
Figure 1.5. TRPs can exhibit overlapping heating and cooling curves (A), a hysteresis (B), or a slow thermo-transition (C). .....	11
Figure 1.6. Transmittance curves for a 0.2 g/L aqueous dispersion of poly(styrene)- <i>b</i> -poly( <i>N</i> -isopropyl acrylamide) (A), <sup>38</sup> and for a 5 g/L dispersion of PEG- <i>b</i> -PMEO <sub>2</sub> MA (B). <sup>10</sup> Figures were taken with permission. ....	13
Figure 1.7. The correlation of the cloud point or LCST with molecular weight of PNIPAM derivatives prepared using different initiators: 2-chloropropionamide (CP), <i>N</i> -isopropyl-2-chloropropionamide ( <i>i</i> -PrCP), methyl 2-chloropropionate (MCP), ethyl 2-chloropropionate (ECP), and <i>N</i> -phenyl-2-chloropropionamide (PhCP). The figure was adapted from Xia et al. with permission. <sup>60</sup> .....	19
Figure 1.8. LCSTs of PNIPAM dispersions with the addition of different types of salts and salt concentrations. The figure was adapted from Eeckman et al. with permission. <sup>62</sup> .....	21
Figure 1.9. Chemical structure of cellulose. ....	23
Figure 1.10. Chemical structures of amylose (A) and amylopectin (B). ....	24

Figure 1.11. Chemical structures of HBPS (A), HIPS (B), BE <sub>n</sub> S (C), TAS (D), PyHES (E) and HB-SNP (F). Substitution is shown only at O-6 while in fact substitution can occur at O-2, O-3 and O-6. ....	26
Figure 1.12. An overview of surface mining operation. This picture was obtained online from <a href="http://www.oilsandsmagazine.com">www.oilsandsmagazine.com</a> with permission. ....	28
Figure 1.13. Schematic diagram showing the proposed microstructure of Athabasca oil sands. Picture was taken with permission. <sup>77</sup> .....	29
Figure 1.14. Schematic representation of bitumen recession and liberation (A), and aeration and flotation (B). The pictures were adapted from Masliyah et al. with permission. <sup>80</sup> .....	30
Figure 1.15. Effect of processing temperature on bitumen recovery in laboratory scale oil sands exactions. Figure was taken with permission. <sup>82</sup> .....	33
Figure 1.16. The effect of the air to slurry ratio by volume (Air:Slurry) on bitumen recovery over extraction time in a laboratory scale oil sands extraction process at 35 °C. Figure was taken with permission. <sup>84</sup> .....	34
Figure 1.17. Schematic representation of slime coating of bitumen droplets in an oil sands slurry in response to divalent cationic concertation. This picture was adapted from Wallace et al. with permission. <sup>96</sup> .....	36
Figure 1.18. Bitumen recoveries of different solvents for oil sands extractions. Solvents used include: n-pentane (1), n-hexane (2), n-heptane (3), cyclohexane (4), <i>o</i> -xylene (5), ethyl acetate (6), toluene (7), methyl ethyl ketone (8), chloroform (9), trichloroethylene (10), acetone (11) and ethanol (12). Figure was adapted from Wang et al. with permission. <sup>106</sup> ....	39
Figure 1.19. Schematic diagram showing conventional oil sands tailings management. Numbers in parenthesis represents the relative volume of components per m <sup>3</sup> of bitumen produced. This diagram was adapted from Vedoy and Soares with permission. <sup>2</sup> .....	41
Figure 1.20. Tetrahedra and octahedra sheets of unit layer of clay. Figure was taken with permission from Antonio Jordán from <a href="http://blogs.egu.eu">blogs.egu.eu</a> . ....	44
Figure 1.21. Layer structures of kaolinite (A) and montmorillonite (B). ....	44
Figure 1.22. Schematic representation of electrical double layer of a colloidal particle and its potential is shown as a function of distance from the particle surface. This picture was adapted from Yingchoncharoen et al. with permission. <sup>113</sup> .....	45
Figure 1.23. Plot of interparticle potentials as a function of distance between the charged surfaces of two particles. This picture was adapted from Gelardi and Flatt with permission. <sup>114</sup> .....	47

Figure 1.24. Graphical representation of charge neutralization (A), bridging (B) and electrostatic patch (C) mechanism. ....	48
Figure 2.1. Chemical structures of PAM- <i>g</i> -PEOMA (A), PAM- <i>g</i> -PPO (B), PNIPAM (C), poly(AEMA- <i>st</i> -NIPAM) (D), chitosan- <i>g</i> -CHPTAC (E) and carboxymethylated starch (F). 60	
Figure 2.2. Preparation of TRS and HMS. Substitution is shown only at O-6 while in fact substitution can occur at O-2, O-3 and O-6. ....	67
Figure 2.3. Light transmittance curves for aqueous dispersions of HB1.5-CS (A), HB1.9-CS (B), and HB2.3-CS (C) with concentrations ranging from 0.025 g/L (25 ppm) to 1 g/L (1000 ppm). ....	69
Figure 2.4. Light transmittance curves for aqueous dispersions of HB1.9-PS from 0.025 g/L (25 ppm) to 1 g/L (1000 ppm). ....	71
Figure 2.5. Initial settling rate (ISR, A), water recovery (B), supernatant turbidity (C), and sediment solids content (D) from the settling tests of 2 wt % MFT using various HB-CSs with MS from 0.6 to 2.3 and at polymer doses from 0 to 1000 ppm (on the dry/slurry basis). ....	75
Figure 2.6. Schematic representation of flocculation of clay particles using thermoresponsive (TR) HB-CS at a low dose (A), at an optimal dose (B) and at overdose (C) at 23 °C.....	76
Figure 2.7. Schematic representation of flocculation of clay particles using thermoresponsive (TR) HB-CS at low (A) and high (B) doses at 50 °C.....	78
Figure 2.8. Initial settling rate (ISR, A), water recovery (B), supernatant turbidity (C), and sediment solids content (D) from the settling tests of 2 wt % MFT using HB1.5-CS at polymer doses from 0 to 1000 ppm (dry/slurry) at settling temperatures of 23, 50, or 65 °C.	81
Figure 2.9. Initial settling rate (ISR, A), water recovery (B), supernatant turbidity (C), and sediment solids content (D) of the settling tests of 2 wt % MFT using HB1.9-CS or HB1.9-PS at polymer doses from 0 to 1000 ppm (on the dry/slurry basis).....	83
Figure 2.10. Schematic representation of flocculation of clay particles using thermoresponsive (TR) HB-PS at low (A) and high (B) doses at 50 °C.....	85
Figure 2.11. Settling tests using 10 wt % MFT. Initial settling rate (ISR, A), water recovery (B), supernatant turbidity (C), and sediment solids content (D) of the settling tests using HB1.9-PS at doses ranging from 0 to 1000 ppm (on the dry/slurry basis). ....	87
Figure 2.12. Initial settling rate (A), water recovery (B), supernatant turbidity (C), and sediment solids content (D) of settling tests of 2 wt % MFT using PHE0.02-PS or PHE0.2-PS at polymer doses from 0 to 1000 ppm (dry/slurry) at 50 °C and compared to HB0.6-PS. ....	91

Figure 2.13. Initial settling rate (ISR, A), water recovery (B), supernatant turbidity (C), and sediment solids content (D) of the settling tests of 10 wt % MFT using PHE0.2-PS at polymer doses from 0 to 1000 ppm (dry/slurry) at 50 °C and compared to HB1.9-PS.....	93
Figure 3.1. Chemical structures of poly(AM- <i>co</i> -DADMAC) (A), poly(DADMAC) (B), poly(AM- <i>co</i> -AMHP) (C), Zetag 8110 (D), dextran-EDHPAC (E), starch- <i>g</i> -PDMC (F), chitosan- <i>g</i> -PAM (G), and chitosan-CHPTAC- <i>g</i> -PAM (H). .....	97
Figure 3.2. Preparation of Cat-CS and Cat-PS. Substitution is shown only at O-6 while in fact substitution can occur at O-2, O-3 and O-6. ....	104
Figure 3.3. Initial settling rate (ISR) of the settling tests of 2 wt % MFT using Cat-CS with MS <sub>Cat</sub> ranging from 0.02 to 0.25. Dosage was reported on the dry/slurry basis.....	105
Figure 3.4. Schematic representation of flocculation of clay particles using Cat-CS at low dose (A), optimal dose (B), and overdose (C). ....	106
Figure 3.5. Water recovery of the settling tests of 2 wt % MFT using Cat-CS with MS <sub>Cat</sub> ranging from 0.02 to 0.25. Dosage was reported on the dry/slurry basis. ....	107
Figure 3.6. Supernatant turbidity of the settling tests of 2 wt % MFT using Cat-CS with MS <sub>Cat</sub> ranging from 0.02 to 0.25. Dosage was reported on the dry/slurry basis.....	109
Figure 3.7. Sediment solids content of the settling tests of 2 wt % MFT using Cat-CS with MS <sub>Cat</sub> ranging from 0.02 to 0.25. Dosage was reported on the dry/slurry basis.....	110
Figure 3.8. Initial settling rate (ISR) of the settling tests of 2 wt % MFT using Cat0.02-PS and Cat0.02-CS with varying doses ranging from 25 to 800 ppm (on the dry/slurry basis). ....	111
Figure 3.9. Water recovery of the settling tests of 2 wt % MFT using Cat0.02-PS and Cat0.02-CS with varying doses ranging from 25 and 800 ppm (on the dry/slurry basis). ...	112
Figure 3.10. Supernatant turbidity of the settling tests of 2 wt % MFT using Cat0.02-PS and Cat0.02-CS with varying doses ranging from 25 and 800 ppm (on the dry/slurry basis). ...	113
Figure 3.11. Sediment solids content of the settling tests of 2 wt % MFT using Cat0.02-PS and Cat0.02-CS with varying doses ranging from 25 and 800 ppm (on the dry/slurry basis). .....	114
Figure 3.12. Partially hydrolyzed Zetag 8110. <sup>127</sup> .....	115
Figure 4.1. Preparation of Cat-HB-CS and Cat-HB-PS. Substitution is shown only at O-6 while in fact substitution can occur at O-2, O-3 and O-6. ....	121
Figure 4.2. Light transmittance curves for aqueous dispersions of Cat0.02-HB2.2-CS (A) and Cat0.02-HB2.0-PS (B) with concentrations ranging from 0.05 g/L (50 ppm) to 1 g/L (1000 ppm). .....	123

Figure 4.3. Initial settling rate (ISR) of the settling tests of 2 wt % MFT using Cat0.02-HB2.2-CS, Cat0.02-CS and HB2.3-CS with varying doses from 25 to 1000 ppm (dry/slurry). .....	124
Figure 4.4. Schematic representation of flocculation of clay particles using Cat0.02-HB2.2-CS at low dose (A), optimal dose (B), and overdose (C) when settling at 23 °C.....	125
Figure 4.5. Schematic representation of flocculation of clay particles using Cat0.02-HB2.2-CS (A), HB2.3-CS (B) and Cat0.02-CS (C) at 600 ppm when settling at 23 °C.....	127
Figure 4.6. Schematic representation of flocculation of clay particles using Cat0.02-HB2.2-CS at low (A) and high (B) doses when settling at 50 °C.....	128
Figure 4.7. Schematic representation of flocculation of clay particles using Cat0.02-HB2.2-CS (A), HB2.3-CS (B) and Cat0.02-CS (C) at 600 ppm when settling at 50 °C.....	129
Figure 4.8. Water recovery of the settling tests of 2 wt % MFT using Cat0.02-HB2.2-CS, Cat0.02-CS and HB2.3-CS with varying doses from 25 to 1000 ppm (dry/slurry).....	131
Figure 4.9. Supernatant turbidity of the settling tests of 2 wt % MFT using Cat0.02-HB2.2-CS, Cat0.02-CS and HB2.3-CS with varying doses from 25 to 1000 ppm (dry/slurry).....	132
Figure 4.10. Sediment solids content of the settling tests of 2 wt % MFT using Cat0.02-HB2.2-CS, Cat0.02-CS and HB2.3-CS with varying doses from 25 to 1000 ppm (dry/slurry). .....	133
Figure 4.11. Initial settling rate (ISR) of the settling tests of 2 wt % MFT using Cat0.02-HB2.0-PS, Cat0.02-PS and HB1.9-PS with varying doses from 25 to 1000 ppm (dry/slurry). .....	135
Figure 4.12. Schematic representation of flocculation of clay particles using Cat0.02-HB2.0-PS at low dose (A), optimal dose (B) and overdose (C) when settling at 23 °C.....	135
Figure 4.13. Schematic representation of flocculation of clay particles using Cat0.02-HB2.0-PS at low (A) and high (B) doses when settling at 50 °C. ....	136
Figure 4.14. Water recovery of the settling tests of 2 wt % MFT using Cat0.02-HB2.0-PS, Cat0.02-PS and HB1.9-PS with varying doses from 25 to 1000 ppm (dry/slurry). ....	137
Figure 4.15. Supernatant turbidity of the settling tests of 2 wt % MFT using Cat0.02-HB2.0-PS, Cat0.02-PS and HB1.9-PS with varying doses from 25 to 1000 ppm (dry/slurry).....	138
Figure 4.16. Sediment solids content of the settling tests of 2 wt % MFT using Cat0.02-HB2.0-PS, Cat0.02-PS and HB1.9-PS with varying doses from 25 to 1000 ppm.....	139

Figure 5.1. Preparation of hydroxybutyl (HB), phenylhydroxyethyl (PHE) and cationic starches derived from CS or PS. Substitution is shown only at O-6 while in fact substitution can occur at O-2, O-3 and O-6.....	143
Figure 5.2. Schematic representation of flocculation of clay particles using Cat0.02-CS (A), HB0.6-CS (B) and the dual flocculant system with two different flocculant addition orders: Cat0.02-CS followed by HB0.6-CS (C) and HB0.6-CS followed by Cat0.02-CS (D). .....	147
Figure 5.3. Dose effect of HB0.6-CS on initial settling rate (ISR, A), water recovery (B), supernatant turbidity (C) and sediment solids content (D) of the flocculation of a 2 wt % MFT with a second flocculant, Cat0.02-CS, at a dose of 600 ppm at 50 °C. Dosage was reported on the dry/slurry basis.....	149
Figure 5.4. Initial settling rates (ISR) of flocculation of 2 wt % MFT using flocculant pairs consisting of HB0.6-CS and Cat0.02-CS (A), HB2.3-CS and Cat0.02-CS (B), HB0.6-CS and Cat0.05-CS (C), and HB2.3-CS and Cat0.05-CS (D) at 50 °C.....	151
Figure 5.5. Schematic representation of flocculation of clay particles using 25 ppm HB0.6-CS and Cat0.02-CS at low dose (A), optimal dose (B) and overdose (C).....	153
Figure 5.6. Schematic representation of flocculation of clay particles using 25 ppm (A), 100 ppm (B), and 600 ppm (C) of HB2.3-CS and Cat0.02-CS at optimal doses at 50 °C. ....	155
Figure 5.7. Water recovery of flocculation of 2 wt % MFT using flocculant pairs consisting of HB0.6-CS and Cat0.02-CS (A), HB2.3-CS and Cat0.02-CS (B), HB0.6-CS and Cat0.05-CS (C), and HB2.3-CS and Cat0.05-CS (D) at 50 °C.....	159
Figure 5.8. Supernatant turbidity of flocculation of 2 wt % MFT using flocculant pairs consisting of HB0.6-CS and Cat0.02-CS (A), HB2.3-CS and Cat0.02-CS (B), HB0.6-CS and Cat0.05-CS (C), and HB2.3-CS and Cat0.05-CS (D) at 50 °C.....	161
Figure 5.9. Sediment solids content of flocculation of 2 wt % MFT using flocculant pairs consisting of HB0.6-CS and Cat0.02-CS (A), HB2.3-CS and Cat0.02-CS (B), HB0.6-CS and Cat0.05-CS (C), and HB2.3-CS and Cat0.05-CS (D) at 50 °C.....	163
Figure 5.10. Initial settling rates (ISR) of flocculation of 2 wt % MFT using flocculant pairs consisting of HB0.6-PS and Cat0.02-PS (A), and HB1.9-PS and Cat0.02-PS (B) at 50 °C. Dosage was reported on the dry/slurry basis. ....	167
Figure 5.11. Schematic representation of flocculation of clay particles using 25 ppm (A), 100 ppm (B), and 600 ppm (C) of HB1.9-PS and Cat0.02-PS at optimal doses at 50 °C. ....	169
Figure 5.12. Water recovery of flocculation of 2 wt % MFT using flocculant pairs consisting of HB0.6-PS and Cat0.02-PS (A), and HB1.9-PS and Cat0.02-PS (B) at 50 °C. Dosage was reported on the dry/slurry basis.....	171

Figure 5.13. Supernatant turbidity of flocculation of 2 wt % MFT using flocculant pairs consisting of HB0.6-PS and Cat0.02-PS (A), and HB1.9-PS and Cat0.02-PS (B) at 50 °C. Dosage was reported on the dry/slurry basis. ....	173
Figure 5.14. Sediment solids content of flocculation of 2 wt % MFT using flocculant pairs consisting of HB0.6-PS and Cat0.02-PS (A), and HB1.9-PS and Cat0.02-PS (B) at 50 °C. Dosage was reported on the dry/slurry basis. ....	175
Figure 5.15. ISR (A), WR (B), ST (C) and SSC (D) of the flocculation of 2 wt % MFT with a flocculant pair, PHE0.2-PS and Cat0.02-PS. The performance of settling with Cat0.02-PS alone or with HB0.6-PS and Cat0.02-PS were included for comparison. ....	178
Figure 5.16. Initial settling rates (ISR) of the flocculation of 10 wt % MFT using flocculant pairs consisting of HB0.6-PS and Cat0.02-PS (A), HB1.9-PS and Cat0.02-PS (B), and HB1.9-PS and Cat0.2-PS (C) at 50 °C. Dosage was reported on the dry/slurry basis.....	186
Figure 5.17. Water recovery of the flocculation of 10 wt % MFT using flocculant pairs consisting of HB0.6-PS and Cat0.02-PS (A), HB1.9-PS and Cat0.02-PS (B), and HB1.9-PS and Cat0.2-PS (C) at 50 °C. Dosage was reported on the dry/slurry basis. ....	188
Figure 5.18. Supernatant turbidity of the flocculation of 10 wt % MFT using flocculant pairs consisting of HB0.6-PS and Cat0.02-PS (A), HB1.9-PS and Cat0.02-PS (B), and HB1.9-PS and Cat0.2-PS (C) at 50 °C. Dosage was reported on the dry/slurry basis. ....	191
Figure 5.19. Sediment solids content of the flocculation of 10 wt % MFT using flocculant pairs consisting of HB0.6-PS and Cat0.02-PS (A), HB1.9-PS and Cat0.02-PS (B), and HB1.9-PS and Cat0.2-PS (C) at 50 °C. Dosage was reported on the dry/slurry basis.....	193
Figure 5.20. The effect of the settling temperatures on the performance regarding initial settling rate (ISR, A), water recovery (B), supernatant turbidity (C), and sediment solids content (D) when flocculating 10 wt % MFT with a dual polymer pair consisting of 600 ppm of HB1.9-PS and Cat0.2-PS at various doses from 0 to 1000 ppm (dry/slurry).....	195
Figure 6.1. Preparation of PHE-HB-SNP. Substitution is shown only at O-6 while in fact substitution can occur at O-2, O-3 and O-6. ....	204
Figure 6.2. <sup>1</sup> H-NMR spectral comparison for PHE-HB-SNP (A), HB-SNP (B), PHE-SNP (C), and unmodified SNP (D). ....	205
Figure 6.3. Light transmittance measurements of various aqueous PHE-HB-SNP dispersions and an HB1.28-SNP dispersion for comparison. ....	207
Figure 6.4. Transmittance plot of 10 g/L PHE-HB-SNP dispersions with different MS <sub>PHE</sub> and MS <sub>HB</sub> . Transmittance values were measured at a wavelength of 500 nm at 15 °C. ....	210

Figure 6.5. Transmittance curves (A) and hydrodynamic diameters ( $D_h$ , B) of PHE0.31-HB0.30-SNPs prepared in different reaction protocols. Light transmittance measurements were conducted at 10 g/L. DLS measurements were conducted at 15 °C and 70 °C with 3 g/L dispersions. SO→BO, BO→SO, and BO+SO represent that the SNPs were subjected to hydrophobic modification prior to hydroxybutylation, the reactions in the reverse order, and the reactions occurred simultaneously, respectively.....	213
Figure 6.6. Preparation of PHE-HB-SNP using the BO+SO protocol. Substitution is shown only at O-6 while in fact substitution can occur at O-2, O-3 and O-6.....	213
Figure 6.7. Correlation between the reaction efficiency of hydroxybutylation ( $RE_{HB}$ ) and the amount styrene oxide (SO) added in the reactions. The dotted lines are binominal fitted trendlines provided for visual guidance only.....	216
Figure 6.8. Comparison of transmittance curves between PHE-HB-SNPs with different $MS_{PHE}$ but the same $MS_{HB}$ : 0.30 (A), 0.76 (B) and 0.82 (C). Light transmittance measurements were conducted at 10 g/L.....	217
Figure 6.9. Comparison of transmittance curves between PHE-HB-SNPs with different $MS_{PHE}$ but identical $MS_{PHE}$ : 0.18 (A), 0.22 (B) and 0.3 (C). Light transmittance measurements were conducted at 10 g/L.....	219
Figure 6.10. Transmittance curves of PHE0.28-HB0.36-SNP (A) and PHE0.27-HB0.72-SNP (B) dispersions in varying concentrations in a range of 1-50 g/L.....	221
Figure 6.11. Transmittance curves for 10 g/L dispersions of PHE0.30-HB0.42-SNP (A) and HB1.74-SNP (B) at low to high pH.....	223
Figure 7.1. Schematic representation of oil recovery procedures using the thermoresponsive block copolymer PEG- <i>b</i> -PMEO <sub>2</sub> MA. This picture was adapted from Yang and Duhamel with permission. <sup>10</sup> .....	228
Figure 7.2. Transmittance curves of the 1 g/L dispersions of Cat-HB1.9-SNP with MS of cationic groups ranging from 0 to 0.036.....	233
Figure 7.3. Bitumen recovery of extractions of fresh oil sands ores using Cat-HB1.9-SNPs with MS of cationic groups ranging from 0 to 0.036 along with 50 mg of toluene. ....	234
Figure 7.4. Transmittance curves of Cat0.036-HB1.9-SNP in a 1 g/L aqueous dispersion with no salts or with NaCl at a concentration of 30 mM. ....	235
Figure 7.5. Preparation of Cat-PHE-HB-SNP. Substitution can occur at O-2, O-3 and O-6. ....	237
Figure 7.6. Transmittance curves of Cat-PHE0.38-HB0.4-SNPs in a 1 g/L aqueous dispersion with no salts or with NaCl at a concentration of 30 or 60 mM.....	237



Figure 7.7. Bitumen recovery of extractions of fresh oil sands ores using 50 mg of toluene and 1 g/L of Cat-SNPs, Cat-PHE0.38-SNPs and Cat-PHE0.38-HB0.4-SNPs with varying MS of cationic groups.....	239
Figure 7.8. A plot of the amount of bitumen obtained from the top layer (“extracted bitumen”), the middle layer (“bitumen in tailings”) and the residual bitumen in the sands at the bottom (“unextracted bitumen”) versus time for the phase separation of the extraction mixture after rotating at 45 °C in an oven. The extraction tests were conducted with fresh oil sands ores using the Cat0.17-SNP (A) and the Cat0.17-PHE0.38-SNP (B) at 1 g/L along with 50 mg of toluene. ....	243
Figure 7.9. Pictures of bitumen extraction mixtures taken after 24 h of phase separation for the Cat0.17-PHE0.38-SNP (A) and the Cat0.17-SNP (B). The dark band on top of the aqueous phase is corresponding to the froth consisting mainly of the toluene diluted bitumen. ....	245
Figure 7.10. Bitumen recovery of extractions of fresh or aged oil sands ores using 50 mg of toluene and 1 g/L of Cat-SNPs with varying MS of cationic groups. ....	247
Figure 7.11. Optimization of the MS <sub>PHE</sub> values of Cat0.17-PHE-SNP in the extractions of the aged oil sands ores were performed (A). The effect of toluene dose (B), extraction temperature (C) and polymer concentration (D) were shown for the extractions of the aged ores using Cat0.17-PHE0.38-SNP at 1 g/L and 50 mg of toluene.....	249
Figure 7.12. Bitumen recovery versus the number of extraction cycles. The extractions started with Cat0.17-PHE0.38-SNP at 1 g/L for the first extraction cycle and 50 mg of toluene for each cycle. ....	251
Figure 8.1. Schematic flow diagram of a proposed method for improving the consolidation and dewatering of MFT. A dual polymer flocculant consisting of 600 ppm of HB1.9-PS and 100 ppm of Cat0.2-PS is used as an example. ....	258

## List of Tables

Table 1.1. A summary of poly( <i>N</i> -alkylacrylamide)s with different monosubstituting alkyl groups and the corresponding LCSTs.....	15
Table 1.2. Poly( <i>N,N</i> -dialkylacrylamide)s with different disubstituting alkyl groups and their corresponding LCSTs. ....	16
Table 1.3. Thermoresponsive celluloses with different substituents and their corresponding LCSTs. ....	23
Table 2.1. LCST values of HB-CS and HB-PS. ....	70
Table 2.2. The decrease in transmittance above the LCSTs of HB1.9-CS and HB1.9-PS.....	71
Table 2.3. Hydrodynamic diameters ( $D_h$ ) of TRS at 25 °C and 65 °C at 1 g/L (1000 ppm). .	72
Table 2.4. Effect of solids content of MFT on flocculation using 600 ppm HB2.3-CS at 50 °C.....	80
Table 5.1. Effect of flocculant addition orders on the settling performance of the dual flocculant system consisting of Cat0.02-CS and HB0.6-CS at 50 °C.....	146
Table 5.2. A summary of flocculation performance of different flocculant pairs with a combined dose under 50 ppm at 50 °C. ....	181
Table 5.3. A summary of performance of various polymers used to flocculate 10 wt % MFT. ....	197
Table 6.1. The molar substitution (MS), reaction efficiency (RE) and LCSTs of PHE-HB-SNPs obtained from modifying the HB-SNPs with styrene oxide. ....	204
Table 6.2. The molar substitution (MS), reaction efficiency (RE) and LCSTs of PHE-HB-SNPs obtained from SNPs subjected to hydrophobic modification prior to hydroxybutylation. ....	209
Table 6.3. Results of SNPs reacting with styrene oxide (SO) and butene oxide (BO) in different protocols. ....	211
Table 6.4. The molar substitution (MS), reaction efficiency (RE), and LCSTs of PHE-HB-SNPs obtained by modifying SNPs with butene oxide (BO) and styrene oxide (SO) simultaneously. ....	214

# Chapter 1

## Introduction

### 1.1 Overview of the Thesis

Canada has one of the largest proven reserves of crude oil, only after Saudi Arabia and Venezuela, and accounting for approximately 15 % of the world's oil reserves and exceeding 3 trillion barrels of oil.<sup>1</sup> Over 97 % of Canada's oil reserves are in the form of oil sands deposits which are mainly located in three areas of Alberta, Canada: Athabasca, Peace River and Cold Lake. Generally, oil sands, also known as tar sands or bituminous sands, consist of minerals, water and bitumen. The bitumen is intuitively the most valuable component to be extracted from the oil sands and can be upgraded to a variety of products such as gasoline, kerosene, petroleum diesel and asphalt. Unfortunately, extracting the bitumen from the sands is not a trivial endeavor. Indeed, since the rise of the oil economy at the beginning of the 20<sup>th</sup> century, governments and private companies alike have tried to develop an economical and environmentally benign extraction process that would enable oil from oil sands to compete with oil obtained from traditional sources on the world market.

Based on the depth of oil sands deposits, two types of bitumen extraction technologies are currently employed by the oil sands industry: surface mining and *in situ* drilling technologies. For oil sands ores located less than 75 meters below the surface, surface mining and water-based extraction is applied, whereas for the ores located deeper than 75 meters below the surface, *in situ* extraction such as steam-assisted gravity drainage (SAGD) or cyclic steam

stimulation (CSS) is applied. Both processes require a considerable amount of energy and resources, mainly water.

In addition to being energy and resource intensive, another major drawback to the current oil sands extraction processes is the creation of tailings ponds. Oil sands tailings, which are composed of water, sands, clay and residual bitumen, are by-products of the bitumen extraction process from oil sands. The tailings collected from extraction plant and from froth treatment are collectively discharged into a large settling basin, which is commonly referred to as a tailings pond.<sup>2</sup> In tailings ponds, coarse sands settle to the bottom by gravity very rapidly to form sand beaches, and the clarified water is recycled back to the extraction process. However, the fine ( $< 44 \mu\text{m}$ ) and ultrafine ( $< 2 \mu\text{m}$ ) solids settle at an extremely slow rate. Hence, the fine tailings settle over the course of two to three years to 30-40 wt % solids, which is known as mature fine tailings (MFT). Without any treatment, MFT remains in a very stable gel-like fluid state for decades before consolidation.

The accumulation of large volume of MFT poses a major environmental concern. Over 50 years of continuous tailings discharge, these tailings have surpassed 1.5 trillion liters currently and their volumes continue to grow each year. Today, tailings ponds cover more than 250 square kilometers, which is about the areas of Waterloo, Kitchener and Guelph combined. The anticipated clean-up costs of the accumulated tailings are estimated to be over \$50 billion dollars. With the expansion of oil sands mining operations, the fast accumulating volume of tailings deepens negative impact on the environment.

Land reclamation, water recycling and environmental contamination are notably the largest environmental concerns which pose a significant challenge to the sustainable development of the oil sands industry. By law, oil sands operators must fully reclaim the land within 10 years once the tailings pond is no longer in use. Hence, it is certainly a priority to minimize and eventually eliminate the tailings ponds, by increasing the solids content of the MFT at the bottom of the tailings ponds, to create trafficable land ready for reclamation. An equally important goal is to recover the process water from the tailings pond, especially the entrapped water from MFT, and recycle it back to the extraction plant in order to reduce the use of fresh water. Moreover, MFT contain a significant amount of naphthenic acids, heavy metals (e.g. mercury and arsenic) and residual toxic hydrocarbonates which have adverse acute and chronic effects on aquatic and wildlife organisms in areas surrounding the tailings ponds. Therefore, effective tailings management should be employed to reduce both the total accumulated MFT volume and the MFT produced per barrel of bitumen produced.

The main focus of this thesis is the development of more environmentally benign processes for the extraction of bitumen from oil sands and the consolidation of MFT in oil sands tailings ponds. In brief, we examine mainly thermoresponsive starch-based polymers as process aids for bitumen extraction and dewatering of MFT. As thermoresponsive polymers, oil sands processing technology and MFT flocculation are central to this thesis, a detailed discussion of each of these topics is given below.

## 1.2 Thermoresponsive Polymers

“Smart polymers”, also known as stimuli-responsive polymers (SRPs), undergo an abrupt change in their physical properties, in most cases, a change in their dispersibility in water, in response to external stimuli. These external stimuli, such as temperature, pH, ionic strength, and photosensitivity, can affect polymer-polymer interactions and polymer-solvent interactions at the molecular level to induce switchable properties of the SRPs. Among the various suites of stimuli, thermal response is arguably the most extensively studied due to its practicality in many applications. Polymers that exhibit a phase transition behavior in response to a change in temperature are commonly known as thermoresponsive polymers (TRPs). Since their discovery in the 1960’s, TRPs have garnered considerable attention as a result of their numerous potential applications in the biomedical fields, such as drug and gene delivery vehicles,<sup>3-5</sup> tissue engineering and cell culturing materials,<sup>6,7</sup> as well as in the non-biologically related fields, such as filtering agents,<sup>8</sup> smart surface coatings,<sup>9</sup> oil extraction additives,<sup>10</sup> and flocculating agents.<sup>11-16</sup>

Due to their potential applications, numerous studies have been conducted on TRPs. Poly(*N*-isopropylacrylamide) (PNIPAM), which exhibits a lower critical solution temperature (LCST) at approximately 32 °C, is arguably among most popular and studied synthetic TRPs.<sup>17</sup> Other well-known TRPs that have also been studied in depth include poly(*N,N*-diethylacrylamide) (PDEAAm) with an LCST of 33 °C,<sup>18</sup> poly(*N*-vinyl caprolactam) (PVCL) with an LCST between 30 and 35 °C,<sup>19</sup> and poly(2-(2-methoxyethoxy) ethyl methacrylate) (PMEO<sub>2</sub>MA) with an LCST around 26 °C,<sup>20</sup> to name a few. More recently, TRPs derived from biodegradable and biocompatible materials have been of interest. Many reports have appeared

in the literature describing modification and applications of TRPs based on natural polymers such as polysaccharides. A common polysaccharide-based TRP is methyl cellulose with an LCST of approximately 30 °C.<sup>21</sup> TRPs derived from starch, which is one of the most abundant and readily available biopolymer in nature, have also been a growing interest.<sup>22–26</sup>

### 1.2.1 Critical Solution Temperatures

Thermoresponsive polymers (TRPs) can exhibit lower critical solution temperature (LCST) or upper critical solution temperature (UCST). Some TRPs can exhibit both an LCST and an UCST. Figure 1.1 shows the schematic phase diagrams for TRP dispersions. Depending on the miscibility gap, the minimum of the phase diagram is referred to as the LCST (Fig. 1.1A) and the maximum of the phase diagram is referred to as the UCST (Fig. 1.1B).<sup>27</sup> The LCST and UCST are the respective temperatures below and above which the polymer and the solvent become completely miscible at any given concentration. More specifically, for LCST-type TRP dispersions, the polymer dispersion undergoes phase separation when the temperature is higher than the LCST and for UCST-type TRP dispersions, phase separation occurs when the solution temperature is lower than the UCST. Phase separation is entropy driven for LCST-type TRPs and enthalpy driven for UCST-type TRPs. In this thesis, we are mainly interested in the LCST-type TRPs. A dispersion with an LCST-type TRP appears to be clear and homogeneous below the LCST, and the dispersion turns cloudy and immiscible above the LCST.

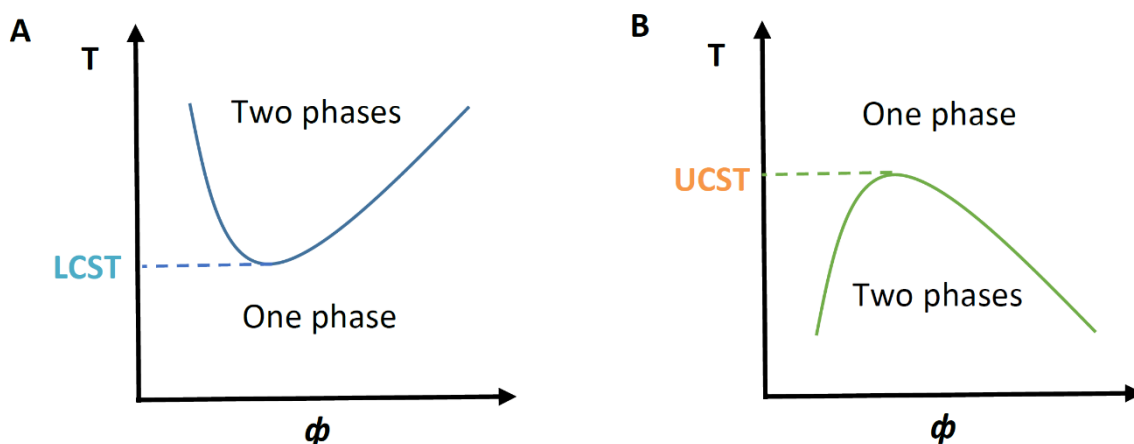


**Figure 1.1.** Schematic phase diagrams plotting critical temperatures,  $T$ , as a function of polymer volume fraction,  $\phi$ , for LCST (**A**) and UCST (**B**).

Phase separation for LCST-type TRPs is energetically favorable due to the increase of entropy in a polymer-water system above the LCST.<sup>28</sup> To elaborate, the polymer in the system can stay solvated below the LCST due to the presence of hydrogen bonding between the hydrophilic regions of the polymer and water molecules. Additionally, it is important to note that the hydrophobic regions of the polymer, which can behave similarly to nonpolar substances in water, are surrounded by an ordered layer of water molecules.<sup>27,29,30</sup> Considering the change in Gibbs free energy ( $\Delta G$ ) below the LCST, the ordered arrangement of water molecules surrounding the hydrophobic regions of the polymer results in a relatively small negative change in entropy ( $\Delta S$ ), which is not energetically favorable for a miscible dispersion. However, the presence of a vast number of polymer-water hydrogen bonds contributes to a large negative change in enthalpy ( $\Delta H$ ) that overcomes the unfavorable negative  $\Delta S$ . Hence,  $\Delta G$  remains negative and a homogenous dispersion is energetically favorable below the LCST.<sup>29,31</sup> On the other hand,  $\Delta H$  becomes less negative as a result of disruption or weakening of the polymer-water hydrogen bonds when temperature increases.<sup>31</sup> Hence, there is a small contribution from the  $\Delta H$  to



the negative  $\Delta G$  of phase separation. Additionally, the dissociation of water molecules from the polymer increases  $\Delta S$  as temperature increases. As a result, the  $\Delta S$  dominates the contribution to the negative  $\Delta G$  and becomes the main driving force for the phase separation above the LCST.<sup>32</sup>

### 1.2.2 Phase Transition Behaviors

Depending on the chemical nature of LCST-type TRPs, the TRPs can exhibit one or both of two distinctive phase transition behaviors: intramolecular aggregation and intermolecular aggregation.<sup>28</sup> The intramolecular aggregation, also known as a coil-to-globule transition, describes a process by which in response to a change in temperature, linear and flexible polymer chains in a dispersion adopt other conformations which are more thermodynamically stable.<sup>17</sup> Below the LCST, the polymer completely disperses in water as a result of extensive hydrogen bonding between the polymer chains and water molecules, and the polymer chains adopt a random coil conformation (Fig. 1.2A). Above the LCST, the polymer, undergoing intramolecular aggregation, collapses into a globular conformation as a result of the disruption of polymer-water hydrogen bonding by the elevated temperature (Fig. 1.2A). As an example, PNIPAM undergoes a coil-to-globule transition at around 32 °C. This phase transition can be observed by monitoring the decrease in hydrodynamic radius ( $R_h$ ) of the polymer as the temperature increases (Fig. 1.2B).<sup>17</sup>

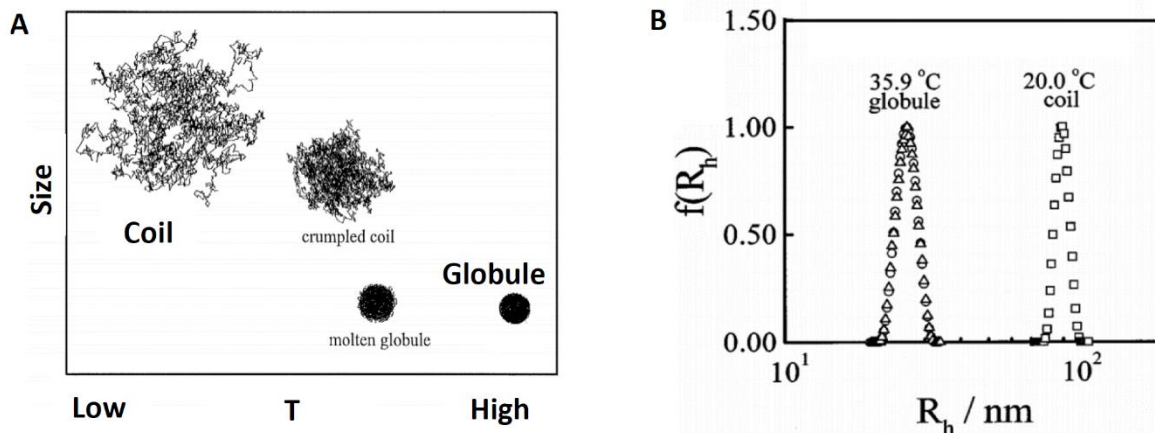


**Figure 1.2.** Schematic representation of a coil-to-globule transition of a TRP with four thermodynamically stable states from low to high temperature (A), and hydrodynamic radius distributions,  $f(R_h)$ , of PNIPAM in a low concentration dispersion at below and above the LCST (B). Both diagrams were adapted from Wu et al. with permission.<sup>17</sup>

TRPs with a phase transition involving intermolecular aggregation are typically amphiphilic block copolymers, which consist of hydrophilic and hydrophobic blocks.<sup>28</sup> Below the LCST, polymer chains in a dispersion typically adopt random coil conformation (Fig. 1.3).<sup>33</sup> As the temperature increases, the coil conformation is no longer thermodynamically stable leading to formation of micelle-like intermolecular aggregates above the LCST (Fig. 1.3).<sup>33</sup> A well-known TRP which exhibits this type of phase transition is a commercially available triblock copolymer known as Pluronics<sup>TM</sup>.<sup>34</sup> This triblock copolymer consists of a hydrophilic poly(ethylene oxide) (PEO) block sandwiched between two hydrophobic poly(propylene oxide) (PPO) blocks.

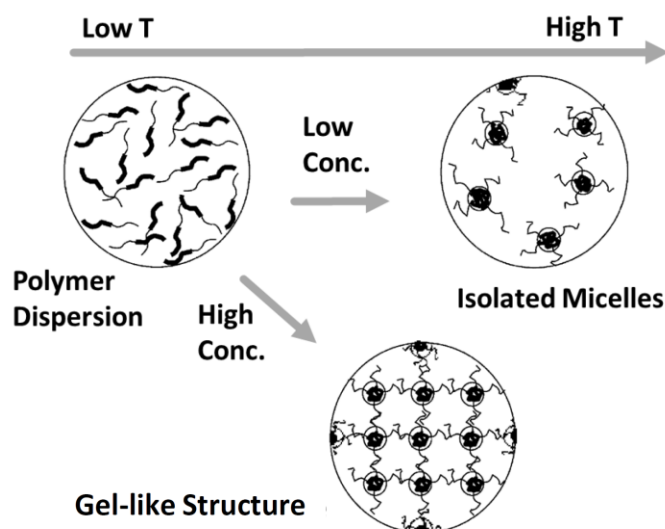


**Figure 1.3.** A schematic representation of conformational changes of amphiphilic block copolymers in an aqueous dispersion. At low concentration, polymer chains assemble into isolated micelles above LCST; at high concentration, these polymeric micelles further assemble into an ordered gel-like structure. This figure was adapted from Gil et al. with permission.<sup>28</sup>

The outcome of the phase transition can often be manipulated by the structure of a thoughtfully designed block copolymer. As an example, a hydrophobic block can be grafted onto a TRP, such as PNIPAM, to enable the formation of micelles with a hydrophobic core and a hydrophilic TRP-based corona below LCST at a relatively low concentration (Fig. 1.4A). The TRP-based corona becomes hydrophobic above the LCST leading to deformation of micelles (Fig. 1.4A).<sup>28</sup> On the contrary, when a hydrophilic block is grafted onto a TRP, the TRP block becomes hydrophobic above LCST which triggers the formation of micelles (Fig. 1.4B).<sup>28</sup>

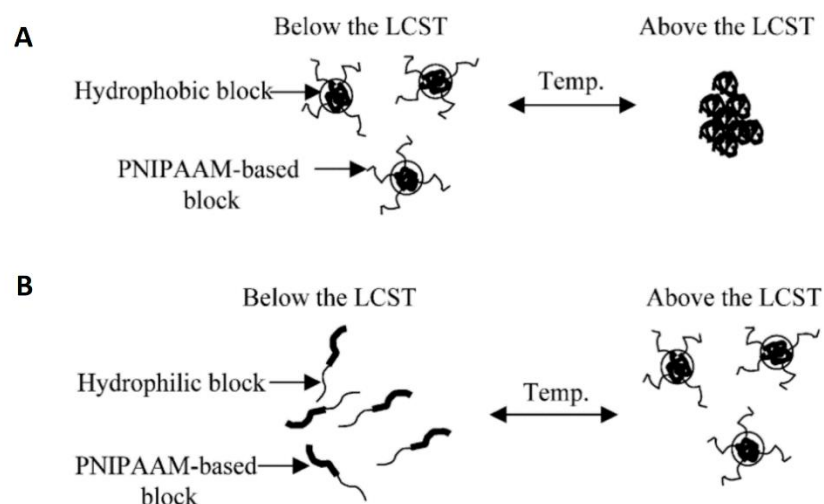


**Figure 1.4.** Schematic representation of two types of micellar structures of PNIPAM grafted block copolymers in an aqueous dispersion: a block copolymer consisting of a hydrophobic block and a thermoresponsive block (**A**), and a block copolymer containing a hydrophilic block and a thermoresponsive block (**B**). Both diagrams were adapted from Gil et al. with permission.<sup>28</sup>

### 1.2.3 TRP Transmittance Curves

The drastic change in dispersibility of a TRP in an aqueous dispersion can be described by its transmittance curve as the dispersion undergoes phase separation in response to a change in temperature. Transmittance curves can be obtained from absorbance measurements over a range of temperature. The absorbance of the TRP dispersion can be monitored with a UV/Visible spectrometer equipped with a temperature controller.

Different TRPs can exhibit different heating and cooling curves (Fig. 1.5).<sup>35</sup> Some TRPs show overlapping transmittance curves for heating and cooling processes (Fig. 1.5A), and others show a notable gap, known as a hysteresis, between their heating and cooling transmittance curves (Fig. 1.5B). Moreover, some TRPs exhibit an abrupt change in

transmittance and a steep transmittance curve (Fig. 1.5A and B) and others show a shallow transmittance curve indicating a relatively slow thermal transition (Fig. 1.5C).

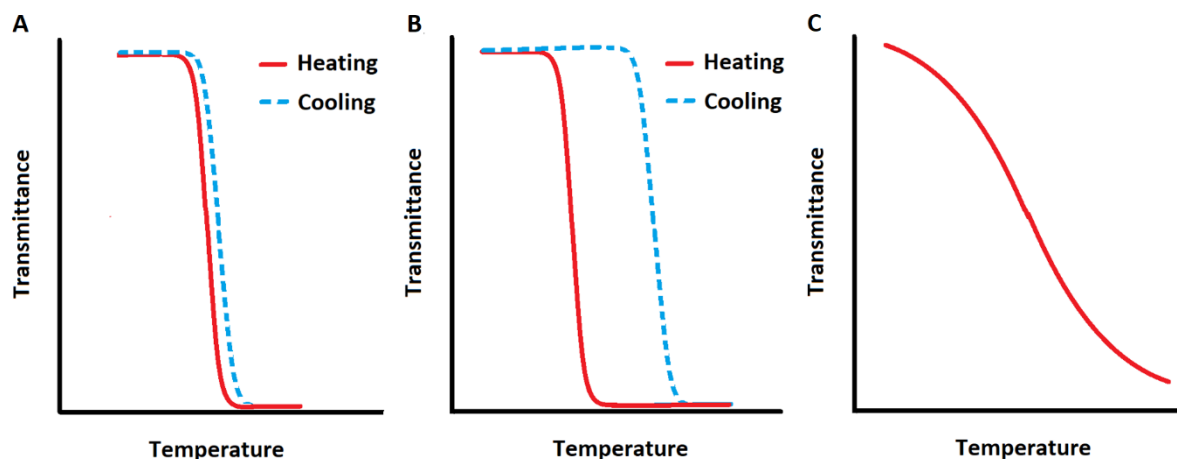


**Figure 1.5.** TRPs can exhibit overlapping heating and cooling curves (A), a hysteresis (B), or a slow thermo-transition (C).

TRPs with overlapping heating and cooling transmittance curves are often amphiphilic block copolymers consisting of hydrophobic and hydrophilic blocks.<sup>35</sup> The hydrophobic-hydrophilic balance enables the copolymers to stay solvated in a dispersion below their LCSTs. As temperature increases, the hydrophobic-hydrophilic balance is disrupted, which triggers assembly of individual polymer chains into micelle-like large aggregates and eventually leads to sol-gel phase separation. TRPs consisting of poly(vinyl ether)s, poly(phosphoester)s as well as acrylate- and methacrylate-based polymers, such as poly(2-(2'-methoxyethoxy)ethyl methacrylate-*co*-oligo(ethylene glycol) methacrylate) (P(MEO<sub>2</sub>MA-*co*-OEGMA)), usually exhibit a thermal transition that displays the overlapping heating and cooling transmittance curves.<sup>20,36</sup>

TRPs with a coil-to-globule thermal transition often show a hysteresis in heating and cooling transmittance curves.<sup>35</sup> The hysteresis can be attributed to the diffusion of water molecules into dense hydrophobic aggregates, which are formed above LCST, is hindered during the cooling process.<sup>36</sup> The hindered diffusion results in a slower dissociation of the aggregates and a decreased rate of re-solvation of individual polymer chains. A common TRP that exhibits a hysteresis is PNIPAM.<sup>37</sup>

The slope of a transmittance curve can often be quite informative. Typically, a sharp transmittance curve indicates a fast thermal transition. When an ON/OFF switch is needed for a potential application, a fast thermal transition is preferred. A fast thermal transition ensures a maximum amount of polymer-water interactions below the LCST, however, such interactions are rapidly minimized above the LCST.<sup>35</sup> On the contrary, a shallow transmittance curve indicates a relatively slow thermal transition. This type of transmittance curves often involves the formation or collapse of micelles above the LCST depending on the design of the TRPs. As an example, poly(styrene)-*b*-poly(*N*-isopropyl acrylamide) diblock copolymers (PSt-*b*-PNIPAM)) form micelles in an aqueous dispersion below the LCST.<sup>38</sup> As temperature increases, the micelles collapse to form insoluble aggregates and consequently, a continuous decrease in the transmittance over a range of temperature can be observed with the increasing number of insoluble aggregates (Fig. 1.6A). Another example is poly(ethylene glycol)-*b*-poly(2-(2-methoxyethoxy)ethyl methacrylate) (PEG-*b*-PMEO<sub>2</sub>MA), which forms micelles above its LCST and exhibits a shallow transmittance curve (Fig. 1.6B).<sup>10</sup>

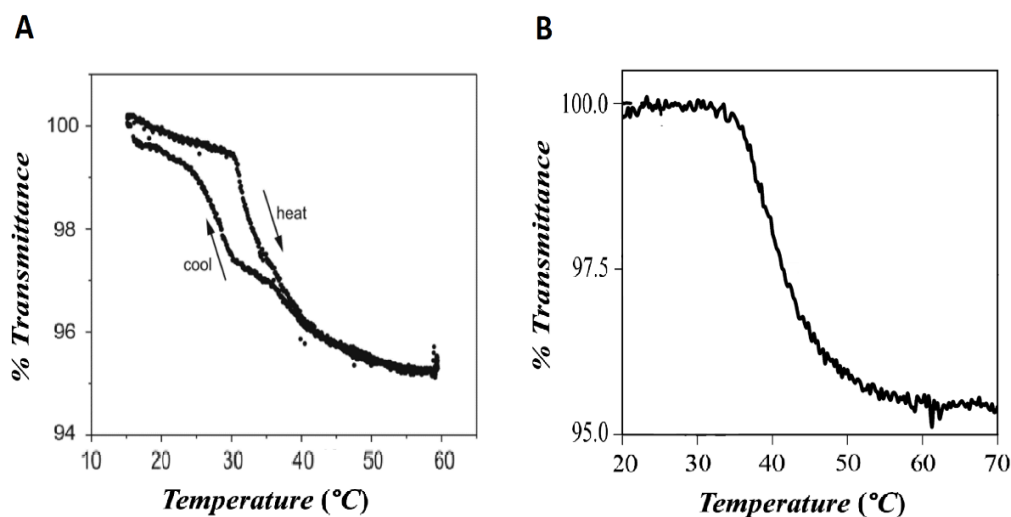


**Figure 1.6.** Transmittance curves for a 0.2 g/L aqueous dispersion of poly(styrene)-*b*-poly(*N*-isopropyl acrylamide) (A),<sup>38</sup> and for a 5 g/L dispersion of PEG-*b*-PMEO<sub>2</sub>MA (B).<sup>10</sup> Figures were taken with permission.

#### 1.2.4 Factors affecting LCST

One of the biggest advantages of TRPs is that their LCSTs can be conveniently adjusted to satisfy different requirements for various potential applications. Investigating factors that can affect the LCST of TRPs has always been one of the focuses of the studies involving TRPs in the literature. Molecular structure, molecular weight, polymer concentration, and salt content in a dispersion are common factors affecting the LCST.

##### 1.2.4.1 Effect of Molecular Structure on LCST

TRPs with different molecular structures often exhibit different LCSTs. In other words, LCSTs can be tuned by a careful design of TRPs, more specifically, by introduction of hydrophobic or hydrophilic chemical groups to adjust hydrophobicity of TRPs. The presence of more hydrophobic groups on a TRP should intuitively result in a lower LCST. The

hydrophobic or hydrophilic groups can be small chemical moieties, oligomers or large polymeric blocks.

Altering small chemical moieties on TRPs, such as alkyl groups, can adjust the LCSTs of the original TRPs. As an example, PNIPAM with isopropyl groups has an LCST of approximately 32 °C (Table 1.1, entry 2).<sup>39</sup> Substituting the isopropyl groups with other alkyl groups such as n-propyl, cyclopropyl, and ethyl groups can yield poly(*N*-alkylacrylamide)s with respective LCSTs of 23, 58, and 74 °C (Table 1.1, entries 1, 8 and 9).<sup>32,40,41</sup> Other examples of poly(*N*-alkylacrylamide)s are summarized in Table 1.1. Generally, the LCSTs decrease with increasing hydrophobicity of the alkyl groups as a result of stronger hydrophobic effects induced by the alkyl groups during thermal transition. Moreover, when a relatively hydrophilic hydroxyl group is attached, in case of poly(*N*-(2-hydroxyisopropyl)acrylamide) (PHIPAM), the LCST can increase drastically to 80 °C when compared to the LCST of PNIPAM (Table 1.1, entries 2 and 10).<sup>39,42</sup> The increase in the LCST can be due to an extra amount of energy that is required to break the additional hydrogen bonding between water molecules and the hydrophilic groups during thermal transition.



**Table 1.1.** A summary of poly(*N*-alkylacrylamide)s with different monosubstituting alkyl groups and the corresponding LCSTs.

Entry	Poly( <i>N</i> -alkylacrylamide)	LCST (°C)
1	poly( <i>N</i> - <i>n</i> -propylacrylamide)	23 <sup>41</sup>
2	poly( <i>N</i> -isopropylacrylamide)	32 <sup>39</sup>
3	poly(ethoxypropylacrylamide)	33 <sup>43</sup>
4	poly( <i>N</i> -(1-hydroxymethyl)propylmethacrylamide)	34 <sup>44</sup>
5	poly( <i>N</i> -(2-ethoxyethyl)acrylamide)	38 <sup>45</sup>
6	poly(aminomethoxypropylacrylamide)	43 <sup>46</sup>
7	poly( <i>N</i> -(2-ethoxyethyl)methacrylamide)	50 <sup>45</sup>
8	poly( <i>N</i> -cyclopropylacrylamide)	58 <sup>40</sup>
9	poly( <i>N</i> -ethylacrylamide)	74 <sup>32</sup>
10	poly( <i>N</i> -(2-hydroxyisopropyl)acrylamide)	80 <sup>42</sup>

LCSTs can also be manipulated by the substitution of a second alkyl group. Poly(*N*-ethylacrylamide) has an LCST of 74 °C (Table 1.1, entry 9),<sup>32</sup> however, with the second ethyl group on the amide nitrogen atom, poly(*N,N*-diethylacrylamide) exhibits a much lower LCST of 32 °C (Table 1.2, entry 1).<sup>47</sup> When the two ethyl groups are replaced by two relatively less hydrophobic methyl groups, poly(*N,N*-dimethylacrylamide) shows a substantially higher LCST of 216 °C (Table 1.2, entry 2).<sup>48</sup> Moreover, when one of the methyl groups is substituted with increasingly hydrophobic alkyl groups, the resultant poly(*N,N*-dialkylacrylamide)s exhibit much lower LCSTs (Table 1.2, entries 2-4).<sup>48,49</sup>

**Table 1.2.** Poly(*N,N*-dialkylacrylamide)s with different disubstituting alkyl groups and their corresponding LCSTs.

Entry	Poly( <i>N,N</i> -alkylacrylamide)	LCST (°C)
1	poly( <i>N,N</i> -diethylacrylamide)	32 <sup>47</sup>
2	poly( <i>N,N</i> -dimethylacrylamide)	216 <sup>48</sup>
3	poly( <i>N,N</i> -ethylmethylacrylamide)	60 <sup>49</sup>
4	poly( <i>N,N</i> -propylmethylacrylamide)	15 <sup>48</sup>

The placement of hydrophobic moieties can also affect the LCST. Poly(*N,N*-ethylmethylacrylamide), which has an extra methyl group on the amide nitrogen atom compared to poly(*N*-ethylacrylamide), exhibits a lower LCST than the latter (Table 1.2, entry 3 and Table 1.1, entry 9).<sup>32,49</sup> Typically, the LCST decreases as the hydrophobicity of TRPs increases, however, there are exceptions to this. Poly(*N*-isopropylmethacrylamide), which has an additional methyl group on the hydrocarbon backbone compared to poly(*N*-isopropylacrylamide), exhibits an LCST of 46 °C, which is higher than the LCST of PNIPAM.<sup>39,50</sup> It was speculated by Djokpe et al. that steric hindrance might be the cause of the increase in LCST due to the methyl group on the hydrocarbon backbone. This methyl group may interfere with the hydrophobic interactions of the *N*-isopropyl groups leading to a delay in aggregation and phase separation.<sup>51</sup>

Moreover, the insertion of hydrophilic oligomers can also adjust the LCST. Hydrophilic oligomers, such as ethylene glycol oligomers, can be introduced into monomers of a hydrophobic polymer and the LCST of the resultant polymer can be tuned by the length of the ethylene glycol oligomers. For example, methyl methacrylate (MMA) is the monomer

of the hydrophobic polymer, poly(methyl methacrylate) (PMMA), and when ethylene glycol oligomers are inserted in between the methyl and methacrylate groups of the monomer, the resultant poly(methyl ethoxymethacrylate)s (PMEO<sub>n</sub>MA)s become thermoresponsive. When the number of ethylene glycol units increases from 2, 3 to 4 (i.e.  $n = 2, 3$  or 4), the LCSTs of the respective PMEO<sub>n</sub>MA)s increase from 26 °C, 52 °C to 68 °C.<sup>52,53</sup> Similarly, when ethylene glycol oligomers are inserted into poly(ethyl methacrylate), the resultant poly(ethyl ethoxymethacrylate)s (PEEO<sub>n</sub>MA)s exhibit LCSTs of 4 °C, 27 °C and 42 °C as the oligomer unit number,  $n$ , equals 2, 3 and 4, respectively.<sup>52</sup> Due to the more hydrophobic ethyl terminal groups of PEEO<sub>n</sub>MA)s compared to PMEO<sub>n</sub>MA)s, the PEEO<sub>n</sub>MA)s intuitively have lower LCSTs, given that the number of ethylene glycol oligomer units on both polymers are the same.

In some cases, the LCST can also be affected by grafting of a polymeric block to a TRP. For example, when PNIPAM, which has an LCST of about 32 °C, is grafted with a hydrophilic polymeric block, the resultant polymer often results in a higher LCST. Block copolymers consisting of PNIPAM and poly(*N*-hydroxyethylacrylamide) (PHEA) have LCSTs in a range of 37 °C and 56 °C, depending on the molar fraction of PHEA.<sup>54</sup> Similarly, cellulose-*g*-PNIPAM exhibits higher LCSTs in a range from 37 °C to 41 °C.<sup>55</sup> Another prevalent TRP is poly(2-(2-methoxyethoxy) ethyl methacrylate) (PMEO<sub>2</sub>MA) with an LCST of 26 °C. With the grafting of a hydrophilic block, poly(ethylene glycol) (PEG), PEG-*g*-PMEO<sub>2</sub>MA was reported to have a higher LCST (34 °C) than PMEO<sub>2</sub>MA.<sup>10</sup> On the other hand, when a hydrophobic block, poly(*N*-acryloyl-2,2-dimethyl-1,3-oxazolidine) (PADMO), was grafted to PEO, which has an LCST typically higher than 100 °C,<sup>56</sup> it yielded PEO-*b*-PADMO samples with LCSTs

in a 20 - 35 °C temperature range depending on the degree of polymerization of the PADMO block.<sup>57</sup>

#### **1.2.4.2 Effect of Molecular Weight on LCST**

Typically, the LCST decreases with an increase in molecular weight of a TRP. The effect of molecular weight on the LCST becomes more pronounced when the molecular weight is relatively small.<sup>58</sup> On the contrary, the LCST becomes less dependent of molecular weight as the molecular weight gets larger. Generally, the effect of molecular weight is due to the hydrophobic terminal groups of a TRP.<sup>59</sup> The terminal groups of a polymer are usually determined by the type of initiator used in a polymerization reaction. Xia et al. showed that the polymerization of PNIPAM using different initiators can produce PNIPAM derivatives with different terminal groups and with different LCSTs.<sup>60</sup> The effect of the terminal groups on the LCSTs becomes less pronounced as the molecular weight of the TRPs increase (Fig. 1.7).<sup>60</sup> In other words, the LCST becomes less dependent on the molecular weight for TRPs with a high molecular weight (>10 kDa). On the contrary, at low molecular weight (<10 kDa), the molecular weight has a more pronounced effect on the LCSTs of the PNIPAM derivatives with different terminal groups (Fig. 1.7).<sup>60</sup>

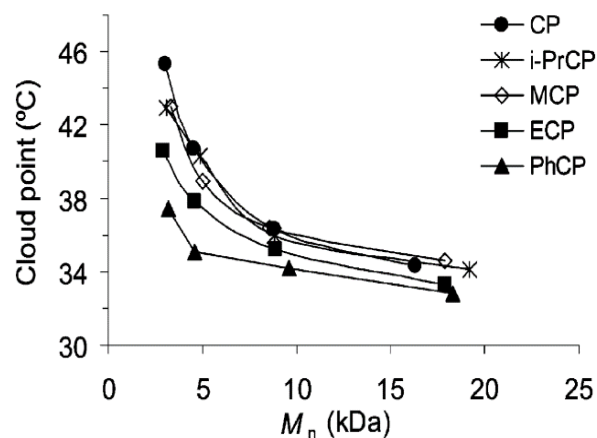


**Figure 1.7.** The correlation of the cloud point or LCST with molecular weight of PNIPAM derivatives prepared using different initiators: 2-chloropropionamide (CP), *N*-isopropyl-2-chloropropionamide (*i*-PrCP), methyl 2-chloropropionate (MCP), ethyl 2-chloropropionate (ECP), and *N*-phenyl-2-chloropropionamide (PhCP). The figure was adapted from Xia et al. with permission.<sup>60</sup>

#### 1.2.4.3 Effect of Polymer Concentration on LCST

Generally, the LCST of a TRP increases as the polymer concentration decreases. When a TRP dispersion is diluted, the chance of interparticle interactions between the polymer chains is decreased, and phase separation due to the formation of large aggregates occurs at a higher temperature. Many examples which describe the effect of polymer concentration on the LCST can be found in the literature. Uğuzdoğan et al. reported that the LCST of poly(ethoxypropylacrylamide) decreased from 42 °C to 32 °C when the polymer concentration was increased from 0.1 to 5 wt %.<sup>43</sup> Chen et al. also reported that when the concentration increased from 0.1 to 2 wt %, the LCST of poly(*N*-acryloylsarcosine methyl ester) decreased from 54 °C to 42 °C.<sup>61</sup> Ju et al. reported that the LCST decreased to 2.5 °C as the concentration of a dispersion of 2-hydroxy-3-isopropoxypropyl starch increased from 0.2 to 1 wt %.<sup>25</sup> The

determination of the concentration effect on the LCST of a TRP is quite necessary for potential applications of such TRP.

#### **1.2.4.4 The Effect of the Type of Salts and Salt Concentration on LCST**

Generally, the LCST is affected by any molecules in a TRP dispersion that can affect polymer-water interactions. Salts are known to affect LCST, and kosmotropic salts typically have a larger effect than chaotropic salts. Kosmotropic salts are relatively small and some of them have higher charge density. Water molecules interact with kosmotropic salt molecules more favorably than with polymer, which results in weakened polymer-water interactions. The salt molecules destabilize TRPs in a dispersion, which causes a decrease in LCST. Examples of kosmotropic salts are  $\text{CH}_3\text{CO}_2^-$ ,  $\text{HCO}_2^-$ ,  $\text{F}^-$ ,  $\text{OH}^-$ ,  $\text{HPO}_4^-$ ,  $\text{CO}_3^{2-}$ , and  $\text{SO}_4^{2-}$ . On the contrary, chaotropic salts are relatively large and monovalent. Examples of chaotropic salts include  $\text{ClO}_4^-$ ,  $\text{SCN}^-$ ,  $\text{I}^-$ ,  $\text{Br}^-$  and  $\text{Cl}^-$ . These salts are less effective at affecting the LCST and in fact, they sometimes stabilize the hydrophobic segments of a TRP, resulting in that more energy is required for a phase separation to occur.<sup>25</sup> For example, the LCST of PNIPAM can be decreased with the addition of salts (Fig. 1.8).<sup>62</sup> Kosmotropic salts can induce much lower LCSTs with a relatively low salt concentration compared to chaotropic salts.

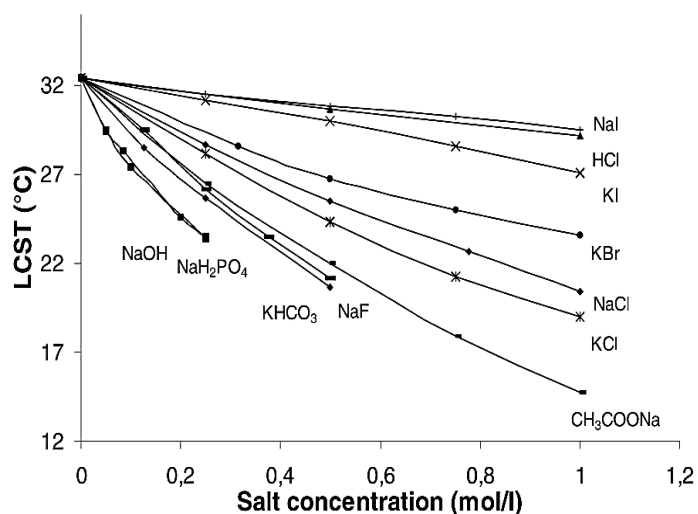


**Figure 1.8.** LCSTs of PNIPAM dispersions with the addition of different types of salts and salt concentrations. The figure was adapted from Eeckman et al. with permission.<sup>62</sup>

### 1.2.5 Thermoresponsive Polysaccharides

A potential problem with thermoresponsive synthetic polymers such as PNIPAM is that the monomers of such polymers are often carcinogenic and teratogenic, which makes this type of TRPs less biocompatible and detrimental to any potential biological applications.<sup>63</sup> Hence, many efforts have been directed towards TRPs derived from biocompatible, biodegradable and non-toxic materials such as polysaccharides. Since the discovery of thermoresponsive cellulose ethers such as methyl and hydroxypropyl celluloses in the early 1990's,<sup>63</sup> numerous reports have appeared in the literature describing their thermoresponsive behavior and applications. Recently, thermoresponsive starches have also emerged in the literature, which is not surprising given the natural abundancy of starch in nature.

### 1.2.5.1 Thermoresponsive Cellulose

Cellulose is the most abundant biopolymer on Earth, which consists of D-anhydroglucose units joined together by  $\beta$ -1,4-glycosidic linkages (Fig. 1.9). Many cellulose derivatives have been reported to show thermoresponsive behavior, and some of the common thermoresponsive celluloses (TRC) and their LCSTs are summarized in Table 1.3. These TRCs are typically prepared by alkylation or etherification at hydroxyl (OH) groups of C-2, C-3 and C-6 positions on anhydroglucose units (AGUs).<sup>64</sup> Similar to thermoresponsive synthetic polymers, hydrophobic substituents can largely affect the LCST of a TRC. For example, methyl cellulose (MC) has an LCST of about 68 °C,<sup>65</sup> whereas the LCST of hydroxypropyl cellulose (HPC) is approximately 46 °C.<sup>66</sup> Other than different hydrophobic substituents, the LCST is also determined by the degree of substitution (DS) and the molar substitution (MS) of the substituents. The DS is defined as the average number of the substituted OH groups on an AGU, and MS is referring to the number of moles of substituents per mole of AGU.<sup>64</sup> For example, hydroxypropyl methyl cellulose (HPMC) with a DS of methyl group ( $DS_{Me}$ ) of 1.9 and an MS of hydroxypropyl group ( $MS_{HP}$ ) of 0.25 has a lower LCST of approximately 65 °C,<sup>67</sup> due to the higher  $DS_{Me}$  and  $MS_{HP}$ , compared to another HPMC with a  $DS_{Me}$  of 1.45 and an  $MS_{HP}$  of 0.11, which has an LCST of 75 °C.<sup>68</sup>



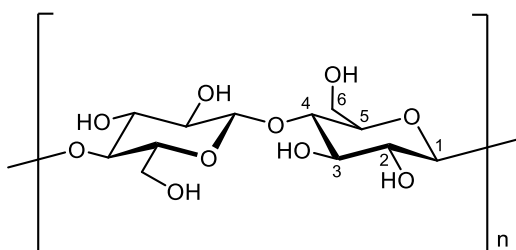


**Figure 1.9.** Chemical structure of cellulose.

**Table 1.3.** Thermoresponsive celluloses with different substituents and their corresponding LCSTs.

Entry	Thermoresponsive Celluloses	Substituents	LCST (°C)
1	Methyl cellulose (MC)	-CH <sub>3</sub>	68 <sup>65</sup>
2	Hydroxypropyl cellulose (HPC)	-CH <sub>2</sub> CH(OH)CH <sub>3</sub>	46 <sup>69</sup>
3	Hydroxyethyl methyl cellulose (HEMC)	-CH <sub>3</sub> or -CH <sub>2</sub> CH <sub>2</sub> OH	74 <sup>70</sup>
4	Hydroxypropyl methyl cellulose (HPMC)	-CH <sub>3</sub> or -CH <sub>2</sub> CH(OH)CH <sub>3</sub>	65 <sup>67</sup>
5	Ethylhydroxyethyl cellulose (EHEC)	-CH <sub>2</sub> CH <sub>3</sub> or -CH <sub>2</sub> CH <sub>2</sub> OH	39 <sup>66</sup>

### 1.2.5.2 Thermoresponsive Starch

Starch, one of the most abundant and readily available biopolymers in nature, is produced by plants for energy storage. Starch has a characteristic granular morphology, which is made up of alternating crystalline and amorphous layers. The size of starch granules varies from submicron to over 100 microns in diameter depending on the source of starch. Starch granules consist of two major compounds: amylose and amylopectin. Starches from corn (maize), rice and potato contain approximately 70 to 80 % amylopectin and 20 to 30 % amylose.<sup>71</sup> Amylose is primarily a linear polysaccharide which is made of D-anhydroglucose units linked together by  $\alpha$ -1,4-glycosidic linkages (Fig. 1.10A). On the other hand, amylopectin

is a highly branched polysaccharide with an  $\alpha$ -1,4-linked D-anhydroglucose main chain and many  $\alpha$ -1,6-linked branches (Fig. 1.10B).

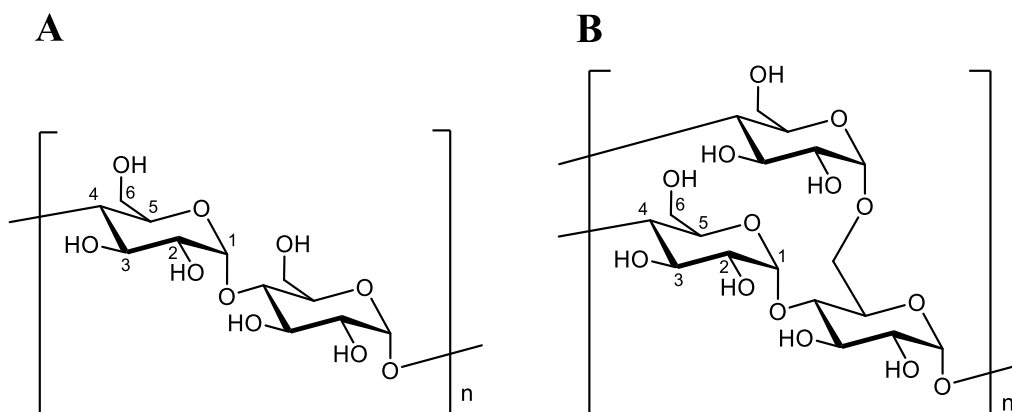


**Figure 1.10.** Chemical structures of amylose (A) and amylopectin (B).

Recently, Ju et al. reported the preparation of thermoresponsive 2-hydroxy-3-butoxypropyl starch (HBPS, Fig. 1.11A) and 2-hydroxy-3-isopropoxypropyl starch (HIPS, Fig. 1.11B) by reacting cooked food grade starch with butyl or isopropyl glycidyl ether under basic conditions.<sup>25,26</sup> HBPS with MS from 0.32 to 0.63 exhibit LCSTs from 32.5 °C to 4.5 °C, whereas HIPS with MS from 0.86 to 2.77 exhibit LCSTs ranging from 69 °C to 28 °C.<sup>25,26</sup> It was also demonstrated that the thermoresponsive HBPS formed micelles below its LCST, but insoluble aggregates were observed above the LCST.<sup>26</sup> Shortly thereafter, Ju and coworkers reported the synthesis of thermoresponsive 3-(2-butoxy(ethoxy)<sub>n</sub>)-2-hydroxypropyl starch ethers (BE<sub>n</sub>S), containing oligo(ethylene glycol) spacers of various lengths (n = 0, 1 or 2), by reacting degraded waxy maize starch with several hydrophobic reagents that differed in the length of the oligo(ethylene glycol) spacers (Fig. 1.11C).<sup>24</sup> BE<sub>n</sub>S exhibit a wide range of

LCSTs from 17.5 °C to 55 °C in response to a change in the length of oligo(ethylene glycol) groups and their molar substitution.<sup>24</sup>

In 2014, Yuan et al. have grafted dipropyl or dibutyl epoxypropylamine onto hydroxyethyl starch yielding pH and temperature responsive tertiary amine starch ether (TAS, Fig. 1.11D) with LCSTs ranging from 26 °C to 72.8 °C.<sup>23</sup> In 2017, Jong and Ju reported thermoresponsive 2-hydroxy-3-(2-propynyloxy) propyl hydroxyethyl starch (PyHES, Fig. 1.11E), obtained by reacting hydroxyethyl starch with 2-propynylglycidyl ether.<sup>22</sup>

In 2019, we described the preparation of thermoresponsive starch nanoparticles (SNPs) by treating SNPs with butene oxide in basic conditions.<sup>72</sup> The resulting hydroxybutyl SNPs (HB-SNPs, Fig. 1.11F) exhibit thermoresponsivity when the MS of the HB groups ( $MS_{HB}$ ) was greater than 1.<sup>72</sup> The LCST of the HB-SNPs could be tuned in a range from 52 °C to 33 °C by adjusting the  $MS_{HB}$  from 0.22 to 1.85.<sup>72</sup> Additionally, The LCST of the HB-SNPs could also be adjusted by varying the concentration of the HB-SNP dispersions and higher concentration resulted in a decrease in the LCST. The addition of salts and alcohols also greatly affected the LCSTs. By dynamic light scattering (DLS), the hydrodynamic diameter ( $D_h$ ) of the thermoresponsive HB-SNPs increased substantially from approximately 10 nm to greater than 200 nm as the dispersion temperature increased from below to above the LCST of the HB-SNPs, indicating the formation of large insoluble aggregates above the LCST. Thermoresponsive HB-SNPs were shown to contain HB oligomers on hydroxyl (OH) groups of the SNPs.

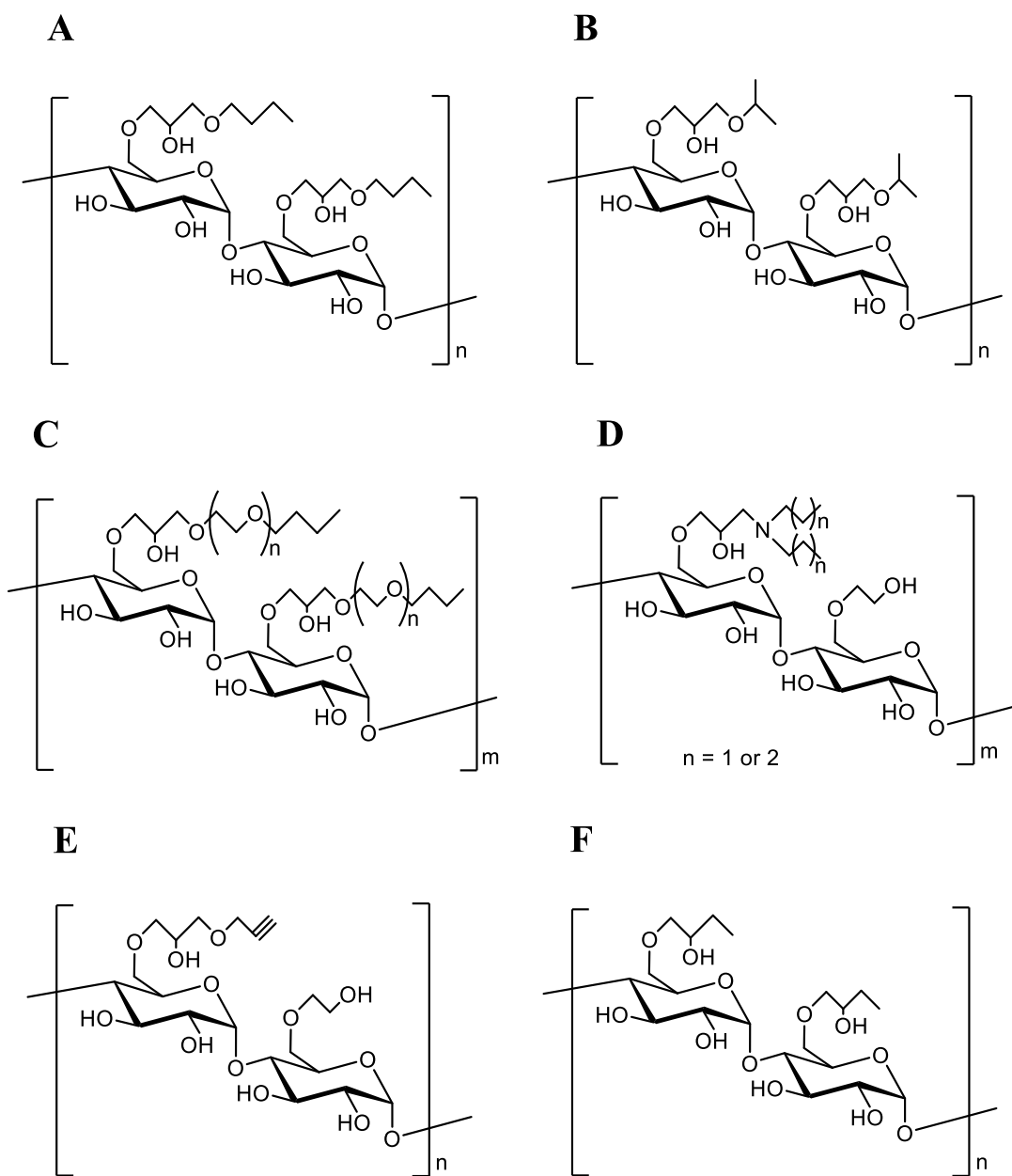


**Figure 1.11.** Chemical structures of HBPS (A), HIPS (B),  $BE_nS$  (C), TAS (D), PyHES (E) and HB-SNP (F). Substitution is shown only at O-6 while in fact substitution can occur at O-2, O-3 and O-6.

## **1.3 Oil Extraction from Oil Sands**

### **1.3.1 *In situ* Extraction Process**

*In situ* extraction technologies such as steam-assisted gravity drainage (SAGD) and cyclic steam stimulation (CSS) are commonly applied to extract bitumen from oil sands that are buried deep underground. Since bitumen in oil sands naturally has much higher viscosity than conventional crude oil, the bitumen reservoir must be heated to sufficiently reduce the viscosity of bitumen before being extracted from the ground. Generally, high pressure and high temperature steam is injected into oil sands deposits to heat up and liquify the bitumen. The emulsion of bitumen and condensed water is then collected and pumped to the surface and transported to downstream upgrading plants.<sup>73,74</sup> The *in situ* technologies typically have a high water recycling rate and do not produce tailings ponds. However, bitumen recovery is relatively low at about 35 to 60 %. Moreover, an enormous amount of energy is required to generate the steam, which generates relatively high emission of greenhouse gases.

### **1.3.2 Surface Mining Extraction Process**

Oil sands ores near the surface are amenable to surface mining and water-based extraction to recover bitumen. In the 1930s, the Clark hot water extraction (CHWE) process was developed by Clark and coworkers, and this process has been widely implemented by different commercial surface mining operations.<sup>75</sup> An overview of bitumen extraction in a surface mining operation is shown in Figure 1.12. Oil sands are first mined and transported to an ore preparation plant by haul trucks. Then, the lumps of raw oil sands are crushed down to smaller size in rotary breakers and mixed with warm water to produce a slurry. This slurry is

conditioned and fed to hydro-transport pipelines. At this stage, the typical operation temperature of the slurry is between 40 and 55 °C. In the pipelines, the ore size is further reduced, and the bitumen starts to liberate from sand grains as bitumen droplets which can attach to air bubbles and reduce the density of the bitumen droplets. The conditioned slurry is then pumped into a primary separation vessel, where the bitumen droplets can float to the top to form a primary froth and heavier coarse solids settle to the bottom to be discharged as primary tailings. Subsequently, the primary froth is pumped to de-aerators and froth treatment tanks, where the froth is screened and diluted with solvents such as naphtha and paraffin. The solvent diluted bitumen is finally sent for upgrading. The middling stream, which contains mainly fine solids and residual bitumen in the primary separation vessel, is further treated in flotation cells for secondary bitumen recovery. The remaining fine solids and the primary tailings are treated and discharged into a tailings pond for dewatering before the process water can be recycled for subsequent extractions.

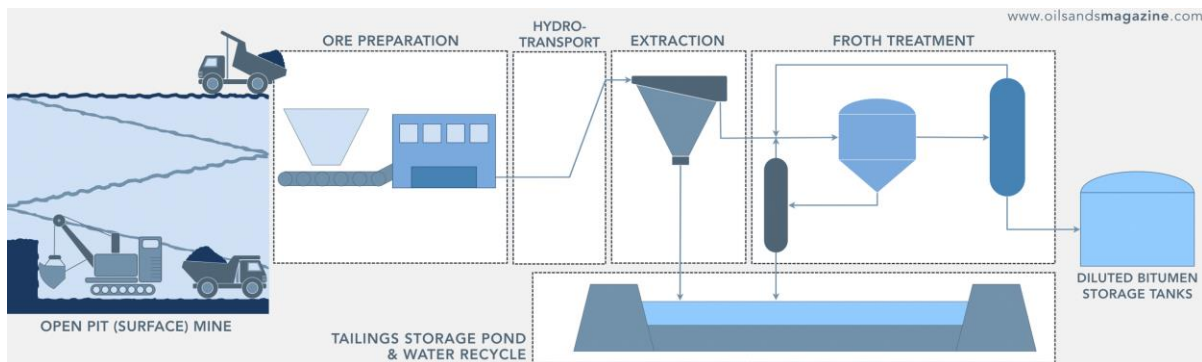


**Figure 1.12.** An overview of surface mining operation. This picture was obtained online from [www.oilsandsmagazine.com](http://www.oilsandsmagazine.com) with permission.

### 1.3.3 Key Aspects in Water-based Bitumen Extraction Process

#### 1.3.3.1 General Properties of Oil Sands Ores

A typical composition of mineable oil sands ore is 7-12 % bitumen, 4-7 % innate water, and 84 % minerals by mass. Oil sands ores with a bitumen content higher than 10 wt % and a low clay content are referred to as good processing ores.<sup>76</sup> Conversely, oil sands ores with low bitumen and high clay content are referred to as poor processing ores. The CHWE process performs well with good processing ores, while poor processing ores only yield poor bitumen recovery using this process.<sup>76</sup> A microstructure of oil sands ores has been proposed by Takamura in the early 1980s (Fig. 1.13).<sup>77</sup> It is widely accepted that a thin film of water is sandwiched between the interfaces of sand grains and bitumen.<sup>78</sup> The film of water with a thickness of approximately 10 nm is stabilized by electrostatic forces arising from electrical double layers at the water-oil and water-sand grain interfaces. This hydrophilic nature of the oil sands enhances bitumen recovery in the water-based extractions.<sup>78</sup>

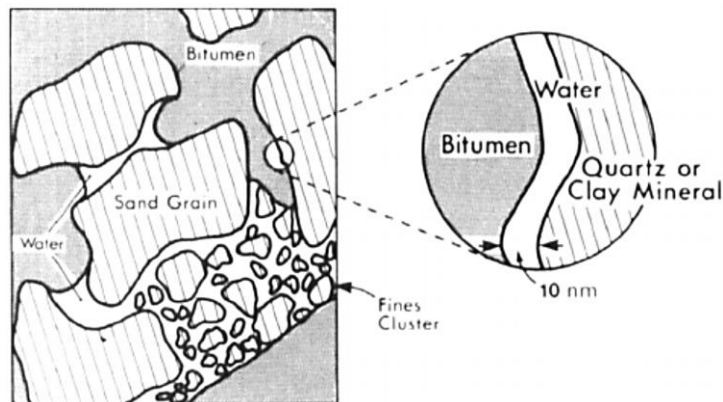


**Figure 1.13.** Schematic diagram showing the proposed microstructure of Athabasca oil sands. Picture was taken with permission.<sup>77</sup>

### 1.3.3.2 Bitumen Recession and Liberation

The recovery of bitumen begins with bitumen recession on the sand grains and liberation from the sand grains. Bitumen recession refers to the process of decreasing the contact area between the film of bitumen and sand grains to eventually form bitumen droplets, and bitumen liberation is defined as the detachment of the bitumen droplets from the sand grains to the aqueous phase (Fig. 1.14). In a typical extraction operation, chemical aids such as caustics are added to facilitate the recession and liberation processes, in that the surface of sand grains is hydrolyzed in alkaline conditions and becomes more hydrophilic. As the surface of sand grains becomes more hydrophilic, the affinity of the sand grain surface for bitumen decreases. Hence, the contact area between the bitumen and the sand grains surface decreases and the bitumen recesses to bitumen droplets, which is eventually liberated from the sand grains (Fig. 1.14A). Other than the addition of chemical aids, the recession and liberation processes are influenced by the processing temperature, shear rate and interfacial properties.<sup>79</sup>

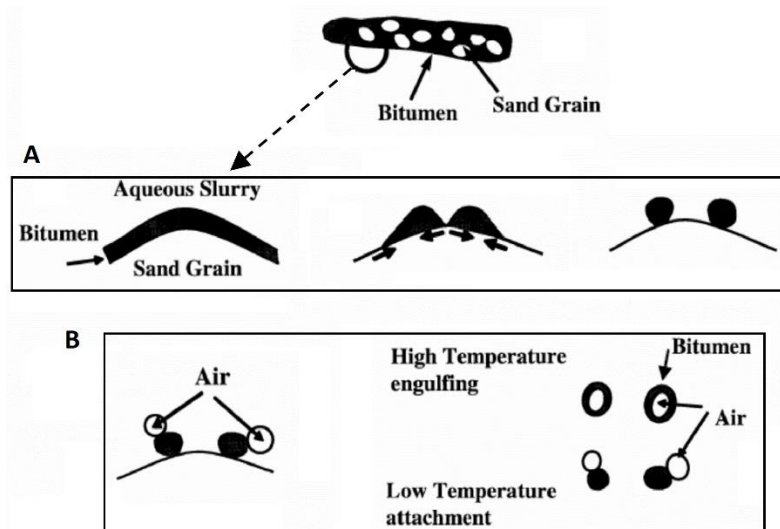


**Figure 1.14.** Schematic representation of bitumen recession and liberation (A), and aeration and flotation (B). The pictures were adapted from Masliyah et al. with permission.<sup>80</sup>



### **1.3.3.3 Aeration and Flotation of Bitumen**

Aeration and flotation are important processes in bitumen extraction, which generally occur in hydrotransport pipelines, separation vessels and flotation cells. After the bitumen droplets are liberated from the sand grains, they are often suspended in the aqueous phase, as their density is similar to that of water. To reduce the density of the bitumen droplets, air bubbles are introduced in the extraction process. As bitumen is inherently hydrophobic, the air bubbles tend to attach to the suspended bitumen droplets, which produces relatively low-density bitumen-air bubble complexes (Fig. 1.14B). At a temperature below 35 °C, air bubbles weakly attach to the surface of bitumen droplets.<sup>80</sup> However, at a temperature above 45 °C, bitumen has a low viscosity resulting in the spreading of bitumen onto the surface of air bubbles and engulfing the air bubbles. The engulfment of air bubbles dominates during the aeration step in a hot/warm water extraction process. The aerated bitumen floats to the top of the aqueous phase in a separation vessel and eventually forms a layer of bitumen-rich froth. The froth from the primary separation vessel in a typical oil sands operation consists of approximately 66 wt % bitumen, 25 wt % water and 9 wt % solids.<sup>81</sup>

### **1.3.4 Factors Affecting Bitumen Extraction from Oil Sands**

Bitumen recovery is affected by a number of factors that can be generally grouped into three categories: the oil sands ore properties, the extraction conditions, and the water chemistry of the extraction mixture. Ore properties such as the bitumen content, fines content and types, wettability, aging/weathering of ores are key factors to be considered. Operating conditions such as the processing temperature, air injection, shear rate and mechanical mixing time greatly

affect bitumen recovery as well. Moreover, it is also important to investigate water chemistry in an aqueous extraction mixture such as the pH, valence and concentration of ions, types and concentration of surfactants and carbonates naturally present in oil sand ores, and chemical aids introduced during bitumen extraction.

#### **1.3.4.1 Effect of Processing Temperature**

Since the establishment of the first commercial surface mining operation in the 1960s, the CHWE process has been adopted and initially required a processing temperature higher than 70 °C. Many efforts have been made to reduce the processing temperature in order to cut down energy costs and greenhouse gas emissions. Starting in the 2000s, the majority of the commercial oil sands operations have adopted a lower processing temperature around 35 to 50 °C.

As shown in many laboratory extraction tests, the processing temperature plays an important role in bitumen recovery in that the processing temperature greatly affects bitumen liberation, aeration and flotation.<sup>82</sup> Masliyah et al. reported that the bitumen can be liberated at a significantly faster rate at 50 °C than at 35 °C.<sup>80</sup> Zhou et al. also reported a faster bitumen recovery rate when extractions were conducted at 50 and 80 °C as compared to at 25 °C.<sup>83</sup> Long et al. concluded that the rate of bitumen recovery from oil sands was significantly lower at an operating temperature below 35 °C, and the effect of the operating temperature on bitumen recovery was negligible above 50 °C (Fig. 1.15).<sup>82</sup>

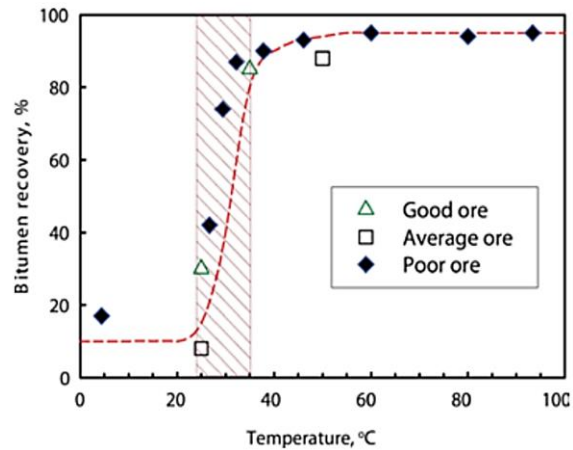


**Figure 1.15.** Effect of processing temperature on bitumen recovery in laboratory scale oil sands exactions. Figure was taken with permission.<sup>82</sup>

#### 1.3.4.2 Effect of Air Bubbles

The availability of air bubbles in an oil sand-water slurry during the conditioning and flotation processes is an important factor for high-recovery extractions. The availability of air depends on the amount of indigenous air (i.e. air entrapped in oil sand ores), dissolved air in the slurry, air entrained into the slurry by stirring, and injected air during the processes. Wallwork et al. showed that air injection significantly improved bitumen recovery at low processing temperatures, and bitumen recovery increased with increasing amounts of injected air (Fig. 1.16).<sup>84</sup> Flynn et al. and Sanders et al. also reported that bitumen recovery improved with the addition of air.<sup>85,86</sup> Moreover, it is widely accepted that small air bubbles, with the same or smaller size compared to the size of bitumen droplets, are able to attach themselves to the bitumen droplets more effectively than large air bubbles, and the small air bubbles usually lead to more efficient aeration and flotation of the bitumen droplets.<sup>87-89</sup> Sanders et al. suggested that an insufficient amount of air bubbles in an oil sands slurry resulted in an

ineffective flotation process and low bitumen recovery when the extractions were conducted in a laboratory-scale pipeline loop.<sup>86</sup>

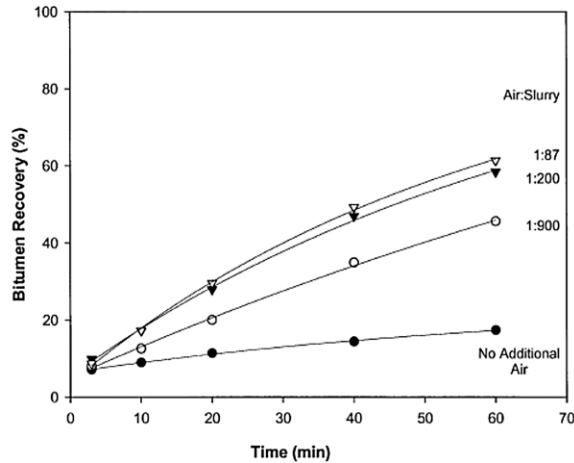


**Figure 1.16.** The effect of the air to slurry ratio by volume (Air:Slurry) on bitumen recovery over extraction time in a laboratory scale oil sands extraction process at 35 °C. Figure was taken with permission.<sup>84</sup>

### 1.3.4.3 Effect of Aging/Weathering of Ores

Aging or weathering of oil sands ores often leads to deteriorated extractability of bitumen. Aging is referred to as natural or laboratory processes that degrade oil sands ores, and such processes include dehydration, oxidation of inorganics and evaporation of light hydrocarbons. Ren et al. studied the effect of aging on the processability of oil sands ores, and found that the deteriorated processability of the aged ores was a consequence of the decreased the wettability of the aged ores as well as the increased attractive interactions between bitumen and the hydrophobic ore surface.<sup>90-92</sup> It was proposed that the loss of innate water, which was responsible for separating the surfaces of mineral solids and bitumen, could result in an intimate contact of bitumen, with strong bitumen adsorption on the mineral solids, leading to a difficult bitumen liberation process for the aged oil sands ores.<sup>90</sup>

#### **1.3.4.4 Effect of Clays and Divalent Cations**

The presence of clays is detrimental to the aeration and flotation processes. Slime coating is a phenomenon describing the coverage of bitumen by fines/clays. Liu et al. reported that the slime coating of montmorillonite on bitumen droplets significantly deteriorated bitumen recovery in the presence of calcium and magnesium ions.<sup>93</sup> Moran et al. also reported that montmorillonite and illite strongly interact with bitumen, which can hinder bitumen-air bubbles attachment, while kaolinite only interacts weakly with the bitumen surface.<sup>94</sup> Gu et al. suggested that divalent cations can bridge between bitumen and clays, and the clay coated bitumen surfaces become more hydrophilic which makes the attachment of air bubbles more difficult.<sup>95</sup> Wallace et al. also showed that the adsorption of clays onto bitumen droplets (i.e. slime coating) greatly impaired the floatation of bitumen (Fig. 1.17), leading to a poor froth formation.<sup>96</sup> It is widely accepted that increasing the pH of an oil sands slurry and elimination of divalent cations can effectively minimize bitumen-clay interactions and improve bitumen recovery.

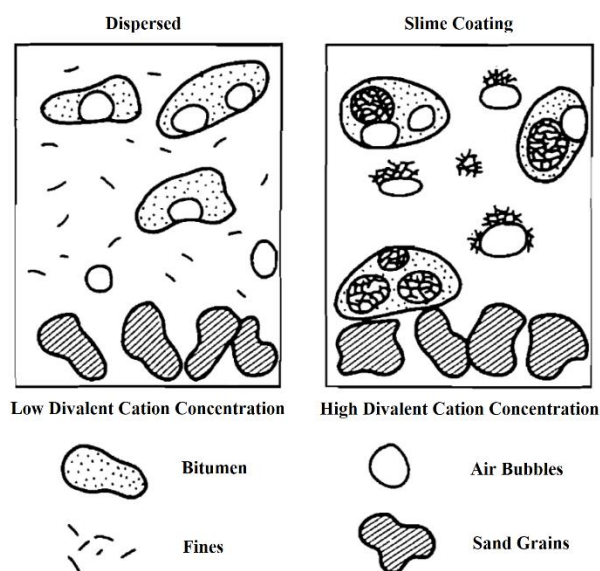


**Figure 1.17.** Schematic representation of slime coating of bitumen droplets in an oil sands slurry in response to divalent cationic concentration. This picture was adapted from Wallace et al. with permission.<sup>96</sup>

### 1.3.5 Chemical Aids for Bitumen Extraction of Oil Sands

Processing aids are often required in the oil sands extraction process to improve bitumen recovery, and they are particularly important for low temperature extractions or extractions of poor processing ores. Processing aids can be categorized into three groups: inorganic metal salts, organic solvents and polymeric aids.

#### 1.3.5.1 Inorganic Chemical Aids

Caustics are the most widely used inorganic chemical additives to enhance bitumen liberation and bitumen recovery. NaOH, a typical caustic, can enhance bitumen liberation by increasing the pH of an oil sands slurry and deprotonating natural surfactants, which facilitates the release of natural surfactants from oil sands ores.<sup>97</sup> The ionized surfactants become more surface active and reduce the interfacial tension between bitumen droplets and water, hence,

improving bitumen liberation. Moreover, NaOH increases the wettability of sand grains by hydrolyzing the surface of the sand grains, which facilitates the detachment of bitumen from the sand grains. However, the addition of NaOH makes the attachment of bitumen droplets to air bubbles more difficult, which is detrimental to bitumen aeration.

CaO or Ca(OH)<sub>2</sub> (also known as lime) was reported to also enhance bitumen recovery.<sup>98</sup> Lime promotes the release of asphaltic acids acting as surfactants, which reduces the concentration of divalent ions in the slurry and eliminates the attachment of clays to bitumen droplets. This promotes the attachment of bitumen droplets to air bubbles, thereby enhancing bitumen recovery. Flury et al. reported that the use of ammonium hydroxide (NH<sub>4</sub>OH) led to a higher bitumen recovery than the use of NaOH, especially at a high slurry pH.<sup>97</sup> Li et al. deployed acidified sodium silicates to increase flotation rate and improve bitumen recovery in bitumen extractions from poor processing ores.<sup>99</sup> The acidified sodium silicates were used as a depressant of clay particles in the slurry, which also precipitates divalent cations and promotes bitumen aeration.

### **1.3.5.2 Liquid Hydrocarbons and Organic Solvents**

In 1990, Sury patented a cold-water extraction process with the addition of a mixture of kerosene and methyl isobutyl carbinol (MIBC).<sup>100</sup> Kerosene tends to spread on the surface of bitumen and leads to the formation of a thin coating which enhances bitumen attachment to air bubbles. MIBC, commonly used as a froth agent in mineral flotation, promotes the formation of stable air bubbles. Later in 1999, Allcock et al. also reported a warm water extraction process using kerosene and MIBC to recover bitumen from low processing ores and

achieved a high bitumen recovery of 91 %.<sup>101</sup> In 2012, Hooshiar et al. employed a composite solvent consisting of toluene and heptane in a non-aqueous bitumen extraction process to extract bitumen from oil sands ores with high fine contents and achieved a recovery of close to 70 %.<sup>102</sup> Li et al. also reported that a solvent mixture of heptane and toluene (3:1 v/v) was able to effectively extract bitumen from oil sands with bitumen recoveries ranging from 63 to 87 % depending on experimental conditions such as solvent-to-oil sands ratio, stirring rate, solvent-bitumen contact time and extraction temperature.<sup>103</sup> In 2012, Yang et al. described a hybrid extraction process using a mixture of water and solvents such as petroleum ether, naphtha, cyclohexane and toluene to achieve bitumen recoveries of 67 %, 74 %, 85 % and 95 %, respectively.<sup>104</sup> Shortly after, a similar aqueous and non-aqueous hybrid process for bitumen extraction was reported by Harjai et al.<sup>105</sup> In their process, diluents such as kerosene and naphtha were added to oil sands ores prior to preparation of an oil sands slurry, and resulted in a decrease in bitumen viscosity and an improved bitumen liberation process. In 2014, Wang et al. conducted comprehensive studies on solvent extractions of bitumen from aged oil sands ores using a series of solvents and among the investigated solvents, *o*-xylene, toluene, methyl ethyl ketone, chloroform and trichloroethylene showed excellent bitumen recovery at approximately 75 % (Fig. 1.18).<sup>106</sup>



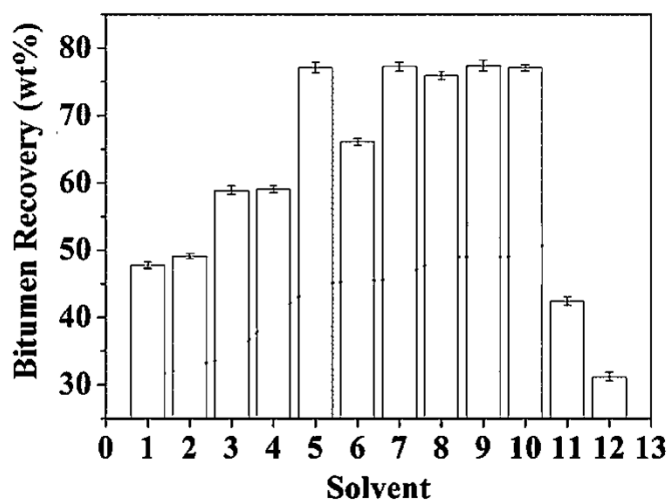


**Figure 1.18.** Bitumen recoveries of different solvents for oil sands extractions. Solvents used include: n-pentane (1), n-hexane (2), n-heptane (3), cyclohexane (4), *o*-xylene (5), ethyl acetate (6), toluene (7), methyl ethyl ketone (8), chloroform (9), trichloroethylene (10), acetone (11) and ethanol (12). Figure was adapted from Wang et al. with permission.<sup>106</sup>

### 1.3.5.3 Polymeric Processing Aids

Polymers are also used as processing aids to enhance bitumen recovery, particularly for bitumen extraction from poor processing ores. In 2005, Li et al. presented a study on the synergetic effect of anionic hydrolyzed PAM on both bitumen extraction and treatment of tailings.<sup>107</sup> They reported that the addition of 30 ppm of the hydrolyzed PAM in the extraction of bitumen from poor processing ores resulted in an optimized bitumen recovery of more than 80 %, which was 20 % higher compared to the extractions without the addition of polymers. In 2008, the same group of researchers synthesized a hybrid Al(OH)<sub>3</sub>-PAM which was used in combination with a hydrolyzed PAM to extract bitumen from poor processing ores.<sup>108</sup> A combination of 5 ppm of Al(OH)<sub>3</sub>-PAM and 15 ppm of the hydrolyzed PAM was used to achieve an optimal bitumen recovery of 86 %. In 2011, Long et al. deployed a thermoresponsive polymer, PNIPAM, in bitumen extraction from poor processing ores and

found that when the flotation process was conducted at 40 °C (above the LCST of PNIPAM) after slurry conditioning at room temperature, the addition of PNIPAM enhanced bitumen recovery and promoted flocculation of tailings.<sup>109</sup> In 2015, Yang and Duhamel prepared several thermoresponsive block copolymers consisting of PEG and poly(2-(2-methoxyethoxy) ethyl methacrylate) (PMEO<sub>2</sub>MA) with an LCST of 35 °C and showed that with the addition of 65 mg of toluene and 1 g/L of PEG-*b*-PMEO<sub>2</sub>MA, a 100 % extraction recovery was obtained.<sup>10</sup> The block copolymer-containing aqueous solution could be recycled up to five times while still maintaining a satisfactory bitumen recovery. Lin et al. investigated the effect of ethyl cellulose as a demulsifier along with a diluent, toluene, on bitumen recovery and froth quality in a low temperature aqueous and solvent hybrid extraction process.<sup>110</sup> The addition of 100-200 ppm of ethyl cellulose clearly showed a significant improvement in froth quality with a negligible effect on bitumen recovery.

## **1.4 Flocculation of Mature Fine Tailings**

### **1.4.1 Current Industrial Practices for Tailings Management**

As mentioned in Section 1.3.2, the tailings collected from the extraction plant and from froth treatment are collectively discharged into a large settling basin, which is commonly referred to a tailings pond (Fig. 1.19).

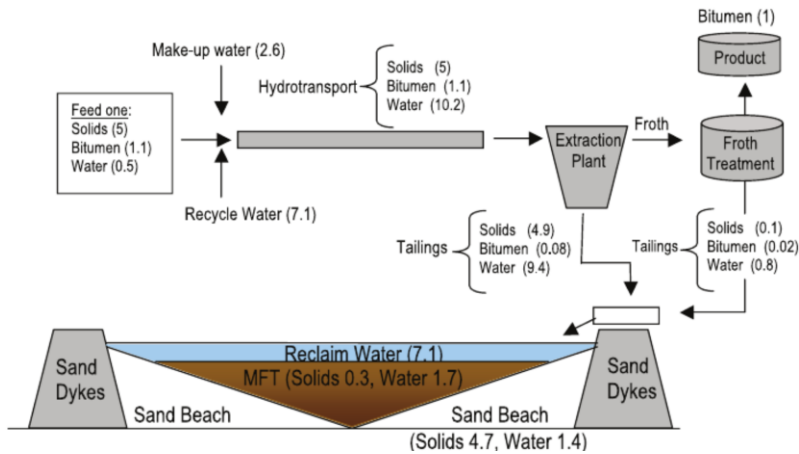


**Figure 1.19.** Schematic diagram showing conventional oil sands tailings management. Numbers in parenthesis represents the relative volume of components per  $\text{m}^3$  of bitumen produced. This diagram was adapted from Vedoy and Soares with permission.<sup>2</sup>

Dewatering technologies for tailings management, aiming to enhance the settling rate of fine solids, to increase solids content and to recover the maximum amount of recyclable water, have been an important subject to be studied in the past few decades. Composite tailings (CT) and paste tailings (PT) are the primary technologies that are employed in commercial-scale operations for tailings treatment.

#### 1.4.1.1 Composite Tailings Technology

Composite tailings (CT) (also referred to consolidated tailings) technology, being employed by Syncrude, Suncor and Canadian Natural, involves the addition of a coagulant, calcium sulfate (also known as gypsum), to a tailings slurry comprising of MFT from tailings ponds and fresh tailings from the extraction process. The mixture is then transferred to a settling basin, where the sediment consolidates to a homogeneous deposit in less than a month. This consolidated deposit allows relatively rapid reclamation to finally obtain a trafficable

deposit. Moreover, clear water is released from the CT deposit in a relatively short period of time instead of decades for untreated MFT. The CT process is relatively effective and low cost, however, the use of gypsum results in a high dose of divalent ions in the released water, which has a detrimental effect on the recovery of bitumen extraction and significantly impedes the reuse of the released water.

#### **1.4.1.2 Paste Tailings Technology**

Paste tailings (PT) technology is an effective solution to rapidly consolidate fresh tailings, which is mainly employed by Shell Albian Sands. In the PT process, polymeric flocculants, based on anionic PAM with high molecular weight, are used to flocculate fresh tailings from the extraction process to achieve a fast settling rate. The thickened tailings have solids content of about 30-40 wt %, and without the flocculants, it would take years for the fresh tailings to achieve such solids content. Moreover, the warm process water can be readily recycled back to the extraction process due to the rapid settling rate by the use of the flocculants, hence, the decrease in the temperature of the recycled process water is minimized such that energy cost and greenhouse gas emission can be reduced. However, the PT process does not deal with the legacy MFT. In addition, the thickened tailings require additional tailings treatments such as centrifugation to further increase the solids content of the tailings and to release more entrapped water.

#### **1.4.2 Mature Fine Tailings Composition**

Typically, MFT contains about 30-40 wt % solids, 1-3 wt % residual bitumen and water to make up the rest. Over 90 wt % of the MFT solids are fines/clays with size under 44  $\mu\text{m}$  in

diameter.<sup>111</sup> The major clay components of MFT are 40-70 wt % kaolinite, 28-45 wt % illite and 1-15 wt % montmorillonite, and a small amount of smectite can often be found.<sup>112</sup> It has been widely accepted that clays, due to their small particle size, high surface areas and negatively charged surfaces, are responsible for water retention and viscoelastic properties of MFT.<sup>111</sup>

### **1.4.3 Clay Mineralogy**

Clay particles are composed of tetrahedral sheets of silicon-oxygen and octahedral sheets of magnesium- or aluminum-oxygen (Fig. 1.20). Different types of clays can display different arrangements of the tetrahedral and octahedral sheets. For example, kaolinite is two-layered clay particles which have a unit layer of one tetrahedral sheet and one octahedral sheet stacking together by van der Waals force and hydrogen bonds (Fig. 1.21A). Illite and montmorillonite are three-layered clay particles that have a unit layer of one octahedral sheet sandwiched between two tetrahedral sheets (Fig. 1.21B). Typically, clay particles carry permanent negative charges arising from isomorphic substitution which occurs when a tetravalent silicon ion is replaced by a trivalent aluminum ion in tetrahedra sheets or when a trivalent aluminum ion is replaced by a divalent magnesium ion in octahedra sheets. As MFT contains mostly clay, negative charges on the clay particles are responsible for colloidal stabilization.

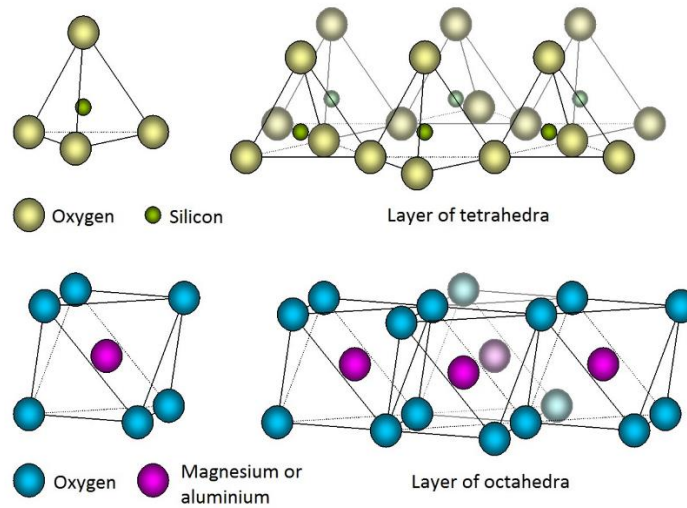


**Figure 1.20.** Tetrahedra and octahedra sheets of unit layer of clay. Figure was taken with permission from Antonio Jordán from blogs.egu.eu.

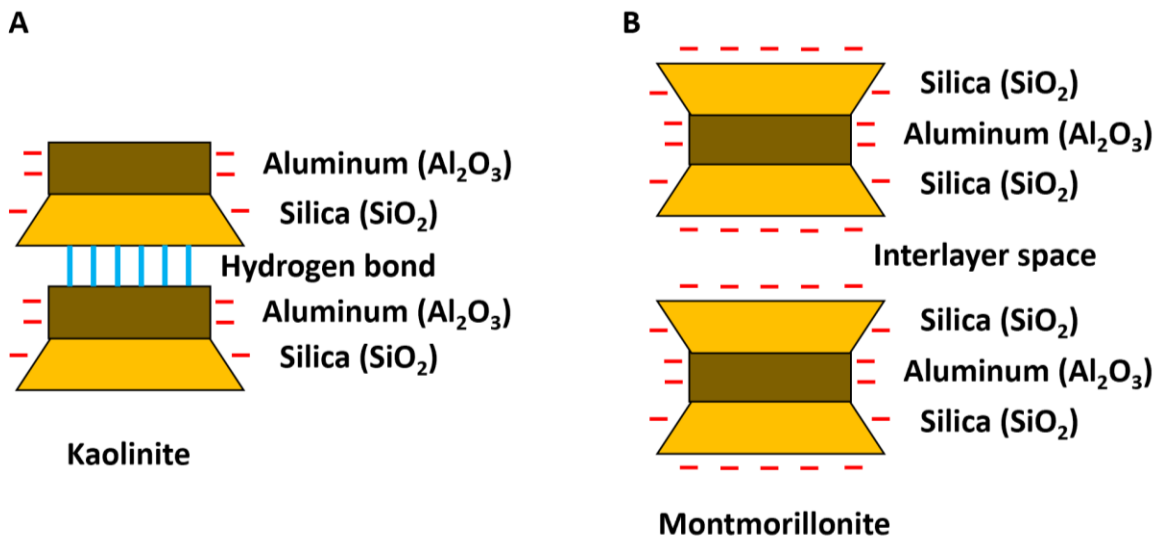


**Figure 1.21.** Layer structures of kaolinite (A) and montmorillonite (B).

#### 1.4.4 Electrical Double Layer

In a colloidal system, the behavior of clay particles is strongly influenced by the electrical charges on the particle surface. A double layer model is often used to explain the

presence of electrical repulsive force of a negatively charged clay particle in an ionic environment (Fig. 1.22). In this model, counter-ions (i.e. oppositely charged ions) are attracted towards the negatively charged particle surface which creates a layer of counter-ions (known as the Stern layer) resulting in an electrical potential known as the Stern potential. A second layer, where the counter-ion concentration is higher than that of co-ions, between the Stern layer and the bulk phase is referred to a diffuse layer. The potential is the highest at the particle surface and decreases exponentially with increasing distance from the surface, and eventually approaches zero outside of the diffuse layer. The potential between the Stern layer and the diffuse layer is called zeta potential, which determines the repulsive force between two particles and the stability of the particle dispersion.

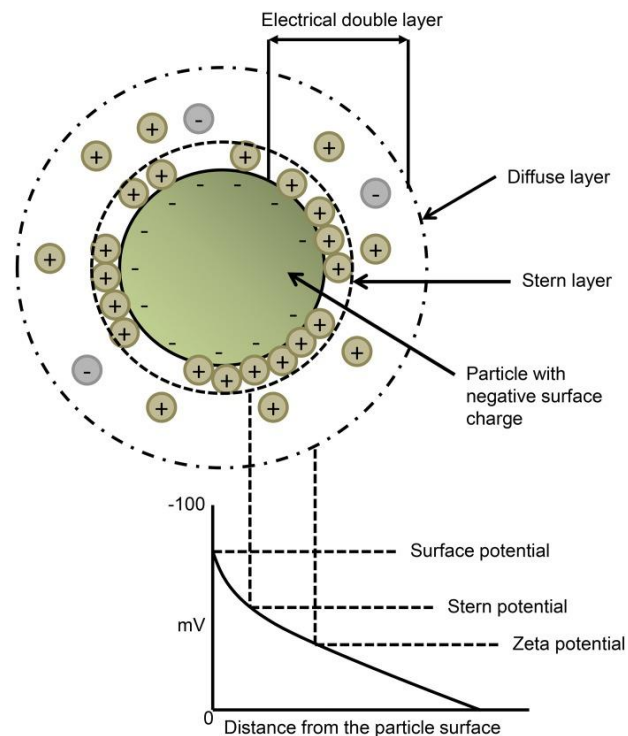


**Figure 1.22.** Schematic representation of electrical double layer of a colloidal particle and its potential is shown as a function of distance from the particle surface. This picture was adapted from Yingchoncharoen et al. with permission.<sup>113</sup>

### 1.4.5 Colloidal Stability and the DLVO Theory

In a suspension, the stability of colloidal particles is determined by interfacial interactions resulting from both electrostatic repulsive and van der Waals attractive forces. The DLVO theory, which is named after Derjaguin, Landau, Verwey, and Overbeek, is often used to describe the stability of colloidal particles. Figure 1.23 illustrates the interfacial potentials of two charged particles approaching each other in a suspension. As the two particles approach each other, the net interaction potential increases to a maximum potential energy (known as energy barrier). When the thermal kinetic energy is below the energy barrier, the net interaction potential is repulsive, hence, the particles repel each other giving a stable suspension. On the contrary, if the energy barrier is overcome, van der Waals attraction dominates as the particles approach each other and as a result, the particles aggregate, and the suspension becomes unstable. Moreover, the energy barrier can be reduced by neutralization of surface charges through the addition of an appropriate amount of counter ions or by bridging via large molecules such as a polymeric flocculant.



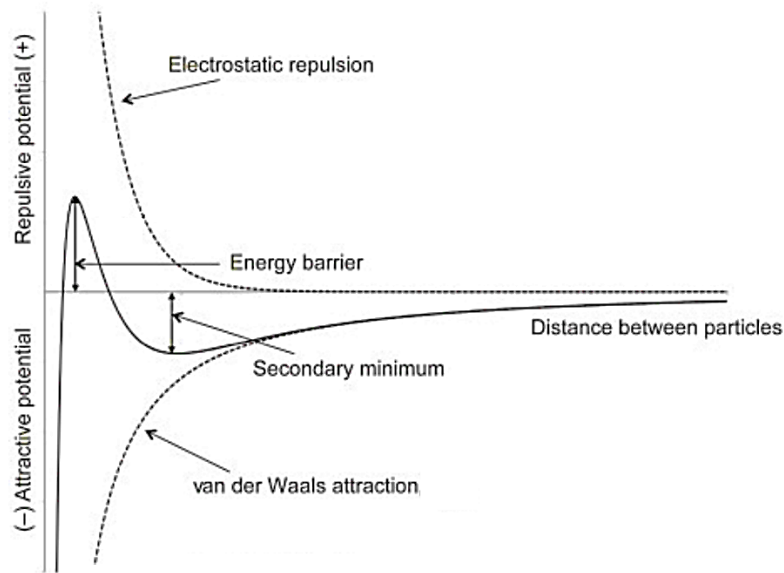


**Figure 1.23.** Plot of interparticle potentials as a function of distance between the charged surfaces of two particles. This picture was adapted from Gelardi and Flatt with permission.<sup>114</sup>

### 1.4.6 Coagulation

Coagulation describes a process by which coagulants with an opposite charge, such as gypsum in the composite tailings process, are added to neutralize surface charges in a colloidal suspension. To elaborate, with the addition of coagulants, the surface charges are neutralized, and the charges may also be locally reversed (Fig. 1.24A). The electrostatic repulsion is greatly reduced, and the interaction may become attractive when a particle encounters another particle with partially reversed charges. As a result, the energy barrier of aggregation is drastically reduced, and the colloidal suspension becomes unstable. Coagulation usually leads to small and loosely bound flocs which are relatively fragile when compared to the flocs formed by flocculation.

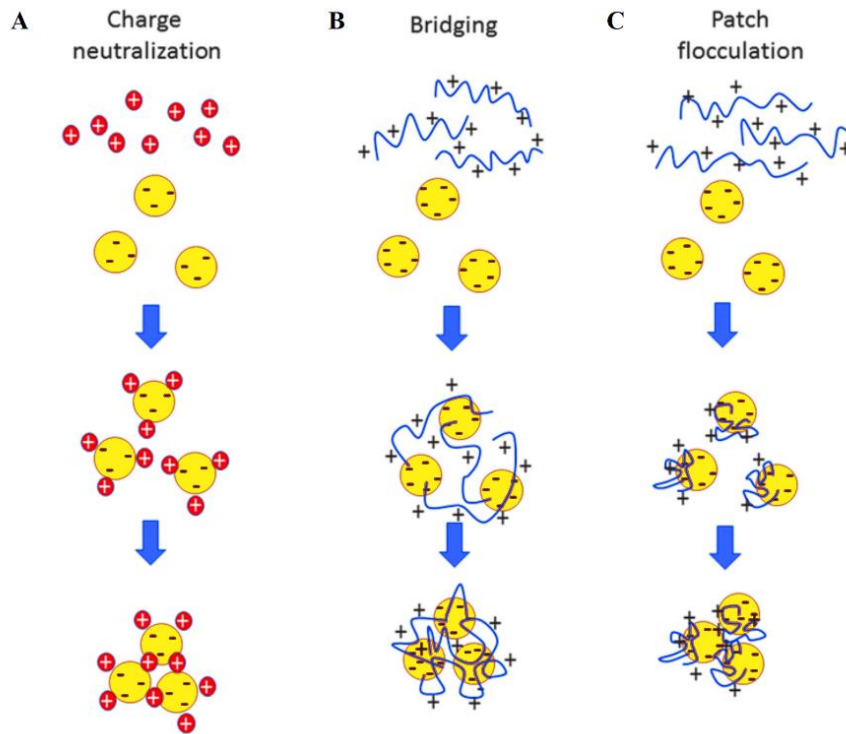


**Figure 1.24.** Graphical representation of charge neutralization (A), bridging (B) and electrostatic patch (C) mechanism.

### 1.4.7 Flocculation

Flocculation is a process by which particles or small aggregates formed by coagulation are brought together by bridging with polymeric flocculants to form larger aggregates known as flocs. Bridging requires sufficient polymers adsorption onto the surface of colloidal particles. The polymers typically have a high molecular weight so that the polymer chains are capable of spanning the gap (i.e. double layer barrier) between the particles to minimize the electrostatic repulsion (Fig. 1.24B). The adsorption of polymer to particles is mainly by hydrogen bonding and electrostatic interactions. Moreover, when a cationic flocculant or an anionic flocculant with a coagulant is added to a colloidal system with negatively charged

particles, the charged polymers create highly charged patches on the surface of the particles upon their adsorption onto the particles. The particles with the charged patches interact with each other and with the flocculant and free particles in the colloidal system to produce large and stable flocs resulting in a destabilized suspension (Fig. 1.24C).

An important factor that can affect the effectiveness of bridging and electrostatic patch flocculation is flocculant dose. Optimal dose is reached when half of the particle surfaces are covered by the flocculants. An excess polymer dose leads to excessive polymer coverage on the particle surfaces and few available sites for interparticle interaction. Consequently, the particles are re-stabilized by the adsorbed polymer which provides steric stabilization. On the other hand, insufficient flocculant dose leads to inadequate interparticle interaction between the colloidal particles, hence, impeding the formation of flocs.

Agitation also plays an important role in flocculation. Insufficient agitation may cause local overdose which results in poor flocculation performance. However, excessive agitation may cause the formation of small flocs due to floc breakage, thus, an optimal agitation rate is desirable during a flocculation process.

Polymers with higher molecular weight often perform better as flocculants. The flocculants with higher molecular weight may increase particle radius, which in turn improve collision efficiency and settling rate.<sup>115</sup> Polymer structure also affects flocculation in that more branched polymers often provide greater surface area for particle adsorption.

### **1.4.8 Previous Studies on Flocculation of Oil Sands Fine Tailings**

The challenge posed by the legacy as well as accumulating MFT is a major problem for oil sands operations. It has been an ongoing goal to improve settling rate and consolidation of fresh tailings and MFT in an economical and environmentally friendly manner for better tailings management. There have been numerous reports in the literature regarding flocculation studies using existing flocculants, which are effective for other types of wastewater such as tailings from mineral mining, as well as novel flocculants being developed towards consolidation and dewatering of fresh tailings and MFT.

#### **1.4.8.1 Poly(acrylamide)-based Flocculants**

Non-ionic poly(acrylamide) (PAM) is rarely an effective flocculant due to the lack of ionic charge and therefore inadequate polymer-particle interactions.<sup>116</sup> In 1999, Cymerman et al. reported that the use of high molecular weight, anionic PAM (Magnafloc 1011) with medium charge density was capable of flocculating fresh tailings.<sup>117</sup> A fast settling rate was observed but the supernatant contained about 1.5 wt % solids which was highly turbid. Shortly after in 2000, Sworska et al. reported that anionic PAM with a charge density of 25 % showed good flocculation performance for Syncrude fine tailings (fresh tailing from the extraction process), especially when divalent cations such as  $\text{Ca}^{2+}$  and  $\text{Mg}^{2+}$  were introduced.<sup>118</sup> It was suggested that the divalent cations are responsible for bridging the anionic polymer chains and negatively charged clay particle surfaces. This hypothesis was also supported by Long et al.<sup>119</sup> Sworska et al. also reported that adequate mixing (at 200 revolutions per minute, rpm) allows complete distribution of the polymer in the Syncrude fine tailings which results in good

flocculation at a relatively low dose (10 ppm).<sup>120</sup> In 2008, Li et al. reported the flocculation of fresh tailings produced from a laboratory extraction system when 20 ppm of partially hydrolyzed PAMs (HPAM) with various molecular weight from 0.01 to 40 million Daltons (MDa) were used in the extraction system.<sup>121</sup> The researchers found out that the addition of the high molecular weight HPAM (> 17.5 MDa) produced a clear supernatant after the settling of the fresh tailings for 24 h, while no flocculation was observed for the fresh tailings with the low molecular weight HPAMs (< 1 MDa).<sup>121</sup> Anionic PAM was reported to be ineffective in flocculating MFT due to the inadequate distribution of the polymer in MFT as MFT has a high solids content of greater than 30 wt %.<sup>2</sup> However, once MFT was diluted to 10 wt % or below, the anionic PAM became quite effective.<sup>122</sup> Alamgir et al. reported that an initial setting rate (ISR) of 8.8 m/h, supernatant turbidity (ST) of 156 NTU and sediment solids content (SSC) of 30 wt % were achieved when 100 ppm of Magnafloc 1011 (a commercial anionic PAM) were used to flocculate 10 wt % MFT.<sup>122</sup> In 2018, Strandman et al. also showed that good flocculation results were obtained by treating 5 wt % MFT with a series of in-house synthesized anionic PAM.<sup>123</sup>

Cationic PAM has been used in the flocculation of oil sands tailings to avoid the need of divalent cations. In 2006, Zhou and Franks discussed the effect of cationicity of PAM on flocculation of a silica suspension as a modeling system for oil sands tailings and suggested that the flocculation mechanisms are bridging, a combination of charge neutralization and bridging or electrostatic patch flocculation when PAMs with low (10 %), medium (40 %) or high (100 %) cationicity were used.<sup>124,125</sup> Later in 2009, Wang et al. showed that a cationic copolymer of acrylamide and acryloylamino-2-hydroxypropyl trimethyl ammonium chloride

effectively flocculated a kaolinite clay suspension at a low pH.<sup>126</sup> Recently, Wang et al. introduced a method to use commercial cationic PAM (Zetag 8110) in the flocculation of 5 wt % MFT.<sup>127</sup> In their method, preconditioning of a Zetag 8110 dispersion (1.5 kg/t) by hydrolyzing at 70 °C for 16 h at pH of 8.5 prior to be used in settling tests was necessary to achieve an effective flocculation and to obtain a supernatant of less than 200 nephelometric turbidity unit (NTU). In 2017, Vajihinejad et al. synthesized a series of poly(acrylamide-co-diallyldimethylammonium chloride) polymers with different compositions and molecular weights and found that both the composition and the molecular weights were important for their flocculation performance on 5 wt % MFTs.<sup>128</sup> Cationic PAM often shows promising flocculation ability; however, the associated high cost prevents its commercial applications.

Inorganic-organic hybrid flocculants often show superior flocculation efficiency due to the synergistic effect of the two components in the hybrid flocculants. In 2004, Yang et al. synthesized a hybrid flocculant, aluminum hydroxide-PAM (Al-PAM), and showed that this hybrid flocculant was more effective than PAM and the PAM/aluminum chloride blend when tested with a 0.25 wt % kaolinite clay suspension as modeling tailings.<sup>129</sup> Later in 2008, Sun et al. used single molecule force spectroscopy to show that the adhesion force between Al-PAM and kaolinite clay particle surface was five-fold stronger than that between PAM and the particle surface.<sup>130</sup> Two years later, Wang et al. compared the flocculation performance of Al-PAM on oil sands tailings produced from laboratory extraction tests to the performance of Magnafloc 1011, and concluded that Al-PAM was more effective in flocculating fine particles.<sup>131</sup> Lee et al. reported the synthesis of calcium chloride-PAM and ferric chloride-PAM hybrid polymers and showed that both polymers can effectively flocculate kaolinite

suspensions.<sup>132,133</sup> In 2012, Alamgir et al. deployed Al-PAM to flocculate MFT with solids content from 5 to 31 wt % and showed that although Al-PAM was ineffective in flocculating MFT with solids content greater than 15 wt %, Al-PAM was capable of flocculating diluted MFT with solids content of 10 wt % or lower.<sup>122</sup>

#### **1.4.8.2 Hydrophobically Modified Flocculants**

Hydrophobic modification on a flocculant often improves its flocculation performance due to the enhanced interactions between the flocculant and colloidal particles. The hydrophobic modification also improves dewatering due to the increase in the hydrophobicity of the flocculant. In 2009, Shang et al. reported the synthesis of a novel hydrophobically modified cationic PAM (HCPAM) containing hydrophobic groups, methacryloxypropyltrimethoxy silane, and showed that the HCPAM performed better than cationic PAM when flocculating a kaolin suspension, and better performance was achieved by the HCPAM with higher hydrophobicity.<sup>134</sup> In 2016, Reis et al. introduced hydrophobicity to PAM by grafting propylene oxide (PPO) groups and demonstrated that PAM-g-PPO dewatered and densified 2 wt % MFT more efficiently than the commercial PAM by reducing the amount of water entrapped in flocs.<sup>135</sup> Shortly after, Hripko et al. systematically investigated the effect of comonomer composition, hydrophobic chain length and molecular weight of PAM-g-PEO and concluded that all three variables significantly affected the flocculation performance, in terms of initial settling rate (ISR), supernatant turbidity (ST) and capillary suction time (CST), and optimal performance could be obtained by manipulating the variables.<sup>136</sup> Very recently, Bazoubandi and Soares synthesized a series of amylopectin-g-PAM with different grafting frequencies and lengths and showed that the amylopectin-g-PAM, which was less hydrophilic

due to the amylopectin grafts compared to PAM, was able to flocculate 5 wt % MFT and formed sediments with higher solids content than the commercial PAM.<sup>137</sup>

#### **1.4.8.3 Thermo-responsive Flocculants**

The use of polymers with a thermo-responsive phase transition as flocculants can potentially facilitate the formation of more compact and stronger flocs during flocculation and dewatering of oil sands tailings. Typically, thermo-responsive flocculants are added to oil sands tailings at a temperature below their LCSTs, which allows for the adsorption of the flocculants onto fine particle surfaces and initiates the flocculation process. When the temperature is raised above the LCSTs, the polymers become hydrophobic, which may increase interparticle interactions due to hydrophobic interactions and enhance the capturing of fine particles. Moreover, the increase in the hydrophobicity of thermo-responsive flocculants above their LCSTs can potentially decrease the amount of water entrapped in flocs, which helps dewatering and consolidation of sediments. In 2007, Li et al. first applied a thermo-responsive polymer, PNIPAM, to flocculate 10 wt % kaolin suspensions and showed that higher settling rates and better solid compaction were achieved when the settling temperature (40 °C) was above the LCST of PNIPAM than below.<sup>12</sup> Later on, they determined that PNIPAM with high molecular weight resulted in more effective flocculation and sediment consolidation compared to that with low molecular weight.<sup>138</sup> In 2011, Long et al. reported that the settling rate of laboratory extraction tailings increased by 12-fold due to the addition of 400 ppm of PNIPAM, when the flocculation tests were conducted above its LCST at 40 °C.<sup>109</sup> In 2015, Li et al. reported that flocculation of MFT with PNIPAM was much more effective than a commercial PAM in that when 120 ppm of PNIPAM were used to flocculate 10 wt % MFT, a high ISR of



22.5 m/h and a relatively clear supernatant with an ST of 93 NTU were achieved.<sup>139</sup> They also reported that when PNIPAM was used for settling tests at room temperature, no flocculation was observed.

#### **1.4.8.4 Dual Functionality Flocculants**

Flocculants with more than one functionality show superior flocculation performance due to the synergistic effect of the different functionalities. In 2009, Shang et al. discussed the synthesis of a novel hydrophobically modified and cationic flocculant, poly(acrylamide-methacryloxyethyltrimethyl ammonium chloride-methacryloxypropyltrimethoxy silane) (P(AM-DMC-MAPMS)), and found that this dual functionalized flocculant gave greater flocculation performance, in terms of clay removal, than a commercial cationic PAM when flocculating a 0.1 wt % kaolinite clay suspension.<sup>134</sup> Zhang et al. reported that the synthesis of copolymers of acrylamide, DADMAC and diallylmethyl dehydroabiatic acid propyl ester ammonium bromide and showed that this rosin-based, hydrophobically modified, cationic PAM had a better clay removal ability and a larger flocculation window (i.e. a larger difference between the maximum and minimum doses at which a satisfactory flocculation performance can be achieved) than cationic PAM when flocculating 3-5 wt % kaolin suspensions.<sup>140</sup> In 2015, Lu et al. synthesized a random copolymer comprising of NIPAM, 2-aminoethyl methacrylamide hydrochloride (AEMA) and 5-methacrylamido-1,2-benzoboroxole (MAAmBo).<sup>141</sup> The NIPAM and AEMA segments render the copolymer thermoresponsivity and cationicity, respectively, whereas the benzoboroxole moieties may strongly interact with hydroxyl groups on kaolinite at slightly basic conditions. They reported that the copolymer accelerated the settling of a 5 wt % kaolin suspension and an ISR of 3 m/h was achieved at a

dose of 25 ppm under the conditions of pH 9 and 50 °C, however, the ST was extremely high.<sup>141</sup> In 2017, Zhang et al. reported the flocculation of 10 and 15 wt % MFTs with PNIPAM and a thermoresponsive cationic copolymer of NIPAM and AEMA.<sup>11</sup> Both polymers were effective flocculants for 10 wt % MFT at 25 °C (below their LCSTs) and 50 °C (above the LCSTs). However, the thermoresponsivity of these polymers appeared to have only very modest effect on flocculation performance as there was very little difference in the ISR, ST and water recoveries (WR) between the settling tests conducted at 25 °C and 50 °C with either polymer. Very recently, Gumfekar and Soares reported the synthesis of a series of multifunctional copolymers based on thermoresponsive NIPAM, cationic 2-(methacryloyloxy) ethyl trimethyl ammonium chloride, and hydrophobic *N*-tert-butylacrylamide segments.<sup>142</sup> They demonstrated that the terpolymer can be optimized to effectively flocculate 10 wt % MFT and an ISR of 7 m/h was achieved.

#### **1.4.8.5 Dual Polymer Flocculants**

A dual component flocculation system often improves flocculation performance in that the first component serves as an anchor for the adsorption of the second component through interactions such as electrostatic attraction and hydrogen bonding. Loeke et al. showed that better filterability can be achieved when MFT was treated with a dual polymer flocculant consisting of anionic PAM and cationic poly(diallyldimethylammonium chloride) (poly(DADMAC)) or PEO.<sup>143</sup> In 2016, Lu et al. reported a dual flocculant system for the flocculation of fresh tailings from laboratory extractions and showed that after treating the tailings with 20 ppm of anionic PAM followed by the addition of 200 ppm of cationic chitosan,

ISR was as high as 7.7 m/h and ST was relatively low at 71 NTU.<sup>144</sup> They also reported that the setting tests using either polymer alone showed unsatisfactory results.

#### **1.4.8.6 Polysaccharide-based Flocculants**

As inorganic and synthetic polymer flocculants sometimes lead to secondary pollution and new environment challenges, effective biopolymer-based flocculants are highly desired. In 2009, Ghimici and Nichifor reported an efficient flocculation of a kaolin suspension using a cationic dextran modified with quaternary ammonium salt groups, *N*-ethyl-*N,N*-dimethyl-2-hydroxypropylene ammonium chloride.<sup>145</sup> In 2013, Wang et al. showed the capability of starch-graft-poly (2-methacryloyloxyethyl) trimethyl ammonium chloride (starch-*g*-PDMC) to remove clay particles from a kaolin suspension.<sup>146</sup> In 2011, Lu et al. reported a study of flocculating properties of 3-chloro-2-hydroxypropyl trimethyl ammonium chloride (CHPTAC) modified chitosan-graft-PAM (chitosan-CHPTAC-*g*-PAM) and showed that as the CHPTAC content increased, the flocculating performance in terms of ST increased.<sup>147</sup> Molatlhegi and Alagha also reported that chitosan-*g*-PAM had a better settling behavior compared to chitosan or PAM when treating a 5 wt % kaolin suspension.<sup>148</sup> Very recently, Oliveira et al. used chitosan-*g*-PAM to flocculate 5 wt % MFT and reported that 10000 ppm chitosan-*g*-PAM was able to dewater the MFT at an ISR of 20.7 m/h and an ST below 10 NTU.

### **1.5 Objectives of the Thesis**

The objectives of this thesis are to develop effective starch-based flocculants for the consolidation and dewatering of oil sands MFT and to investigate the use of starch-based processing aids in the extraction of bitumen from oil sands. The ultimate goal of this project is

to develop starch-based flocculants that are capable of flocculating MFT with a high settling rate ( $> 20$  m/h), recovering a maximum amount of water that has high clarity ( $< 30$  NTU), and yielding a reclaimable sediment with very high solids content ( $> 60$  wt %). Flocculation performance was evaluated in terms of initial settling rate, water recovery, supernatant turbidity and sediment solids content. The flocculation performance of thermoresponsive starch, hydrophobically modified starch, cationic starch, cationic thermoresponsive starch and a dual polymer flocculation system consisting of a thermoresponsive starch and a cationic starch were examined in detail. The performance of the flocculants derived from corn starch and potato starch was also explored throughout the thesis. The effectiveness of the use of charge stabilized, thermoresponsive starch nanoparticles as processing aids in an aqueous-solvent hybrid extraction process to recover bitumen from poor processing oil sands ores was investigated. Cationic hydrophobically modified starch nanoparticles were employed as a demulsifier in the bitumen extraction process and their ability to improve the recovery of bitumen from poor processing ores and aged oil sands ores was evaluated.

## Chapter 2

# Thermoresponsive Starch for the Flocculation of Oil Sands Mature Fine Tailings

### 2.1 Introduction

As stated in Chapter 1, MFT form extremely stable suspensions that can take decades to consolidate and dewater if no further treatment is applied. Many efforts have been made to develop technologies, such as coagulation and flocculation, to accelerate the consolidation and dewatering of MFT, but none have been employed in an industrial scale. Anionic polyacrylamide (PAM) with a high molecular weight and medium charge density is currently used by Shell Albian Sands to flocculate fresh tailings but it has shown to be an ineffective flocculant for MFT.<sup>2</sup> Moreover, since PAM has a high affinity for water, the flocs produced by PAM often contain a considerable amount of water which leads to a sediment with low solids content. Another disadvantage of PAM is that the recycled water can be contaminated with carcinogenic monomers as it has been shown that the commercial-grade PAM can contain up to 500 ppm of acrylamide and more acrylamide is released during the degradation of PAM under certain conditions.<sup>149–151</sup>

Many examples of hydrophobic flocculants are reported in the literature and it has been shown that the hydrophobic flocculants can reduce the entrapment of water inside flocs and improve sediment solids content.<sup>134–137</sup> Hripko et al. have reported that optimized flocculation performance of 5 wt % MFT can be achieved when PAM is grafted with poly(ethylene oxide methyl ether methacrylate) (PEOMA) chains, which increased its hydrophobicity (Fig.

2.1A).<sup>136</sup> Reis et al. also showed that the grafting of hydrophobic propylene oxide (PPO) groups to PAM improved flocculation and dewatering of 2 wt % MFT (Fig. 2.1B).<sup>135</sup> The study of hydrophobic polymers for MFT flocculation has been extended to thermoresponsive polymers (TRPs). As summarized in Chapter 1, TRPs are polymers that undergo a phase transition from being a soluble hydrophilic coil to an insoluble hydrophobic globule when the lower critical solution temperature (LCST) is reached. The most common TRP is poly(*N*-isopropylacrylamide) (PNIPAM, Fig. 2.1C) which has an LCST of approximately 32 °C.

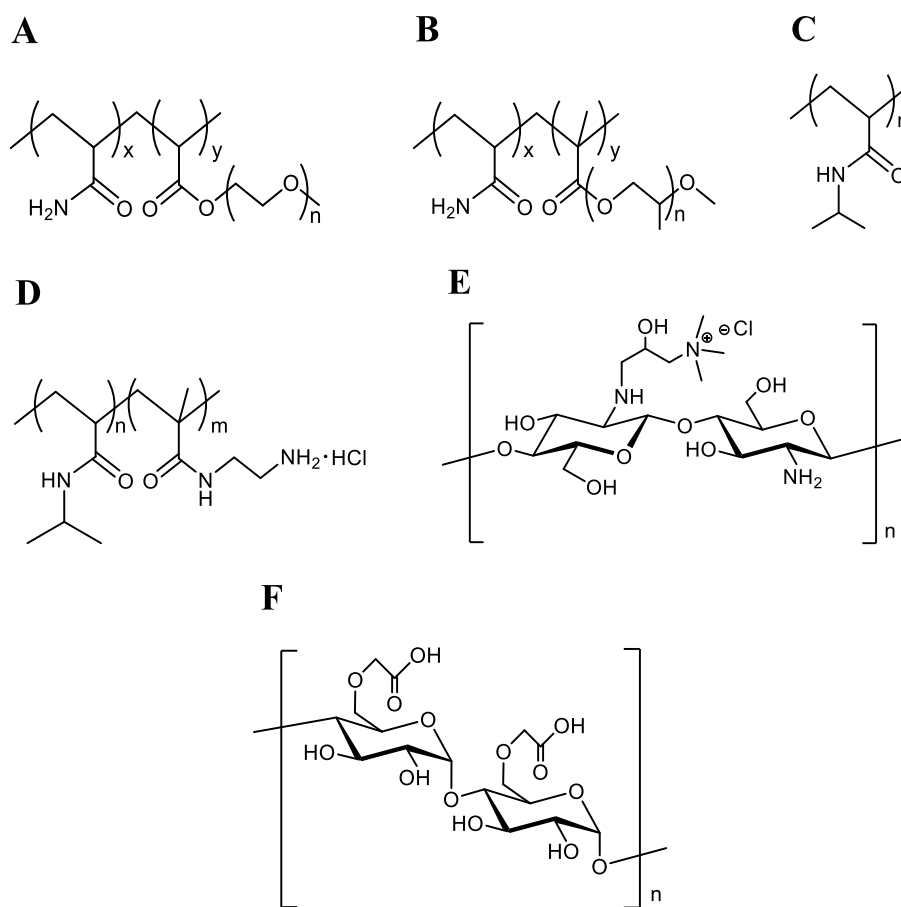


**Figure 2.1.** Chemical structures of PAM-g-PEOMA (A), PAM-g-PPO (B), PNIPAM (C), poly(AEMA-*st*-NIPAM) (D), chitosan-g-CHPTAC (E) and carboxymethylated starch (F).

The classic thermoresponsive polymer, PNIPAM, has been used extensively in the studies examining the effect of thermoresponsivity on flocculation performance.<sup>11,12,109,138,139</sup> In 2011, Long et al. reported a synergistic improvement of both bitumen recovery and settling rate of the extraction tailings when PNIPAM was added to oil sands slurry and the extraction was conducted at 40 °C instead of at room temperature.<sup>109</sup> They also reported that the sediment volume was significantly reduced but the bitumen froth quality was deteriorated by the PNIPAM. In 2015, Li et al. used PNIPAM to flocculate 10 wt % MFT and showed that the PNIPAM, when settling at 50 °C, gave considerably faster initial settling rates (ISR), lower supernatant turbidity (ST), and more consolidated sediments than a commercial PAM did.<sup>139</sup> The authors also reported that no flocculation was observed when the settling test using PNIPAM was conducted at room temperature. In 2017, Zhang and coworkers showed that a thermoresponsive copolymer of NIPAM and 2-amino ethyl methacrylamide hydrochloride (AEMA) (poly(AEMA-*st*-NIPAM), LCST = 45 °C, Fig. 2.1D) effectively flocculated 10 wt % MFT while the use of PNIPAM gave a high ISR but very poor ST.<sup>11</sup> In their studies, the thermoresponsivity of these polymers appeared to have only very modest effect on flocculation performance as very little difference was observed for the ISR, ST and water recoveries (WR) between the settling tests conducted at 25 °C and 50 °C.

To eliminate the potential health concerns with the use of synthetic polymer-based flocculants, flocculants derived from natural biomaterials, such as starch, chitosan, cellulose, alginate, and guar gum, are being examined as potential alternatives in industrial flocculation applications. Quite recently, two reports concerning the use of modified biopolymers as flocculants for oil sands tailings have emerged. In 2018, Oliveira et al. reported that the

flocculation of 5 wt % MFT was successful with the use of a cationic flocculant which was derived from a natural polysaccharide, chitosan, and modified with 3-chloro-2-hydroxypropyl trimethylammonium chloride (chitosan-g-CHPTAC, Fig. 2.1E).<sup>152</sup> Zhao et al. employed an anionic carboxymethylated starch (Fig. 2.1F) to flocculate 5.5 wt % oil sands fresh tailings and showed that an ISR of 2.6 m/h and sediment solids content (SSC) at 36 wt % were achieved with the use of 50 ppm of the anionic starch.<sup>153</sup>

In 2019, we reported the synthesis of thermoresponsive starch (TRS) by hydroxybutylation,<sup>154</sup> and hydrophobically modified starch (HMS) by reacting the starch with styrene oxide.<sup>154</sup> The potential improvements on flocculation performance by using polymers with thermoresponsive or hydrophobic functionalities along with the benefits of using starch as base materials prompted us to explore TRS and HMS as flocculants for MFT. In this chapter, we report the performance of TRS and HMS derived from corn starch or potato starch in the flocculation of MFT.

## **2.2 Materials and Methods**

### **2.2.1 Materials**

Cooked, high amylopectin waxy corn starch (CS) was obtained from EcoSynthetix Inc. (Burlington, Ontario, Canada). Neutral, pre-gelatinized, high amylopectin potato starch (PS) was a gift from Coöperatie AVEBE U.A. (Veendam, The Netherlands). 1,2-Butene oxide and styrene oxide were obtained from Sigma-Aldrich Co. (USA). Oil sands MFT (about 35 wt %, D10: 1.6  $\mu\text{m}$ , D50: 6.9  $\mu\text{m}$  and D90: 19.2  $\mu\text{m}$ ) was originally obtained from Syncrude Canada Ltd and provided to us by Joao Soares, University of Alberta, Canada. Magnafloc 1011 was



obtained from BASF Co. (USA). Other reagents and solvents were commercially available and used without further purification unless stated otherwise.

### **2.2.2 Preparation of TRS and HMS**

CS or PS (1 g) was dispersed in deionized water at 40 °C for 2 h to give an approximately 25 wt % dispersion. The dispersion was cooled to room temperature (rt) followed by the dropwise addition of 10 M NaOH with vigorous stirring to give a dispersion with a pH of 13. Butene oxide or styrene oxide was added to the mixture and stirred vigorously at 40 °C for 24 h. The mixture was cooled to rt then neutralized by the dropwise addition of 1 M HCl with vigorous stirring. The neutralized mixture was subjected to dialysis against deionized water for 2 days using a dialysis bag with molecular weight cut-off ( $MW_{\text{cutoff}}$ ) of 1 kD. A minimum of 5 water replacements were performed over the course of 2 days to give an overall dilution ratio of approximately 1:10<sup>10</sup>. The dialyzed, modified starches were lyophilized for at least 3 days to yield a white powder.

### **2.2.3 Determination of the Molar Substitution of the Modified Starches**

The molar substitution (MS) was determined using <sup>1</sup>H-NMR spectroscopy on a Bruker Avance 500 NMR spectrophotometer. The modified starch (10 mg) was dispersed in deuterium oxide (D<sub>2</sub>O, 600 μL) for 16 h at 4 °C then allowed to warm to rt before obtaining the spectra. An example of NMR spectra of hydroxybutyl corn starch (HB-CS) and hydroxybutyl potato starch (HB-PS) with a molar substitution (MS) of 1.9 (HB1.9-CS and HB1.9-PS) and phenylhydroxyethyl potato starch (PHE-PS) with an MS of 0.2 (PHE0.2-PS) are shown in Figures A1-3 in Appendix A. The MS of HB groups ( $MS_{\text{HB}}$ ) was defined as the molar ratio of

the HB substituents to the anhydroglucose units (AGU) of the starch molecules. The  $MS_{HB}$  was calculated using Eq. 2.1:

$$MS_{HB} = \frac{I_{CH_3}/3}{I_{H_a}}$$

**Equation 2.1**

where  $I_{CH_3}$  is the integral value for the methyl group peak of HB groups at 0.70-1.05 ppm and  $I_{H_a}$  is the integral value for the anomeric proton ( $H_a$ ) at 5.20-5.85 ppm. The MS of PHE groups ( $MS_{PHE}$ ) was defined as the molar ratio of the PHE substituents to AGU and was calculated using Eq. 2.2:

$$MS_{PHE} = \frac{I_{\text{phenyl-H}}/5}{I_{H_a}}$$

**Equation 2.2**

where  $I_{\text{phenyl-H}}$  is the integral value for the phenyl proton peak at 7.20-7.60 ppm.

## 2.2.4 Determination of LCST by Light Transmittance

Light transmittance values were determined using a Cary 4000 Bio UV-Visible spectrophotometer equipped with a multi-cuvette holder and a temperature controller. The modified starches were dispersed in deionized water to concentrations ranging from 0.025 g/L to 1 g/L for 16 h at 4 °C before the light transmittance studies were conducted. The temperature of the dispersion was measured by a temperature probe in a reference cell. The transmittance was recorded at a wavelength of 500 nm with a heating rate of 10 °C/min, which approximated the heating rate in the flocculation process. The modified polymer dispersions were equilibrated for at least 5 minutes at 20 °C in the cuvette holder before the measurements commenced. Absorbance data points were taken every 1 °C and recorded up to 60 °C. The

absorbance data was then converted to transmittance and plotted against dispersion temperature to give a transmittance curve. The LCST is defined as the temperature at the inflection point of the transmittance curve of a 1 g/L polymer dispersion.

### **2.2.5 DLS Measurements**

The modified starch was dispersed in deionized water to a concentration of 1 g/L. The dispersions were stirred for 2 h at 4 °C and left undisturbed for 16 h at 4 °C. The dynamic light scattering (DLS) measurements were performed at 25 °C and 65 °C using the Zetasizer Nano (Malvern Instruments, Worcestershire, UK). The dispersions were equilibrated for 5 minutes at each temperature settings before starting the measurements.

### **2.2.6 Settling Tests**

The solids content of undiluted MFT is approximately 35 wt % and previous studies on the flocculation of undiluted MFT have shown that the flocculation process was impeded because the high solids content of MFT did not allow for the proper distribution of the flocculants.<sup>122</sup> To mitigate this problem, tap water was added to the undiluted MFT to produce dilutions of MFT with solids contents of 2, 5 or 10 wt %. All MFT dilutions were prepared fresh and homogenized with a mechanical stirrer for 2 h before use. Stocks of non-thermoreponsive starch or hydrophobically modified starch dispersions were prepared to a concentration of 50 g/L and stored at rt before use. The stocks of thermoresponsive starch dispersions were also prepared to 50 g/L but stored at 4 °C before use. For each settling test, 50 g of the diluted MFT were used. The diluted MFT were stirred in a 100 mL beaker for 2 min at 600 rpm. A pre-determined dose of polymer dispersion was added dropwise to the MFT

mixture at 23 °C over 2 min. The polymer doses were expressed with reference to total MFT weight. The mixture was stirred at 23 °C or in a 50 °C water bath at a stirring speed of 200 rpm with a magnetic stirrer. After stirring for 8 min, the mixture was poured into a 50 mL graduated cylinder followed by inverting 3 times. The graduated cylinder was then left undisturbed at 23 °C or at 50 °C (water bath). For settling tests at 50 °C, the graduated cylinder was removed from the 50 °C water bath after 30 min. Mudline height was recorded as a function of settling time. Normalized mudline height is referred to the mudline height divided by initial mudline height ( $H_i$ ). Initial settling rate (ISR) is defined as the slope of the initial linear portion of the normalized mudline height as a function of settling time plot (Figure A4 in Appendix A). After 24 h of settling, final mudline height ( $H_f$ ) was recorded, and water recovery (WR) was calculated using Eq. 2.3:

**Equation 2.3**

$$WR = \left(1 - \frac{H_f}{H_i}\right) \times 100 \%$$

Approximately 5 mL of the supernatant were withdrawn from the middle of the upper layer in the graduated cylinder and transferred to a cuvette which was then measured by an SPER Scientific 860040 turbidity meter to obtain supernatant turbidity (ST) in nephelometric turbidity units (NTU). The sediment was transferred from the graduated cylinder to a glass beaker, dried overnight at 110 °C and weighed. The sediment solid content (SSC) was determined from the weight of the solid residue after drying. All experiments were conducted at least 3 times to obtain representative results.

## 2.3 Results and Discussion

### 2.3.1 Modified Starches and their Thermoresponsivity

Hydroxybutyl corn starch (HB-CS) with  $MS_{HB}$  of 0.6 (HB0.6-CS), 1.5 (HB1.5-CS), 1.9 (HB1.9-CS) and 2.3 (HB2.3-CS), hydroxybutyl potato starch with an  $MS_{HB}$  of 1.9 (HB1.9-PS), and phenylhydroxyethyl potato starch (PHE-PS) with  $MS_{PHE}$  of 0.02 (PHE0.02-PS) and 0.2 (PHE0.2-PS) were prepared from hydroxyalkylation of cooked CS or PS at basic conditions (Fig. 2.2). The molar substitutions were obtained from  $^1\text{H-NMR}$  analysis

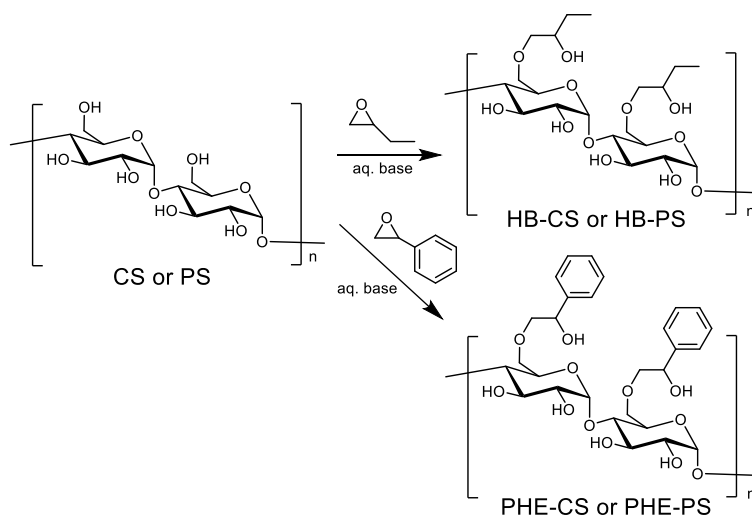


**Figure 2.2.** Preparation of TRS and HMS. Substitution is shown only at O-6 while in fact substitution can occur at O-2, O-3 and O-6.

The hydrophobically modified starches (HMS), PHE0.02-PS and PHE0.2-PS, were not thermo-responsive. HB0.6-CS was not thermo-responsive either, while the HB1.5-CS, HB1.9-CS and HB2.3-CS were thermo-responsive, which was indicated by the light transmittance measurements at different concentrations of the aqueous dispersions of the three thermo-responsive HB-CSs (Fig. 2.3A-C). At low concentrations (<100 ppm) of the HB1.5-,

HB1.9- and HB2.3-CS, the decrease in transmittance above the LCST was small, which indicated that the polymers remained relatively stable in the dispersions and the formation of insoluble aggregates did not occur. When the concentration of the polymers was greater than 100 ppm, the decrease in transmittance became larger after the phase transition. For HB2.3-CS dispersions at 600 ppm or above, the transmittance values decreased close to 0 % above the LCST (Fig. 2.3C), which indicated the formation of insoluble aggregates and a complete phase separation. For all three thermoresponsive HB-CSs, the LCST values decreased only by a few degrees with the increasing concentrations (Table 2.1), similar to that reported for PNIPAM.<sup>42</sup>

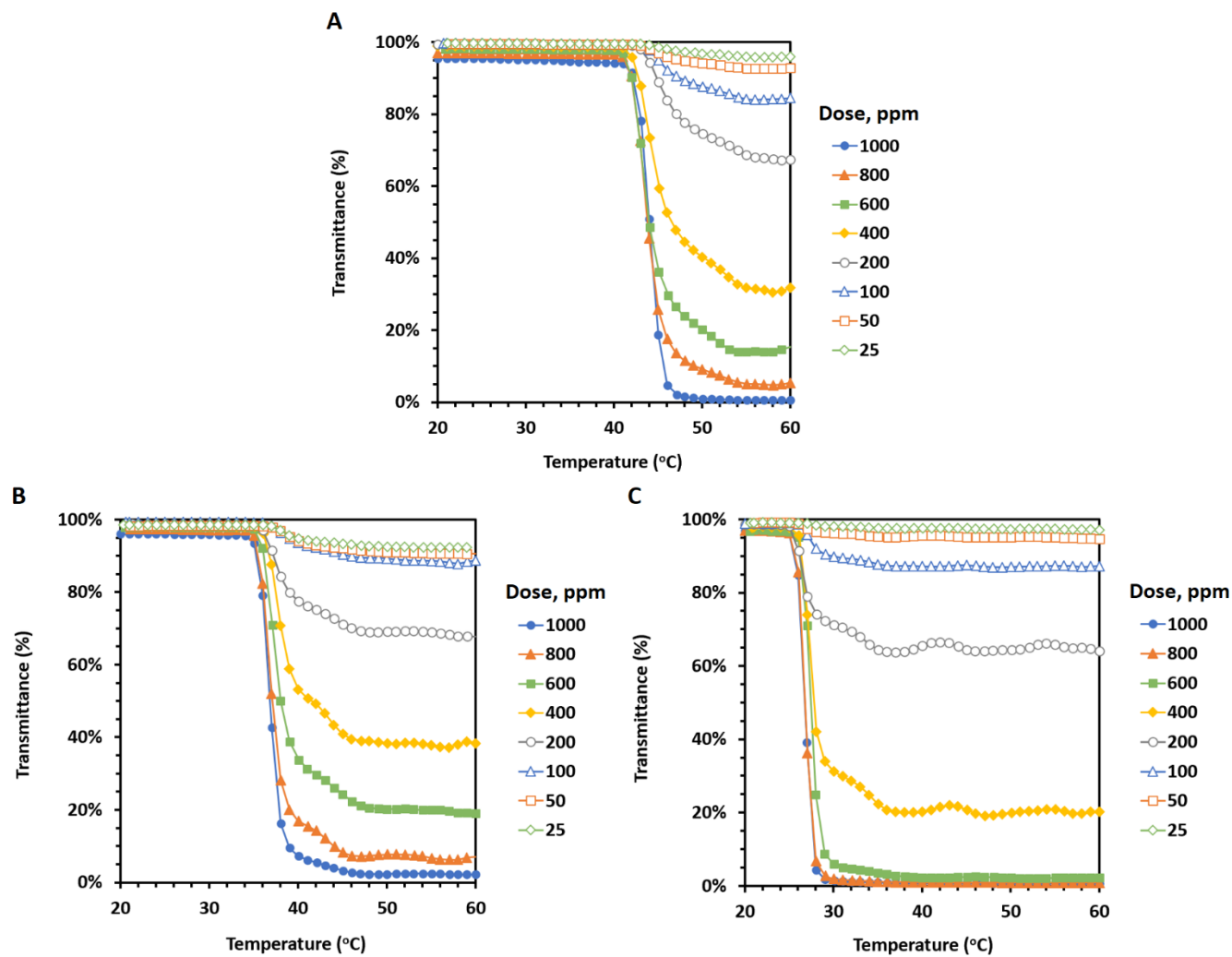


**Figure 2.3.** Light transmittance curves for aqueous dispersions of HB1.5-CS (A), HB1.9-CS (B), and HB2.3-CS (C) with concentrations ranging from 0.025 g/L (25 ppm) to 1 g/L (1000 ppm).

**Table 2.1.** LCST values of HB-CS and HB-PS.

Starch		LCST (°C) <sup>a</sup>							
		25 <sup>b</sup>	50 <sup>b</sup>	100 <sup>b</sup>	200 <sup>b</sup>	400 <sup>b</sup>	600 <sup>b</sup>	800 <sup>b</sup>	1000 <sup>b</sup>
1	HB1.5-CS	n.d.	n.d.	45	45	45	44	44	44
2	HB1.9-CS	39	39	38	38	38	38	37	37
3	HB2.3-CS	n.d.	n.d.	28	28	28	28	27	27
4	HB1.9-PS	n.d.	n.d.	38	37	37	36	36	36

<sup>a</sup> Temperature at the inflection point of the transmittance curve.

<sup>b</sup> Dose (ppm)

HB1.9-PS was also thermoresponsive, but it exhibited transmittance curves that were very different from those of the HB1.9-CS (Fig. 2.4 and Fig. 2.3B). The transmittance curves of the HB1.9-PS were shallower than the HB1.9-CS ones. At a concentration of 100 ppm or below, the decrease in transmittance above the LCST was no more than 3 % and the transmittance curves were extremely shallow, which made the accurate determination of the LCSTs at these concentrations very difficult. At concentrations greater than 100 ppm and at temperatures close to the LCST, the transmittance values decreased sharply initially but the curves became shallower afterwards (Fig. 2.4). Unlike the curves of HB-CSs, the transmittance curves of HB1.9-PS never plateaued, and the transmittance values continued to decrease slowly with the increasing temperature (up to 60 °C), indicating a slow but continuous dehydration of the polymer chains. Despite the differences in transmittance curves, the LCST of the HB1.9-PS was very similar to that of the HB1.9-CS (Table 2.1, entries 2 and 4). However, the maximum decrease in transmittance values above the LCST was only 21 % for the HB1.9-PS (Table 2.2, entry 2), indicating that the polymers could remain relatively stable in the dispersion due to the incomplete dehydration of the polymer chains. On the other hand, a much larger maximum decrease in transmittance values (94 %) above the LCST was observed for the HB1.9-CS (Table 2.2, entry 1), indicating an almost



completely destabilized dispersion and phase separation. Overall, these observations suggested that the HB1.9-PS formed semi-stable mesoglobules rather than insoluble aggregates above its LCST and similar findings were reported elsewhere.<sup>155</sup>

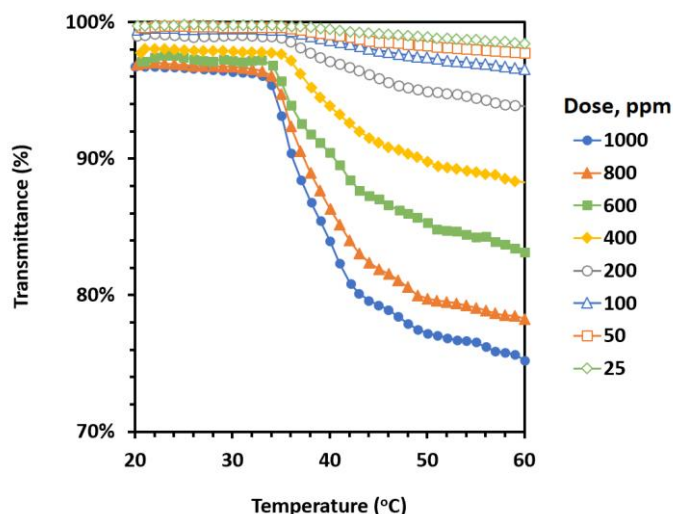


**Figure 2.4.** Light transmittance curves for aqueous dispersions of HB1.9-PS from 0.025 g/L (25 ppm) to 1 g/L (1000 ppm).

**Table 2.2.** The decrease in transmittance above the LCSTs of HB1.9-CS and HB1.9-PS.

	Starch	Decrease in Transmittance (%) <sup>a</sup>							
		25 <sup>b</sup>	50 <sup>b</sup>	100 <sup>b</sup>	200 <sup>b</sup>	400 <sup>b</sup>	600 <sup>b</sup>	800 <sup>b</sup>	1000 <sup>b</sup>
1	HB1.9-CS	6	7	10	31	60	79	90	94
2	HB1.9-PS	1	2	3	5	10	14	19	21

<sup>a</sup> Difference in transmittance values at 20 °C and 60 °C.

<sup>b</sup> Dose (ppm)

The hydrodynamic diameters ( $D_h$ ) of the thermoresponsive starches increased significantly when the dispersion temperature increased from below (25 °C) to above their LCSTs (65 °C) (Table 2.3). At 65 °C, the  $D_h$  of the HB1.9-PS aggregates was 84 nm, which was considerably smaller than those formed by the HB1.9-CS (with a  $D_h$  of 220 nm). This

observation again supported that the HB1.9-PS was forming mesoglobules rather than large insoluble aggregates above its LCST.

**Table 2.3.** Hydrodynamic diameters ( $D_h$ ) of TRS at 25 °C and 65 °C at 1 g/L (1000 ppm).

	Starch	$D_h$ (nm)	
		25 °C	65 °C
1	HB1.5-CS	39	215
2	HB1.9-CS	38	220
3	HB2.3-CS	39	157
4	HB1.9-PS	23	84

The reason for the differences in thermoresponsive behaviors between the HB1.9-PS and the HB1.9-CS was not entirely clear. Both polymers were derived from high amylopectin starches. One difference between the two starches is their molecular weights in that the weight-average molecular weight ( $M_w$ ) of the HB1.9-PS ( $3900 \pm 203$  kDa) is greater than that of the HB1.9-CS ( $2300 \pm 187$  kDa). But the difference in molecular weight does not necessarily explain the difference in their thermoresponsive behaviors. Another notable difference is that potato starch naturally contains phosphate esters while corn starch usually does not. We subjected the CS and PS to degradation by amylase, and the  $\alpha$ -limited products were examined by  $^{31}\text{P}$ -NMR. Peaks corresponding to starch phosphate esters were clearly evident in the  $^{31}\text{P}$ -NMR spectrum of the  $\alpha$ -limited PS but were absent in that of the  $\alpha$ -limited CS (see Fig. A5 and A6 in Appendix A). This is consistent with the studies by others who have shown that PS has a considerably higher phosphate ester content than CS.<sup>156,157</sup> The phosphate esters in the PS confer a small amount of negative charge to the HB-PS as evidenced by the difference in zeta potential between the HB1.9-PS (-12 mV) and the HB1.9-CS (-0.3 mV) at 50 °C (above their LCST). It is possible that the phosphate

esters buried within the HB1.9-PS migrate to the surface as the polymer becomes more hydrophobic above its LCST and consequently, the exposed phosphate esters may cause the incomplete dehydration of the polymer chains and induce the formation of semi-stable mesoglobules instead of insoluble aggregates due to electrostatic repulsions between the polymers.

### **2.3.2 Settling Tests using HB-CS**

The non-thermoreponsive HB0.6-CS and the thermoresponsive HB1.5-, HB1.9-, and HB2.3-CS were used to flocculate 2 wt % MFT. The settling tests were performed at 23 °C (below the LCSTs of the three HB-CSs) and at 50 °C (above their LCSTs). For the settling tests conducted at 50 °C, a three-step process, similar to that employed by Zhang et al.<sup>11</sup> and Li et al.,<sup>138</sup> was used to obtain a more consolidated sediment. In this protocol, a dispersion of the HB-CS was added to a stirring MFT mixture at 23 °C and then the mixture was placed in a water bath at 50 °C and continued to stir for 8 min. The mixture was then transferred to a graduated cylinder at 50 °C and left undisturbed for settling to occur at a 50 °C water bath. After 30 min, the mixture was removed from the warm water bath and left standing at 23 °C for the rest of 24 h settling time.

Without the addition of any polymer, the 2 wt % MFT remained in the suspension state after 24 h of settling at either 23 °C or 50 °C. The addition of unmodified CS or PS as negative controls at a dose up to 1000 ppm did not flocculate the 2 wt % MFT either. Moreover, when the thermoresponsive HB-CS stock dispersions were heated to 50 °C before adding to the MFT mixture, the polymers only induced formation and settling of a small amount of flocs leading

to a very turbid supernatant. So, it was impossible to determine the rate of settling as the mudline could not be clearly tracked in the turbid mixture. Under these conditions, the HB-CS molecules associated with each other to form insoluble aggregates before they could deposit onto the clay particle surfaces. As a consequence, the formation of flocs did not readily occur due to the lack of bridging, and the flocculation ability of the HB-CS was impeded. Similar findings have been reported elsewhere using PNIPAM to flocculate a silica suspension.<sup>14</sup>

The flocculation performance of the HB-CSs was evaluated in terms of initial settling rate (ISR), water recovery (WR), supernatant turbidity (ST), and sediment solids content (SSC) at various polymer doses and at settling temperatures of 23 °C and 50 °C (Fig. 2.5A-D). At low doses (< 200 ppm), the ISRs for all four HB-CSs increased with the increasing dose (Fig. 2.5A) while the STs decreased with the increasing dose (Fig. 2.5C). A maximum ISR and a minimum ST were reached at about 100-200 ppm for the non-thermoresponsive HB0.6-CS at both 23 °C and 50 °C and for the thermoresponsive HB-CSs at 23 °C. At doses of 200 ppm or below, the predominant flocculation mechanism could be bridging between the free particles and polymer adsorbed particles via hydrogen bonding and van der Waals forces (Fig. 2.6A and B).

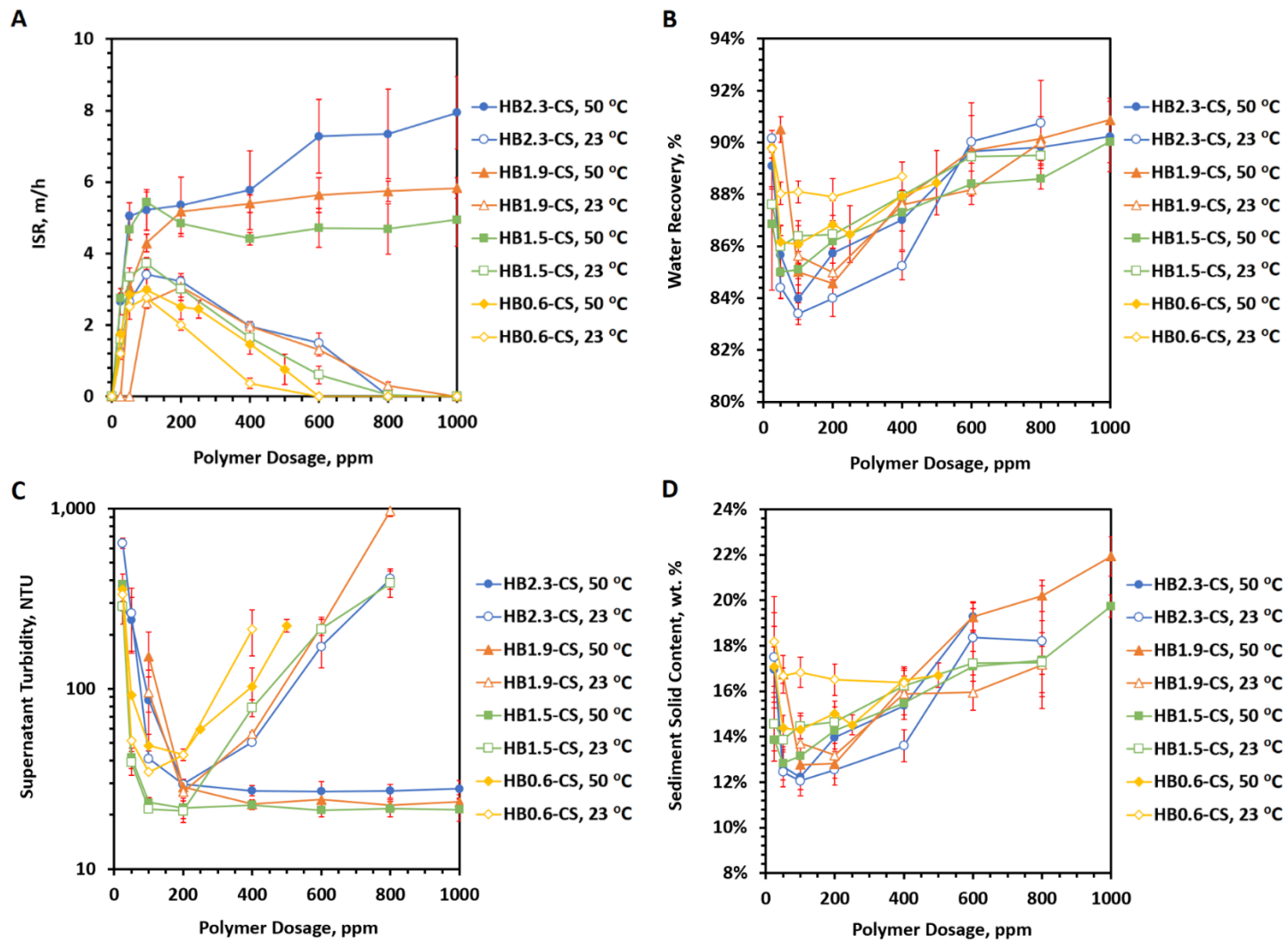


**Figure 2.5.** Initial settling rate (ISR, **A**), water recovery (**B**), supernatant turbidity (**C**), and sediment solids content (**D**) from the settling tests of 2 wt % MFT using various HB-CSs with MS from 0.6 to 2.3 and at polymer doses from 0 to 1000 ppm (on the dry/slurry basis).

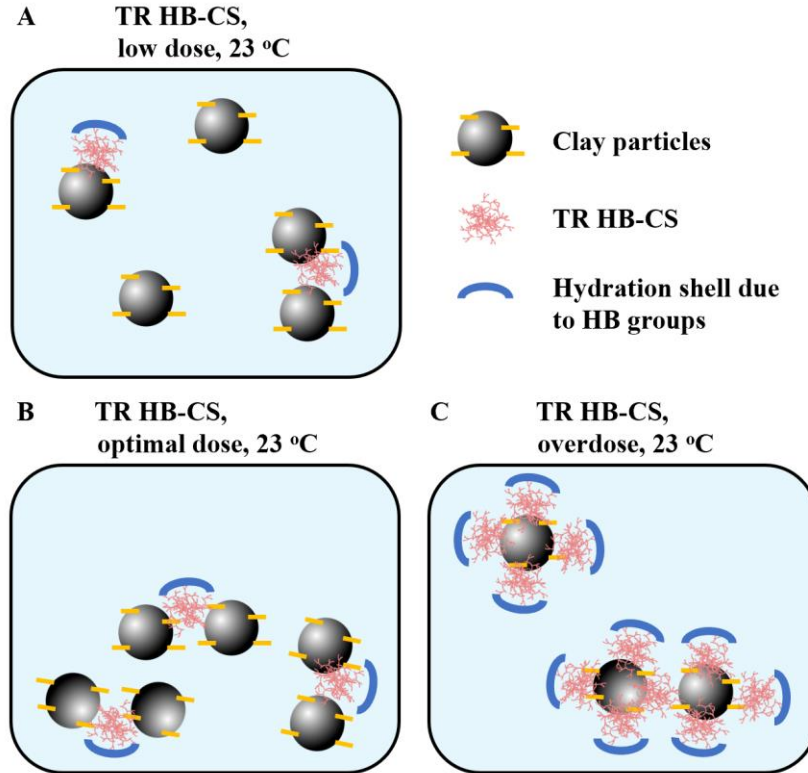


**Figure 2.6.** Schematic representation of flocculation of clay particles using thermoresponsive (TR) HB-CS at a low dose (**A**), at an optimal dose (**B**) and at overdose (**C**) at 23 °C.

At doses of 200 ppm and beyond, the ISR decreased (Fig. 2.5A) and the ST increased (Fig. 2.5C) when the non-thermoreponsive HB0.6-CS dose increased for settling tests conducted at both 23 °C and 50 °C. At doses greater than 400 ppm for HB0.6-CS regardless of the settling temperatures, although a small amount of flocs formed and settled quickly, a significant amount of clay particles still remained suspended in the supernatant even after the 24 h settling. Hence, it was no longer practical to determine the ISR or ST, and the WR or SSC would not be meaningful due to the highly turbid supernatant. Consequently, HB0.6-CS failed to flocculate the 2 wt % MFT when used at a dose higher than 400 ppm.

Similar to HB0.6-CS, at doses of 200 ppm and above, the ISRs decreased (Fig. 2.5A) and the STs increased (Fig. 2.5C) with the increasing doses of the thermoresponsive HB-CSs

but only at 23 °C which was below their LCSTs. When the dose was greater than 800 ppm, the HB1.5-, HB1.9-, and HB2.3-CS lost their flocculating ability at 23 °C, similar to HB0.6-CS when overdosed (> 400 ppm). This is consistent with the studies by others who have shown that overdosing flocculants greatly deteriorated their flocculation performance.<sup>122,138,158</sup> At these high polymer doses, the clay particles in the suspension may no longer be destabilized by the polymers due to insufficient free particle surface for the anchoring of polymers and for bridging to occur. Moreover, the adsorbed polymer layer may provide steric stabilization to the suspended clay particles (Fig. 2.6C).

For the thermoresponsive HB-CS settling tests conducted at 50 °C, the ISRs were slow at low doses (< 100 ppm, Fig. 2.5A) due to inadequate polymers for sufficient bridging and for the thermoresponse to occur (Fig. 2.7A). The ISRs increased with the increasing dose and reached a plateau at around 100-200 ppm (Fig. 2.5A). The ISRs of the thermoresponsive HB-CSs were approximately 1.5-2 folds greater at 50 °C than those at 23 °C. Moreover, at 50 °C, the ISRs did not decrease, and at the same time, the STs stayed at their minimum when the doses of the thermoresponsive HB-CSs increased above 200 ppm (Fig. 2.5C). More specifically, at 50 °C and at doses from 100 to 1000 ppm, the ISRs of the HB1.5- and HB1.9-CSs remained more or less constant as did the supernatant turbidity. At 50 °C and at doses between 100 and 1000 ppm, the ST of the HB2.3-CS remained constant, and the ISR stayed constant till 400 ppm and increased slightly beyond that. It is clear that, even at high doses, the thermoresponsive HB-CSs still successfully flocculated the 2 wt % MFT at 50 °C, which implied that the flocculation window was greatly broadened due to the hydrophobic HB-CSs above their LCSTs. The broadening effect was also observed by others who used hydrophobic

polymers to flocculate kaolin suspensions.<sup>140,159</sup> Moreover, at high doses and at 50 °C, it can be hypothesized that the interactions between clay particles become attractive because the thermoresponsive HB-CS adsorbed clay particle surfaces become hydrophobic (Fig. 2.7B), unlike at 23 °C, where the interactions are repulsive due to the steric effects induced by the hydrated polymer layer on the clay particle surfaces (Fig. 2.6C). This suggested that the flocculation mechanism at 50 °C predominantly involved hydrophobic interactions between the hydrophobic polymers on the clay particle surfaces and was less dependent upon the bridging interactions between the polymer and the clay particles. A similar hypothesis was proposed by Li et al. who studied the flocculation performance of PNIPAM on silica suspensions,<sup>138</sup> and also by Masliyah and coworkers who examined the flocculation of kaolin suspensions using PNIPAM.<sup>12</sup>

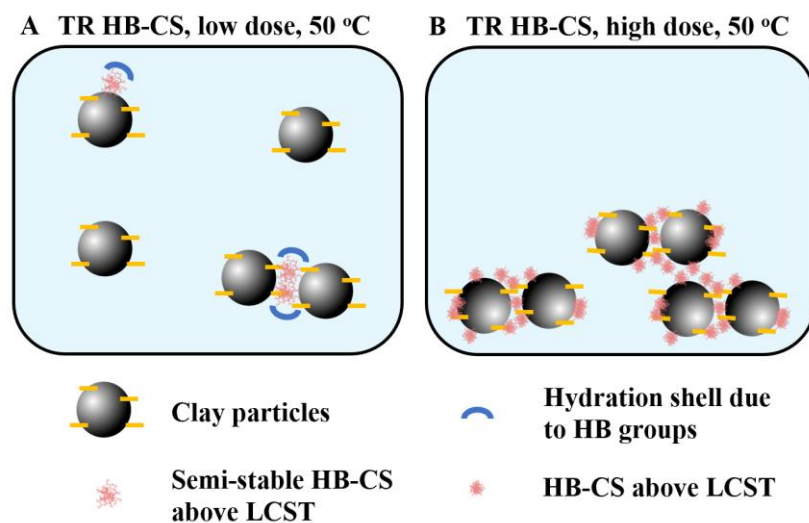


**Figure 2.7.** Schematic representation of flocculation of clay particles using thermoresponsive (TR) HB-CS at low (A) and high (B) doses at 50 °C.

Generally, when supernatant turbidity was high, water recovery was also high (Fig. 2.5B and C). This could be because when the supernatant contained a large amount of



suspended particles, either due to an insufficient dose of polymers for bridging or due to overdosing of the polymers which caused re-stabilization of the particles, fewer particles were being consolidated which led to a lower final mudline height and higher WR. Moreover, when ST was high, sediment solids content was also high in general (Fig. 2.5C and D). At low flocculant doses, the supernatant could still contain a large amount of small, hydrophilic clay particles while the larger, less hydrophilic solids could be flocculated first and form a sediment which was relatively high in solids content. As the supernatant was being clarified, the sediment formed by the small, hydrophilic clay particles might entrap more water which led to a relatively low SSC. At high flocculant doses, these small, hydrophilic clay particles could be re-stabilized due to overdosing, hence, resulting in the sediment with a high SSC again. However, this was not the case of the thermoresponsive HB-CSs at 50 °C and at a dose higher than 200 ppm. Both WR and SSC increased but the ST still remained at a low level (Fig. 2.5B-D) indicating a real improvement in the flocculation performance. This may be due to the close packing of the TRP-adsorbed clay particles as a consequence of hydrophobic interactions between the TRPs above their LCSTs (Fig. 2.7B).

As it has been reported in a flocculation study that when the settling temperature (38 °C) was close to the LCST of PNIPAM (32 °C), the PNIPAM and alumina particles formed smaller flocs compared to those settled at 52 °C, hence, resulting in slower settling rates.<sup>160</sup> Since the HB1.5-CS had an LCST of 45 °C which was close to the settling temperature of 50 °C, settling tests were also conducted at 65 °C using the HB1.5-CS to determine if an increase in the settling temperature would enhance its flocculation performance. Flocculating with the HB1.5-CS at 65 °C resulted in a slightly higher ISR compared to 50 °C (Fig. 2.8A), possibly

due to the formation of slightly larger flocs when settling at 65 °C. The effect of polymer dose on ISR was similar at 50 °C and 65 °C, in that a maximum ISR occurred at 100 ppm and as the dose increased, the ISR remained more or less constant. The ST values were at a low level for both settling temperatures at a dose of 100 ppm and higher (Fig. 2.8C). At 65 °C, both WR and SSC were slightly higher than at 50 °C (Fig. 2.8B and D), indicating that less water was entrapped within the sediment when settling occurred at a higher temperature.

The effect of solids content of MFT on flocculation performance was examined with the use of 600 ppm of the HB2.3-CS and MFT with solids content of 2, 5, and 10 wt % at 50 °C (Table 2.4). The ISR decreased by over 10-fold when the solids content of the MFT was increased from 2 to 5 wt % and decreased by 20-fold when the solids content further increased to 10 wt %. The WR also decreased significantly from 90 % to 50 % as the solids content increased from 2 to 10 wt % while both ST and SSC were more or less unchanged. The flocculation performance of the HB2.3-CS, in terms of ISR and WR, reduced significantly with the increasing solids content of MFT. Similar observations were reported by other researchers who also saw a substantial decrease in flocculation performance as the solids content of MFT increased.<sup>11,122</sup>

**Table 2.4.** Effect of solids content of MFT on flocculation using 600 ppm HB2.3-CS at 50 °C.

	<b>MFT, wt %</b>	<b>ISR, m/h</b>	<b>WR, %</b>	<b>ST, NTU</b>	<b>SSC, wt %</b>
1	2	7.3 ± 1.0	90 ± 1.4	27 ± 3.6	19.3 ± 0.6
2	5	0.6 ± 0.1	68 ± 1.5	34 ± 2.8	18.2 ± 0.4
3	10	0.37 ± 0.04	50 ± 0.8	27 ± 2.7	19.5 ± 0.4

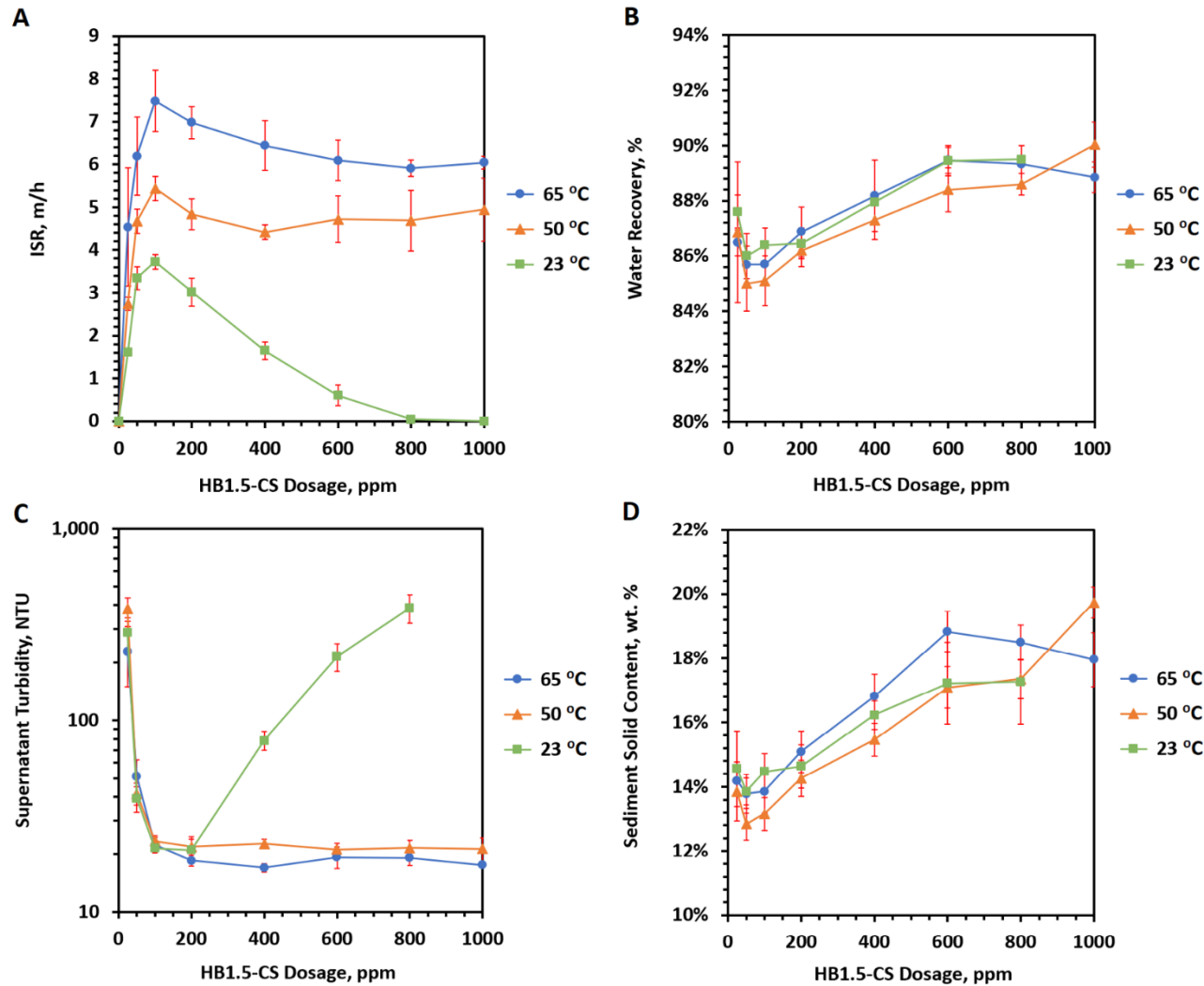


**Figure 2.8.** Initial settling rate (ISR, **A**), water recovery (**B**), supernatant turbidity (**C**), and sediment solids content (**D**) from the settling tests of 2 wt % MFT using HB1.5-CS at polymer doses from 0 to 1000 ppm (dry/slurry) at settling temperatures of 23, 50, or 65 °C.

### **2.3.3 Settling Tests using HB-PS**

Thermoresponsive HB1.9-PS were initially used to flocculate 2 wt % MFT at 23 °C and 50 °C, and its flocculation performance was evaluated by ISR, WR, ST and SSC and compared to that of the HB1.9-CS (Fig. 2.9A-D). At 23 °C which was below the LCST of HB1.9-PS, the ISR increased as the dose of the HB1.9-PS increased from 25 to 200 ppm, and a maximum ISR was reached at 200 ppm while higher doses resulted in a decrease in the ISR (Fig. 2.9A). At 23 °C and 200 ppm, the HB1.9-PS had an ISR which was close to 4 folds higher than that of the HB1.9-CS at the same dose.

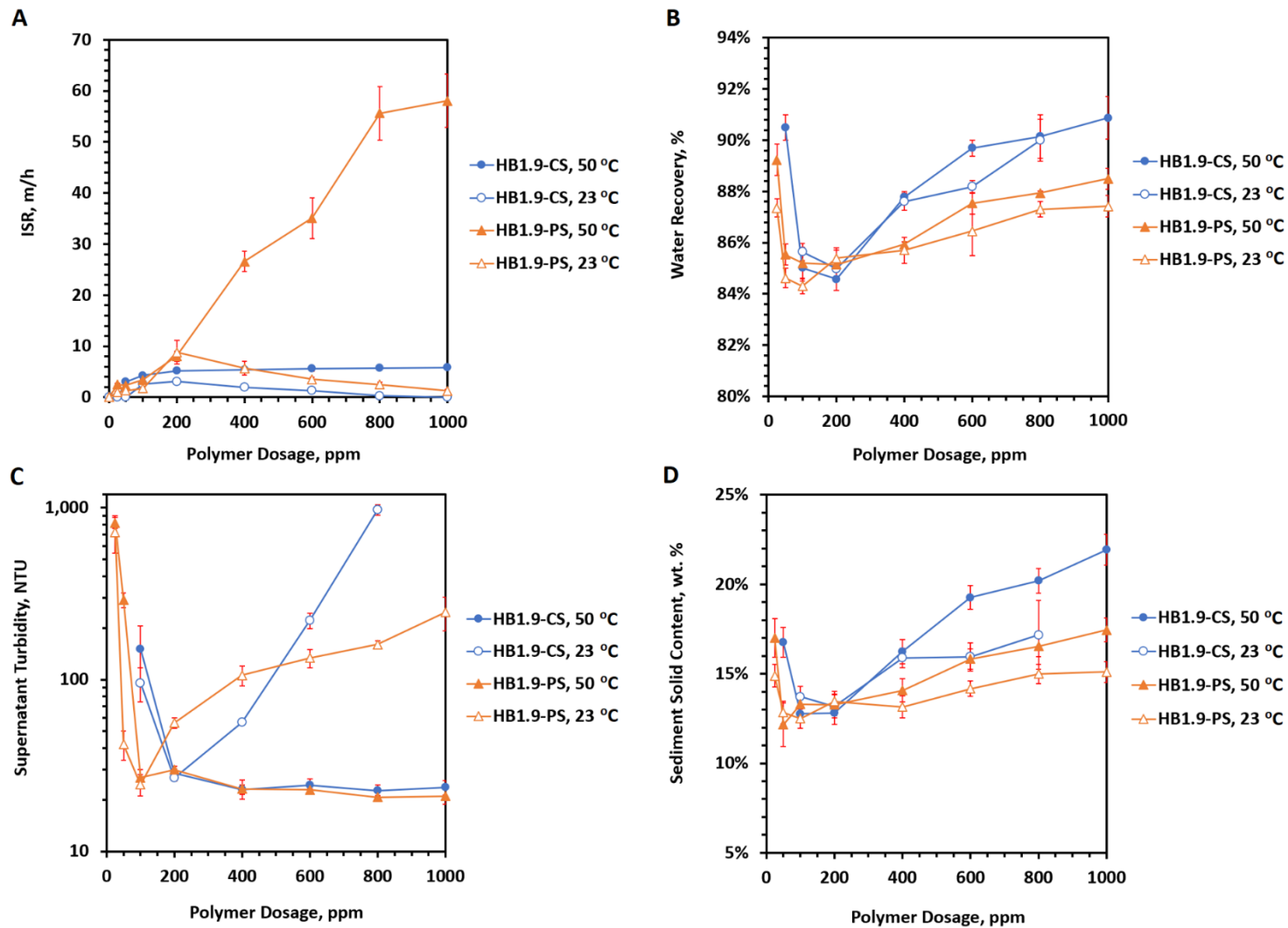


**Figure 2.9.** Initial settling rate (ISR, **A**), water recovery (**B**), supernatant turbidity (**C**), and sediment solids content (**D**) of the settling tests of 2 wt % MFT using HB1.9-CS or HB1.9-PS at polymer doses from 0 to 1000 ppm (on the dry/slurry basis).

At a dose of 200 ppm or below, the ISRs produced by the HB1.9-PS at 50 °C were slow due to insufficient bridging (Fig. 2.10A) and were very similar to those at 23 °C (Fig. 2.9A). However, the ISR continued to increase at 50 °C while the ISR started to decrease at 23 °C as the dose of the HB1.9-PS was higher than 200 ppm. This observation still supported the hypothesis that the flocculation mechanism at 50 °C involved hydrophobic interactions between the hydrophobic polymers on the clay particle surfaces. However, this flocculation mechanism may no longer be predominant since the HB1.9-PS does not form insoluble hydrophobic globules above its LCST as discussed in Section 2.3.1. The presence of a small amount of phosphate esters in PS along with the presence of divalent cations in MFT suggested another possible flocculation mechanism due to electrostatic attractions in that the divalent cations could bridge the PS, free clay particles and the PS adsorbed clay particles (Fig. 2.10B). This mechanism was only possible at 50 °C because the phosphate esters, which would otherwise be buried within the HB1.9-PS molecules below the LCST, could migrate to the surface as the polymer went through the hydrophilic to hydrophobic transition above its LCST. A similar mechanism was also proposed by Wang et al. who employed a cationic thermoresponsive polymer to flocculate kaolin suspensions at a settling temperature above the LCST of the polymer.<sup>13</sup> At 1000 ppm, the ISR of the HB1.9-PS was 58 m/h which was more than 7-fold higher than that obtained by the use of the HB1.9-CS at the same dose (Fig. 2.9A). This large increase in ISR could be explained by the formation of larger flocs due to the synergistic effect of the hydrophobic interactions and electrostatic attractions induced by the HB1.9-PS above its LCST.

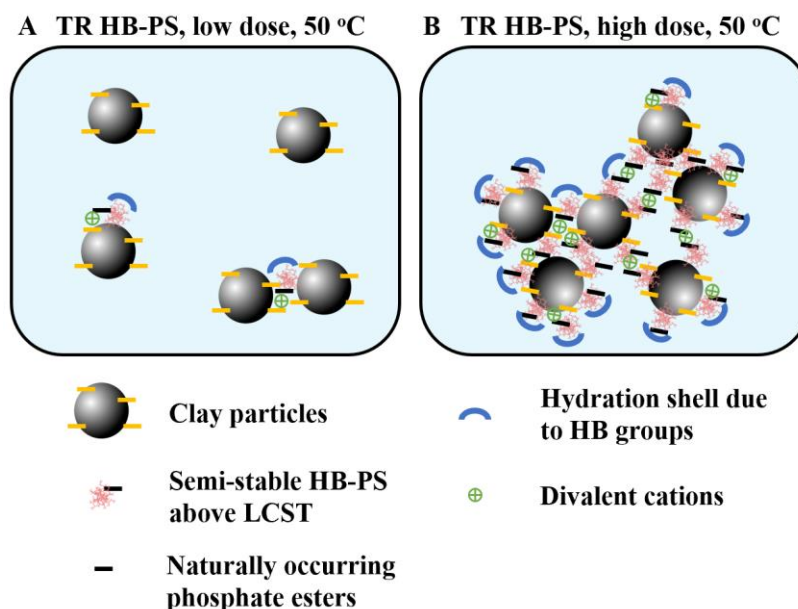


**Figure 2.10.** Schematic representation of flocculation of clay particles using thermoresponsive (TR) HB-PS at low (**A**) and high (**B**) doses at 50 °C.

At 23 °C, the ST produced by the HB1.9-PS decreased drastically from 722 to 25 NTU as its dose increased from 25 to 100 ppm (Fig. 2.9C). At 23 °C and at doses above 100 ppm, the ST increased, which was similar to the behavior of the HB1.9-CS. The lowest ST (25 NTU) was reached at an optimal dose of 100 ppm for the HB1.9-PS, which was at a lower dose compared to that for the HB1.9-CS. At 50 °C, both the HB1.9-PS and HB1.9-CS produced clean supernatants with ST at about 20-30 NTU as their doses increased above 100 ppm.

The trends of WR and SSC were quite similar between the HB1.9-PS and HB1.9-CS regardless of the settling temperatures, in that these parameters both decreased at low doses (25-200 ppm) and then increased as the doses increased (Fig. 2.9B and D). At 50 °C, though the WR and SSC increased with the increasing doses for both polymers, the HB1.9-PS exhibited lower WR and SSC than those obtained by the HB1.9-CS. This could be due to the

incomplete dehydration of the HB1.9-PS above its LCST, which may not expel water from the flocs as effectively as the HB1.9-CS did. Additionally, it could also be due to the presence of naturally occurring phosphate esters in the PS-based flocculants, which caused the entrapment of more water in the flocs.

When the HB1.9-PS was used to flocculate 10 wt % MFT at a dose of 400 ppm or below, the ISR values were similar for the settling tests conducted at 23 °C and 50 °C (Fig. 2.11A). At the HB1.9-PS dose of 400 ppm or above, the ISR increased significantly at 50 °C as the polymer dose increased, while the ISR increased only marginally at 23 °C. The highest ISR (2.6 m/h) was reached at 50 °C when 1000 ppm of the HB1.9-PS was used, while at 23 °C, the ISR at the same dose was 3.4-fold lower. It should also be noted that when 600 ppm of the HB1.9-PS was dosed at 50 °C rather than at 23 °C (i.e. the polymer underwent thermal transition before being added to MFT), the polymer lost its flocculation ability entirely. Overall, these findings once again implied that the thermoresponsivity played an important role in obtaining high settling rates.

At 23 °C, the ST of the HB1.9-PS decreased to a minimum of 110 NTU at a dose of 600 ppm and then increased as the dose increased (Fig. 2.11C). At 50 °C, ST decreased to a minimum of 109 NTU at the same optimal dose as that at 23 °C but remained more or less the same above 600 ppm, indicating a wider flocculation window. Both WR and SSC increased slightly with the increasing dose of HB1.9-PS (Fig. 2.11B and D), and the values were quite similar across the dose range for the settling tests performed at 23 °C and 50 °C.



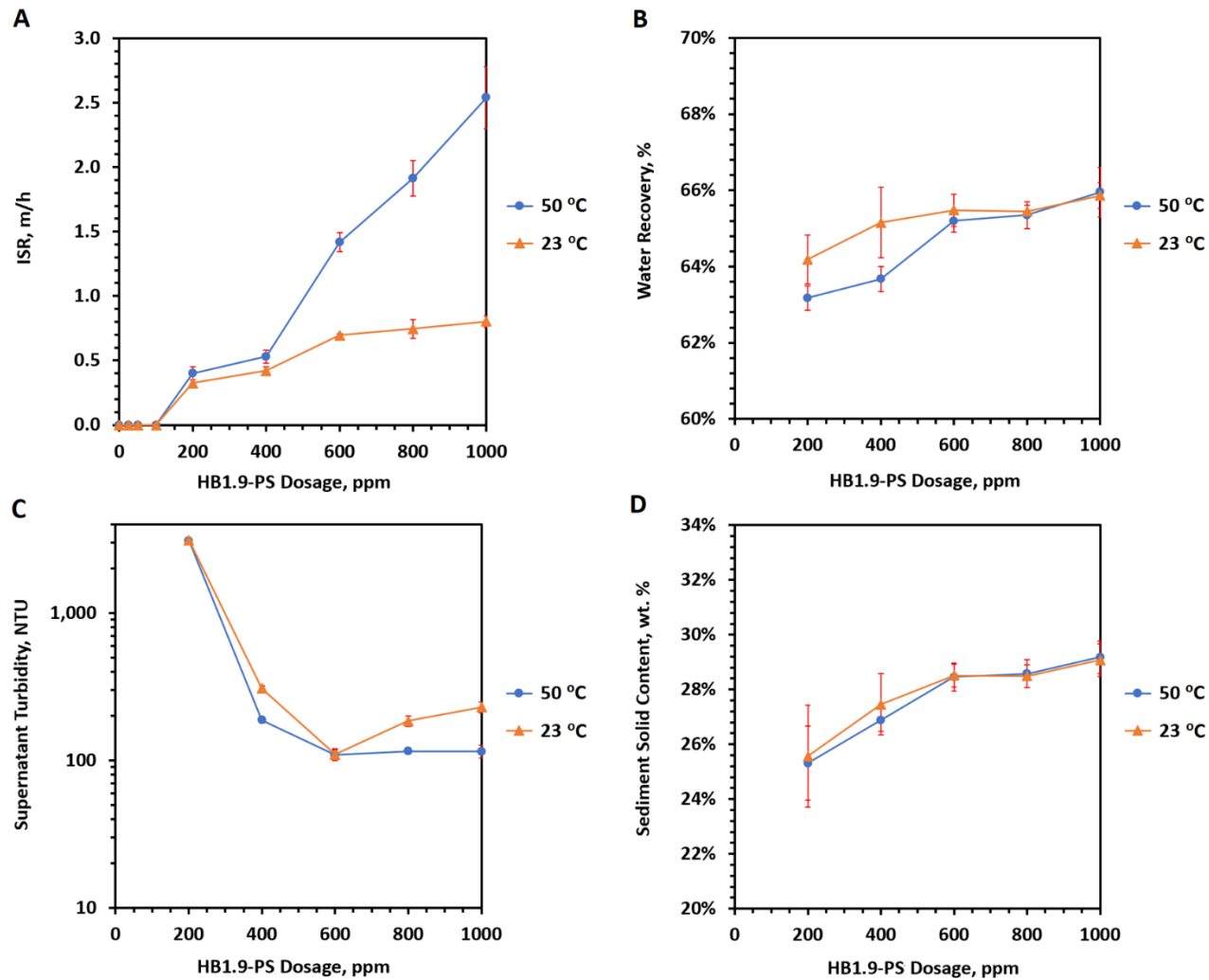


**Figure 2.11.** Settling tests using 10 wt % MFT. Initial settling rate (ISR, **A**), water recovery (**B**), supernatant turbidity (**C**), and sediment solids content (**D**) of the settling tests using HB1.9-PS at doses ranging from 0 to 1000 ppm (on the dry/slurry basis).

The HB1.9-PS was more effective, in terms of ISR, WR and SSC, for flocculating 10 wt % MFT compared to the HB1.9-CS. At 600 ppm and 50 °C, the HB1.9-PS exhibited an ISR that was 5-fold greater than that obtained by the HB1.9-CS (0.28 m/h). At 600 ppm, the WR and SSC using the HB1.9-PS were 65 % and 28 wt % but were only 51 % and 19 wt % using the HB1.9-CS. At 600 ppm and 50 °C, ST was superior using the HB1.9-CS (35 NTU) compared to the HB1.9-PS (109 NTU).

When flocculating 2 and 10 wt % MFT, the HB1.9-PS was superior to the HB1.9-CS, at least in terms of ISR. The superior performance of the HB1.9-PS could be due to the higher a molecular weight of the HB1.9-PS (3900 kDa) compared to the HB1.9-CS (2300 kDa), as higher molecular weight often improves the flocculating ability of thermoresponsive,<sup>138,161</sup> and non-thermoresponsive polymers.<sup>162,163</sup> It is also worth noting that though both the HB1.9-CS and HB1.9-PS at a dose of 600 ppm would have undergone a phase transition at 50 °C, the latter did not become completely dehydrated at this temperature. As a result, the HB1.9-PS at 600 ppm could form semi-stable mesoglobules at 50 °C, unlike in the case of the HB1.9-CS, which formed unstable, hydrophobic aggregates. Moreover, as the HB1.9-PS became more hydrophobic at 50 °C, the negatively charged, naturally occurring phosphate esters could migrate to the surface of the mesoglobules, hence, leading to an increase in the surface charges which could facilitate the capturing of free clay particles. The findings that the HB1.9-PS exhibited significantly better flocculation performance when the settling tests were conducted at temperatures above its LCST (50 °C) compared to below its LCST (23 °C), and was superior in several aspects to the HB1.9-CS when flocculating 2 and 10 wt % MFT, suggested that the slightly negatively charged HB1.9-PS mesoglobules were quite capable of acting as highly

effective flocculants. The mesoglobules are in some ways similar to those obtained with the negatively charged, high molecular weight PAM, which are apparently the most prevalent flocculants used in the oil sands industry.<sup>127</sup> Alamgir et al. reported that Magnafloc 1011, a commercial anionic PAM with high molecular weight, was a very effective flocculant of 10 wt % MFT and the polymer produced an ISR of 8.8 m/h and an ST of 162 NTU at a dose of 100 ppm.<sup>122</sup> We examined Magnafloc 1011 as a flocculant of 10 wt % MFT and found it to be a very poor flocculant at 50, 100 and 1000 ppm (see Fig. A7 in Appendix A). The difference between our results and Alamgir et al. is most likely due to the differences in the MFT.

#### **2.3.4 Settling Tests using PHE-PS**

Phenylhydroxyethyl PS (PHE-PS), which contains phenyl functional groups, is strongly hydrophobic; however, we found that PHE-PS is not thermoresponsive.<sup>154</sup> Nevertheless, we evaluated the flocculation performance of this hydrophobic, non-thermoresponsive starch. Settling tests were first conducted using PHE-PSs with  $MS_{PHE}$  of 0.02 (PHE0.02-PS) and 0.2 (PHE0.2-PS) and 2 wt % MFT, and their ISR, WR, ST and SSC were compared to HB0.6-PS (Fig. 2.12A-D). Below a dose of 100 ppm, the ISR of both PHE-PSs increased with the increasing dose and a maximum ISR was reached at 100 ppm (Fig. 2.12A). The maximum ISR of the PHE0.2-PS was 37 m/h, which was slightly higher than that of the PHE0.02-PS (30.5 m/h). The ST of both PHE-PSs decreased to a minimum as their doses increased from 25 to 50 ppm (Fig. 2.12C). The lowest ST (59 NTU) was produced using PHE0.2-PS while the PHE0.02-PS gave a much higher ST. Though the WR and SSC of the PHE0.2-PS were lower compared to the PHE0.02-PS (Fig. 2.12B and D), it was possibly due

to the highly turbid supernatant produced by the latter as discussed earlier for HB-CSs. Overall, the PHE0.2-PS performed better than the PHE0.02-PS, indicating that the hydrophobic groups could facilitate the flocculation.

The PHE-PSs exhibited a very narrow flocculation window in that the ISR decreased significantly and the ST increased sharply as the dose of the polymers increased beyond their optimal doses (Fig. 2.12A and C). The ST obtained using the PHE0.2-PS sample was very similar to that of the HB0.6-PS sample which also had a narrow flocculation window in terms of the ST (Fig. 2.12C). At 100 ppm, PHE0.2-PS exhibited an ISR that was more than 5-fold higher than HB0.6-PS (Fig. 2.12A). Moreover, at 100 ppm, PHE0.2-PS also exhibited lower ST and higher WR and SSC than HB0.6-PS (Fig. 2.12B-D), indicating that PHE0.2-PS is a remarkably effective flocculant for 2 wt % MFT.

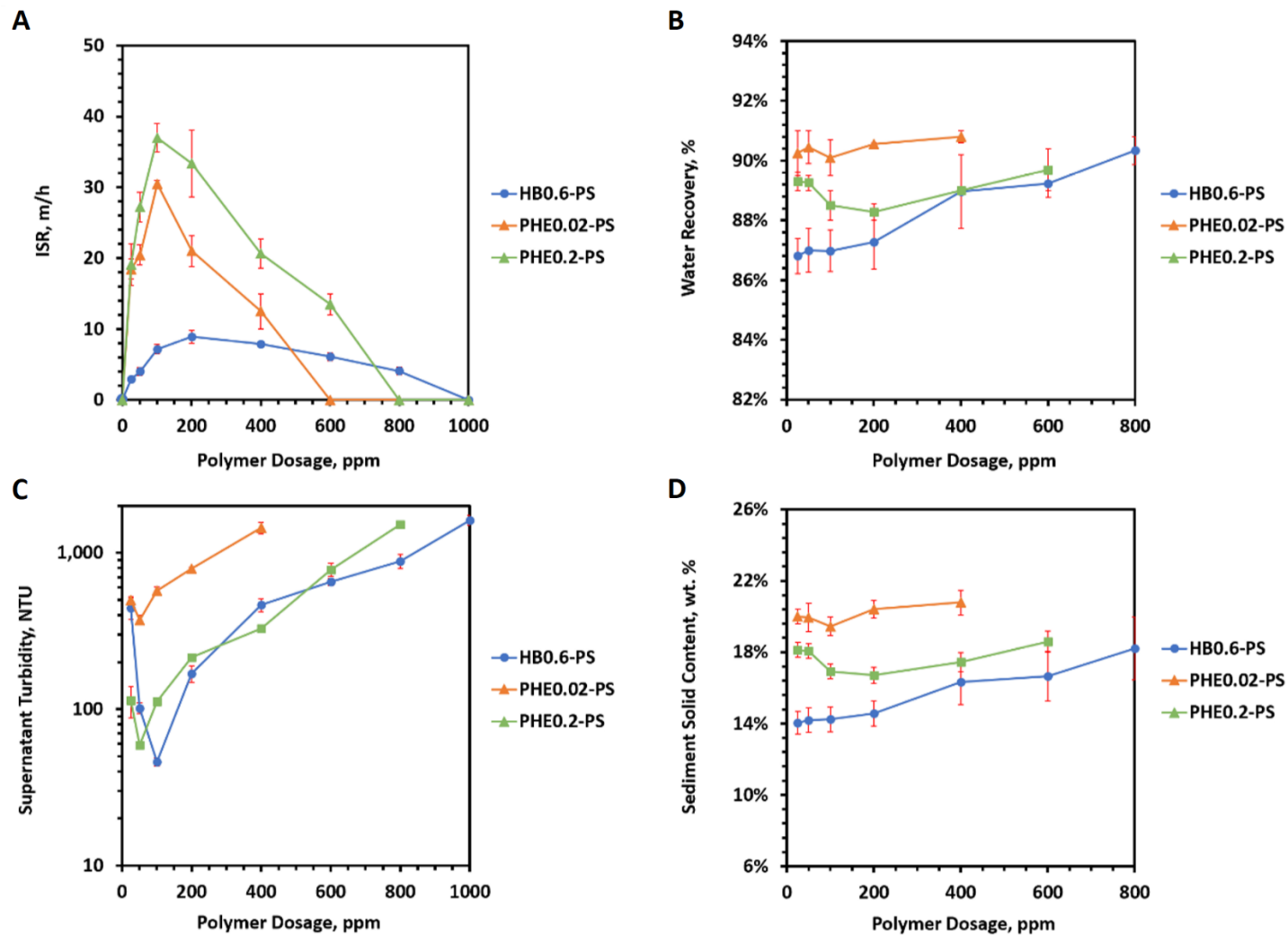


**Figure 2.12.** Initial settling rate (A), water recovery (B), supernatant turbidity (C), and sediment solids content (D) of settling tests of 2 wt % MFT using PHE0.02-PS or PHE0.2-PS at polymer doses from 0 to 1000 ppm (dry/slurry) at 50 °C and compared to HB0.6-PS.

We next employed PHE0.2-PS for the flocculation of 10 wt % MFT and its performance was plotted against the polymer dose and compared to the thermoresponsive HB1.9-PS sample (Fig. 2.13A-D). No flocculation was observed until a dose of 100 ppm was reached for PHE0.2-PS, which was at a lower dose compared to HB1.9-PS that required 200 ppm to show its flocculating ability. At 100 ppm or above, the ISR of PHE0.2-PS increased only marginally with increasing dose while the ISR of HB1.9-PS increased at a faster rate starting from 400 ppm (Fig. 2.13A). Moreover, at 400 ppm and above, HB1.9-PS exhibited significantly lower ST and higher WR and SSC than PHE0.2-PS (Fig. 2.13B-D). It is worth mentioning that the thermoresponsive effect of HB1.9-PS became more pronounced with increasing dose, indicated by the increase in the change in transmittance (Table 2.2, entry 2). These findings suggested that at 400 ppm or above, the HB1.9-PS sample exhibited superior flocculation performance for 10 wt % MFT due to its thermoresponsivity, when compared to the non-thermoresponsive PHE0.2-PS sample.

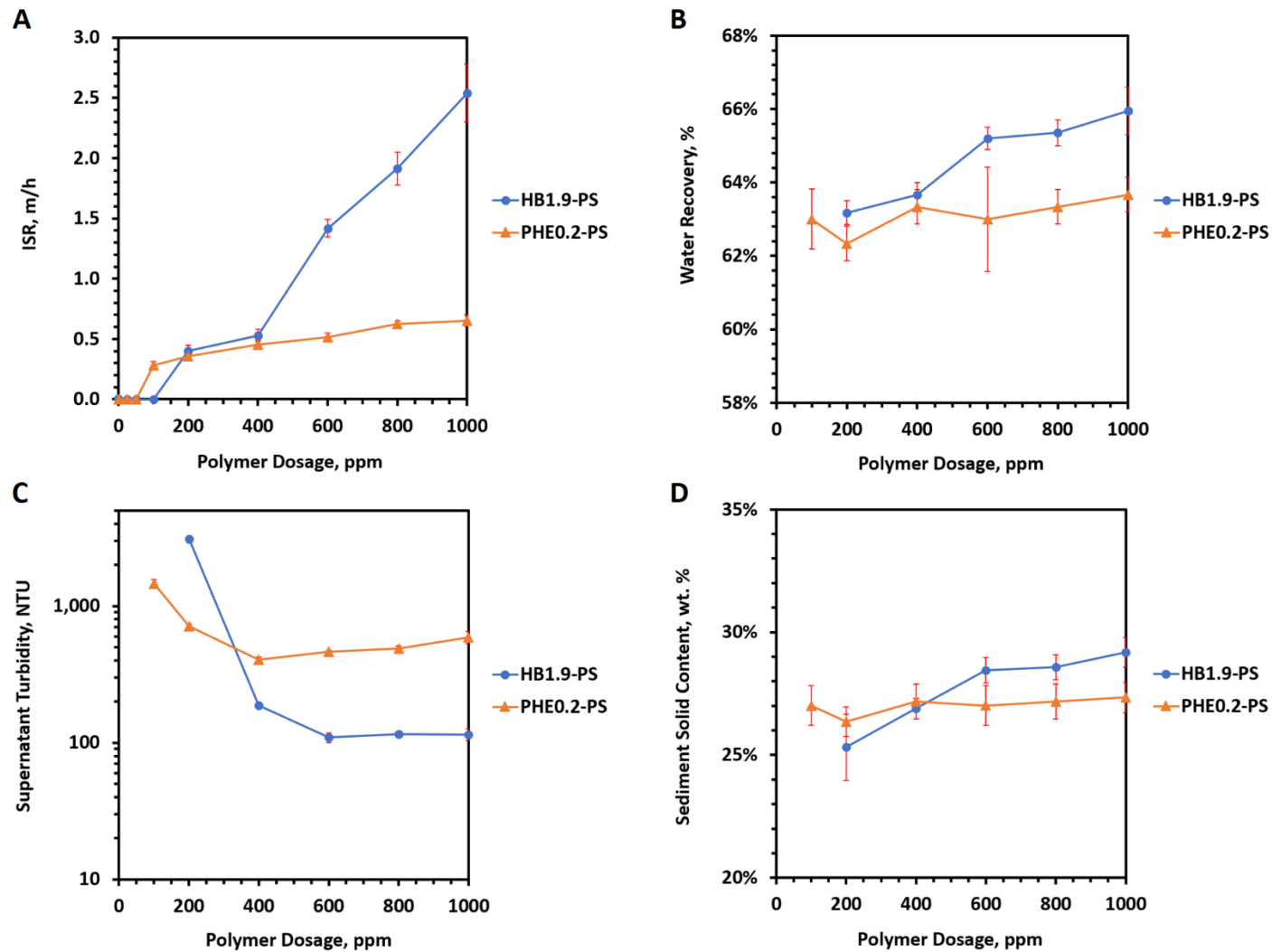


**Figure 2.13.** Initial settling rate (ISR, **A**), water recovery (**B**), supernatant turbidity (**C**), and sediment solids content (**D**) of the settling tests of 10 wt % MFT using PHE0.2-PS at polymer doses from 0 to 1000 ppm (dry/slurry) at 50 °C and compared to HB1.9-PS.

### 2.3.5 Comparison with other Thermoresponsive Polymers

Comparing the performance of other thermoresponsive polymers as flocculants of MFT using data reported in the literature is of interest; however, it should be noted that the results are highly dependent upon the test conditions and the MFT themselves. As mentioned in the introduction, there has only been a few other studies reporting the flocculation of MFT using thermoresponsive polymers. A study, by Li et al. in 2015, reported that the flocculation of 10 wt % MFT fractions, which contained  $< 2 \mu\text{m}$  or  $< 10 \mu\text{m}$  fine particles, was quite successful using PNIPAM (LCST =  $32 \text{ }^\circ\text{C}$ ) with an unspecified molecular weight.<sup>139</sup> At doses of 120-160 ppm, the PNIPAM exhibited very high ISRs of 21.3-22.5 m/h and relatively low STs of 93-95 NTU at  $50 \text{ }^\circ\text{C}$  while no flocculation was observed at  $25 \text{ }^\circ\text{C}$ . For comparison, HB1.9-PS was able to flocculate 10 wt % MFT and produced a supernatant with a similar turbidity (109 NTU) but at a significantly lower ISR (1.4 m/h) at a dose of 600 ppm. The difference in the settling rates is most likely due to the difference in MFT in that the MFT fractions used by Li et al. were more homogenous in particle size,<sup>139</sup> and it has been shown that the heterogeneous composition of MFT makes the flocculation process more difficult.<sup>111</sup>

Another study, by Zhang et al. in 2017, also reported the flocculation of 10 wt % MFT using PNIPAM ( $M_n = 324 \text{ kDa}$ , LCST =  $32 \text{ }^\circ\text{C}$ ).<sup>11</sup> Surprisingly, in contrast to the studies by Li et al.,<sup>139</sup> only very modest differences were found in the flocculation performance of the PNIPAM between the settling tests conducted at  $25 \text{ }^\circ\text{C}$  and  $50 \text{ }^\circ\text{C}$ .<sup>11</sup> At 1000 ppm, the PNIPAM exhibited an ISR of 3.6 m/h and an ST of 420 NTU,<sup>11</sup> and both parameters were significantly worse than the data reported by Li et al.<sup>139</sup> The significantly different results obtained by these two groups with PNIPAM may be due to differences in the molecular weight of the PNIPAM,



the test conditions and the MFT. With the use of 1000 ppm of the PNIPAM, the WR and SSC were reported to be 64 % and 31 wt %, respectively.<sup>11</sup> At the same dose, the HB1.9-PS exhibited an ISR of 2.5 m/h, an ST of 115 NTU, a WR of 66 % and an SSC of 29.2 wt %, and these results were comparable to those of the PNIPAM discussed above.

## **2.4 Conclusion**

We have demonstrated that thermoresponsive HB-CSs and HB-PS were capable of flocculating MFT. Thermoresponsivity was absolutely required for optimal flocculation performance in that they were considerably more effective in several respects at temperatures above their LCST than below. In terms of ISRs, the HB1.9-PS was considerably better than the HB1.9-CS and this was especially so with 10 wt % MFT. Moreover, the hydrophobically modified, non-thermoresponsive PHE-PSs were also capable of flocculating MFT but they usually performed worse than the thermoresponsive starches, especially when flocculating 10 wt % MFT. Overall, the best flocculant to be used for 2 wt % MFT was HB1.9-PS at 1000 ppm (ISR: 58 m/h, WR: 89 %, ST: 21 NTU and SSC: 17.4 wt %) or PHE0.2-PS at 50 ppm (ISR: 27 m/h, WR: 89 %, ST: 59 NTU and SSC: 18.1 wt %), and the best performer for 10 wt % MFT was HB1.9-PS at 1000 ppm (ISR: 2.5 m/h, WR: 66 %, ST: 115 NTU and SSC: 29.2 wt %).

## Chapter 3

# Cationic Starches for the Flocculation of Oil Sands Mature Fine Tailings

### 3.1 Introduction

The flocculants that appear to be the most widely used by the oil sands industry are anionic polyacrylamides (PAM). However, the supernatants generated with these flocculants are quite turbid, which is mainly due to the negative charges on the clays and other ultrafines. As a result, cationic polymers have begun to attract more attention and have been examined as flocculants of MFT and of so-called MFT models such as kaolin or silica suspensions. Some examples are discussed below.

Cationic PAM, prepared by modification of PAM or copolymerization of acrylamide and comonomers with cationic moieties, is one of the most used and studied polymeric flocculants.

In 2006, Zhou and Franks employed two cationic copolymers of acrylamide and diallyldimethylammonium chloride (poly(AM-*co*-DADMAC), Fig. 3.1A) with charge densities of 10 % and 40 % as well as a cationic homopolymer of DADMAC (poly(DADMAC), Fig. 3.1B) with a charge density of 100 % to flocculate a 0.16 wt % silica particle suspension.<sup>125</sup> The authors suggested that the 10 % charged polymer facilitated the bridging of the silica particles, the 40 % charged polymer induced charge neutralization at its

optimal dose while the 100 % charged polymer flocculated the particles by electrostatic patch mechanism at its optimal dose.

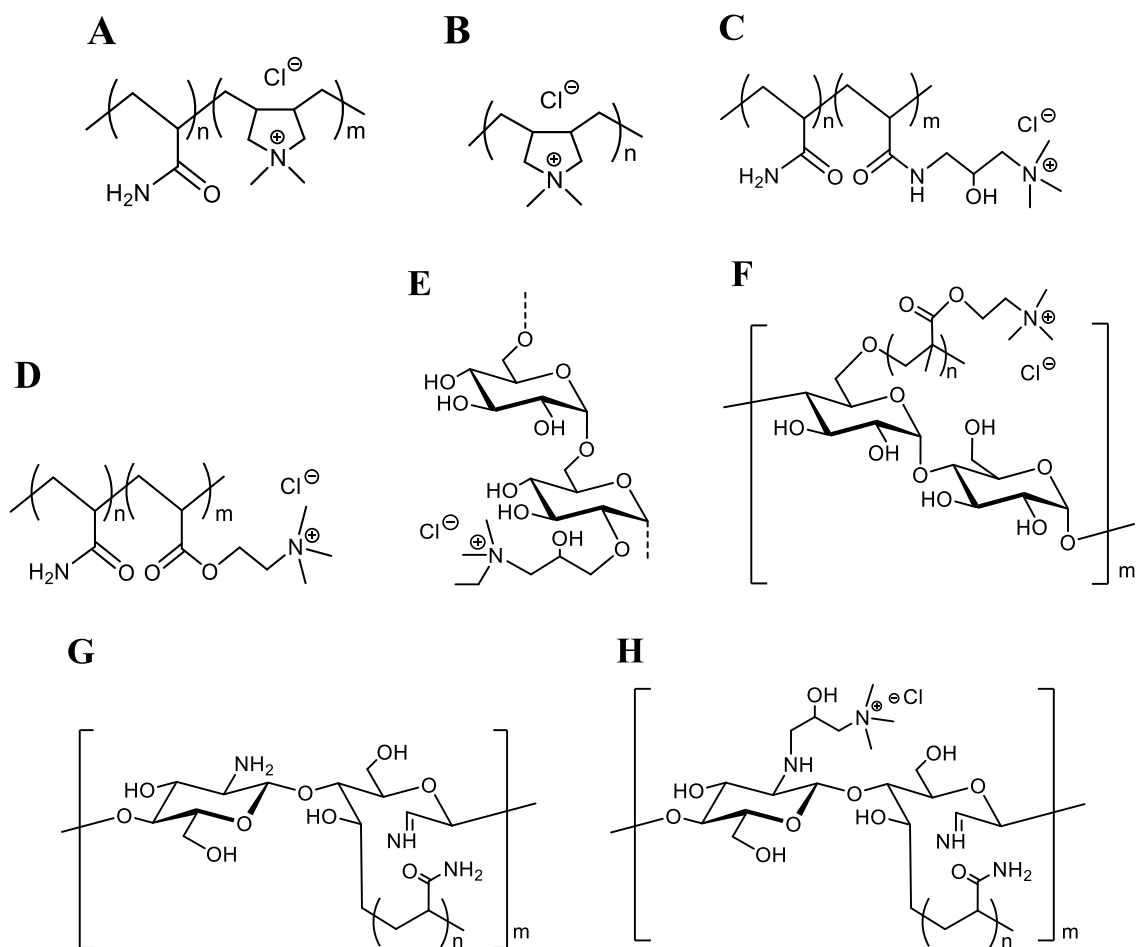


**Figure 3.1.** Chemical structures of poly(AM-*co*-DADMAC) (A), poly(DADMAC) (B), poly(AM-*co*-AMHP) (C), Zetag 8110 (D), dextran-EDHPAC (E), starch-*g*-PDMC (F), chitosan-*g*-PAM (G), and chitosan-CHPTAC-*g*-PAM (H).

In 2009, Wang et al. flocculated 0.25 wt % kaolin suspensions using a cationic copolymer of acrylamide and acryloylamino-2-hydroxypropyltrimethylammonium chloride (poly(AM-*co*-AMHP), Fig. 3.1C).<sup>126</sup> They showed that by the use of 0.2 ppm of this cationic copolymer, the transmittance of the kaolin suspension with a pH of 4 increased from below 25

% to 97 %, and upon the increase of the polymer dose, the transmittance reduced because of overdosing. More recently, Wang et al. examined a commercial cationic PAM (Zetag 8110, Fig. 3.1D) as a flocculant of 5 wt % MFT.<sup>127</sup> They found that the flocculation performance became much better when the Zetag 8110 was hydrolyzed at a slightly alkaline condition at 70 °C for 18 h before use. A supernatant turbidity (ST) as low as 153 NTU was achieved when the hydrolyzed Zetag 8110 at a dose of 1.5 kg per ton of MFT solids was used.

Vajihinejad et al. synthesized a series of poly(AM-co-DADMAC)s (Fig. 3.1A) with different composition and molecular weights to investigate the effect of chemical composition and molecular weight of poly(AM-co-DADMAC) on its flocculation performance of 5 wt % MFT.<sup>128</sup> They found that the copolymer with a high molecular weight (about 1.8 million Da) resulted in a fast ISR but suffered from a high ST, and the copolymer with a high DADMAC composition led to a low ST. One of the best results obtained (an ISR of 0.24 m/h and an ST of 3.5 NTU) was achieved with the use of 4000 ppm of poly(AM-co-DADMAC) with an acrylamide molar ratio of 0.24 and a molecular weight of 200 kDa.

Recently, biopolymer-based flocculants have been reported to effectively flocculate kaolin, clay, quartz and MFT. Biopolymers such as starch, chitosan, cellulose, dextran and guar gum are usually used as base materials to prepare the biopolymer-derived flocculants.

Ghimici and Nichifor used cationic dextrans (Fig. 3.1E), prepared by reacting dextran with epichlorohydrin and *N,N*-dimethylethylamine to obtain the cationic *N*-ethyl-*N,N*-dimethyl-2-hydroxypropylene ammonium chloride (EDHPAC) groups with molar substitution (MS) ranging from 0.18 to 1.10, to flocculate 1 wt % clay suspensions containing kaolinite,

montmorillonite and quartz.<sup>145</sup> They observed that the optimal dose decreased from 24 to 1.6 ppm with the increasing MS of the cationic groups from 0.18 to 1.10. They also reported that the ST values decreased with increasing flocculant dose but reached a minimum which was followed by an increase in the ST at higher dose.

In 2013, Wang et al. reported the flocculation of a 0.25 wt % kaolin clay suspension using starch, PAM and starch-graft-poly(2-methacryloyloxyethyl) trimethylammonium chloride (starch-*g*-PDMC, Fig. 3.1F).<sup>146</sup> The authors found that starch was not able to flocculate the clay particles while under 1 ppm of starch-*g*-PDMC effectively flocculated the clay particles to achieve an ST of under 25 NTU at the pH range from 4 to 10. The starch-*g*-PDMC showed superior performance to PAM, especially under alkaline conditions.

Yuan et al. reported the use of chitosan-*g*-PAM (Fig. 3.1G) to flocculate a 0.07 wt % kaolin suspension and showed that 0.1 ppm of the chitosan-*g*-PAM produced the most clarified supernatant.<sup>164</sup> Shortly thereafter, the same group of researchers reported the flocculation of *N*-(3-chloro-2-hydroxypropyl) trimethyl ammonium chloride (CHPTAC) modified chitosan-*g*-PAM (chitosan-CHPTAC-*g*-PAM, Fig. 3.1H) with various MS of CHPTAC from 0.282 to 0.447.<sup>147</sup> The chitosan-CHPTAC-*g*-PAM with an MS of 0.447 successfully flocculated a kaolin suspension with initial turbidity of 90 NTU to give a clean supernatant with 98.5 % transparency at an optimal dose of 0.2 ppm. Molatlhegi and Alagha also used chitosan-*g*-PAM to flocculate a kaolin suspension with a solid content of 5 wt %.<sup>148</sup> The use of 40 ppm chitosan-*g*-PAM significantly accelerated the settling rate from 1.1 m/h without polymer addition to a maximum of 24.84 m/h. The effect of polymer stock concentration was investigated, and a

higher concentration stock dispersion resulted in a higher ISR. The chitosan-*g*-PAM performed much better than chitosan and performed almost similar to commercial PAM.

In 2018, Oliveira et al. prepared cationic chitosan (chitosan-CHPTAC) by reacting chitosan with CHPTAC and chitosan grafting with PAM (chitosan-*g*-PAM).<sup>152</sup> Both chitosan-based flocculants were used to flocculate 5 wt % MFT and compared to cationic PAM. Chitosan-*g*-PAM showed higher ISR than chitosan-CHPTAC when a dose range from 3000 to 10000 ppm was examined but the cationic PAM did not flocculate the MFT. The highest ISR achieved was 20.7 m/h with the addition of 10000 ppm chitosan-*g*-PAM. Moreover, chitosan-*g*-PAM caused a much lower ST than chitosan-CHPTAC at a polymer dose below 7000 ppm.

Many researchers have showed that starch is an effective biopolymer-based flocculant for silica or clay suspensions after attaching cationic moieties on the hydroxyl (OH) groups on the starch. In 2005, Pal et al. synthesized a series of cationic starch using CHPTAC with MS from 0.42 to 0.86 and used them to flocculate 0.25 wt % silica suspension.<sup>165</sup> The lowest ST of 4 NTU was achieved when 0.75 ppm of the cationic starch synthesized with a molar ratio of 0.72 was used. In 2007, Chen et al. reported the flocculation of 1 wt % kaolin suspension using cationic corn starch (Cat-CS) modified with CHPTAC and an MS of 0.47.<sup>166</sup> The authors suggested that the adsorption of the cationic starch on the clay particle surface was fast, but the rate of aggregation and frequency of collisions were slow, which were the rate determining step of flocculation. Later on, the same group of researchers reported the flocculation of 1 wt % kaolin suspension by Cat-CS with MS from 0.32 to 0.63 and showed that the Cat-CS with an MS of 0.51 had the highest flocculation efficiency.<sup>167</sup> Bratskaya et al. reported high flocculation efficiency when flocculating 0.01 to 0.5 wt % kaolin suspension using cationic

potato starch (Cat-PS) with the MS of CHPTAC ranging from 0.25 to 1.54.<sup>168</sup> The authors suggested that both bridging and electrostatic patch mechanisms occurred for flocculation of kaolin suspension by Cat-PS. Sableviciene et al. modified hydroxyethyl starch or potato starch with 2,3-epoxypropyltrimethylammonium chloride to obtain cationic starches with MS ranging from 0.21 to 0.57 and used them to flocculate a 5 wt % kaolin suspension.<sup>169</sup> The cationic hydroxyethyl starch was more soluble than Cat-PS and it was suggested that the Cat-PS formed a transparent colloidal dispersion. The flocculation performance of Cat-PS was overall much better than that of the cationic hydroxyethyl starch. The best performing Cat-PS had an MS of 0.32 and the optimal dose was 16000 ppm.

The above results suggest that cationic starches may be an effective flocculant of MFT. To our best knowledge, cationic starch has not been examined as a flocculant of MFT. In this chapter, we describe the preparation of a series of cationic starches, prepared by modifying starch with CHPTAC, and their flocculation performance on oil sands MFT.

## **3.2 Materials and Methods**

### **3.2.1 Materials**

Cooked, high amylopectin waxy corn starch (CS) was obtained from EcoSynthetix Inc. (Burlington, Ontario, Canada). Neutral, pre-gelatinized, high amylopectin potato starch (PS) was a gift from Coöperatie AVEBE U.A. (Veendam, The Netherlands). Oil sands MFT (about 35 wt %, D10: 1.6  $\mu\text{m}$ , D50: 6.9  $\mu\text{m}$  and D90: 19.2  $\mu\text{m}$ ) was originally obtained from Syncrude Canada Ltd and provided to us by Joao Soares, University of Alberta, Canada. *N*-(3-Chloro-2-hydroxypropyl) trimethyl ammonium chloride (CHPTAC) (60 wt % solution in H<sub>2</sub>O) was

obtained from Sigma-Aldrich Co. (USA). Other reagents and solvents were commercially available and used without further purification unless stated otherwise.

### **3.2.2 Preparation of CS and PS Modified with CHPTAC**

CS or PS (1 g) was dispersed in deionized water at 40 °C for 2 h to give an approximately 25 wt % dispersion. The dispersion was cooled to room temperature (rt) followed by the dropwise addition of 10 M NaOH with vigorous stirring which gave a dispersion with a pH of 13. A pre-determined amount of CHPTAC was added and the mixture was stirred vigorously at 50 °C for 18 h. After that, the mixture was cooled to rt and 1 M HCl was added to neutralize the mixture under vigorous stirring. The neutralized mixture was subjected to dialysis against deionized water for 2 days using a dialysis bag with molecular weight cut-off ( $MW_{\text{cutoff}}$ ) of 1 kD. A minimum of 5 water replacements were performed over the course of 2 days. The overall dilution ratio was approximately 1:10<sup>10</sup>. The dialyzed cationic starches were lyophilized for at least 3 days to yield a white powder.

### **3.2.3 Determination of Molar Substitution of Cationic Starches**

The molar substitution (MS) was determined using <sup>1</sup>H-NMR spectroscopy on a Bruker Avance 500 NMR spectrophotometer. The cationic starches (10 mg) were dispersed in deuterium oxide (D<sub>2</sub>O, 600 μL) to obtain their spectra. The molar substitution of cationic groups ( $MS_{\text{Cat}}$ ) was defined as the molar ratio of the cationic substituents to the anhydroglucose units (AGUs) of the starch molecules. The  $MS_{\text{Cat}}$  was calculated using Eq. 3.1:



$$MS_{\text{Cat}} = \frac{I_{\text{CHOH}}}{I_{\text{H}_a}}$$

### Equation 3.1

where  $I_{\text{CHOH}}$  is the integral value for the proton peak of the carbon atom bearing an OH group on the CHPTAC substituent at 4.30-4.45 ppm and  $I_{\text{H}_a}$  is the integral value for the anomeric proton ( $\text{H}_a$ ) at 5.20-5.85 ppm.

### 3.2.4 Settling Tests

The MFT had a solids content of approximately 35 wt % and was diluted to 2 or 10 wt % by the addition of tap water. All dilutions of MFT were prepared fresh and homogenized with a mechanical stirrer for 2 h before use in all settling tests. Cationic starch stock dispersions were prepared to a concentration of 50 g/L and stored at rt before use. For each settling test, 50 mL of the diluted MFT were stirred in a 100 mL beaker for 2 min at 600 rpm. A pre-determined amount of cationic starch dispersion was added dropwise to the diluted MFT over 2 min. The mixture was stirred in a 50 °C water bath for 8 min at 200 rpm. After that, the mixture was poured into a 50 mL graduated cylinder and inverted 3 times. The graduated cylinder was left undisturbed in a 50 °C water bath for 30 min before it was removed from the water bath and left at rt for the rest of the settling time. Mudline height was recorded as a function of settling time. For settling tests with high settling rates (> 50 m/h), a camera equipped with a close-up lens was used to record the position of the mudline over time. Initial settling rate (ISR), water recovery (WR), supernatant turbidity (ST) and sediment solids content (SSC) were determined as described in Section 2.2.6. All experiments were conducted at least 3 times to obtain representative results.

### 3.3 Results and Discussion

#### 3.3.1 Preparation of Cat-CS and Cat-PS

Cationic starches derived from corn starch and potato starch were synthesized in basic conditions using CHPTAC in varying mole equivalents from 0.04 to 0.4 (Fig. 3.2). The resultant cationic starches showed  $MS_{Cat}$  ranging from 0.02 to 0.25. An example of  $^1H$ -NMR spectra of Cat-CS and Cat-PS with an  $MS_{Cat}$  of 0.02 (Cat0.02-CS and Cat0.02-PS) is shown in Figures B1 and B2 in Appendix B. The reaction efficiency of the cationization reactions was around 60 %, which was comparable to that reported in the literature.<sup>170</sup>

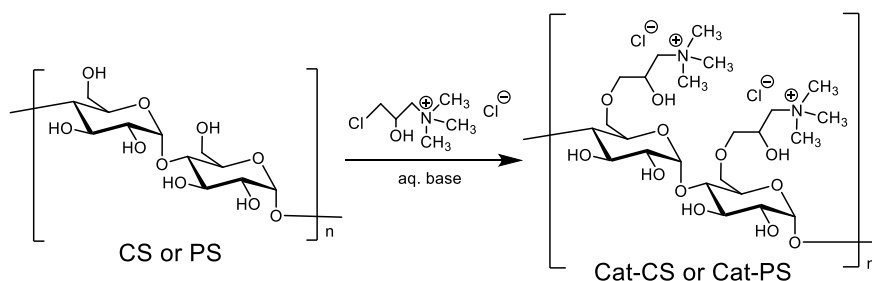


**Figure 3.2.** Preparation of Cat-CS and Cat-PS. Substitution is shown only at O-6 while in fact substitution can occur at O-2, O-3 and O-6.

#### 3.3.2 Settling Tests of 2 wt % MFT using Cat-CS

Settling tests were first conducted using Cat-CS with  $MS_{Cat}$  in a range from 0.02 to 0.25 and 2 wt % MFT. The settling tests were carried out at varying doses starting from 25 ppm till an optimal dose was reached.

##### 3.3.2.1 Initial Settling Rate

The effect of polymer dose on ISR was investigated using a series of Cat-CS (Fig. 3.3). Below a dose of 200 ppm, Cat0.02-CS failed to flocculate the 2 wt % MFT (Fig. 3.4A).

Cat0.02-CS started to flocculate at an ISR of 10 m/h from a dose of 200 ppm. The ISR continued to increase as the polymer dose increased until a maximum value was reached at 600 ppm where large flocs could be formed (Fig. 3.4B). Then, the ISR values decreased as the polymer dose increased to 800 ppm. The same trend was observed by Sableviciene et al. who used a cationic starch to flocculate a 5 wt % kaolin suspension.<sup>169</sup> The flocculant dose giving rise to the maximum ISR is considered as the optimal dose. The flocculation mechanism with Cat-CS can be explained mostly by charge neutralization but bridging and electrostatic patch mechanisms may play a role. At a dose higher than the optimal dose, the particle surfaces should be saturated with the cationic polymers, hence, the decreased ISR may be due to insufficient free particle surfaces for interparticle interactions (i.e. bridging and charge neutralization) to occur. Moreover, the adsorbed layers may also be causing steric repulsion between the particles (Fig. 3.4C). Most importantly, the overdose of Cat-CS may re-stabilize the particles and lead to a loss in flocculation ability.

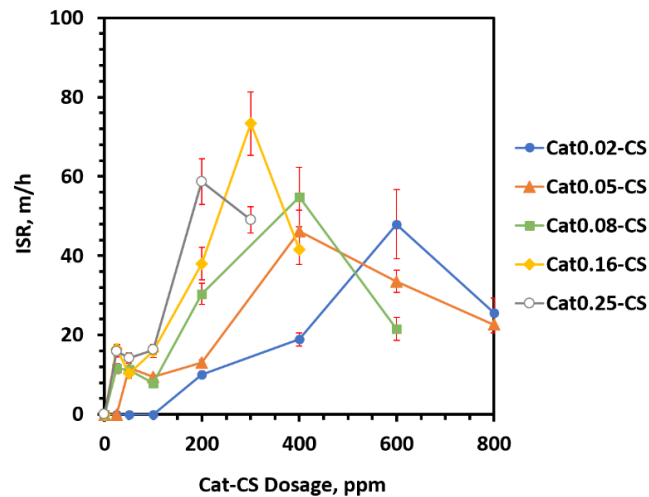


**Figure 3.3.** Initial settling rate (ISR) of the settling tests of 2 wt % MFT using Cat-CS with  $MS_{Cat}$  ranging from 0.02 to 0.25. Dosage was reported on the dry/slurry basis.

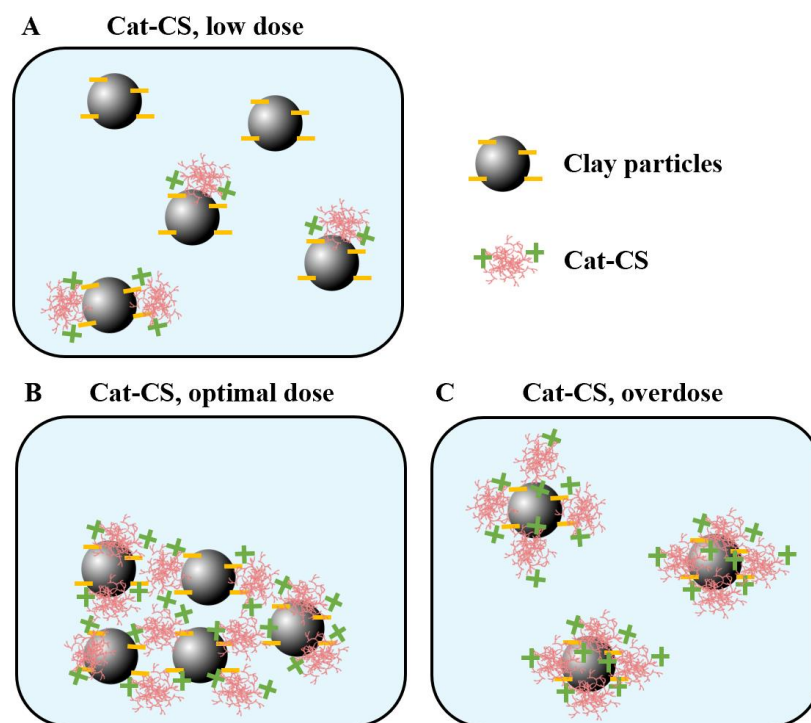


**Figure 3.4.** Schematic representation of flocculation of clay particles using Cat-CS at low dose (A), optimal dose (B), and overdose (C).

Cat0.05-CS started to flocculate the MFT from a dose of 50 ppm (Fig. 3.3). The ISR decreased slightly at a dose of 100 ppm and then increased with increasing flocculant dose to reach a maximum value at 400 ppm. A similar phenomenon was observed for Cat0.08-CS in that a dose of 25 ppm gave an ISR of 11.6 m/h and the optimal dose was 400 ppm. Moreover, optimal doses for Cat0.16-CS and Cat0.25-CS were 300 and 200 ppm, respectively. The optimal doses decreased from 600 to 200 ppm as the  $MS_{\text{Cat}}$  of Cat-CS increased from 0.02 to 0.25. The increase in the  $MS_{\text{Cat}}$  should increase the electrostatic attraction between the polymer and the negatively charged surface of the clay particles, hence, facilitating bridging and charge neutralization at a lower dose. The maximum ISRs of Cat0.02-, Cat0.05-, Cat0.08- and Cat0.25-CS were in a range from 46 to 58 m/h while the maximum ISR of Cat0.16-CS (73

m/h) was the highest among the five Cat-CS. The maximum ISRs seemed to become higher as the  $MS_{Cat}$  increased, however, this finding was somewhat inconclusive considering the experimental errors.

### 3.3.2.2 Water Recovery

Water recovery (WR) generally decreased as the cationic content increased, either by an increase in  $MS_{Cat}$  or the polymer dose. Using Cat0.25-CS as an example, WR decreased from 88 % to 80 % when the Cat0.25-CS dose increased from 25 to 300 ppm (Fig. 3.5). At a dose of 200 ppm, WR decreased from 88 % to 81 % when the  $MS_{Cat}$  increased from 0.02 to 0.25. It is intuitive that high cationic content can result in a more hydrophilic cationic starch. As the cationic starch becomes more hydrophilic, more water should be retained by the polymer and the water typically ends up in sediment and consequently, leading to a lower WR.

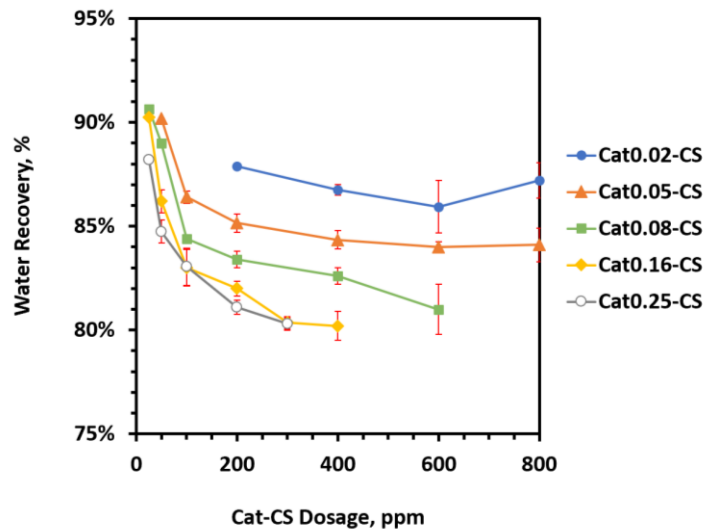


**Figure 3.5.** Water recovery of the settling tests of 2 wt % MFT using Cat-CS with  $MS_{Cat}$  ranging from 0.02 to 0.25. Dosage was reported on the dry/slurry basis.

### 3.3.2.3 Supernatant Turbidity

Supernatant turbidity (ST) describes the quality of the water recovered from the flocculation process. A high ST is a result of the presence of a large amount of stable clay particles in the supernatant. ST was relatively high at low Cat-CS doses (Fig. 3.6). Especially in the case of Cat0.02-CS, ST was higher than 1000 NTU when the Cat-CS dose was below 200 ppm. Moreover, although Cat0.08-, Cat0.16- and Cat0.25-CS were able to flocculate the 2 wt % MFT, the recovered water had high turbidity values of 965, 635, and 250 NTU, respectively. In general, ST decreased as the flocculant dose increased until a minimum was reached. This is also intuitive as a larger amount of Cat-CS in the MFT should cause the formation of new flocs or the growth of flocs to give larger flocs. The flocculant dose giving rise to a minimum ST is considered as the optimal dose regarding supernatant clarity. The optimal doses for Cat-CS decreased as the  $MS_{\text{Cat}}$  increased (Fig. 3.6). The optimal doses from the ST plot matched the optimal doses from the ISR plot. The lowest ST at 6 NTU was achieved by the addition of 300 ppm Cat0.16-CS.

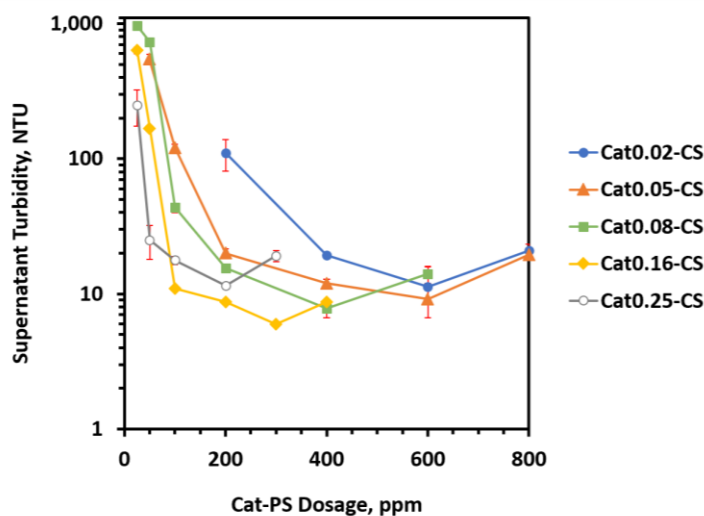


**Figure 3.6.** Supernatant turbidity of the settling tests of 2 wt % MFT using Cat-CS with  $MS_{Cat}$  ranging from 0.02 to 0.25. Dosage was reported on the dry/slurry basis.

### 3.3.2.4 Sediment Solids Content

SSC generally decreased with the increasing cationic content, for example, Cat0.16-CS decreased from 17.8 to 10 wt % as the polymer dose increased from 25 to 300 ppm (Fig. 3.7). At 200 ppm or above, Cat0.02-CS generally gave the highest SSC among the five Cat-CS tested. The low SSC given by Cat0.25-CS was most likely due to the high hydrophilicity which could entrap a relatively large amount of water in the flocs.

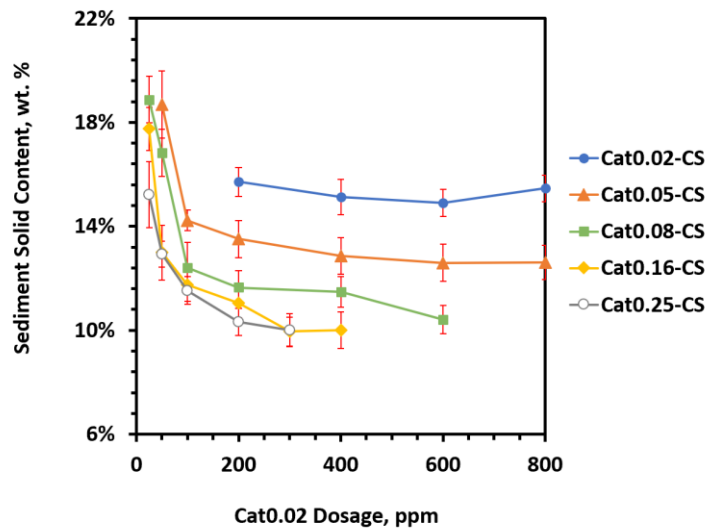


**Figure 3.7.** Sediment solids content of the settling tests of 2 wt % MFT using Cat-CS with  $MS_{Cat}$  ranging from 0.02 to 0.25. Dosage was reported on the dry/slurry basis.

### 3.3.3 Settling Tests of 2 wt % MFT using Cat-PS

Settling tests were conducted using Cat0.02-PS with an  $MS_{Cat}$  of 0.02 and 2 wt % MFT. The settling tests were carried out at varying doses from 25 to 800 ppm and compared to the flocculation performance given by the Cat0.02-CS.

#### 3.3.3.1 Initial Settling Rate

Cat0.02-PS successfully flocculated the 2 wt % MFT starting at a dose of 100 ppm (Fig. 3.8), which was 100 ppm lower than the dose that Cat0.02-CS started to show its flocculation ability. As the dose of Cat0.02-PS increased to 400 ppm, the ISR increased to 92 m/h at which point the maximum ISR was reached. The optimal dose of Cat0.02-PS was 200 ppm lower than that of Cat0.02-CS and the maximum ISR of Cat0.02-PS was almost two times higher. It was clear that the flocculant derived from potato starch had a much higher ISR than the one derived from corn starch, given that the  $MS_{Cat}$  was the same. This could be due to the



presence of naturally occurring phosphate esters on potato starch but absence in corn starch, which was determined by the  $^{31}\text{P}$ -NMR analysis discussed in Section 2.3.1. The anionic phosphate groups should enhance the electrostatic interactions, thus, leading to the formation of larger flocs and a higher ISR for the PS-based flocculants. Further increasing the Cat0.02-PS dose resulted in a decrease in ISR (Fig. 3.8) and this phenomenon was also observed in the settling tests using Cat0.02-CS.

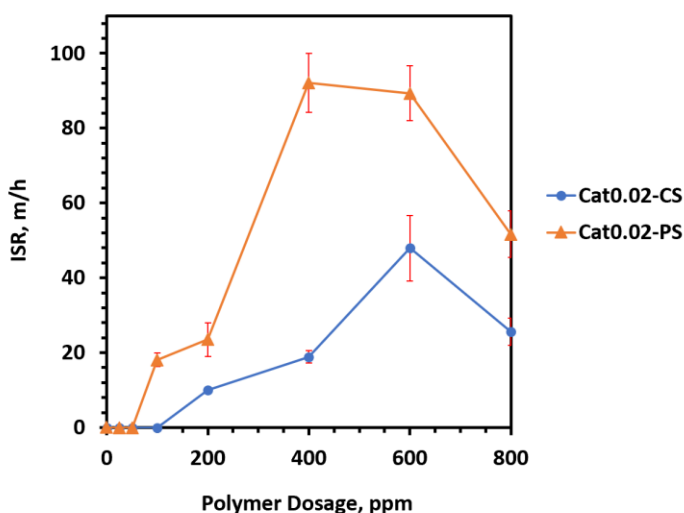


**Figure 3.8.** Initial settling rate (ISR) of the settling tests of 2 wt % MFT using Cat0.02-PS and Cat0.02-CS with varying doses ranging from 25 to 800 ppm (on the dry/slurry basis).

### 3.3.3.2 Water Recovery

At a Cat0.02-PS dose of 100 ppm, WR was at 89 % and the WR decreased to 86 % when the flocculant dose increased to 200 ppm (Fig. 3.9). The WR stayed at around 85-86 % from 200 to 800 ppm, which was generally lower than the WR resulting from Cat0.02-CS. This observation supported that the flocs produced by Cat0.02-PS could hold more water due

to the higher hydrophilicity of PS and consequently, the dewatering ability of Cat0.02-PS was slightly lower than that of Cat0.02-CS.

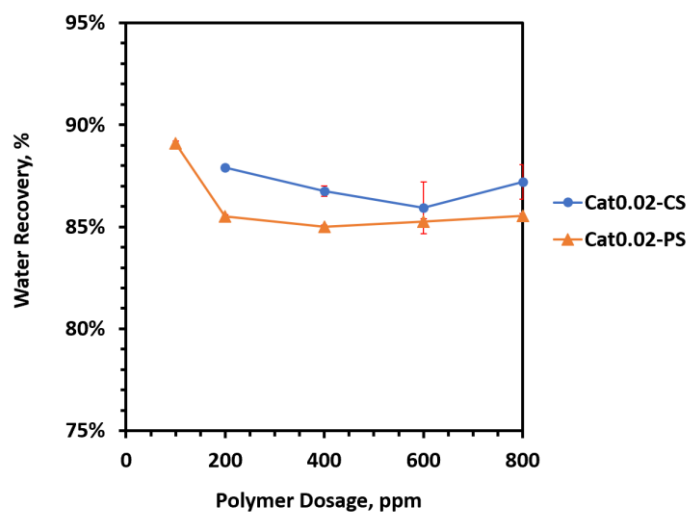


**Figure 3.9.** Water recovery of the settling tests of 2 wt % MFT using Cat0.02-PS and Cat0.02-CS with varying doses ranging from 25 and 800 ppm (on the dry/slurry basis).

### 3.3.3.3 Supernatant Turbidity

The lowest ST (19 NTU) was achieved by the use of 400 ppm of Cat0.02-PS (Fig. 3.10). The optimal dose for Cat0.02-PS was 200 ppm lower than that of Cat0.02-CS. Below 400 ppm, the use of Cat0.02-PS resulted in a cleaner supernatant than using Cat0.02-CS and the opposite was observed when the dose was above 400 ppm.

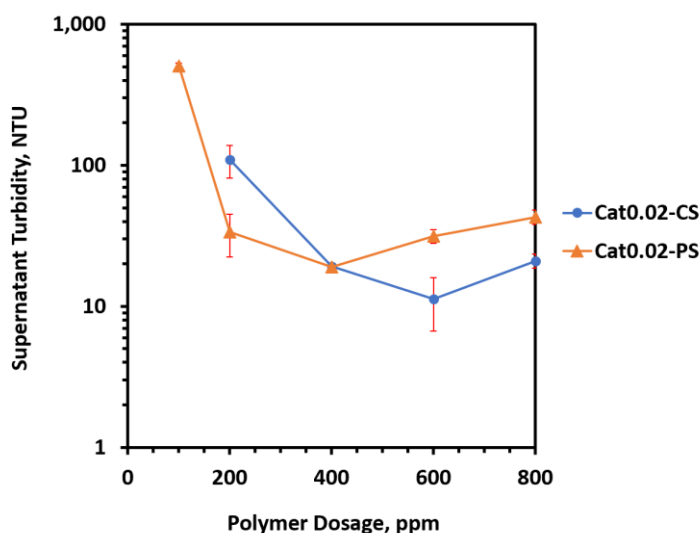


**Figure 3.10.** Supernatant turbidity of the settling tests of 2 wt % MFT using Cat0.02-PS and Cat0.02-CS with varying doses ranging from 25 and 800 ppm (on the dry/slurry basis).

### 3.3.3.4 Sediment Solids Content

When 100 ppm of Cat0.02-PS was used, sediment was relatively dense at an SSC of 16.4 wt % (Fig. 3.11). The SSC decreased to 13.7 wt % when the dose of Cat0.02-PS increased to 200 ppm and remained more or less constant at approximately 13 wt % at doses ranging from 200 to 800 ppm. As discussed in Section 3.3.3.3, ST was relatively high at 505 NTU when 100 ppm of Cat0.02-PS was used. This observation suggested that despite some solids particles were flocculated after treating the MFT with 100 ppm of Cat0.02-PS, a considerable amount of hydrophilic clay particles still remained suspended in the supernatant. When the Cat0.02-PS dose increased to 200 ppm or above, most of the suspended clay particles would be flocculated by the additional amount of Cat0.02-PS. Floccs containing hydrophilic clay particles may retain more water than other solids particles, which could explain the decrease in SSC with the increasing dose of Cat0.02-PS. SSC was generally higher for Cat0.02-CS

compared to Ca0.02-PS at the same dose (Fig. 3.11), which suggested that the Cat0.02-CS formed a denser sediment than the Cat0.02-PS did.

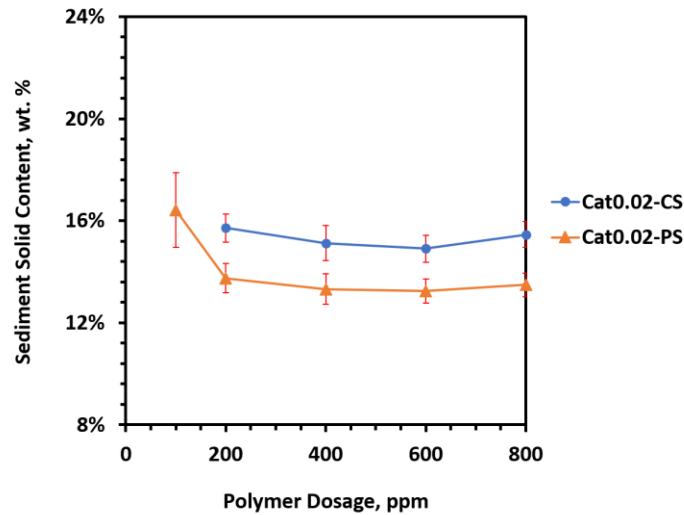


**Figure 3.11.** Sediment solids content of the settling tests of 2 wt % MFT using Cat0.02-PS and Cat0.02-CS with varying doses ranging from 25 and 800 ppm (on the dry/slurry basis).

### 3.3.4 Settling Tests of 10 wt % MFT using Cat-CS and Cat-PS

Flocculation of 10 wt % MFT was unsuccessful with the use of Cat0.02-CS or Cat0.02-PS at a dose up to 1000 ppm. However, the settling tests using 1000 ppm of Cat0.2-PS exhibited good performance in that an ISR of 9.3 m/h, a WR of 59 %, an ST of 21 NTU and an SSC of 23.2 wt % were achieved. The WR and SSC were somewhat unsatisfactory due to the high tendency of water retention by the PS-based flocculants, which is a common problem encountered in the flocculation of 2 wt % MFT by Cat-PS.

### 3.4 Comparison with other Polymers

It is interesting to compare the results obtained with our cationic starch (presented above) to the results obtained by others using other cationic polymers for MFT flocculation. However, we should point out that it is not possible to draw firm conclusions, in terms of whether one cationic polymer is more effective than another, from such a comparison as the results are affected by a number of factors, such as the source of MFT, that are difficult to control.

As mentioned in the introduction, a commercial cationic PAM, Zetag 8110, was examined by Wang et al. to flocculate 5 wt % MFT.<sup>127</sup> The Zetag 8110 has a cationic charge density of 10 % and a molecular weight of 12.7 million Da. After hydrolyzing Zetag 8110 at 70 °C for 18 h, cationic choline ions were released and the hydrolyzed Zetag 8110 became partially anionic (Fig. 3.12). The combination of the cationic and anionic Zetag 8110 caused an effective flocculation of 5 wt % MFT. The optimal ST of 153 NTU was achieved with the use of 75 ppm of the hydrolyzed Zetag 8110. Our results with cationic starch compared quite favorably to the Zetag 8110 in that the use of 50 ppm of Cat0.25-CS to flocculate 2 wt % MFT was able to achieve an ST of 50 NTU and the flocculation of 10 wt % MFT by 1000 ppm of Cat0.2-PS exhibited an impressively low ST of 21 NTU.

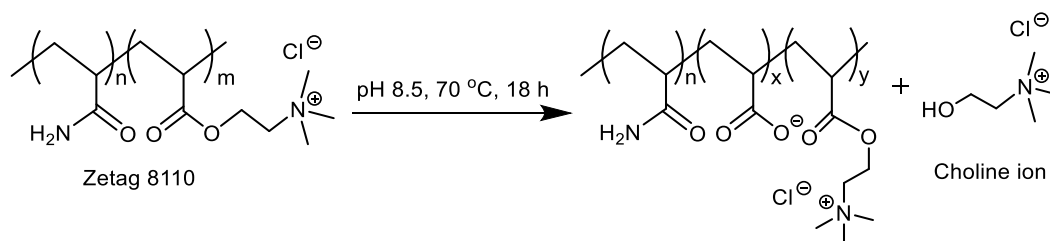


**Figure 3.12.** Partially hydrolyzed Zetag 8110.<sup>127</sup>

Vajihinejad et al. investigated the flocculation ability of a series of poly(AM-co-DADMAC) with different compositions.<sup>128</sup> The authors reported the use of 200 ppm (or 4000 ppm if calculated on the dry polymer/dry MFT solids basis, see Table B1 in Appendix B for the conversion between doses calculated on the dry/slurry and dry/dry basis). poly(AM-co-DADMAC) with an acrylamide molar ratio of 0.24 and a molecular weight of 200 kDa to flocculate 5 wt % MFT and achieved an ISR of 0.24 m/h and an ST of 3.47 NTU. For comparison, with the use of 1000 ppm of Cat0.2-PS to flocculate 10 wt % MFT, a relatively high ISR of 9.3 m/h and a reasonably low ST of 21 NTU were achieved. The use of Cat0.2-PS resulted in a much higher ISR, but a higher dose was required compared to poly(AM-co-DADMAC).

In 2018, Oliveira et al. examined the flocculation performance of a cationic chitosan (chitosan-CHPTAC) and chitosan-g-PAM, and showed that both polymers were effective in flocculating 5 wt % MFT.<sup>152</sup> At a dose of 500 ppm (or 10000 ppm calculated on the dry polymer/dry MFT solids basis), chitosan-CHPTAC and chitosan-g-PAM produced an ISR of 18.27 and 20.72 m/h, respectively and an ST of < 10 NTU. For comparison, 300 ppm of Cat0.16-CS successfully flocculated 2 wt % MFT with a high ISR of 73.3 m/h and an ST under 10 NTU.

### **3.5 Conclusion**

Overall, these results are promising in that both Cat-CS and Cat-PS can successfully flocculate 2 wt % MFT at relatively high settling rates and clean supernatants can be obtained. Cationic starch with a higher  $MS_{\text{Cat}}$  generally requires a lower dose to reach a maximum ISR

and a minimum ST, but it often causes a decrease in WR and SSC. A much higher ISR can be obtained by Cat-PS compared to Cat-CS but the Cat-PS often suffers from slightly deteriorated WR and SSC. Cationic starch with a low  $MS_{Cat}$  (0.02) failed to flocculate 10 wt % MFT but Cat0.2-PS was quite successful in the flocculation of 10 wt % MFT. Flocculation performance of our cationic starches is comparable to other cationic polymers.

## Chapter 4

# Dual Functional Starches for the Flocculation of Oil Sands Mature Fine Tailings

### 4.1 Introduction

In chapter 2, we demonstrated that thermoresponsive hydroxybutyl starch was capable of flocculating MFT and that the thermoresponsive nature of the polymer was essential for optimal results. In chapter 3, we demonstrated that cationic starch, in the form of starch modified with CHPTAC, was also an effective flocculant of MFT. These results prompted us to determine whether a superior MFT flocculant could be developed by combining these two features (thermoresponsivity and cationicity) in a single flocculant. In this chapter, we prepare starches bearing both features and examine them as MFT flocculants.

### 4.2 Materials and Methods

#### 4.2.1 Materials

Cooked, high amylopectin waxy corn starch (CS) was obtained from EcoSynthetix Inc. (Burlington, Ontario, Canada). Neutral, pre-gelatinized, high amylopectin potato starch (PS) was a gift from Coöperatie AVEBE U.A. (Veendam, The Netherlands). Oil sands MFT (about 35 wt %, D10: 1.6  $\mu\text{m}$ , D50: 6.9  $\mu\text{m}$  and D90: 19.2  $\mu\text{m}$ ) was originally obtained from Syncrude Canada Ltd and provided to us by Joao Soares, University of Alberta, Canada. *N*-(3-chloro-2-hydroxypropyl) trimethyl ammonium chloride (CHPTAC) (60 wt % solution in H<sub>2</sub>O) and 1,2-



butene oxide were obtained from Sigma-Aldrich Co. (USA). Other reagents and solvents were commercially available and used without further purification unless stated otherwise.

#### **4.2.2 The preparation of the Dual Functional CS and PS**

CS or PS (1 g) was dispersed in deionized water at 40 °C for 2 h to give an approximately 25 wt % dispersion. The dispersion was cooled to room temperature (rt) followed by the dropwise addition of 10 M NaOH with vigorous stirring which gave a dispersion with a pH of 13. Butene oxide was added and the mixture was stirred vigorously at 40 °C for 24 h. The mixture was cooled to rt and adjusted to a pH of 13. Subsequently, CHPTAC was added and the mixture was stirred vigorously at 50 °C for 18 h. After that, the mixture was cooled to rt and 1 M HCl was added to neutralize the mixture under vigorous stirring. The neutralized mixture was subjected to dialysis against deionized water for 2 days using a dialysis bag with molecular weight cut-off ( $MW_{\text{cutoff}}$ ) of 1 kD. A minimum of 5 water replacements were performed over the course of 2 days. The overall dilution ratio was approximately 1:10<sup>10</sup>. The cationic hydroxybutyl corn starch or potato starch (Cat-HB-CS or Cat-HB-PS) were lyophilized for at least 3 days after dialysis to yield a white powder.

#### **4.2.3 Determination of the Molar Substitution of the Dual Functional Starches**

The molar substitution (MS) was determined using <sup>1</sup>H-NMR spectroscopy on a Bruker Avance 500 NMR spectrophotometer. The Cat-HB-CS and Cat-HB-PS (10 mg) were dispersed in deuterium oxide (D<sub>2</sub>O, 600 μL) to obtain their spectra. The molar substitution of hydroxybutyl groups ( $MS_{\text{HB}}$ ) and that of cationic groups ( $MS_{\text{Cat}}$ ) were determined as described in Section 2.2.3 and Section 3.2.3, respectively.

#### **4.2.4 Determination of the LCST by Light Transmittance**

Light transmittance values were determined using a Cary 4000 Bio UV-Visible spectrophotometer equipped with a multi-cuvette holder and a temperature controller. The Cat-HB-CS and Cat-HB-PS were dispersed in deionized water to concentrations ranging from 0.025 g/L to 1 g/L for 16 h at 4 °C before measuring their transmittance. The temperature of the dispersion was measured by placing a temperature probe in a reference cell. The transmittance was recorded at 500 nm with a heating rate of 10 °C/min. The polymer dispersions were equilibrated for at least 5 minutes at 20 °C in a cuvette before starting the measurements. Absorbance data points were taken every 1 °C and recorded up to 60 °C. LCST is defined as the temperature at the inflection point of the transmittance curve of a 1 g/L polymer dispersion.

#### **4.2.5 Settling Tests**

The solids content of undiluted MFT is approximately 35 wt %. Tap water was used to dilute the MFT to 2 wt %, which was prepared fresh and homogenized with a mechanical stirrer for 2 h before use in settling tests. The stocks of the Cat-HB-CS and Cat-HB-PS dispersions were prepared and stored at 4 °C to a concentration of 50 g/L before use. For each settling test, 50 mL of the diluted tailings were used. The diluted tailings were stirred in a 100 mL beaker for 2 min at 600 rpm. A pre-determined amount of the polymer dispersion was added dropwise to the MFT mixture at 23 °C over 2 min. The mixture was stirred at 23 °C or in a 50 °C water bath for 8 min at 200 rpm. Subsequently, the mixture was poured into a 50 mL graduated cylinder followed by inverting 3 times. The graduated cylinder was then left undisturbed at 23

°C or at 50 °C (water bath). For settling tests at 50 °C, the graduated cylinder was removed from the 50 °C water bath after 30 min. Mudline height was recorded as a function of settling time. Flocculation performance was examined in terms of ISR, WR, ST and SSC, which were determined as described in Section 2.2.6. All experiments were conducted at least 3 times to obtain representative results.

## 4.3 Results and Discussion

### 4.3.1 Preparation of the Dual Functional Starches and their Thermoresponsivity

Cationic thermo-responsive starches were prepared by first hydroxybutylating cooked CS or PS to yield thermo-responsive starches and subsequently reacting with the cationic agent, CHPTAC, to yield Cat-HB-CS and Cat-HB-PS with both cationic and thermo-responsive functionalities (Fig. 4.1). An example of <sup>1</sup>H-NMR spectra of Cat-HB-CS with a molar substitution (MS) of cationic groups (MS<sub>Cat</sub>) of 0.02 and an MS of hydroxybutyl groups (MS<sub>HB</sub>) of 2.2 (Cat0.02-HB2.2-CS) and Cat-HB-PS with an MS<sub>Cat</sub> of 0.02 and an MS<sub>HB</sub> of 2.0 (Cat0.02-HB2.0-PS) is shown in Figures C1 and C2 in Appendix C.

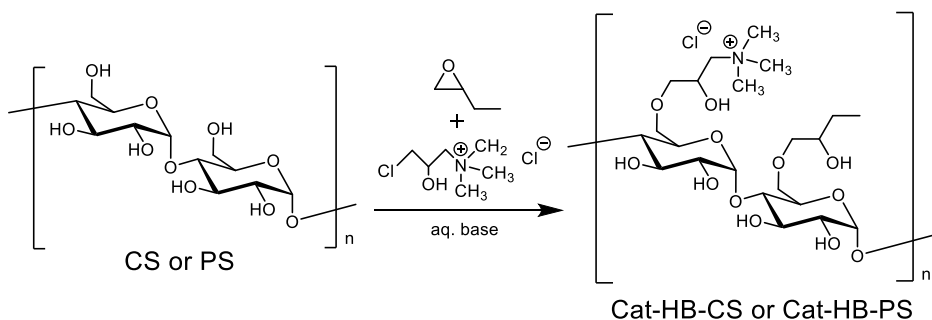


**Figure 4.1.** Preparation of Cat-HB-CS and Cat-HB-PS. Substitution is shown only at O-6 while in fact substitution can occur at O-2, O-3 and O-6.

Transmittance curves showing the phase transition due to temperature were obtained using Cat0.02-HB2.2-CS and Cat0.02-HB2.0-PS in aqueous dispersions with concentrations ranging from 50 to 1000 ppm (Fig. 4.2). The thermoresponsivity of Cat0.02-HB2.2-CS became noticeable at a concentration of 400 ppm or above (Fig. 4.2A) while Cat0.02-HB2.0-PS only began to show thermoresponsivity at 600 ppm or higher (Fig. 4.2B). At these concentrations, both polymers exhibited the LCST values lower than the settling temperature of 50 °C. Moreover, neither of the polymers experienced a complete dehydration of the polymer chains above their LCSTs indicated by the relatively high transmittance values of the dispersions at temperatures higher than their LCSTs. This was most likely due to charge stabilization provided by the cationic substituents on the polymers.

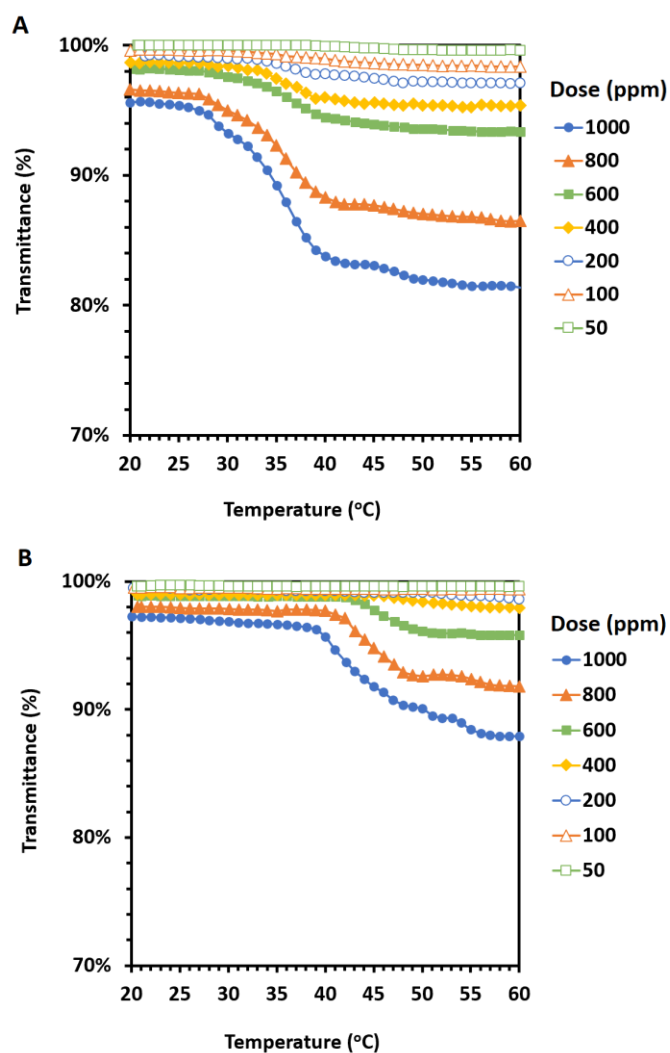


**Figure 4.2.** Light transmittance curves for aqueous dispersions of Cat0.02-HB2.2-CS (A) and Cat0.02-HB2.0-PS (B) with concentrations ranging from 0.05 g/L (50 ppm) to 1 g/L (1000 ppm).

### 4.3.2 Settling Tests of 2 wt % MFT using Cat-HB-CS

Settling tests were conducted using Cat0.02-HB2.2-CS and 2 wt % MFT at 23 °C and 50 °C. The settling tests were carried out at varying doses from 25 to 1000 ppm and compared to the flocculation results given by the HB2.3-CS and Cat0.02-CS samples.

### 4.3.2.1 Initial Settling Rate

At a settling temperature of 23 °C and at 50 ppm, Cat0.02-HB2.2-CS successfully flocculated the 2 wt % MFT with an ISR of 3.8 m/h (Fig. 4.3). At a low dose, the clay particles were only partially flocculated due to an insufficient amount of the polymers (Fig. 4.4A). The ISR continued to increase with the increasing flocculant dose, and a maximum ISR of 8.8 m/h was reached at the optimal dose of 200 ppm (Fig. 4.3). At the optimal dose, the majority of the clay particles could be effectively flocculated via bridging (Fig. 4.4B). Moreover, a lower ISR was obtained at a flocculant dose higher than 200 ppm and as the dose increased, the ISR decreased due to overdosing (Fig. 4.3). When overdosed, the polymers tend to stabilize the clay particles via steric stabilization, and as the polymers contain cationic groups, the charged groups may induce charge repulsion between the clay particles which impede the formation of flocs (Fig. 4.4C).

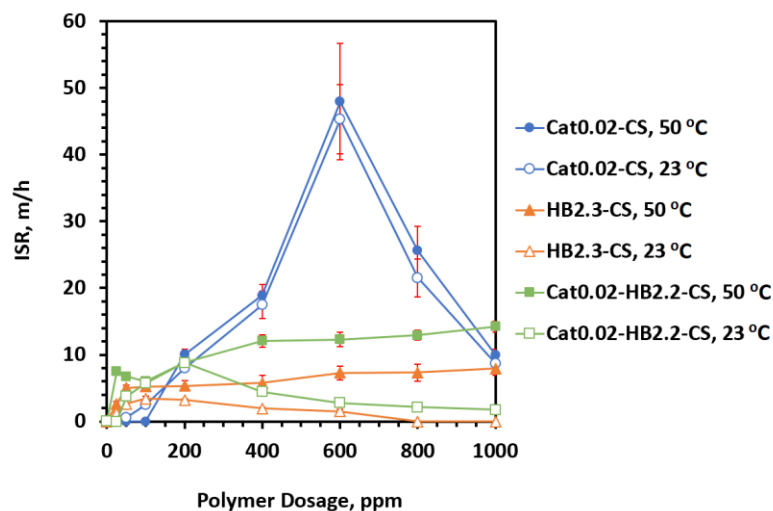


**Figure 4.3.** Initial settling rate (ISR) of the settling tests of 2 wt % MFT using Cat0.02-HB2.2-CS, Cat0.02-CS and HB2.3-CS with varying doses from 25 to 1000 ppm (dry/slurry).

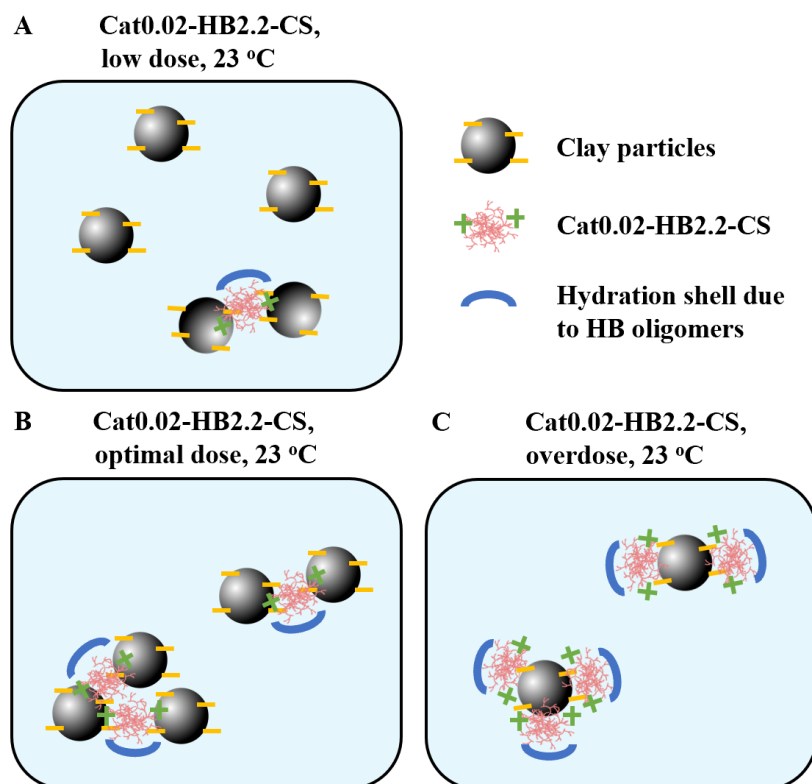


**Figure 4.4.** Schematic representation of flocculation of clay particles using Cat0.02-HB2.2-CS at low dose (**A**), optimal dose (**B**), and overdose (**C**) when settling at 23 °C.

At 23 °C, the HB2.3-CS, with a maximum ISR of 3.4 m/h at 100 ppm (Fig. 4.3), performed worse than the Cat0.02-HB2.2-CS across the dose range examined. The additional cationic charges on the Cat0.02-HB2.2-CS could facilitate the charge neutralization of clay particles as well as the adsorption of the polymers to the surfaces of clay particles via electrostatic attractions. The Cat0.02-CS had a slightly lower ISR at doses from 25 to 200 ppm but had a much higher maximum ISR (45 m/h) at an optimal dose of 600 ppm compared to Cat0.02-HB2.2-CS at 23 °C. At such concentration, clay particles could be charge neutralized and large flocs could form and cause the rapid settling (Fig. 4.5C). Since the Cat0.02-HB2.2-CS had a similar amount of cationic groups as the Cat0.02-CS did, one would expect the

Cat0.02-HB2.2-CS to have a similar ISR as Cat0.02-CS but the settling results suggested otherwise. This may be caused by the fact that clay particles are re-stabilized by the adsorbed layer of Cat0.02-HB2.2-CS, which contains a large number of hydroxybutyl (HB) substituents that are well hydrated below the LCST of the polymer. From previous studies on HB starch nanoparticles (HB-SNPs), the HB groups were found to be oligomerizing on the hydroxyl (OH) groups of HB-SNPs with a high  $MS_{HB}$ .<sup>154</sup> The well-hydrated HB oligomers may provide stability to the polymer adsorbed flocs via the formation of hydration shells on their surface below the LCST of the polymer (Fig. 4.5A and B). At a dose of 600 ppm, although the clay particles could be charged neutralized (by the cationic groups), the adsorbed layer of Cat0.02-HB2.2-CS may prevent the formation of large flocs due to steric stabilization (Fig. 4.5A), hence, a low ISR value was obtained.



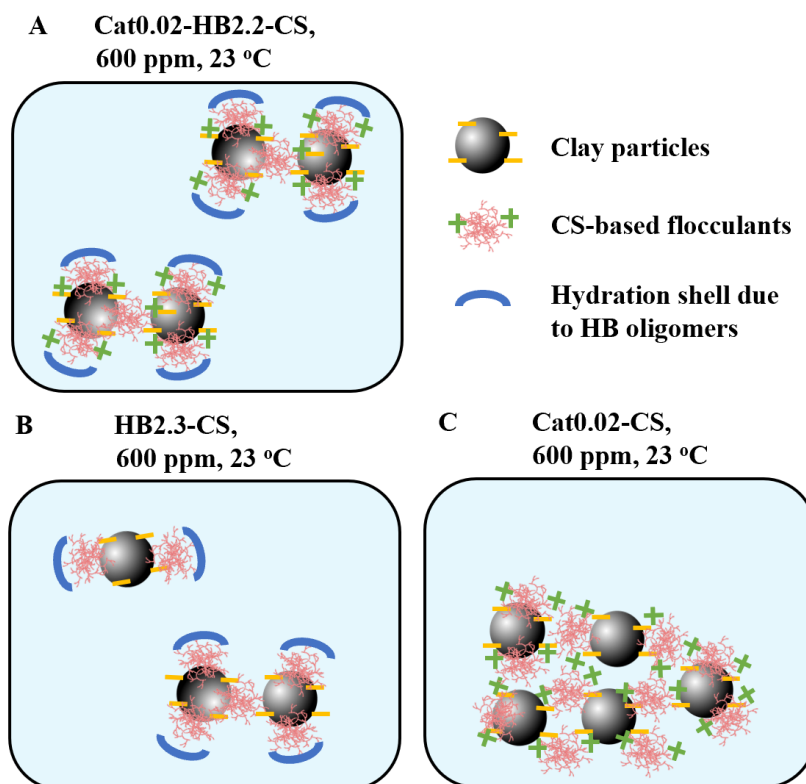


**Figure 4.5.** Schematic representation of flocculation of clay particles using Cat0.02-HB2.2-CS (A), HB2.3-CS (B) and Cat0.02-CS (C) at 600 ppm when settling at 23 °C.

At a settling temperature of 50 °C, 25 ppm of Cat0.02-HB2.2-CS flocculated the 2 wt % MFT with an ISR of 7.5 m/h (Fig. 4.3) but the flocculation was incomplete due the lack of polymers to bridge the remaining clay particles (Fig. 4.6A). A very turbid supernatant obtained after the flocculation at low doses also supported this claim (see Fig. 4.9 in Section 4.3.2.3). The ISR first decreased slightly to 5.7 m/h at a dose of 100 ppm and then increased quickly to 12.1 m/h as a dose of 400 ppm was reached (Fig. 4.3). The ISR had a maximum at 14.3 m/h with the use of 1000 ppm of Cat0.02-HB2.2-CS. At high doses, the presence of hydrophobic interactions may facilitate the aggregation of the polymer adsorbed clay particles as the Cat0.02-HB2.2-CS becomes more hydrophobic and the hydration shells surrounding the HB

oligomers were partially disrupted above its LCST (Fig. 4.6B). The polymers could be partially dehydrated above the LCST due to the presence of the hydrophilic cationic groups.

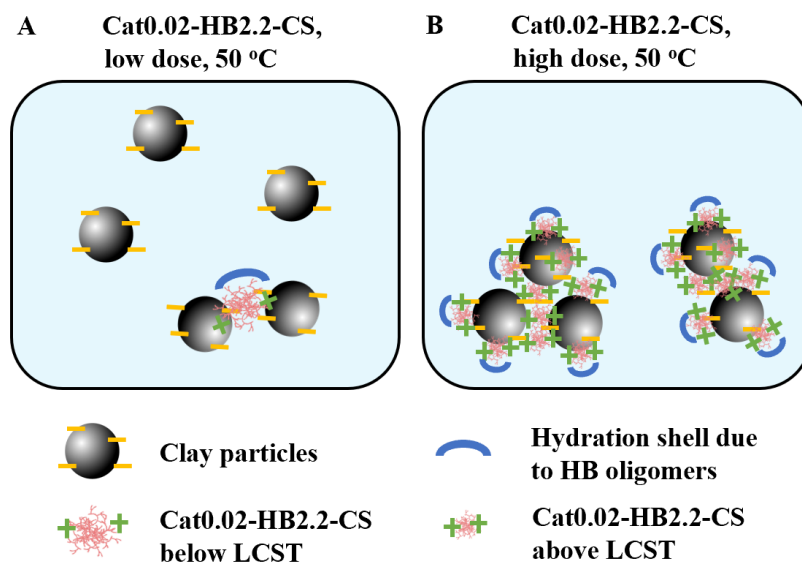


**Figure 4.6.** Schematic representation of flocculation of clay particles using Cat0.02-HB2.2-CS at low (A) and high (B) doses when settling at 50 °C.

The most obvious difference in ISR between the settling temperatures occurred at a dose of 400 ppm or above (Fig. 4.3). A similar phenomenon was observed when settling with HB2.3-CS at a high dose. The overdose effect occurred when settling at 23 °C was greatly mitigated when the settling tests were conducted at 50 °C, which might be due to the increase in intermolecular hydrophobic interactions induced by the thermoresponsive flocculant above its LCST. Cat0.02-HB2.2-CS had higher ISR values compared to HB2.3-CS across the dose range examined. This could be due to the additional cationic groups which may facilitate the adsorption of the polymers onto the clay particle surfaces as a result of electrostatic interactions and leading to a more efficient bridging mechanism (Fig. 4.7A and B). Additionally, at a dose below 200 ppm, Cat0.02-HB2.2-CS was a more effective flocculant than Cat0.02-CS in terms

of ISR (Fig. 4.3). However, at higher doses (400-800 ppm), Cat0.02-CS substantially outperformed Cat0.02-HB2.2-CS. At these high doses, the adsorbed layer of Cat0.02-HB2.2-CS, which may not be completely dehydrated, could provide steric stability to the polymer adsorbed flocs, hence, retarding the aggregation of these flocs to form larger flocs that can settle rapidly (Fig. 4.7A and C).

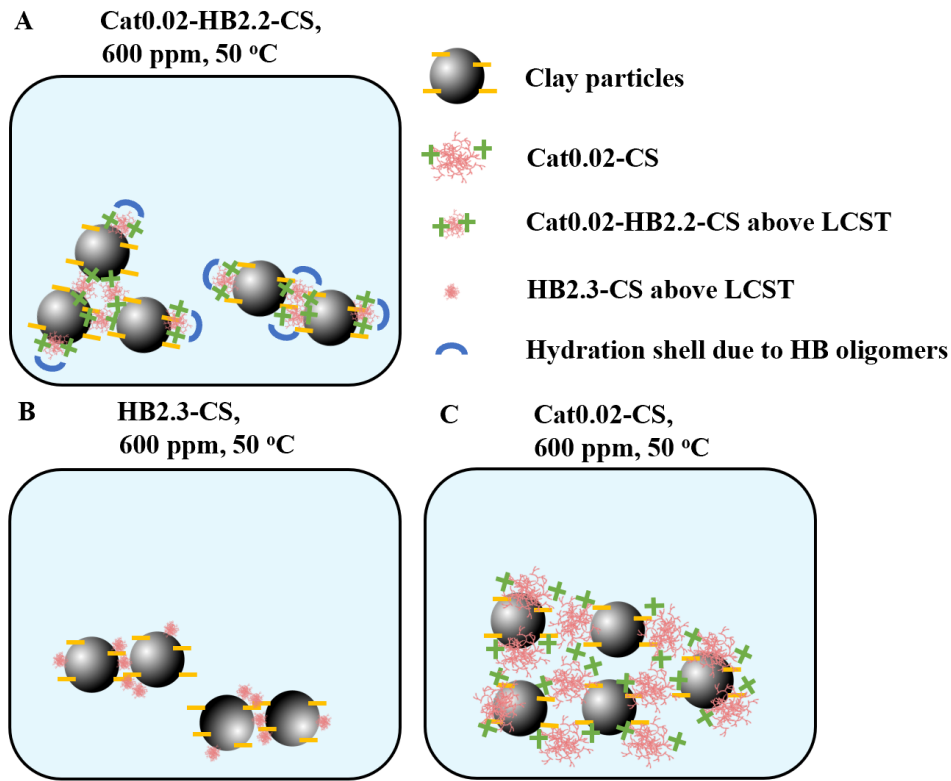


**Figure 4.7.** Schematic representation of flocculation of clay particles using Cat0.02-HB2.2-CS (A), HB2.3-CS (B) and Cat0.02-CS (C) at 600 ppm when settling at 50 °C.

#### 4.3.2.2 Water Recovery

At doses of 400 ppm and below, WR by the use of Cat0.02-CS was generally higher than Cat0.02-HB2.2-CS or HB2.3-CS (Fig. 4.8), while at higher doses, the WR obtained by using HB2.3-CS was at about 90 %, which was slightly higher than the WR by Cat0.02-HB2.2-

CS or Cat0.02-CS. At doses of 400 ppm and above, Cat0.02-HB2.2-CS is demonstrated to be thermoresponsive by the light transmittance measurements (Fig. 4.2A). One would expect that since Cat0.02-HB2.2-CS would undergo a thermal transition above its LCST, Cat0.02-HB2.2-CS could cause a release of more water from sediments and a higher WR than Cat0.02-CS when flocculating at 50 °C. However, Cat0.02-HB2.2-CS did not result in any improvement in WR compared to Cat0.02-CS at a dose of 400 ppm or above while HB2.3-CS showed an improvement over Cat0.02-CS (Fig. 4.8). This could be due to the fact that Cat0.02-HB2.2-CS may not be completely dehydrated due to the cationic groups and may form partially hydrated mesoglobules above its LCST while HB2.3-CS could be completely dehydrated and form insoluble aggregates above the LCST causing the release of water from sediments. This is evidenced by the comparison of the transmittance values of the two thermoresponsive polymers above their LCSTs. To elaborate, at 1000 ppm, HB2.3-CS showed a transmittance value of 0.8 % (Fig. 2.3C) while Cat0.02-HB2.2-CS showed a transmittance value of 81.5 % above their LCSTs (Fig. 4.2A). The Cat0.02-HB2.2-CS has shown to be relatively stable in the dispersion above the LCST which supported that the polymer may not be completely dehydrated. Overall, HB2.3-CS at high doses or Cat0.02-CS at low doses was superior to Cat0.02-HB2.2-CS in terms of WR regardless of the settling temperatures.

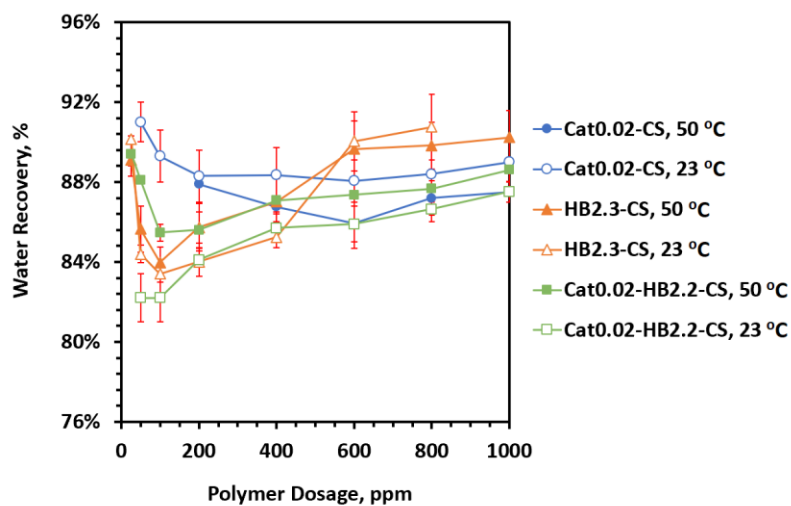


**Figure 4.8.** Water recovery of the settling tests of 2 wt % MFT using Cat0.02-HB2.2-CS, Cat0.02-CS and HB2.3-CS with varying doses from 25 to 1000 ppm (dry/slurry).

#### 4.3.2.3 Supernatant Turbidity

The supernatant was very turbid at low Cat0.02-HB2.2-CS doses and became less turbid as the dose increased from 25 to 200 ppm regardless of the settling temperatures (Fig. 4.9). As the Cat0.02-HB2.2-CS dose continued to increase up to 1000 ppm, the ST increased from a minimum of 20 NTU to 54 NTU at 23 °C, while the ST continued to decrease marginally to 11 NTU at 50 °C (Fig. 4.9). This suggested a broadened flocculation window for using the Cat0.02-HB2.2-CS above its LCST. A similar phenomenon was also observed for HB2.3-CS. Above their LCSTs, both Cat0.02-HB2.2-CS and HB2.3-CS became more hydrophobic which may explain the observation that the flocculation window became larger when settling at 50 °C. The broadening phenomenon due to an increase in the hydrophobicity of the flocculants was also reported in the literature.<sup>140,159</sup> Overall, the use of Cat0.02-HB2.2-CS gave a lower ST compared to either Cat0.02-CS or HB2.3-CS at 50 °C.

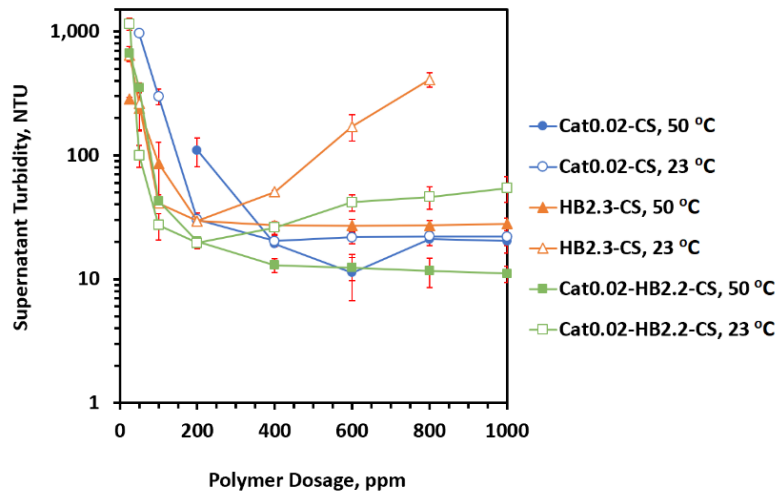


**Figure 4.9.** Supernatant turbidity of the settling tests of 2 wt % MFT using Cat0.02-HB2.2-CS, Cat0.02-CS and HB2.3-CS with varying doses from 25 to 1000 ppm (dry/slurry).

#### 4.3.2.4 Sediment Solids Content

At flocculant doses from 50 to 200 ppm, Cat0.02-CS resulted in a denser sediment and higher SSC than HB2.3-CS or Cat0.02-HB2.2-CS (Fig. 4.10). This may be due to the fact that at these low doses, HB2.3-CS and Cat0.02-HB2.2-CS may not be completely dehydrated at 50 °C. As a result, HB2.3-CS and Cat0.02-HB2.2-CS could retain more water due to the presence of hydration shells surrounding the HB substituents compared to Cat0.02-CS. However, a denser sediment was given by using a high dose (600-1000 ppm) of HB2.3-CS at 50 °C (Fig. 4.10) and at such doses, HB2.3-CS became hydrophobic and dehydrated, hence, could expel water from the sediment. But as discussed earlier, Cat0.02-HB2.2-CS may not be completely dehydrated due to its cationic groups, hence, the ability of expelling water from the sediment could be weakened. Overall, Cat0.02-HB2.2-CS showed the worst performance at the dose range we examined since it could hold more water than Cat0.02-CS at low doses due to the

hydration shells surrounding its HB groups and it failed to expel more water from the sediment than HB2.3-CS at high doses due to its cationic substituents.

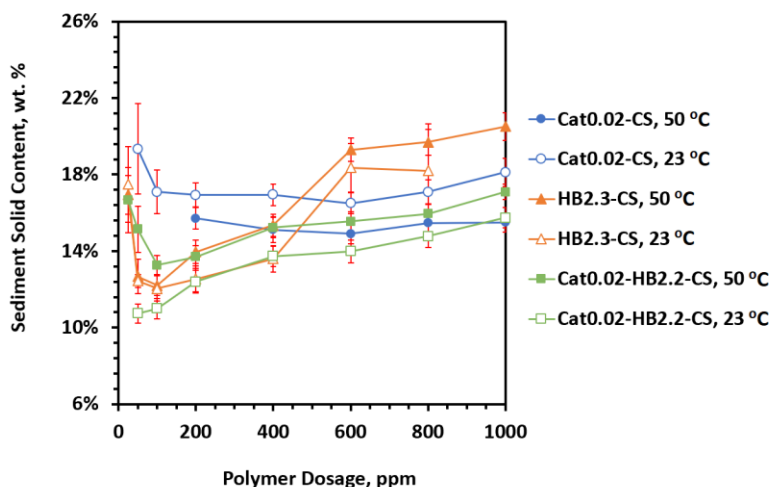


**Figure 4.10.** Sediment solids content of the settling tests of 2 wt % MFT using Cat0.02-HB2.2-CS, Cat0.02-CS and HB2.3-CS with varying doses from 25 to 1000 ppm (dry/slurry).

### 4.3.3 Settling Tests of 2 wt % MFT using Cat-HB-PS

Settling tests were conducted using Cat0.02-HB2.0-PS and 2 wt % MFT at 23 °C and 50 °C. The settling tests were carried out at varying doses from 25 to 1000 ppm and compared to the flocculation results given by the HB1.9-PS and Cat0.02-PS samples.

#### 4.3.3.1 Initial Settling Rate

At doses of 400 ppm or below, the ISR of the settling tests using Cat0.02-HB2.0-PS performed at 23 °C and 50 °C were similar (Fig. 4.11). Below 400 ppm, Cat0.02-HB2.0-PS did not exhibit thermoresponsivity at 50 °C according to the light transmittance studies (Fig. 4.2B), which could explain the similar settling rates at 23 °C and 50 °C. Moreover, at a low dose, the

bridging of the clay particles by polymers may not be very effective due to the insufficient amount of polymers in the MFT mixture (Fig. 4.12A and Fig. 4.13A).

At 23 °C and with the use of Cat0.02-HB2.0-PS, the ISR was maximized at a dose of 400 ppm (Fig. 4.11). At 23 °C, the maximum ISR (22.8 m/h) produced by Cat0.02-HB2.0-PS was much greater than the maximum ISR (8.8 m/h) of HB1.9-PS (Fig. 4.11). This is possibly due to the fact that the cationic groups of Cat0.02-HB2.0-PS provide stronger polymer-clay attractions (Fig. 4.12B), hence, leading to a more effective bridging mechanism compared to HB1.9-PS. However, at 400 ppm, the ISR produced by Cat0.02-HB2.0-PS was considerably lower than that by Cat0.02-PS (Fig. 4.11), which could be a consequence of the formation of sterically stabilized flocs by the hydration shells surrounding the HB substituents of Cat0.02-HB2.0-PS adsorbed on the surface of the flocs.

At 23 °C and with the use of Cat0.02-HB2.0-PS, the ISR decreased from 22.8 m/h to 2.9 m/h as the doses increased from 400 to 1000 ppm (Fig. 4.11). At a dose of 600 ppm or above, the decrease in ISR could be caused by the overdose of the flocculants that could re-stabilize the clay particles (Fig. 4.12C). At doses from 600 to 1000 ppm and at 50 °C which is above the LCST of Cat0.02-HB2.0-PS, the ISR value increased with the increasing dose (Fig. 4.11). The highest ISR (70.3 m/h) was obtained at a dose of 1000 ppm and a settling temperature of 50 °C. A similar trend can also be observed for HB1.9-PS when comparing the ISR values at 23 °C to those at 50 °C (Fig. 4.11).



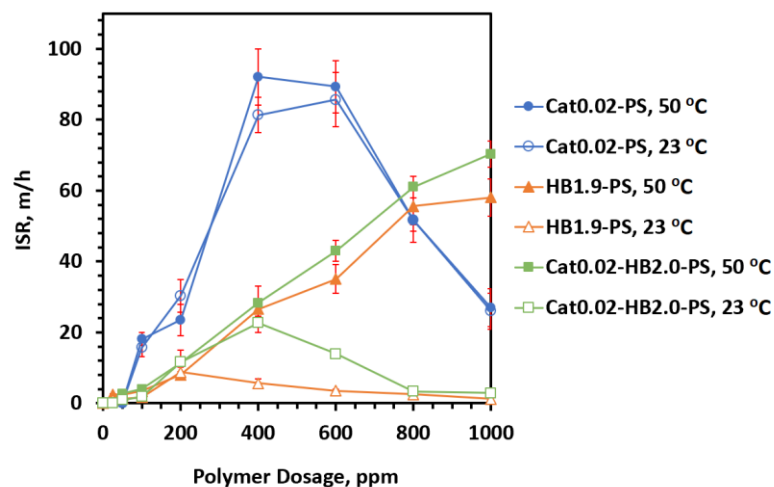


**Figure 4.11.** Initial settling rate (ISR) of the settling tests of 2 wt % MFT using Cat0.02-HB2.0-PS, Cat0.02-PS and HB1.9-PS with varying doses from 25 to 1000 ppm (dry/slurry).

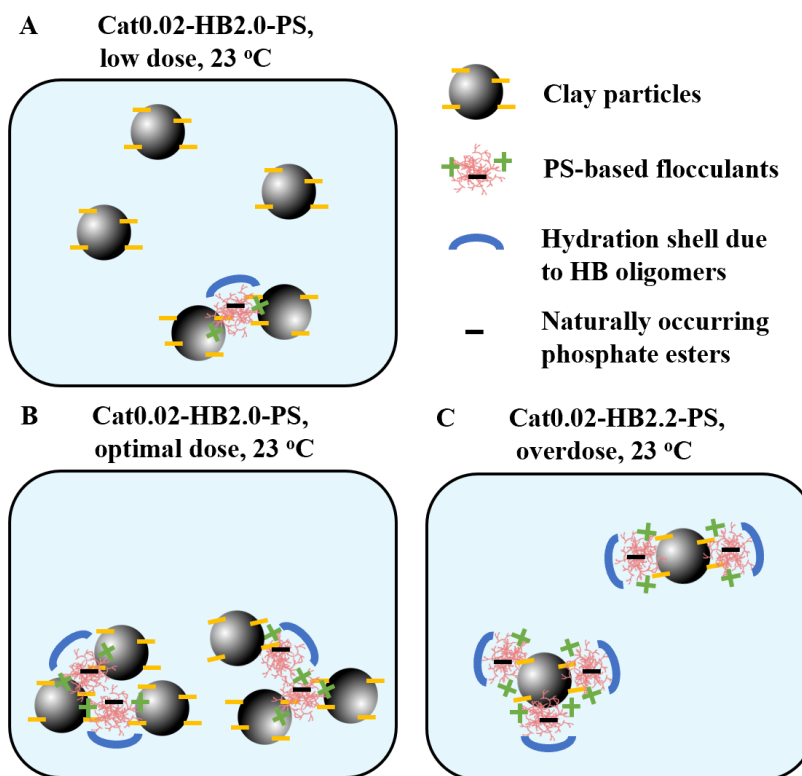


**Figure 4.12.** Schematic representation of flocculation of clay particles using Cat0.02-HB2.0-PS at low dose (A), optimal dose (B) and overdose (C) when settling at 23 °C.

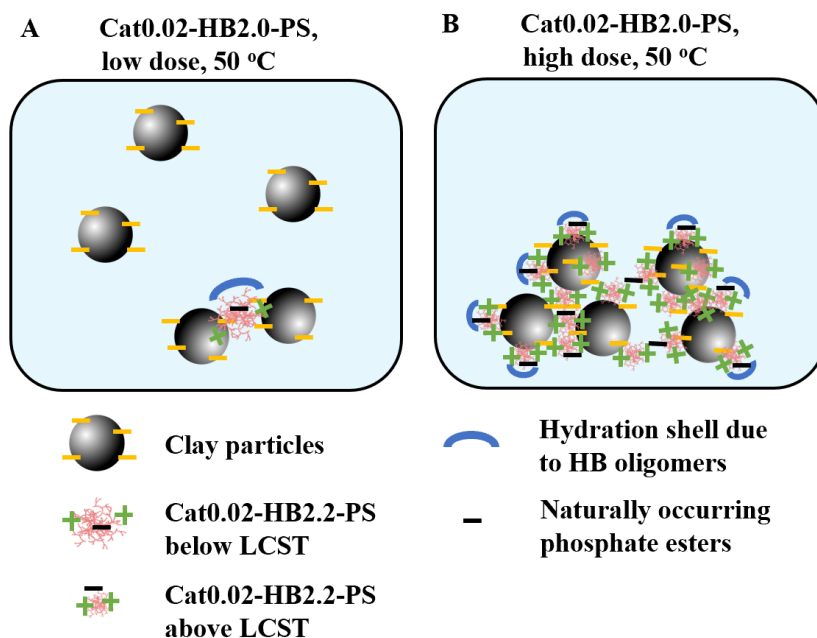


**Figure 4.13.** Schematic representation of flocculation of clay particles using Cat0.02-HB2.0-PS at low (A) and high (B) doses when settling at 50 °C.

Compared to the maximum ISR (14.3 m/h) achieved by Cat0.02-HB2.2-CS at a dose of 1000 ppm (Fig. 4.3), the maximum value (70.2 m/h) obtained by Cat0.02-HB2.0-PS at the same dose was significantly higher (Fig. 4.11). As mentioned earlier in this chapter, the flocs formed by the addition of high doses of Cat0.02-HB2.2-CS could be held together by hydrophobic interactions at 50 °C. However, the formation of large flocs may be prohibited as the flocs could be stabilized by cationic charges and the adsorbed layer of partially dehydrated polymers. Although the MS of both type of substituents on the Cat0.02-HB2.0-PS were similar to those of the Cat0.02-HB2.2-CS, the potato starch-based flocculant had a much faster settling rate. In the literature, it is widely accepted that PS naturally contains covalently bound phosphate groups.<sup>171,172</sup> As Cat0.02-HB2.0-PS went through the hydrophilic to hydrophobic transition at its LCST, the anionic phosphate groups, which were possibly hidden inside the

core of the starch molecule below its LCST, could migrate to the surface of the starch molecule. Consequently, the negative charged phosphate groups could facilitate the capturing of free Cat0.02-HB2.0-PS molecules and/or Cat0.02-HB2.0-PS bound flocs via electrostatic attractions and could lead to the formation of larger flocs (Fig. 4.13B), hence, a higher ISR. Similar observations were made by Wang et al. and Zhang et al. using cationic thermoresponsive flocculants derived from PNIPAM.<sup>11,13</sup>

### 4.3.3.2 Water Recovery

For a flocculant dose ranging from 100 to 1000 ppm, WR resulting from the use of Cat0.02-PS decreased from a maximum of 89 % to 86 %, while HB1.9-PS increased from a minimum of 85 % to 89 % (Fig. 4.14). At low doses, Cat0.02-HB2.0-PS could attract more water than Cat0.02-PS due to the hydration shells while at any dose, Cat0.02-HB2.0-PS could attract more water than HB1.9-PS due to the cationic substituents. So not surprisingly, Cat0.02-HB2.0-PS had the worst WR compared to Cat0.02-PS and HB1.9-PS from 0-1000 ppm.

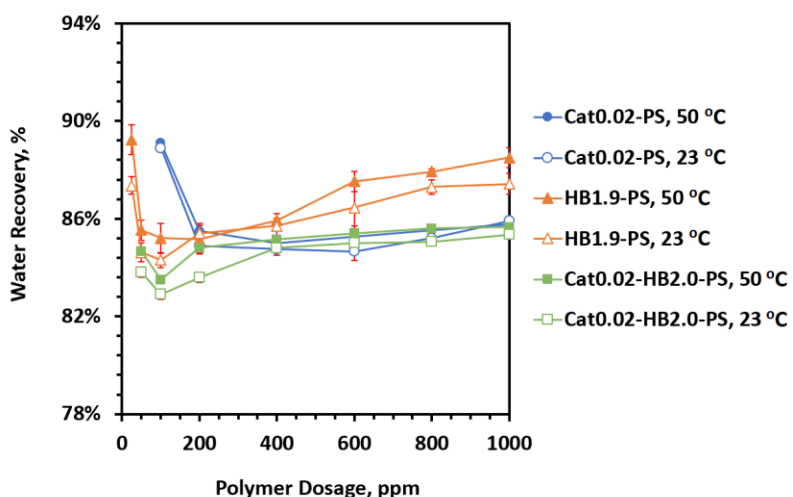


**Figure 4.14.** Water recovery of the settling tests of 2 wt % MFT using Cat0.02-HB2.0-PS, Cat0.02-PS and HB1.9-PS with varying doses from 25 to 1000 ppm (dry/slurry).

### 4.3.3.3 Supernatant Turbidity

To achieve an ST of under 30 NTU, 400 ppm of Cat0.02-PS was required when settling at 50 °C while all other doses gave a higher ST (Fig. 4.15). At a settling temperature of 23 °C, the use of 100 ppm of HB1.9-PS or 200 to 400 ppm of Cat0.02-HB2.0-PS was able to yield a relatively clean supernatant with an ST under 30 NTU. When settling at 50 °C, the use of 100 to 1000 ppm of HB1.9-PS or 400 to 1000 ppm of Cat0.02-HB2.0-PS was also able to achieve an ST of under 30 NTU. Large flocculation windows were observed when using HB1.9-PS (100-1000 ppm) or Cat0.02-HB2.0-PS (200-1000 ppm) at 50 °C while Cat0.02-PS only gave a small flocculation window (200-400 ppm).

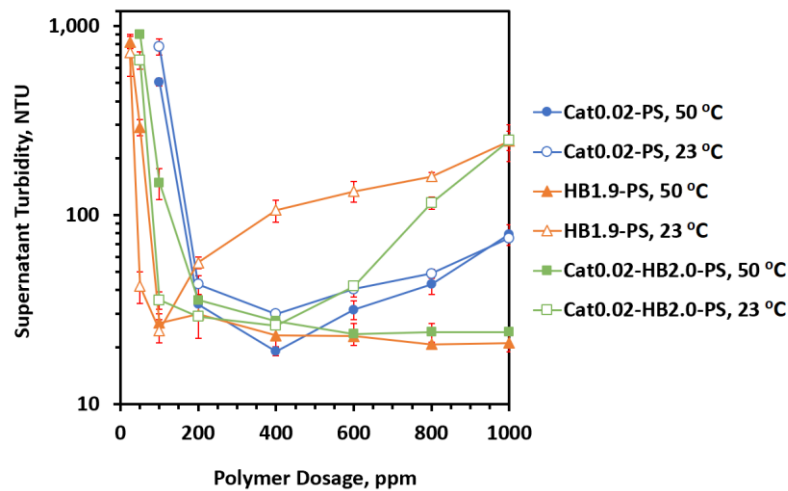


**Figure 4.15.** Supernatant turbidity of the settling tests of 2 wt % MFT using Cat0.02-HB2.0-PS, Cat0.02-PS and HB1.9-PS with varying doses from 25 to 1000 ppm (dry/slurry).

### 4.3.3.4 Sediment Solids Content

Below 200 ppm, SSC resulted from using Cat0.02-PS was higher than both HB1.9-PS and Cat0.02-HB2.0-PS (Fig. 4.16). Above 200 ppm, SSC of Cat0.02-HB2.0-PS approached that of Cat0.02-PS while HB1.9-PS showed the best performance in terms of SSC at 50 °C.

Comparing to the flocculants derived from CS (Fig. 4.10), the PS-based flocculants overall produced lower SSC, which again supported that the PS-based flocculants could retain more water in the sediments.

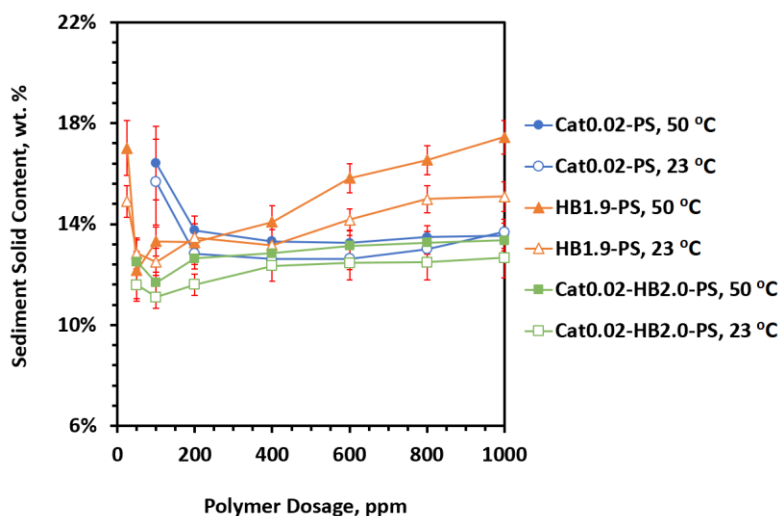


**Figure 4.16.** Sediment solids content of the settling tests of 2 wt % MFT using Cat0.02-HB2.0-PS, Cat0.02-PS and HB1.9-PS with varying doses from 25 to 1000 ppm.

#### 4.4 Comparison with other Dual Functional Polymers

In this section, we compare the performance of our dual functional polymers to that of another dual functional polymer used to flocculate 2 wt % MFT in the literature. In 2018, Gumfekar and Soares reported the flocculation of 2 wt % kaolin suspensions using a dual functional co-polymer consisting of NIPAM (for the thermoresponsive functionality) and acrylic acids (for the anionic functionality).<sup>142</sup> The co-polymer with 20 mol % acrylic acids had an LCST of 36 °C. 20 ppm of the polymer was used in a flocculation test at a settling temperature of 50 °C to produce an ISR of 0.65 m/h and an ST of approximately 100 NTU. Compared to Cat0.02-HB2.2-CS, 100 ppm was required to flocculate 2 wt % MFT with an

ISR of 6 m/h and an ST of 43 NTU at a settling temperature of 50 °C. If a high ISR was of great importance for certain applications, the use of 1000 ppm Cat0.02-HB2.0-PS could lead to a remarkably high ISR of 70.3 m/h and an excellent ST of 24 NTU. The co-polymers consisting of NIPAM and acrylic acids used by Gumfekar and Soares had the advantage of achieving a reasonable flocculation performance at a relatively low polymer dose.

#### **4.5 Conclusion**

Cat0.02-HB2.2-CS showed higher ISR than HB2.3-CS but worse than Cat0.02-CS. Cat0.02-HB2.2-CS showed an ST similar to HB2.3-CS and better than Cat0.02-CS. Additionally, Cat0.02-HB2.2-CS produced lower WR and SSC compared to Cat0.02-CS and HB2.3-CS depending on the flocculant doses. Cat0.02-HB2.0-PS produced considerably higher ISR than Cat0.02-HB2.2-CS but the PS-based flocculants generally gave lower WR and SSC values. Overall, the dual functional starches performed better in ST but worse in ISR, WR and SSC than the cationic starches while they performed better in ISR but worse in WR and SSC than the thermoresponsive starches.

## Chapter 5

# Flocculation of Oil Sands Mature Fine Tailings by Starch-based Dual Polymer Flocculant System

### 5.1 Introduction

Dual polymer flocculation systems generally demonstrate improved flocculation performance on treating oil sands tailings over the single flocculant systems.<sup>143,144,173</sup> Loecke et al. reported that the undiluted MFT treated with a dual polymer system consisting of anionic PAM and cationic poly(diallyldimethylammonium chloride) (poly(DADMAC)), showed better filterability and led to higher solids content after pressure plate filtration compared to treating with the anionic PAM or poly(DADMAC) alone.<sup>143</sup> In 2016, Lu et al. demonstrated that the use of a dual polymer flocculation system involving a commercial anionic PAM (Magnafloc 1011) and chitosan, a cationic biopolymer, greatly improved the settling of fresh oil sands tailings (with 26 wt % solids) collected from an oil sands extraction facility in Alberta compared to the single flocculants.<sup>144</sup> The authors reported that the use of 20 ppm of Magnafloc 1011 and 200 ppm of chitosan produced an ISR of 7.7 m/h and a supernatant with a turbidity of 71 NTU. The dual polymer system showed better performance than Magnafloc 1011 or chitosan when used alone in that 20 ppm of the Magnafloc 1011 yielded very turbid supernatants (>1000 NTU) while 600 ppm of chitosan showed a slow settling rate at only 1.27 m/h.

To the best of our knowledge, the flocculation of MFT using a dual biopolymer-based flocculant system has not been reported in the literature. Here we report a novel dual starch-

based flocculant system, consisting of thermoresponsive hydroxybutyl starches and cationic starches (CHPTAC-modified starches), for the flocculation of MFT.

## **5.2 Materials and Methods**

### **5.2.1 Materials**

Cooked, high amylopectin waxy corn starch (CS) was obtained from EcoSynthetix Inc. (Burlington, Ontario, Canada). Neutral, pre-gelatinized, high amylopectin potato starch (PS) was a gift from Coöperatie AVEBE U.A. (Veendam, The Netherlands). Oil sands MFT was a gift from Joao Soares, University of Alberta, Canada. *N*-(3-Chloro-2-hydroxypropyl) trimethyl ammonium chloride (CHPTAC) (60 wt % solution in H<sub>2</sub>O), 1,2-butene oxide and styrene oxide were obtained from Sigma-Aldrich Co. (USA). Other reagents and solvents were commercially available and used without further purification unless stated otherwise.

### **5.2.2 The Preparation of the CS- and PS-based Flocculants**

Hydroxybutyl (HB) starch and phenylhydroxyethyl (PHE) starch derived from CS or PS were prepared as described in Section 2.2.2 (Figure 5.1). MS of HB groups (MS<sub>HB</sub>) and MS of PHE groups (MS<sub>PHE</sub>) were determined as described in Section 2.2.3. Cationic starch derived from CS or PS was prepared using a cationic agent, CHPTAC, as described previously in Section 3.2.2 (Fig. 5.1) and the determination of the MS of the cationic groups (MS<sub>Cat</sub>) was described in Section 3.2.3.



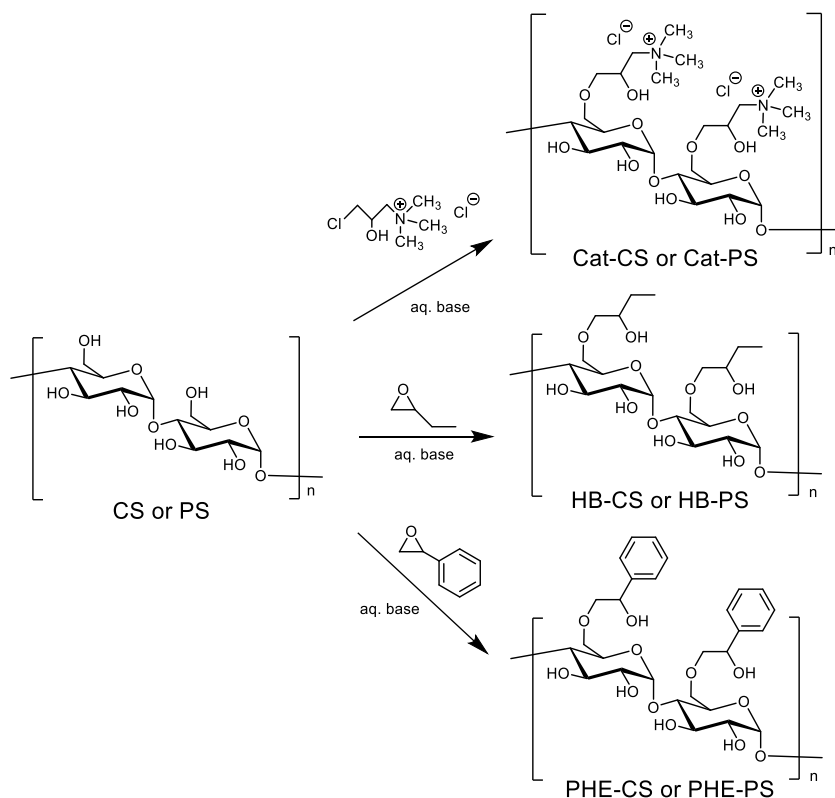


**Figure 5.1.** Preparation of hydroxybutyl (HB), phenylhydroxyethyl (PHE) and cationic starches derived from CS or PS. Substitution is shown only at O-6 while in fact substitution can occur at O-2, O-3 and O-6.

### 5.2.3 Settling Tests

The received MFT had a solids content of approximately 35 wt %, which was diluted to 2 or 10 wt % by the addition of tap water prior to the settling tests. All dilutions of MFT were prepared fresh and homogenized with a mechanical stirrer for 2 h before use in all settling tests. Cationic starch and PHE starch stock dispersions were prepared to a concentration of 50 g/L and stored at rt before use and HB starch stock dispersions were also prepared to a concentration of 50 g/L but kept at 4 °C. For each settling test, 50 mL of the diluted MFT were stirred in a 100 mL beaker for 2 min at 600 rpm. A pre-determined amount of HB starch (or

PHE starch) stock dispersion was added dropwise to the diluted MFT over 2 min, which was followed by the addition of a pre-determined amount of the cationic starch stock dispersion unless stated otherwise. The mixture was stirred for 8 min at 200 rpm in a 50 °C water bath (or at rt for the 23 °C settling tests). After that, the mixture was poured into a 50 mL graduated cylinder and inverted 3 times. The graduated cylinder was left undisturbed in a 50 °C water bath for 30 min before removing from the water bath and placed at rt for the rest of the settling time (or left undisturbed at rt for 24 h for the 23 °C settling tests). Mudline height was recorded as a function of settling time. For the settling tests with a high ISR (> 50 m/h), a camera equipped with a close-up lens was used to record the position of the mudline over time. Flocculation performance was evaluated in the following parameters: ISR, WR, ST and SSC. These parameters were determined as described previously in Section 2.2.6. All experiments were conducted at least 3 times to obtain representative results.

## **5.3 Results and Discussion**

### **5.3.1 Determination of the Order of Addition in the Dual Flocculant System**

With dual flocculant systems, the outcomes of settling tests can vary depending upon the order of addition of flocculants. For example, for a cationic/anionic dual flocculant system to treat undiluted MFT, Loerke et al. reported that addition of a cationic polymer (poly(DADMAC)), after addition of an anionic PAM, produced a better performance in terms of better filterability and higher solids content when the authors compared their results to the data reported previously by Zhu et al., who used the same dual flocculant system but added the cationic polymer first.<sup>143,173</sup> Loerke et al. speculated that the addition of the anionic PAM

formed large negatively charged flocs and upon the subsequent addition of the cationic poly(DADMAC), the negatively charged flocs were bridged to form larger flocs through electrostatic interactions.<sup>143</sup>

We began these studies by determining if the order in which the flocculants were added affected the flocculation results. In a dual flocculant system using cationic corn starch with a molar substitution (MS) of 0.02 (Cat0.02-CS) and hydroxybutyl corn starch with an MS of 0.6 (HB0.6-CS, not thermoresponsive), 50 ppm of the first flocculant was added dropwise to a 2 wt % MFT with stirring over 2 min at rt, followed by the addition of 50 ppm of the second flocculant, in the same way as the first flocculant, at rt. Flocculation results for using HB0.6-CS as the first flocculant and Cat0.02-CS as the second one (HB0.6-CS → Cat0.02-CS) are presented in entry 4 in Table 5.1, and flocculation results obtained when Cat0.02-CS was used as the first flocculant and HB0.6-CS as the second one (Cat0.02-CS → HB0.6-CS) are given in entry 3. The addition order, HB0.6-CS → Cat0.02-CS, had a 68 % increase in ISR over the reverse addition order, Cat0.02-CS → HB0.6-CS, and both dual systems gave superior results in terms of ISR, WR, SST and SSC compared to when just HB0.6-CS or Cat0.02-CS were used alone (entries 1 and 2).

**Table 5.1.** Effect of flocculant addition orders on the settling performance of the dual flocculant system consisting of Cat0.02-CS and HB0.6-CS at 50 °C.

	1 <sup>st</sup> Polymer	Dosage, ppm	2 <sup>nd</sup> Polymer	Dosage, ppm	ISR, m/h	WR, %	ST, NTU	SSC, wt %
1	Cat0.02-CS	50	-	-	n.d.	n.d.	> 1000	n.d.
2	HB0.6-CS	50	-	-	2.8 ± 0.1	86 ± 0.2	92 ± 2.4	14.4 ± 0.5
3	Cat0.02-CS	50	HB0.6-CS	50	7.1 ± 0.4	88 ± 0.1	35 ± 2.5	16.7 ± 0.6
4	HB0.6-CS	50	Cat0.02-CS	50	11.9 ± 1.6	88 ± 0.2	22 ± 1.7	16.4 ± 0.6

To explain the results in Table 5.1, we propose the following. When 50 ppm of only Cat0.02-CS was used, only a very small portion of the free clay particles could be adsorbed by the Cat0.02-CS and became charge neutralized, and these neutralized particle-polymer complexes could aggregate to form flocs that quickly settled to the bottom of the graduated cylinder. However, the majority of the remaining free clay particles stayed in the suspension because the concentration of the Cat0.02-CS in the suspension was low and so there was an insufficient amount of cationic charges for charge neutralization to occur (Fig. 5.2A). As a result, an extremely turbid supernatant was obtained, and the flocculation was unsuccessful (Table 5.1, entry 1). For the same reason, when 50 ppm of Cat0.02-CS was added as the first flocculant of a dual flocculant system, the Cat0.02-CS could only flocculate a small portion of clay particles, which became unstable and could quickly settle, and the rest of the particles could remain suspended in the mixture. Upon the addition of the second flocculant, HB0.6-CS, the bridging of the remaining, suspended particles was induced which led to floc formation and settling (Fig. 5.2C). On the contrary, when 50 ppm of HB0.6-CS was added first, the HB0.6-CS could produce small negatively charged flocs that remain suspended and could probably break apart easily (Fig. 5.2B), unlike in the case of Cat0.02-CS where the flocs were held strongly together by electrostatic interactions and had a net neutral charge. Moreover,

unlike when Cat0.02-CS was added first in which case the Cat0.02-CS would be quickly consumed due to the flocculation of a small amount of clay particles to form relatively large, strong and highly unstable flocs before the addition of the second flocculant, the HB0.6-CS should not be consumed prior to the addition of the second flocculant, Cat0.02-CS, due to the formation of small, fragile flocs that could still be relatively stable in the mixture. Upon the addition of 50 ppm of Cat0.02-CS, the small flocs previously formed by HB0.6-CS could be brought together by bridging and/or charge neutralization to form bigger flocs which would settle quickly (Fig. 5.2D). Thus, HB0.6-CS → Cat0.02-CS was determined to be the better addition order and used for all settling tests conducted with a dual flocculant system hereafter.

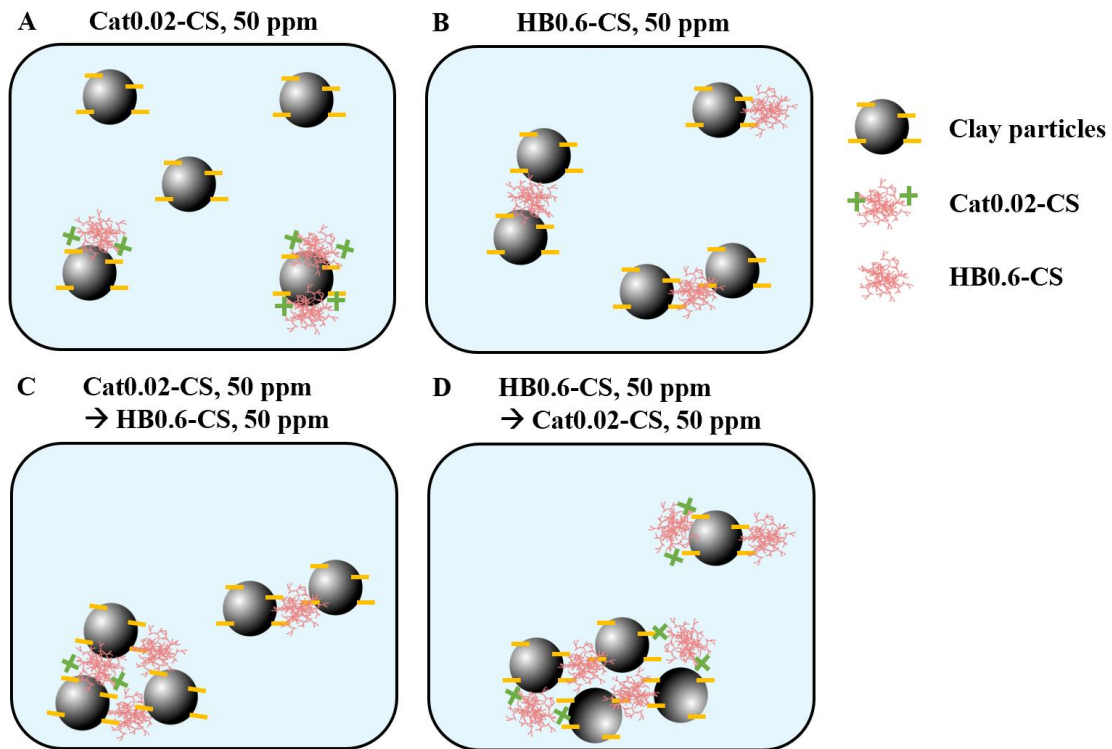


**Figure 5.2.** Schematic representation of flocculation of clay particles using Cat0.02-CS (A), HB0.6-CS (B) and the dual flocculant system with two different flocculant addition orders: Cat0.02-CS followed by HB0.6-CS (C) and HB0.6-CS followed by Cat0.02-CS (D).

### 5.3.2 Dose Effect of HB0.6-CS in a Dual Flocculant System

Settling tests were conducted using varying doses of HB0.6-CS ranging from 25 to 400 ppm as the first flocculant and Cat0.02-CS as the second flocculant. The optimal dose for Cat0.02-CS to achieve an ISR of 47.9 m/h was 600 ppm when used alone (Fig. 3.3). The dose effect of HB0.6-CS was examined with a dose of Cat0.02-CS kept constant at 600 ppm. The ISR increased dramatically from 48 to 193 m/h with the use of only 25 ppm of the first flocculant, HB0.6-CS (Fig. 5.3A). The ISR continued to increase to reach a maximum of 241 m/h at a dose of 100 ppm and then decreased with increasing dose of HB0.6-CS. The optimal dose was also found to be 100 ppm for the use of HB0.6-CS in a single flocculant settling test (Fig. 2.5A). This finding supported that the highest ISR could be achieved when HB0.6-CS was first added to produce small flocs, followed by the addition of the second flocculant, Cat0.02-CS, to cause the flocs to aggregate and to produce much larger flocs by charge neutralization. The water recovery (WR) increased from 85 % to 88 % with the addition of 25 to 400 ppm of HB0.6-CS as the first flocculant (Fig. 5.3B), which was very similar to the WR resulted from using HB0.6-CS alone (Fig. 2.5B). The supernatants were remarkably clean with a supernatant turbidity (ST) below 10 NTU after flocculation with the dual flocculant system (Fig. 5.3C). The sediment solids content (SSC) increased from 13.5 to 16.3 wt % when 25 to 400 ppm of HB0.6-CS were used (Fig. 5.3D). As the HB0.6-CS dose increased, the sediment could contain less water due to hydrophobic interactions of hydroxybutyl groups inside of the flocs. Overall, the flocculation with the dual flocculant system was much more effective than the single polymer flocculation especially concerning the settling rates.

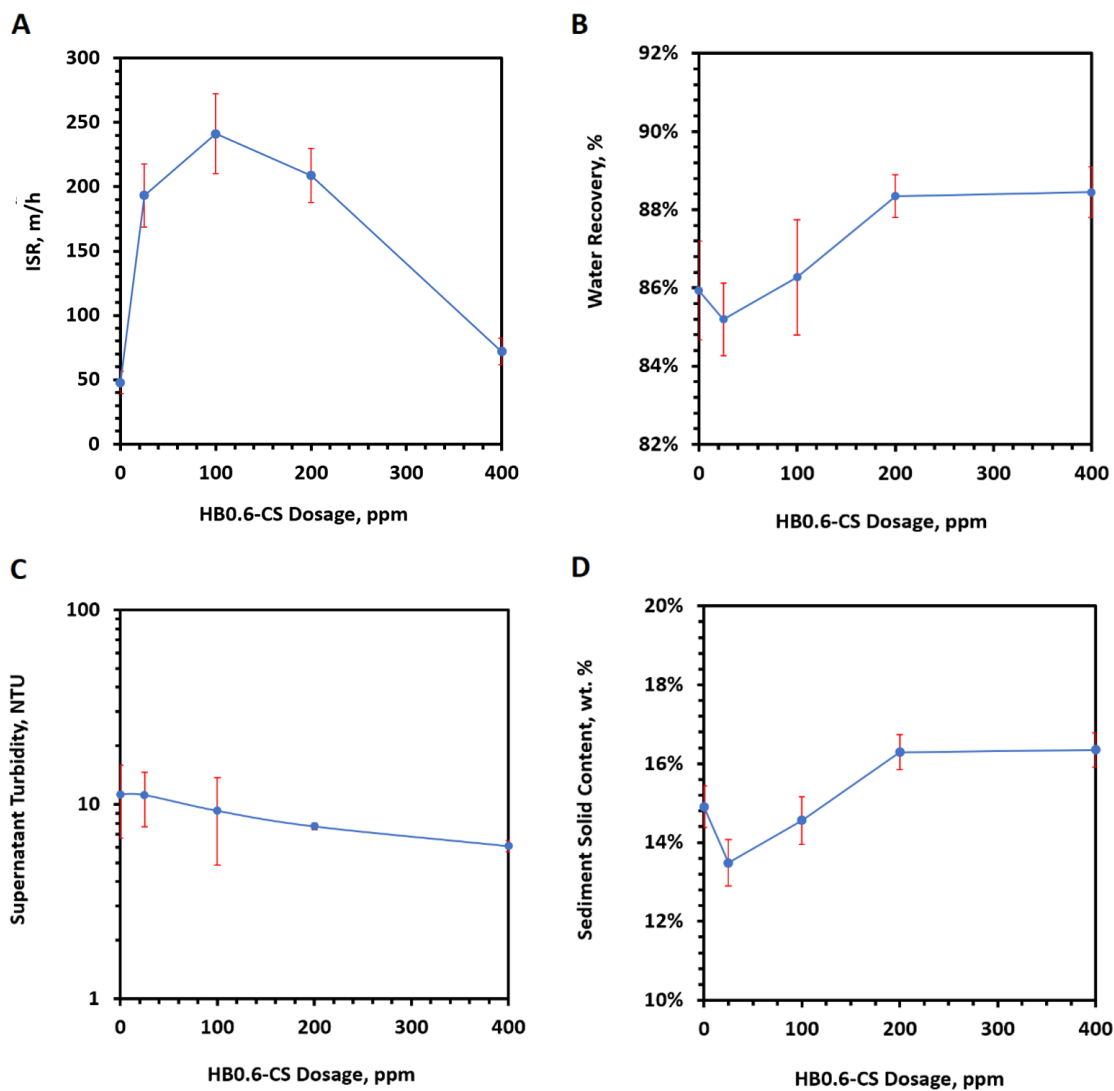


**Figure 5.3.** Dose effect of HB0.6-CS on initial settling rate (ISR, **A**), water recovery (**B**), supernatant turbidity (**C**) and sediment solids content (**D**) of the flocculation of a 2 wt % MFT with a second flocculant, Cat0.02-CS, at a dose of 600 ppm at 50 °C. Dosage was reported on the dry/slurry basis.

### 5.3.3 Settling Tests of 2 wt % MFT using HB-CS and Cat-CS

As shown in the previous section, 25 ppm of HB0.6-CS produced effective flocculation of 2 wt % MFT when used together with 600 ppm of Cat0.02-CS, and the highest ISR was

achieved when 100 ppm of HB0.6-CS was used. In this section, the dose effect of the Cat0.02-CS as the second flocculant was investigated with the use of 25 and 100 ppm of HB0.6-CS as the first flocculant. A thermoresponsive polymer, HB2.3-CS with an LCST of 27 °C, was also employed in order to determine the performance of a novel dual flocculant system consisting of a thermoresponsive polymer and a cationic polymer. The HB2.3-CS at a dose of 600 ppm could cause a hydrophilic to hydrophobic transition due to a complete dehydration of the HB substituents above its LCST. As such, the dose effect of Cat0.02-CS in the dual flocculant system was investigated not only at 25 and 100 ppm but also at 600 ppm of HB2.3-CS as the first flocculant. Moreover, Cat0.05-CS was also used in order to investigate the effect of molar substitution of cationic groups on flocculation performance.

### **5.3.3.1 Initial Settling Rate**

Without the addition of HB0.6-CS, Cat0.02-CS did not produce a clean enough supernatant (i.e. with turbidity under 1000 NTU) and the ISR could not be determined until a dose of 200 ppm was added (Fig. 5.4A). The flocculation was greatly improved when 25 ppm of HB0.6-CS was added as the first flocculant, and an ISR of 7.0 m/h was obtained with the addition of 25 ppm of Cat0.02-CS as the second flocculant. Keeping the HB0.6-CS dose unchanged at 25 ppm, the ISR continued to increase to a maximum of 193 m/h when the dose of Cat0.02-CS increased to 600 ppm. After the maximum, the ISR experienced a decrease to 48 m/h with the increasing Cat0.02-CS dose to 800 ppm. When the dose of HB0.6-CS increased to 100 ppm, the ISR values generally became higher and a maximum of 241 m/h was reached with the use of 600 ppm Cat0.02-CS (Fig. 5.4A).



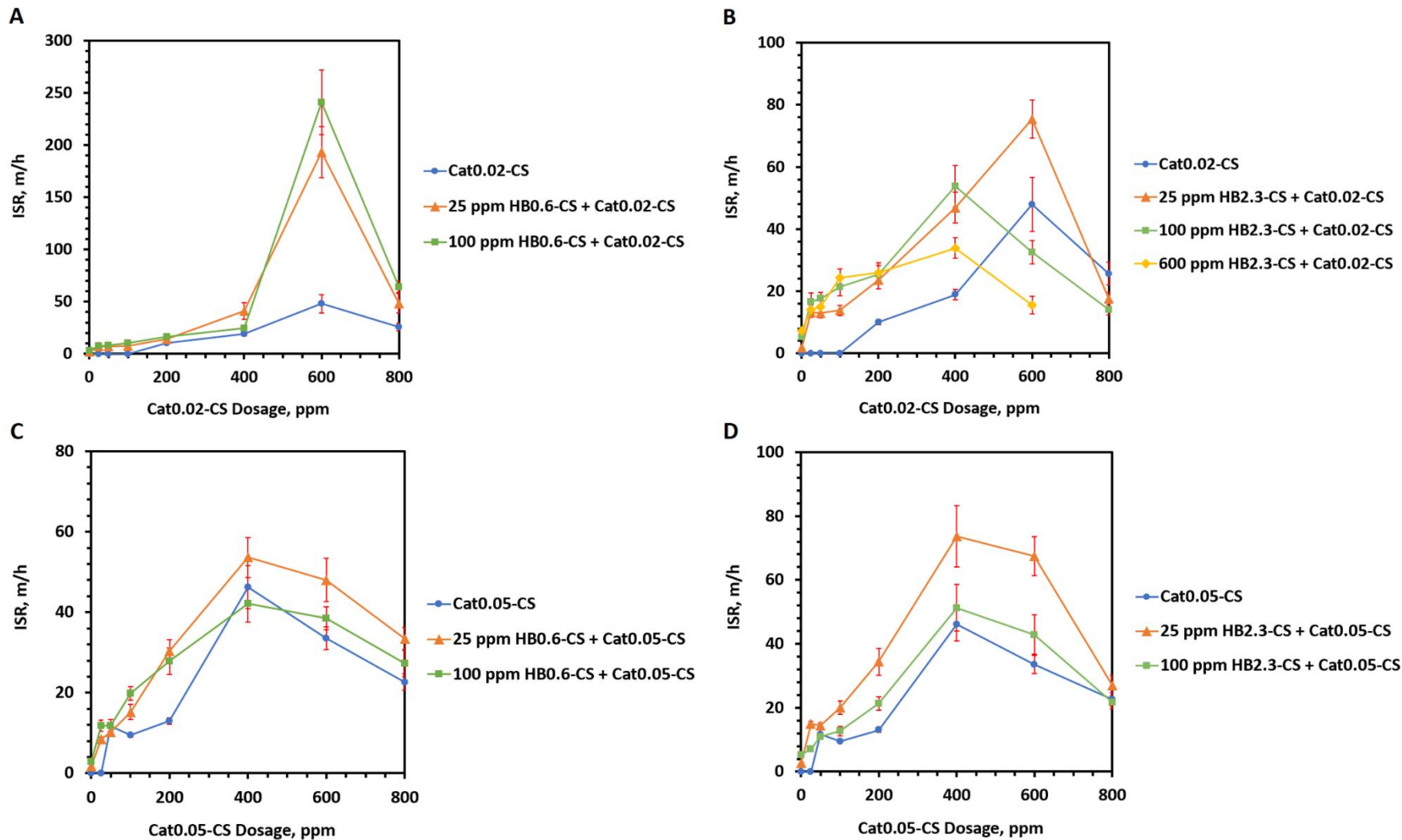


**Figure 5.4.** Initial settling rates (ISR) of flocculation of 2 wt % MFT using flocculant pairs consisting of HB0.6-CS and Cat0.02-CS (A), HB2.3-CS and Cat0.02-CS (B), HB0.6-CS and Cat0.05-CS (C), and HB2.3-CS and Cat0.05-CS (D) at 50 °C.

To explain the results shown in Figure 5.4A, we propose that the addition of the first flocculant, HB0.6-CS, produced small and loosely bound flocs, similar to what was discussed previously (Fig. 5.2B). These flocs could still carry an overall negative surface charge as HB0.6-CS was non-ionic, hence, a slow ISR was resulted with the use of HB0.6-CS alone. However, upon the addition of the second flocculant, Cat0.02-CS, at a low dose, the small flocs previously produced by HB0.6-CS could aggregate to form larger and more strongly bound flocs by bridging or partial charge neutralization (Fig. 5.5A). When an optimal dose of Cat0.02-CS was added, the flocs could be completely charge neutralized and aggregated to produce flocs that were significantly larger in size (Fig. 5.5B). As a consequence, the settling rate was at the highest with the use of Cat0.02-CS at the optimal dose of 600 ppm (Fig. 5.4A). When adding Cat0.02-CS at a dose more than its optimal dose, the large flocs could be re-stabilized and resulted in the break down of the large flocs into smaller flocs causing the decrease in ISR from its maximum value (Fig. 5.5C).

The ISR that resulted from using 25 ppm HB0.6-CS and 600 ppm Cat0.02-CS was approximately 4-fold higher than that resulting from the use of 600 ppm Cat0.02-CS alone (Fig. 5.4A). In both cases, the suspensions were charge neutralized but the two cases could generate flocs that differed in size (Fig. D1 in Appendix D). The flocs produced by Cat0.02-CS could mostly be a result of aggregation of individual neutralized clay particles while the ones generated by the dual flocculant system could be a result of aggregation of small flocs due to the first flocculant, HB0.6-CS. The latter case could produce larger flocs, which explained the higher settling rates.

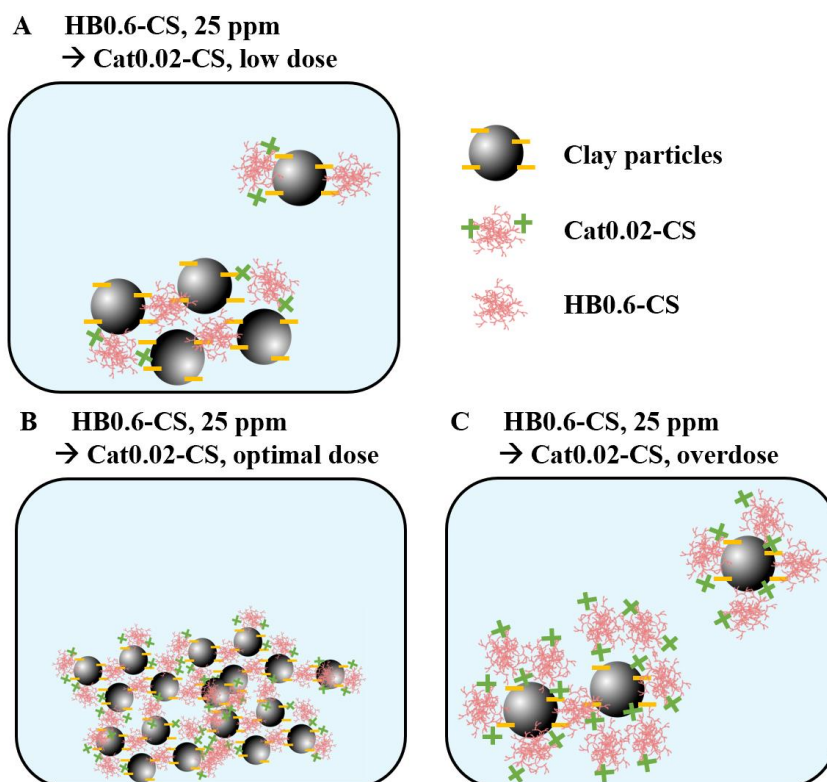


**Figure 5.5.** Schematic representation of flocculation of clay particles using 25 ppm HB0.6-CS and Cat0.02-CS at low dose (A), optimal dose (B) and overdose (C).

The dose effect of Cat0.02-CS was also studied with the use of a thermoresponsive polymer, HB2.3-CS, as the first flocculant in a dual polymer flocculation system. When adding 25 ppm of HB2.3-CS followed by 25 ppm of Cat0.02-CS, an ISR of 13.2 m/h was obtained (Fig. 5.4B). The ISR increased with the increasing dose of Cat0.02-CS and a maximum of 75 m/h was reached at an optimal dose of 600 ppm. Further increase in the Cat0.02-CS dose resulted in a decrease in ISR. The optimal doses of Cat0.02-CS decreased from 600 to 400 ppm with the increase in the dose of the first flocculant, HB2.3-CS, from 25 to 100 ppm. This implied that less cationic charges were required to neutralize the negative charges on the surfaces of free particles or small flocs as the amount of HB2.3-CS increased. We propose that

the additional HB2.3-CS could end up preferably inside of the flocs to form hydrophobic clusters within the intraparticle space of the flocs (compare Fig. 5.6A and B). As the hydrophobic clusters became larger due to the increase in hydrophobic interactions, more anionic charges would be buried inside of the flocs and consequently, a lower dose of Cat0.02-CS was required to neutralize the floc surfaces. When the dose of HB2.3-CS increased to 600 ppm, the HB2.3-CS became more hydrophobic and the hydrophobic clusters could become more compact and covered less amount of negatively charges (Fig. 5.6C). Meanwhile, a larger amount of HB2.3-CS was attracted towards the hydrophobic cluster inside the flocs to physically cover more negative charges due to the increase in the flocculant dose. As a consequence, the optimal dose of the second flocculant, Cat0.02-CS, remained unchanged at 400 ppm even though the dose of the first flocculant increase from 100 to 600 ppm.

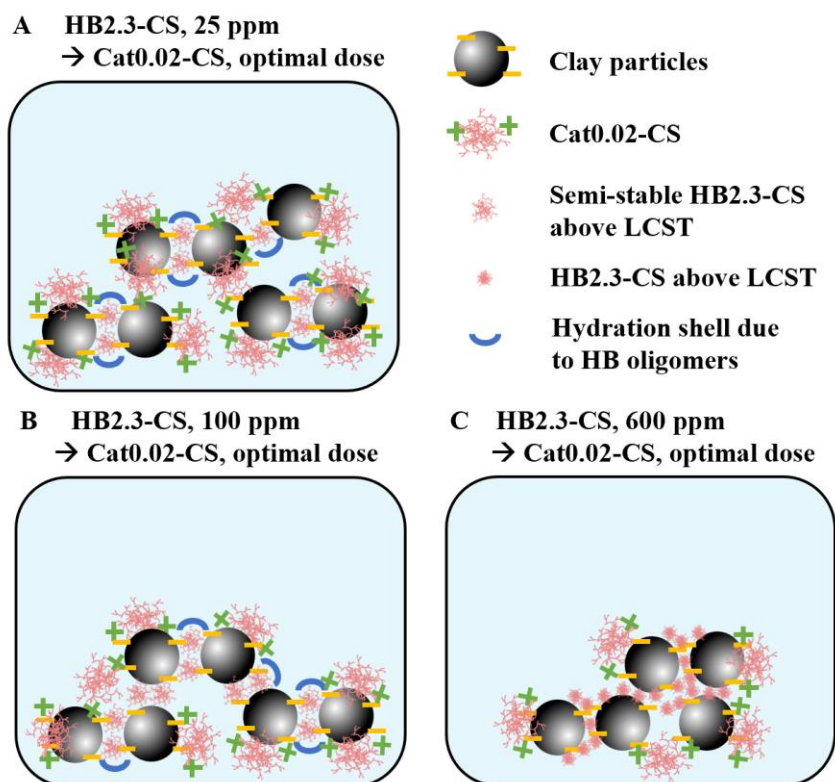


**Figure 5.6.** Schematic representation of flocculation of clay particles using 25 ppm (**A**), 100 ppm (**B**), and 600 ppm (**C**) of HB2.3-CS and Cat0.02-CS at optimal doses at 50 °C.

The maximum ISR values obtained was 75, 54 and 34 m/h for the respective doses of HB2.3-CS at 25, 100 and 600 ppm (Fig. 5.4B). HB2.3-CS could become more dehydrated (i.e. the hydration shells surrounding the HB substituents could be disrupted more) and less stable in a dispersion above its LCST as the polymer dose increases, which was evidenced by the decrease in the transmittance values of the polymer dispersions with increasing doses. For dispersions containing 25, 100 and 600 ppm of HB2.3-CS, the transmittance values recorded at 50 °C were 97 %, 87 % and 2 %, respectively (Fig. 2.3C). At 25 and 100 ppm, the HB2.3-CS could be semi-stable in a dispersion as the polymer may experience an incomplete dehydration (i.e. not all hydration shells surrounding the HB groups were disrupted) while at

600 ppm, the polymer became hydrophobic and completely dehydrated, and no longer stable in the dispersion. Within flocs, the clay particles could be held together more strongly by greater hydrophobic forces due to a higher dose of HB2.3-CS. We speculate that 25 ppm of HB2.3-CS may produce a large number of small, loosely bound flocs (similar to HB0.6-CS) while 600 ppm of HB2.3-CS may generate a small number of large, tightly bound flocs. The addition of the second flocculant, Cat0.02-CS, at optimal doses neutralized the flocs. The large number of the charge neutralized, small flocs may have a higher chance to collide and generate flocs that are large in size. On the contrary, the small number of the charge neutralized, large flocs may have a lower chance to collide and form flocs that are not as large as the ones formed by a large amount of small flocs. Thus, after the addition of Cat0.02-CS to an MFT mixture with 25 ppm of HB2.3-CS, larger flocs could be produced compared to when the Cat0.02-CS was added to the MFT mixture with 100 or 600 ppm of HB2.3-CS. This would explain the finding that the maximum ISR values decreased with the increasing doses of HB2.3-CS (Fig. 5.4B). Moreover, considering HB0.6-CS is much more hydrophilic than HB2.3-CS, a much larger number of smaller, more loosely bound flocs may be generated by the HB0.6-CS. In this case, upon the neutralization by Cat0.02-CS, huge flocs could be produced leading to a much higher ISR than HB2.3-CS.

The dose effect of Cat0.05-CS was also investigated where it was used as the second flocculant instead of Cat0.02-CS. With the use of 25 ppm HB0.6-CS and 25 ppm Cat0.05-CS, an ISR of 8.5 m/h was obtained (Fig. 5.4C). At 200 ppm of Cat0.05-CS, the ISR obtained by the dual flocculant system was more than 2-fold higher than that by using Cat0.05-CS alone. At 400 ppm, which was the optimal dose of Cat0.05-CS, the ISR produced by the dual

flocculant system was just marginally higher. With the use of 100 ppm HB0.6-CS, the ISR values were not better than those with the use of 25 ppm HB0.6-CS for the Cat0.05-CS doses higher than 100 ppm. With the use of 25 ppm of HB2.3-CS and 25 ppm of Cat0.05-CS, an ISR of 15 m/h was achieved (Fig. 5.4D). The maximum ISR was reached at 74 m/h when 400 ppm of Cat0.05-CS was used. The use of 100 ppm of HB2.3-CS did not improve the settling rates across the doses of Cat0.05-CS examined. Overall, replacing the Cat0.02-CS with Cat0.05-CS did not improve the settling rates. Hence, no further attempt has been made to flocculate the 2 wt % MFT using a Cat-CS with a higher  $MS_{Cat}$  as the second flocculant in a dual polymer flocculation process.

### **5.3.3.2 Water Recovery**

At doses from 0 to 100 ppm of Cat0.02-CS, the amount of water recovered from the dual polymer flocculation using 25 ppm of HB0.6-CS was higher than that using 100 ppm of HB0.6-CS (Fig. 5.7A). However, at the same dose range, the supernatants resulted from settling tests using Cat0.02-CS alone contained a large amount of suspended solids, so no water had been recovered from these settling tests. When 200 ppm of Cat0.02-CS was used, WR values resulted from 25 and 100 ppm of HB0.6-CS approached approximately 86 % (Fig. 5.7A). At 400 ppm of Cat0.02-CS or above, WR obtained from the dual polymer flocculation was similar to that when using Cat0.02-CS alone. Hence, the dual polymer flocculation performed better at a dose of 100 ppm or below and had the same performance at high doses compared to Cat0.02-CS used alone.

When HB0.6-CS was replaced with the thermoresponsive HB2.3-CS, at 25 and 100 ppm, WR were slightly lower at a low dose of Cat0.02-CS and became slightly higher with the use of 200 ppm Cat0.02-CS or above (Fig. 5.7B). With the use of HB2.3-CS at 600 ppm, the WR was at the highest (90 %) with the addition of 25 ppm of Cat0.02-CS and decreased marginally to 89 % at higher doses of Cat0.02-CS. The WR values were higher than those resulting from the use of 25 or 100 ppm HB2.3-CS. When using 600 ppm of HB2.3-CS, we suspect that compact flocs were formed, and water could be expelled from the flocs due to the hydrophobic clusters inside of the flocs (Fig. 5.6C).

When Cat0.02-CS was replaced with Cat0.05-CS, WR improved slightly when using a dose of Cat0.05-CS at 100 ppm or below. The improvements were more noticeable when 100 ppm of HB0.6-CS or HB2.3-CS were used (Fig. 5.7C and D). With the use of Cat0.05-CS at a dose of 200 ppm or above, WR generally remained unchanged when 25 or 100 ppm HB0.6-CS was used as the first flocculant, while the WR became slightly lower in the case of HB2.3-CS. The reduction in WR was intuitive because the flocs formed by Cat0.05-CS would hold more water leading to the release of a less amount of water compared to Cat0.02-CS. Replacing Cat0.02-CS with Cat0.05-CS gave a slight improvement in WR only when a low dose of Cat0.05-CS was used.



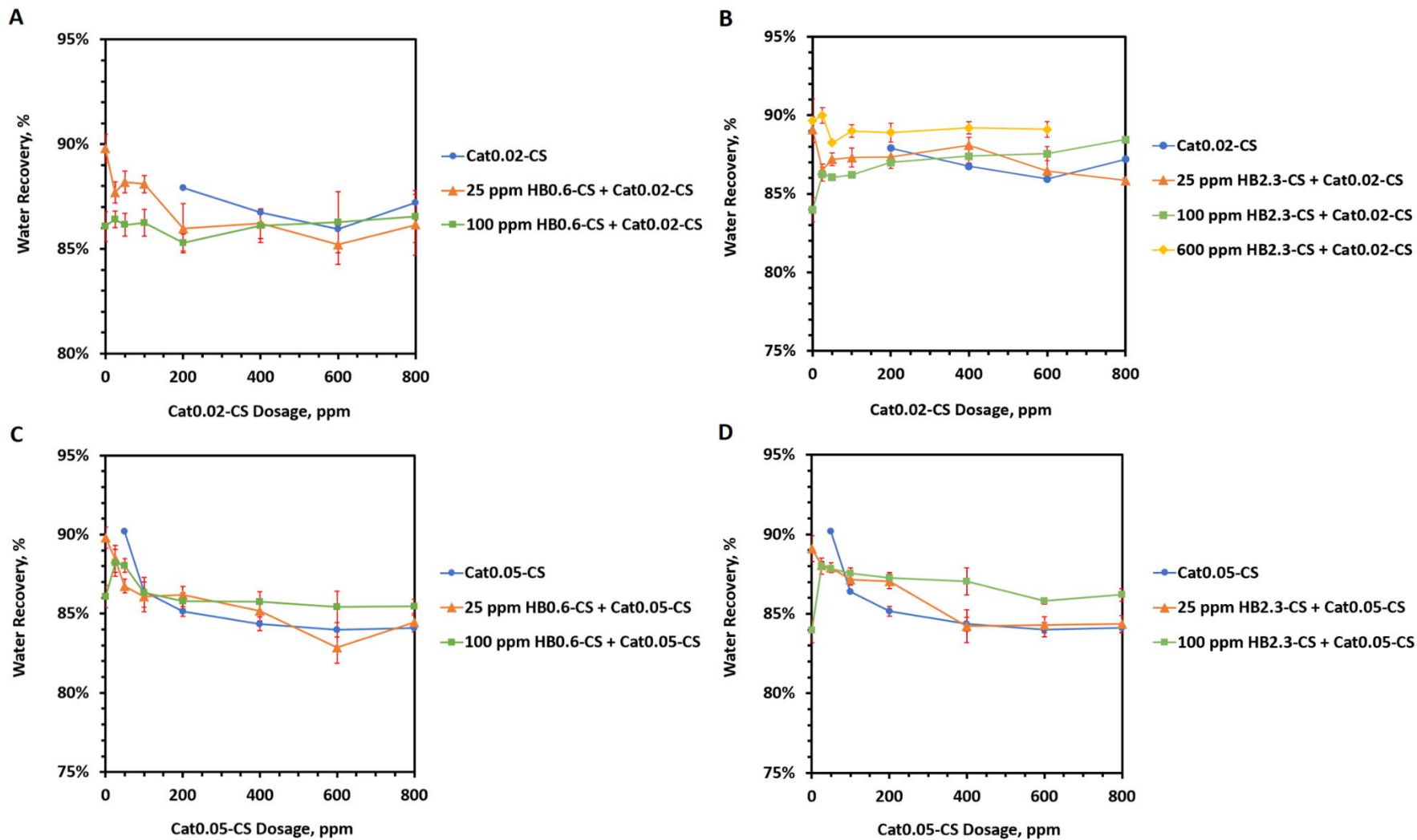


**Figure 5.7.** Water recovery of flocculation of 2 wt % MFT using flocculant pairs consisting of HB0.6-CS and Cat0.02-CS (A), HB2.3-CS and Cat0.02-CS (B), HB0.6-CS and Cat0.05-CS (C), and HB2.3-CS and Cat0.05-CS (D) at 50 °C.

### 5.3.3.3 Supernatant Turbidity

The supernatant was highly turbid ( $> 1000$  NTU) when flocculating with Cat0.02-CS only at a dose below 100 ppm. ST was greatly improved when using the dual flocculant system. With the use of 25 ppm HB0.6-CS and 25 ppm Cat0.02-CS, a reasonably clean supernatant was obtained at an ST of 67 NTU (Fig. 5.8A). With the use of 100 ppm HB0.6-CS and the same dose of Cat-0.02-CS, the ST decreased to 21 NTU. When adding the Cat0.02-CS at a dose higher than 400 ppm, both the dual polymer flocculation and the flocculation with Cat0.02-CS alone produced supernatants with the same turbidity.

When HB2.3-CS was used to replace HB0.6-CS, a very clean supernatant with an ST of 29 NTU was obtained after settling by the dual flocculant system consisting of 25 ppm HB2.3-CS and 25 ppm Cat0.02-CS (Fig. 5.8B). The ST decreased with the increasing dose of Cat0.02-CS until a minimum was reached at 5 NTU when 600 ppm of Cat0.02-CS was added. At 600 ppm of Cat0.02-CS, clay particles were charge neutralized and as a result, very few clay particles remained suspended. Overdosing of Cat0.02-CS led to an increase in ST (Fig. 5.8B). When a low dose of Cat0.02-CS was used, cleaner supernatants were produced with the increasing dose of HB2.3-CS as more polymers were available to bridge the clay particles. When using Cat0.02-CS with a dose of 400 ppm and above, flocculation with either 100 or 600 ppm of HB2.3-CS produced more turbid supernatants due to overdosing of Cat0.02-CS.

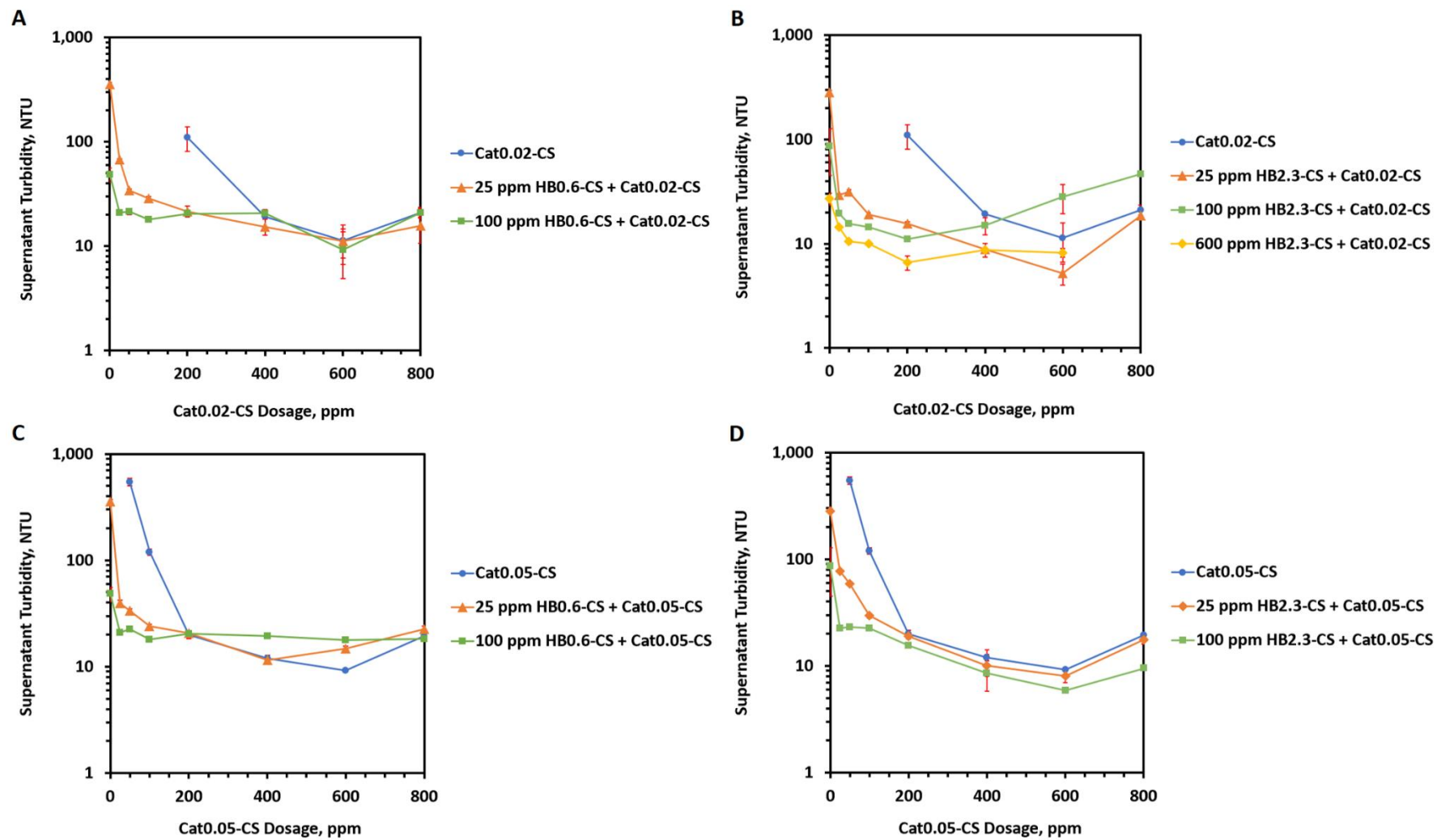


**Figure 5.8.** Supernatant turbidity of flocculation of 2 wt % MFT using flocculant pairs consisting of HB0.6-CS and Cat0.02-CS (A), HB2.3-CS and Cat0.02-CS (B), HB0.6-CS and Cat0.05-CS (C), and HB2.3-CS and Cat0.05-CS (D) at 50 °C.

When Cat0.05-CS was used as the second flocculant and at doses below 200 ppm, the supernatants produced from the dual polymer flocculation had much lower ST than those from the single flocculant flocculation (Fig. 5.8C and D). For example, the supernatant resulted from the dual polymer flocculation using a combined flocculant dose of 50 ppm gave an ST of 40 NTU, which was much lower than the ST of 545 NTU from the flocculation using Cat0.05-CS alone with the same total dose at 50 ppm (Fig. 5.8C). When the Cat0.05-CS dose was at 200 ppm or higher, the difference between the ST values obtained from the dual polymer or single polymer flocculation was small. Overall, the dual flocculant system enabled the recovery of clean water at a relatively low dose of Cat-CS.

#### **5.3.3.4 Sediment Solids Content**

Hydrophilic flocculants generally produce hydrophilic flocs that tend to hold a large amount of water. As well, loose stacking of large sized flocs often leaves a large volume of interparticle spaces that are filled with water molecules. If sediment contained a large amount of water, SSC would be low. When Cat0.02-CS was used at a dose of 100 ppm or under, the use of 25 ppm of HB0.6-CS produced a sediment with higher SSC than using 100 ppm of HB0.6-CS (Fig. 5.9A). HB0.6-CS could retain a considerable amount of water due to the hydration shells surrounding the HB substituents and a higher dose of HB0.6-CS could cause the entrapment of more water in the flocs. When the Cat0.02-CS doses was at 200 ppm or above, the addition of HB0.6-CS generally resulted in a lower SSC (Fig. 5.9A). We speculated that the decrease in SSC with the addition of HB0.6-CS was caused by the formation of large flocs that stacked loosely in the sediment which contained a considerable amount of water.

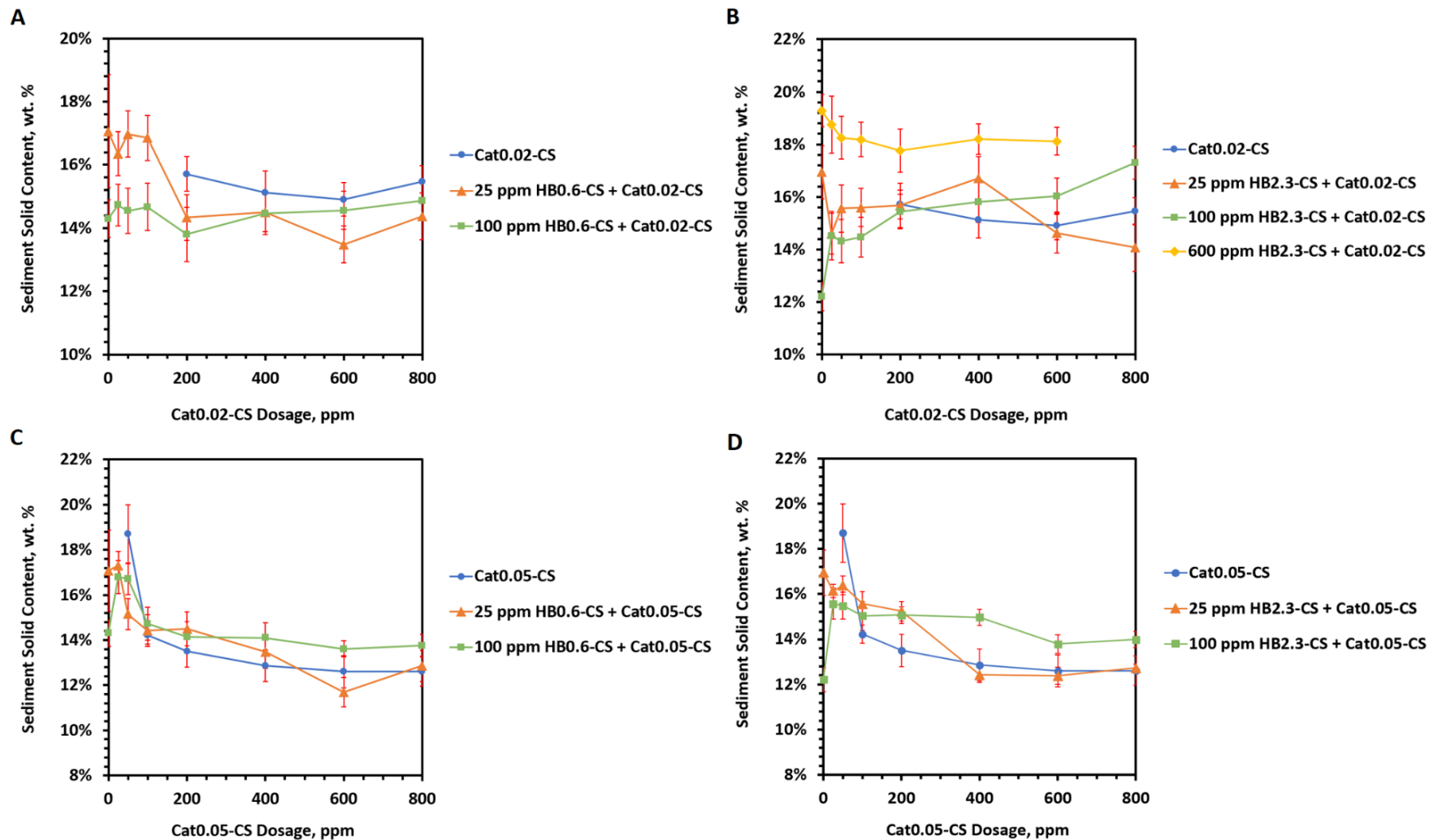


**Figure 5.9.** Sediment solids content of flocculation of 2 wt % MFT using flocculant pairs consisting of HB0.6-CS and Cat0.02-CS (A), HB2.3-CS and Cat0.02-CS (B), HB0.6-CS and Cat0.05-CS (C), and HB2.3-CS and Cat0.05-CS (D) at 50 °C.

At Cat0.02-CS doses from 25 to 100 ppm, the use of 25 ppm HB2.3-CS produced a sediment with an SSC of approximately 15 wt % (Fig. 5.9B), which was lower than that produced by 25 ppm of HB0.6-CS (17 wt %). We speculate that at 25 ppm, the hydration shells surrounding the HB groups on HB2.3-CS may not be disrupted and HB2.3-CS should have a larger amount of hydration shells compared to Cat0.6-CS due to the large number of HB groups of HB2.3-CS. As a result, the HB2.3-CS could retain a larger amount of water in the sediments compared to HB0.6-CS. When the dose of HB2.3-CS was increased to 600 ppm, the hydration shells would be completely disrupted and the polymer would become dehydrated and very hydrophobic at 50 °C, hence, producing flocs and sediments that contained less water. This was supported by the relatively high SSC values (> 18 wt %) obtained when 600 ppm of HB2.3-CS were used compared to 25 or 100 ppm of HB2.3-CS (Fig. 5.9B).

When Cat0.05-CS was used in place of Cat0.02-CS and at a dose of 25 ppm, the SSC values generally became higher. More specifically, at 25 ppm of Cat0.05-CS instead of Cat0.02-CS, the SSC increased from 16.4 to 17.3 wt % and from 14.7 to 16.8 wt % when the HB0.6-CS doses were at 25 and 100 ppm, respectively (Fig. 5.9A and C). As well, the SSC increased from 14.5 to 16.1 wt % and from 14.5 to 15.6 wt % when the respective doses, 25 and 100 ppm, of HB2.3-CS were used (Fig. 5.9B and D). At a dose of 25 ppm, bridging of free clay particles or small flocs produced by HB-CS by the Cat-CS may be the predominant flocculation mechanism. Since Cat0.05-CS contained more cationic groups to anchor onto the particle surfaces than Cat0.02-CS did, Cat0.05-CS should bridge the clay particles or small flocs more effectively and could produce denser sediments with higher SSC values. At higher Cat-CS doses, charge neutralization may become the predominant flocculation mechanism.

Cat-CS with a higher  $MS_{\text{Cat}}$  would not produce denser flocs because of the charge repulsion of the Cat-CS adsorbed flocs as well as the increase in the hydrophilicity of the flocculants. As a consequence, SSC values obtained by Cat0.05-CS were generally lower than that by Cat0.02-CS at high doses.

### **5.3.4 Settling Tests of 2 wt % MFT using HB-PS and Cat-PS**

From Chapter 2 and Chapter 3, we reported that both HB-PS and Cat-PS in the single polymer flocculation had significantly higher settling rates than their corn starch-based derivatives. In this section, the potato starch-based flocculants were employed in the dual flocculant systems to flocculate 2 wt % MFT. In these settling tests, either HB0.6-PS or HB1.9-PS was paired up with Cat0.02-PS. HB0.6-PS is not thermoresponsive while HB1.9-PS exhibits an LCST of 36 °C. All settling tests were conducted at 50 °C.

#### **5.3.4.1 Initial Settling Rate**

Below a dose of 50 ppm, flocculation with Cat0.02-PS alone failed to produce a clean enough supernatant with a turbidity under 1000 NTU, hence, the settling rate was considered to be 0. With the use of 25 ppm of Cat0.02-PS as the second flocculant, 25 ppm of HB0.6-PS resulted in an ISR of 12 m/h, while increasing the dose of HB0.6-PS to 100 ppm increased the ISR significantly to 48 m/h (Fig. 5.10A). The ISR values were much higher compared to those produced by the flocculant pairs consisting of HB0.6-CS and Cat0.02-CS at the same doses. With the increase of the dose of Cat0.02-PS to 600 ppm, the ISR increased to achieve the respective maximum values of 410 m/h and 323 m/h when 25 and 100 ppm of HB0.6-PS were used as the first flocculant. At such high settling rates, the flocculation finished in seconds,

which would be very useful for potential applications that valued the speed of the settling process the most. When compared to the flocculant pairs consisting of HB0.6-CS and Cat0.02-CS, the maximum ISR values from the PS-based flocculant pair were much higher, which was consistent with previous finds that PS-based flocculants usually produced higher settling rates. Moreover, Cat0.02-PS showed an optimal dose at 600 ppm, which was the same as Cat0.02-CS, and this was intuitive as their  $MS_{\text{Cat}}$  values were the same.



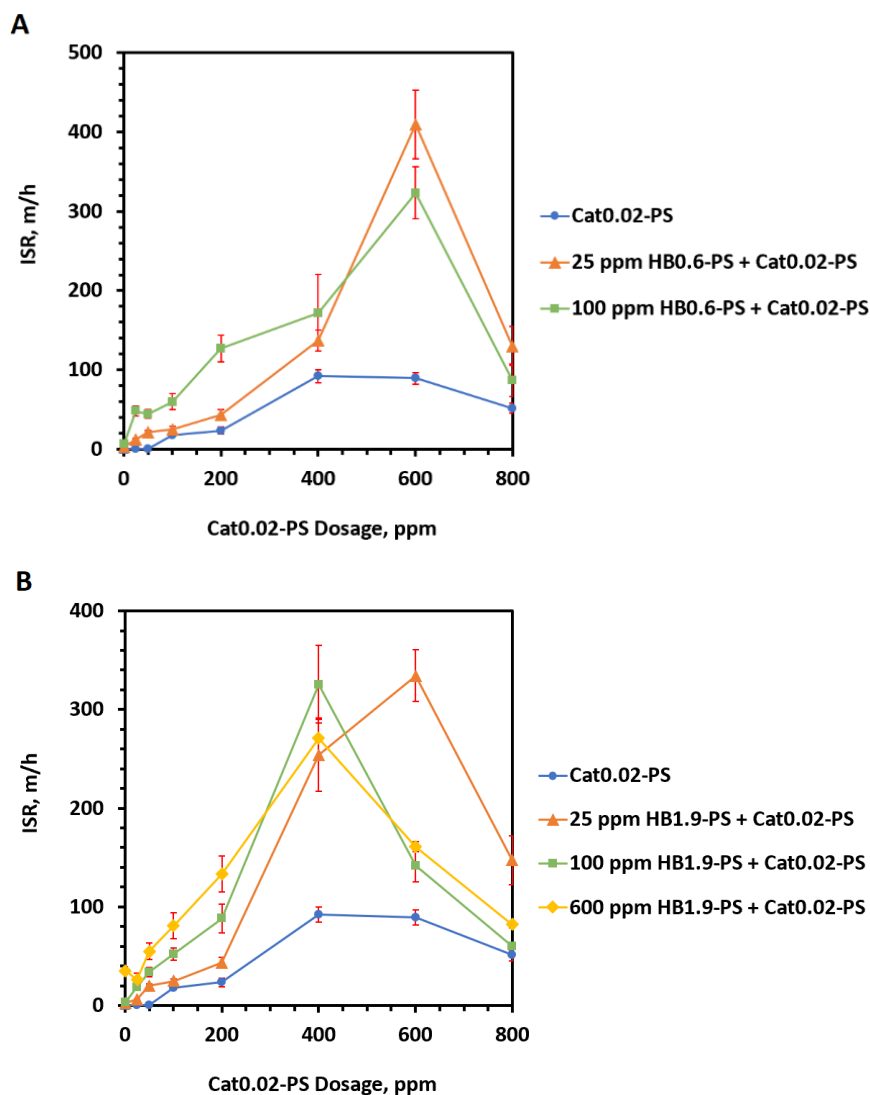


**Figure 5.10.** Initial settling rates (ISR) of flocculation of 2 wt % MFT using flocculant pairs consisting of HB0.6-PS and Cat0.02-PS (**A**), and HB1.9-PS and Cat0.02-PS (**B**) at 50 °C. Dosage was reported on the dry/slurry basis.

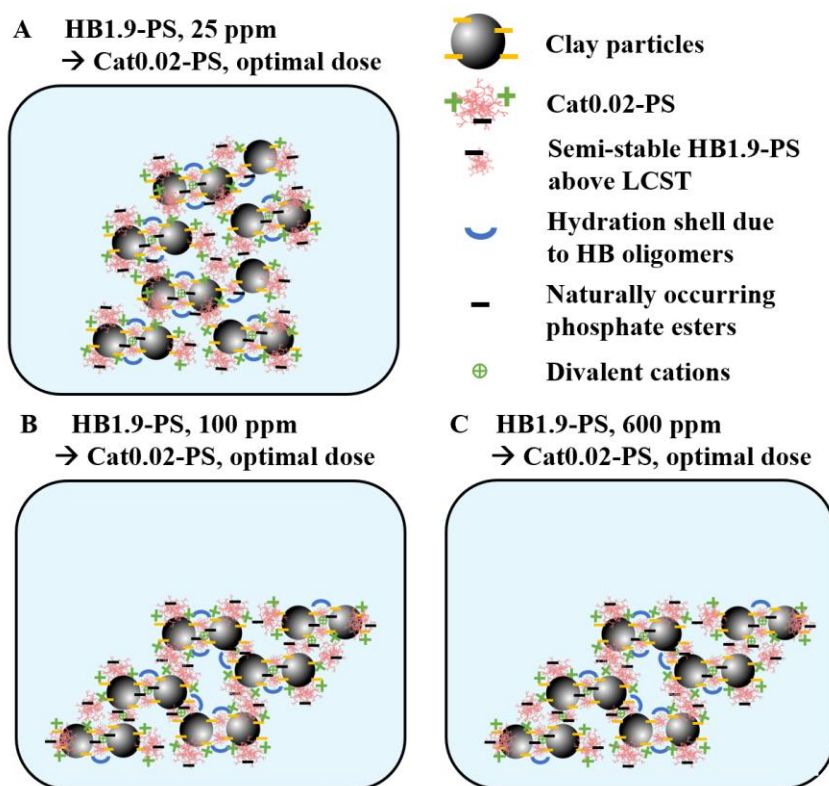
When the thermoresponsive polymer, HB1.9-PS, was paired up with Cat0.02-PS to flocculate 2 wt % MFT, the ISR values were higher with the increasing doses of HB1.9-PS from 25 to 600 ppm at a dose of Cat0.02-PS below 400 ppm (Fig. 5.10B). This increase in ISR could be due to the increase in the hydrophobicity of the HB1.9-PS at higher doses. From

Figure 2.4 in Section 2.3.1, the light transmittance studies of HB1.9-PS showed that HB1.9-PS dispersions at 25, 100 and 600 ppm had the respective transmittance values at 98 %, 96 % and 83 % above the LCST, suggesting that HB1.9-PS may become more dehydrated and form mesoglobules with decreasing stability above its LCST as the polymer dose increases. At Cat0.02-PS dose of 200 ppm or below, HB1.9-PS showed similar settling rates to HB0.6-PS when a dose of 25 or 100 ppm was used (Fig. 5.10A and B). Even when 600 ppm of HB1.9-PS (and Cat0.02-PS at < 200 ppm) were used, the resultant ISR had only a marginal increase over that when 100 ppm of HB0.6-PS were used. At a low dose of Cat0.02-PS, the thermoresponsive feature of HB1.9-PS was somewhat redundant regarding their ISRs.

The maximum ISR at 334 m/h was achieved with the use of 25 ppm HB1.9-PS and 600 ppm Cat0.02-PS, while 100 and 600 ppm HB1.9-PS produced lower maximum values at 326 and 271 m/h, respectively (Fig. 5.10B). This trend was also observed with the flocculant pair, HB2.3-CS and Cat0.02-CS, where the maximum ISR decreased from 75 to 34 m/h as the dose increased from 25 to 600 ppm (Fig. 5.4B).

The maximum ISR was approximately 4.5-, 6-, and 8-fold higher at the respective doses of 25, 100, and 600 ppm when comparing the PS-based flocculant pair to the CS-based pair. The superior performance of the PS-based flocculant pair could be due to the higher molecular weight of the PS-based flocculants compared to the CS-based flocculants, as higher molecular weight often improves the flocculating ability of a flocculant.<sup>162,163</sup> Such increase in the maximum ISR values may also be a result of the negative charges on the flocculants due to the native phosphate esters on potato starch. These negative charges could provide additional

anchoring sites for the attachment of other polymer bound flocs and may eventually lead to the formation of huge flocs (Fig. 5.11A-C). The CS-based flocculants do not contain phosphate groups, which was evidenced by the  $^{31}\text{P}$  NMR analysis of the  $\alpha$ -limited corn starch (Figure A6 in Appendix A). Hence, in the case of CS-based flocculants, the flocs would be less likely to assemble into large flocs (Fig. 5.6A-C).



**Figure 5.11.** Schematic representation of flocculation of clay particles using 25 ppm (A), 100 ppm (B), and 600 ppm (C) of HB1.9-PS and Cat0.02-PS at optimal doses at 50 °C.

The optimal dose of Cat0.02-PS decreased from 600 to 400 ppm when the addition of HB1.9-PS increased from 25 to 100 ppm (Fig. 5.10B). The decrease in the optimal dose suggested a decrease in the amount of Cat0.02-PS that was required for the neutralization of the solids in the MFT. This phenomenon was also observed previously with HB2.3-CS and

Cat0.02-CS (Fig. 5.4B). As the dose of HB1.9-PS increased, we propose that a larger amount of the polymer would aggregate to form hydrophobic clusters inside of the flocs, which could physically occupy the areas with negative charges on the clay particle surfaces and reduce the total number of surface charges of clay particles in the suspension.

#### **5.3.4.2 Water Recovery**

At a dose of Cat0.02-PS below 200 ppm, the use of HB0.6-PS at a dose of 25 or 100 ppm showed similar WR values at about 87 % (Fig. 5.12A). At higher Cat0.02-PS doses, WR stayed unchanged at 87 % with the use of 100 ppm HB0.6-PS, which was higher than that using 25 ppm or without the use of HB0.6-PS. Increasing the dose of HB0.6-PS may increase the chance of the polymers to aggregate inside of flocs and may reduce the amount of water in the intraparticle space of the flocs leading to an increase in recoverable water.

When 25 ppm of HB1.9-PS and Cat0.02-PS with a dose of 50 ppm or below were used, WR greater than 88 % was recorded (Fig. 5.12B), however, the recovered water was very turbid (see Figure 5.13B in the following section). At higher Cat0.02-PS doses, the addition of 25 ppm of HB1.9-PS resulted in lower WR than using Cat0.02-PS alone (Fig. 5.12B). Increasing the dose of HB1.9-PS to 100 and 600 ppm improved the WR but less so than the improvement obtained by 100 ppm of HB0.6-PS and Cat0.02-PS (Fig. 5.12A and B).

Generally, the CS-based polymer pairs consisting of both thermoresponsive and cationic flocculants gave higher WR values than the PS-based pairs. For example, 600 ppm of HB2.3-CS and 25 ppm of Cat0.02-CS yielded a WR of 90 % while 600 ppm of HB1.9-PS and

25 ppm of Cat0.02-PS only produced a WR of 85 %. This suggested that the use of potato starch as the base materials for the flocculants could have a negative impact on WR.

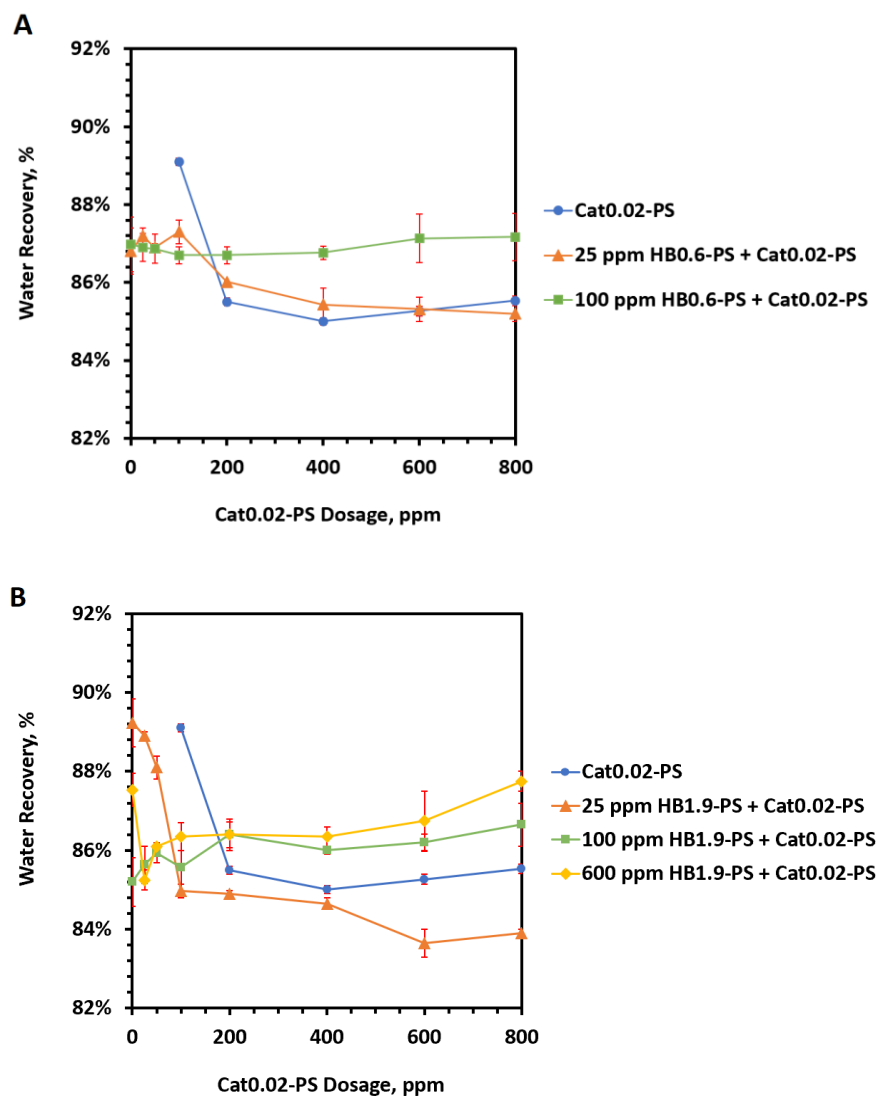


**Figure 5.12.** Water recovery of flocculation of 2 wt % MFT using flocculant pairs consisting of HB0.6-PS and Cat0.02-PS (**A**), and HB1.9-PS and Cat0.02-PS (**B**) at 50 °C. Dosage was reported on the dry/slurry basis.

### 5.3.4.3 Supernatant Turbidity

With the use of 25 ppm HB0.6-PS, the supernatant was very turbid at low Cat0.02-PS doses and the ST decreased drastically with increasing dose of Cat0.02-PS (Fig. 5.13A). As the dose of Cat0.02-PS increased, more flocculants would be available in an MFT mixture for bridging and to neutralize the negatively charged particle surfaces, which could greatly reduce the amount of suspended particles in the supernatant. Similarly, as the dose of HB0.6-PS increased to 100 ppm, the bridging of clay particles should be improved and leading to relatively low ST values.

With a low dose of Cat0.02-PS (< 200 ppm), the use of 100 or 600 ppm of HB1.9-PS produced a cleaner supernatant compared to using only 25 ppm (Fig. 5.13B). The lowest ST value (about 10 NTU) was achieved at 400 ppm of Cat0.02-PS regardless of the doses of HB1.9-PS. Overall, the dual flocculant system generated a lower ST than the single flocculant system.

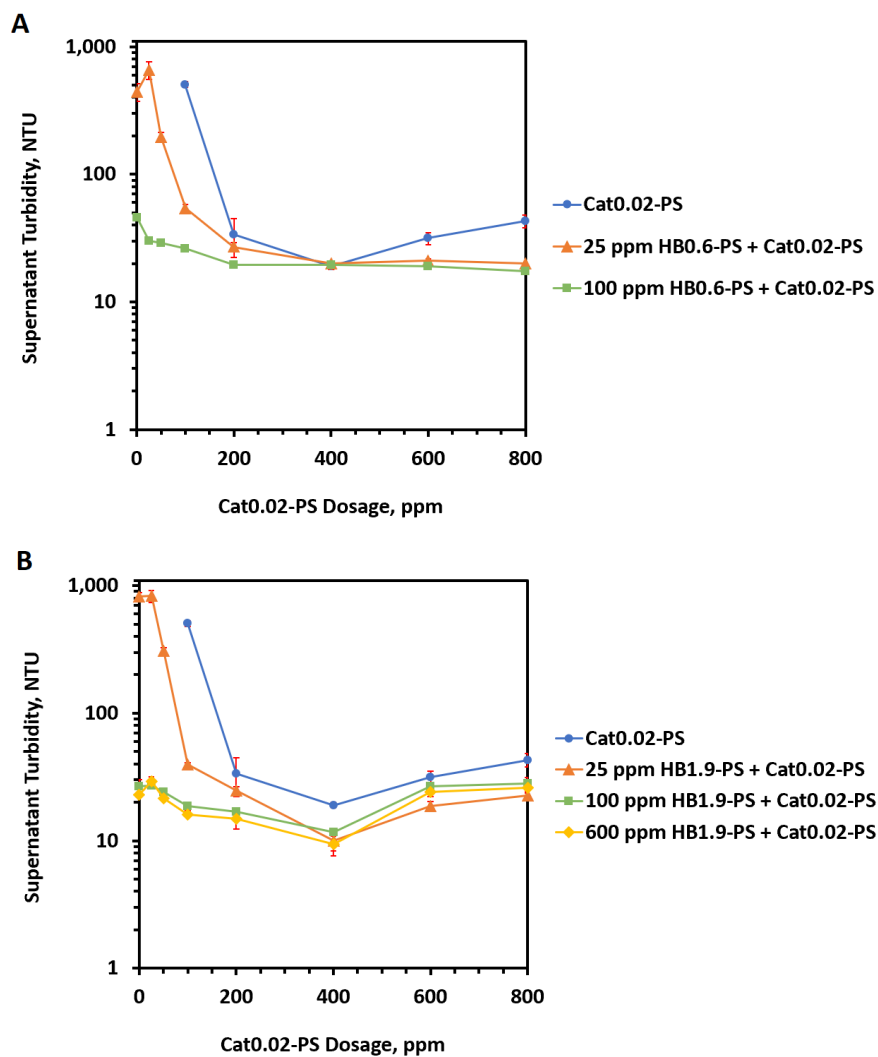


**Figure 5.13.** Supernatant turbidity of flocculation of 2 wt % MFT using flocculant pairs consisting of HB0.6-PS and Cat0.02-PS (**A**), and HB1.9-PS and Cat0.02-PS (**B**) at 50 °C. Dosage was reported on the dry/slurry basis.

#### 5.3.4.4 Sediment Solids Content

At low Cat0.02-PS doses (< 200 ppm), the dual flocculant system produced sediments with similar SSC values (Fig. 5.14A). When the Cat0.02-PS doses were 200 ppm or above, the use of 25 ppm of HB0.6-PS showed little impact on SSC compared to using Cat0.02-PS alone

while the use of 100 ppm of HB0.6-PS yielded slightly higher SSC than using Cat0.02-PS alone (Fig. 5.14A). The SSC values produced by HB0.6-PS and Cat0.02-PS were generally lower than the values obtained by their CS-based equivalents (Fig. 5.9A).

When 25 ppm of HB1.9-PS and 25 ppm of Cat0.02-PS were used, a relatively high SSC (16.9 wt %) was obtained (Fig. 5.14B). However, this flocculation also produced a supernatant with a high turbidity at 830 NTU, indicating that a large amount of hydrophilic solids may still be suspended in the supernatant and consequently, those less hydrophilic solids may form a denser sediment leading to a higher SSC. In general, the SSC increased with the increasing dose of HB1.9-PS (Fig. 5.14B). Compared to the flocculant pair, HB2.3-CS and Cat0.02-CS (Fig. 5.9B), the PS-based flocculants produced sediments with lower SSC values. For example, 600 ppm of HB2.3-CS and 400 ppm of Cat0.02-CS achieved an SSC of 18.2 wt % while the PS-based flocculant pair gave a much lower SSC at 14.2 wt % at the same doses. The higher SSC could be a result of compact flocs produced by HB2.3-CS which are completely dehydrated and very hydrophobic above its LCST at 600 ppm (Fig. 5.6C). On the other hand, HB1.9-PS may not be completely dehydrated above its LCST at 600 ppm due to the presence of negatively charged phosphate groups, hence, producing flocs that are more loosely packed (Fig. 5.11C).



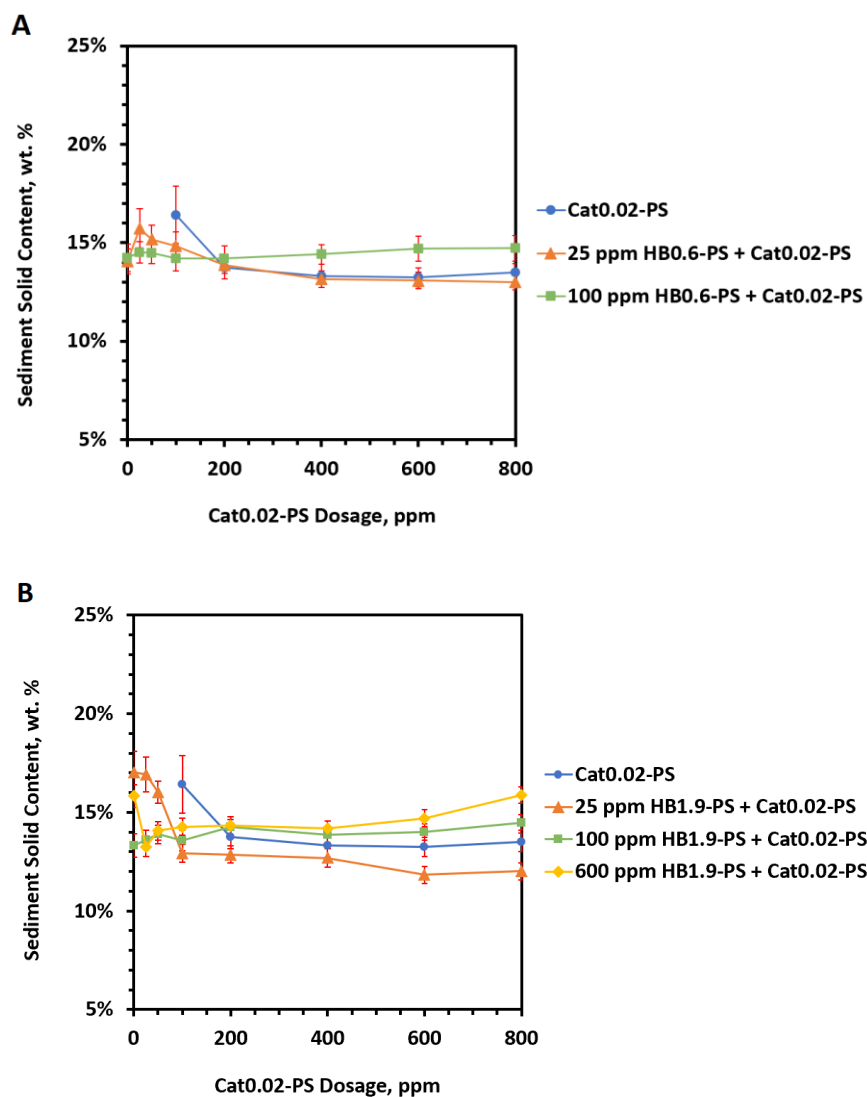


**Figure 5.14.** Sediment solids content of flocculation of 2 wt % MFT using flocculant pairs consisting of HB0.6-PS and Cat0.02-PS (**A**), and HB1.9-PS and Cat0.02-PS (**B**) at 50 °C. Dosage was reported on the dry/slurry basis.

### 5.3.5 Settling Tests of 2 wt % MFT using PHE-PS and Cat-PS

From the previous studies on flocculation of 2 wt % MFT with a dual polymer system, we have established that the PS-based flocculant pairs produced higher ISRs, and the highest ISR achieved was 410 m/h using 25 ppm HB0.6-PS and 600 ppm of Cat0.02-PS. Additionally,

the hydrophobicity of the first flocculant in a dual polymer system played an important role in both WR and SSC, and higher hydrophobicity usually leads to higher WR and SSC. For the aforementioned reasons, a novel hydrophobically modified potato starch, phenylhydroxyethyl potato starch with an  $MS_{PHE}$  of 0.2 (PHE0.2-PS), was synthesized and used in the dual polymer flocculation in place of the HB0.6-PS.

The ISR was 22 m/h with the addition of 25 ppm PHE0.2-PS and 25 ppm Cat0.02-PS (Fig. 5.15A), which was over 80 % higher than the ISR produced by the polymer pair with HB0.6-PS at the same doses. The difference in ISR may arise from the large difference in the ISR values obtained by the use of HB0.6-PS or PHE0.2-PS alone. This was supported by the fact that the flocculation with 25 ppm of PHE0.2-PS produced an ISR of 19 m/h, which was over 6-fold higher than using 25 ppm of HB0.6-PS (Fig. 2.12A). With the increasing dose of Cat0.02-PS, the ISR obtained by HB0.6-PS as the first flocculant quickly approached and surpassed the ISR obtained from PHE0.2-PS (Fig. 5.15A), which suggested that the phenylhydroxyethyl starch may be less cooperative with the cationic starch compared to the hydroxybutyl starch. This was most noticeable when comparing the maximum ISR value produced by the dual polymer flocculation to that by the single polymer flocculation at the optimal dose of Cat0.02-PS. The dual polymer system containing HB0.6-PS produced a maximum ISR that was tremendously higher than using Cat0.02-PS alone while the dual polymer system containing PHE0.2-PS did not improve the maximum ISR of the single polymer flocculation (Fig. 5.15A). Hence, regarding ISR, the dual polymer system with PHE0.2-PS was only beneficial when the dose of Cat0.02-PS was low.

The main purpose of substituting the HB groups for the more hydrophobic PHE groups was to improve WR and SSC. Indeed, flocculation with the dual polymer system containing PHE0.2-PS resulted in higher WR and SSC than with the one containing HB0.6-PS across the doses of Cat0.02-PS examined (Fig. 5.15B and D). The dual flocculant system with PHE0.2-PS also performed better than the single flocculant system in regard to WR and SSC.

Replacing the HB0.6-PS with PHE0.2-PS also improved the clarity of the supernatants. When 25 ppm of PHE0.2-PS was added instead of HB0.6-PS along with 25 ppm of Cat0.02-PS, ST drastically reduced from 659 to 39 NTU (Fig. 5.15C). The ST continued to decrease to a minimum of 13 NTU as the dose of Cat0.02-PS reached 400 ppm.

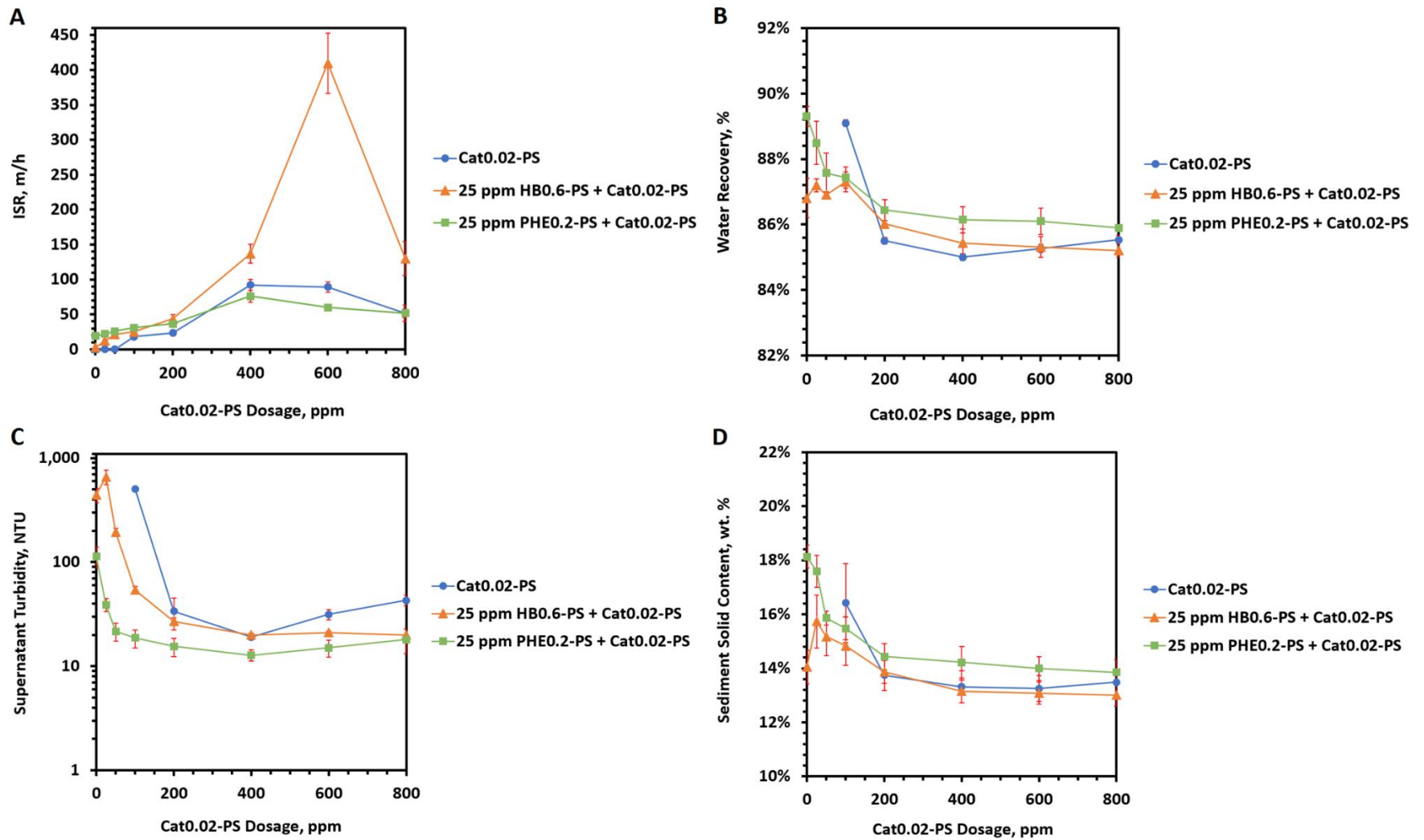


**Figure 5.15.** ISR (A), WR (B), ST (C) and SSC (D) of the flocculation of 2 wt % MFT with a flocculant pair, PHE0.2-PS and Cat0.02-PS. The performance of settling with Cat0.02-PS alone or with HB0.6-PS and Cat0.02-PS were included for comparison.

### 5.3.6 Developing an Economical Flocculant for 2 wt % MFT

An economical flocculant should satisfy the following criteria: firstly, only a low dose is required to achieve an acceptable flocculation performance; secondly, the base material is inexpensive; and thirdly, only a small amount of reagents is needed to produce the flocculants. The base material of the flocculants in testing was either corn starch or potato starch, which is inexpensive. The cost of reagents will mostly determine the cost of the flocculants. Thus, a flocculant or a pair of flocculants which contains the least amount of modification and provides a reasonable performance at a minimal dose is considered to be the best candidate. Table 5.2 summarized the performance of a number of flocculant pairs for the settling of 2 wt % MFT. Comparing entries 1 and 2, the increase in the MS of cationic groups improved the flocculation performance in all four parameters. Similar observations can be made when comparing entry 3 and 4 except for ST. So, in order to reduce the dose required to achieve similar performance, a cationic starch with a higher MS should be used. When comparing entry 1 and 3 or 2 and 4, the increase in the MS of hydroxybutyl groups gave mixed results. Since the thermoresponsive properties were not required for the flocculation of 2 wt % MFT using the dual flocculant system, HB0.6-CS was preferred over HB2.3-CS due to the much higher amount of reagents that were needed to synthesize the latter. Using potato starch as the base material did not improve the performance (i.e. ST was very high) in the dual polymer flocculation using a combined dose of 50 ppm (Table 5.2, entries 6 and 7). Thus, corn starch-based flocculant was more preferable in this case. Due to the reasons discussed above, Cat0.25-CS was synthesized and used together with HB0.6-CS in the settling tests. At a combined dose of 50 ppm, the flocculant pair, HB0.6-CS and Cat0.25-CS, performed considerably better than that when

HB0.6-CS was paired with Cat0.02-CS or Cat0.05-CS (compare entry 9 to entries 1 or 2). With the use of 5 ppm HB0.6-CS and 20 ppm Cat0.25-CS, a reasonable performance was achieved (Table 5.2, entry 10). Moreover, as discussed previously, the flocculants performed more effectively at low doses when substituted with PHE groups instead of HB groups due to the increase in hydrophobicity. As a result, a lower degree of modification on the flocculants would be required. The polymer pair, PHE0.2-CS and Cat0.02-CS, produced better settling results than the one consisting of HB0.6-CS and Cat0.02-CS at the same combined dose of 50 ppm (compare entry 5 to entry 1). When PHE0.2-CS paired with Cat0.25-CS in lieu of Cat0.02-CS, a higher ISR and a lower ST was obtained at a combined dose of 50 ppm (Table 5.2, entry 11). The use of 5 ppm of PHE0.2-CS and 20 ppm of Cat0.25-CS gave a fast ISR at 29 m/h, a good WR at 88 %, an ST under 30 NTU and a high SSC of 17.2 wt % (Table 5.2, entry 12). This pair of flocculants had the least amount of modification with a total MS of 0.45 and used at the lowest dose with a sum of 25 ppm, which was overall the best flocculant pairs to be used for the settling of 2 wt % MFT.

**Table 5.2.** A summary of flocculation performance of different flocculant pairs with a combined dose under 50 ppm at 50 °C.

	1 <sup>st</sup> Polymer	Dosage, ppm	2 <sup>nd</sup> Polymer	Dosage, ppm	ISR, m/h	WR, %	ST, NTU	SSC, wt %
1	HB0.6-CS	25	Cat0.02-CS	25	7.0	88	67	16.4
2	HB0.6-CS	25	Cat0.05-CS	25	8.5	88	40	17.3
3	HB2.3-CS	25	Cat0.02-CS	25	13	86	29	14.5
4	HB2.3-CS	25	Cat0.05-CS	25	15	88	78	16.1
5	PHE0.2-CS	25	Cat0.02-CS	25	15	89	29	17.8
6	HB0.6-PS	25	Cat0.02-PS	25	12	87	659	15.3
7	HB1.9-PS	25	Cat0.02-PS	25	6	89	830	16.9
8	PHE0.2-PS	25	Cat0.02-PS	25	22	88	39	17.6
9	HB0.6-CS	25	Cat0.25-CS	25	29	86	18	14.7
10	HB0.6-CS	5	Cat0.25-CS	20	18	88	41	16.8
11	PHE0.2-CS	25	Cat0.25-CS	25	44	88	16	16.4
12	PHE0.2-CS	5	Cat0.25-CS	20	29	88	29	17.2

### 5.3.7 Comparison with other Polymers used to Flocculate 2 wt % MFT

In this section, we compare the performance of our dual flocculant system to that of other polymers used to flocculate 2 wt % MFT in the literature. A hydrophobically modified polyacrylamide (PAM) was synthesized by copolymerizing different polypropylene oxide macromonomers (PPO) with acrylamide (AM) and the PAM-PPO graft copolymers were used to flocculate 2 wt % MFT by Reis et al. in 2016.<sup>135</sup> The authors reported that with the use of 200 ppm (or 10000 ppm if referred to the mass of MFT solids) of the PAM-*g*-PPO, which had a copolymer composition (AM:PPO-300) of 86:14 and a molecular weight of about 1 million Da, an ISR of 5.2 m/h (or 1.45 mm/s as reported in the paper) and an ST of approximately 280 NTU were obtained. They also reported the performance of a commercial anionic PAM for comparison. The anionic PAM, which had a molecular weight of 17 million Da, was used at a

dose of 40 ppm along with the addition of 20 ppm of calcium ions to produce an ISR of 5.5 m/h and an ST of 1700 NTU. Comparing to a flocculant pair consisting of 25 ppm of PHE0.2-CS and 25 ppm of Cat0.25-CS, the flocculant pair showed much better performance (ISR: 44 m/h, ST: 16 NTU) and required a less amount of additives.

Another study, by Younes et al. in 2018, reported the flocculation of 2 wt % MFT with several variants of the partially hydrolytically degradable cationic polymers and one of such polymers was synthesized with the macromonomer, poly(lactic acid) choline iodide ester methacrylate (PLA<sub>4</sub>ChMA).<sup>174</sup> The authors reported an ISR of 0.34 m/h and an ST of 3 NTU with the use of 180 ppm (or 9000 ppm on the basis of the mass of MFT solids as reported in the paper) of poly(PLA<sub>4</sub>ChMA). As the polymer was degradable at 50 °C over time, an SSC of 20 wt % was achieved when the sediment was kept at 50 °C over a period of 5 days after the flocculation with 200 ppm of the poly(PLA<sub>4</sub>ChMA). For comparison, a settling test with a polymer pair containing 600 ppm of HB2.3-CS and 25 ppm of Cat0.02-CS resulted in a considerably higher ISR and comparable ST and SSC values but required a higher total dose (ISR: 14 m/h, ST: 15 NTU, and SSC after 1 day: 18.7 wt %).

### **5.3.8 Conclusion of the Dual Polymer Flocculation for 2 wt % MFT**

At the optimal dose of cationic starch, the maximum ISR usually decreased with an increasing dose of the first flocculant in a dual polymer settling test. A high hydrophobicity of the first flocculant often caused a decrease in the maximum ISR as well. While at a low dose of the cationic starch, the increasing hydrophobicity of the first flocculant usually increased



the ISR possibly due to more effective bridging. The PS-based dual flocculant system generally resulted in a higher ISR than the CS-based derivatives.

While the PS-based flocculants increased the ISR, the WR and SSC suffered from the increase in hydrophilicity (due to the presence of phosphate groups) of PS. The highest WR and SSC was achieved by the dual flocculant system containing a thermoresponsive polymer at 600 ppm, a dose at which a complete dehydration of the polymer might occur. When used at low doses, the dual polymer system containing PHE groups, which were more hydrophobic than the HB groups, produced relatively high WR and SSC values.

The highest ISR, 410 m/h, was achieved when 25 ppm of HB0.6-PS and 600 ppm of Cat0.02-PS were used. Most of the dual flocculant systems produced clean supernatants and the supernatant with the lowest ST at 5 NTU was produced by the use of 25 ppm of HB2.3-CS and 600 ppm of Cat0.02-CS. The highest WR at 90 % and SSC at 18.7 wt % were achieved by the dual flocculant system consisting of 600 ppm HB2.3-CS and 25 ppm Cat0.02-CS. The most economical flocculant system was the dual polymer pair consisting of 5 ppm of PHE0.2-CS and 20 ppm of Cat0.25-CS, which can flocculate 2 wt % MFT with an ISR at 29 m/h, a WR of 88 %, an ST at 29 NTU and SSC at 17.2 wt %. From the preceding section, it has been found that the dual flocculant systems compared very favorably with other polymers reported in the literature for the flocculation of 2 wt % MFT.

### **5.3.9 Settling Tests of 10 wt % MFT using HB-CS and Cat-CS**

It has been widely established in the literature that increasing the solids content of the MFT drastically increases the difficulty of flocculation, and consequently, the settling rate of

the MFT with a high solids content is often extremely slow.<sup>11</sup> From Section 5.3.3.1, it has been established that the dual flocculant system consisting of 100 ppm of HB0.6-CS and 600 ppm of Cat0.02-CS produced the highest ISR (241 m/h) when used to flocculate 2 wt % MFT. So, the flocculation of 10 wt % MFT was first attempted using this dual flocculant pair; however, this pair of flocculants was not able to effectively flocculate the 10 wt % MFT (ISR: 0.05 m/h, WR: 32 %, ST: 64 NTU and SSC: 14.6 wt %). The CS-based flocculants were not good candidates for the flocculation of 10 wt % MFT.

### **5.3.10 Settling Tests of 10 wt % MFT using HB-PS and Cat-PS**

From Section 5.3.4.1, the dual polymer systems consisting of PS-based flocculants generally exhibited much higher ISR values than the CS-based flocculant systems. This was especially true for the flocculant pair consisting of the thermoresponsive polymer, HB1.9-PS, and Cat0.02-PS. From Section 3.3.4, Cat0.2-PS at a dose of 1000 ppm was capable to flocculating 10 wt % MFT with a reasonable settling rate. In this section, we report the settling of 10 wt % MFT using the PS-based dual flocculant systems. The settling tests were conducted with three different flocculant pairs including HB0.6-PS and Cat0.02-PS, HB1.9-PS and Cat0.02-PS, and HB1.9-PS and Cat0.2-PS.

#### **5.3.10.1 Initial Settling Rate**

The use of Cat0.02-PS alone or a combination of 25 ppm HB0.6-PS and Cat0.02-PS with a dose up to 800 ppm failed to flocculate 10 wt % MFT. When the dose of HB0.6-PS increased to 100 ppm, the dual polymer pair started to show some flocculation ability when the dose of Cat0.02-PS reached 400 ppm or above (Fig. 5.16A). With the use of 100 ppm of

HB0.6-PS and 600 ppm of Cat0.02-PS, an ISR of 0.13 m/h was obtained and was 2.6-fold higher than using the CS-based flocculant pair at the same doses, which demonstrated that the PS-based flocculants are better candidates for the flocculation of 10 wt % MFT. Further increase in the dose of HB0.6-PS to 600 ppm resulted in an increase in the ISR (Fig. 5.16A). The highest ISR, which was recorded at 1.1 m/h, was achieved with the use of 800 ppm Cat0.02-PS. The shape of the ISR curve indicated that the maximum ISR value was not reached until when a higher dose of Cat0.02-PS was added. This flocculant pair was still not a good candidate for the flocculation of 10 wt % MFT since relatively high doses of the flocculants were required and the settling rates were relatively low.

With the use of 25 or 100 ppm of HB1.9-PS and Cat0.02-PS in a dose range from 25 to 800 ppm, no flocculation or flocculation with slow settling rates resulted (Fig. 5.16B). As the dose of HB1.9-PS increased to 600 ppm, the flocculation occurred at much faster settling rates. This observation suggested that the thermoresponsivity of HB 1.9-PS played an important role in ISR in the flocculation of 10 wt % MFT. As discussed previously, we speculate that HB1.9-PS may not be completely dehydrated due to the presence of phosphate groups above its LCST, but an increase in the polymer dose could cause the polymer to dehydrate more above the LCST due to the presence of more hydrophobic HB groups. With the presence of more hydrophobic HB groups in an MFT mixture, the formation of flocs could be facilitated by the increase in hydrophobic interactions between HB1.9-PS and the HB1.9-PS adsorbed clay particles, hence, increasing the settling rates.

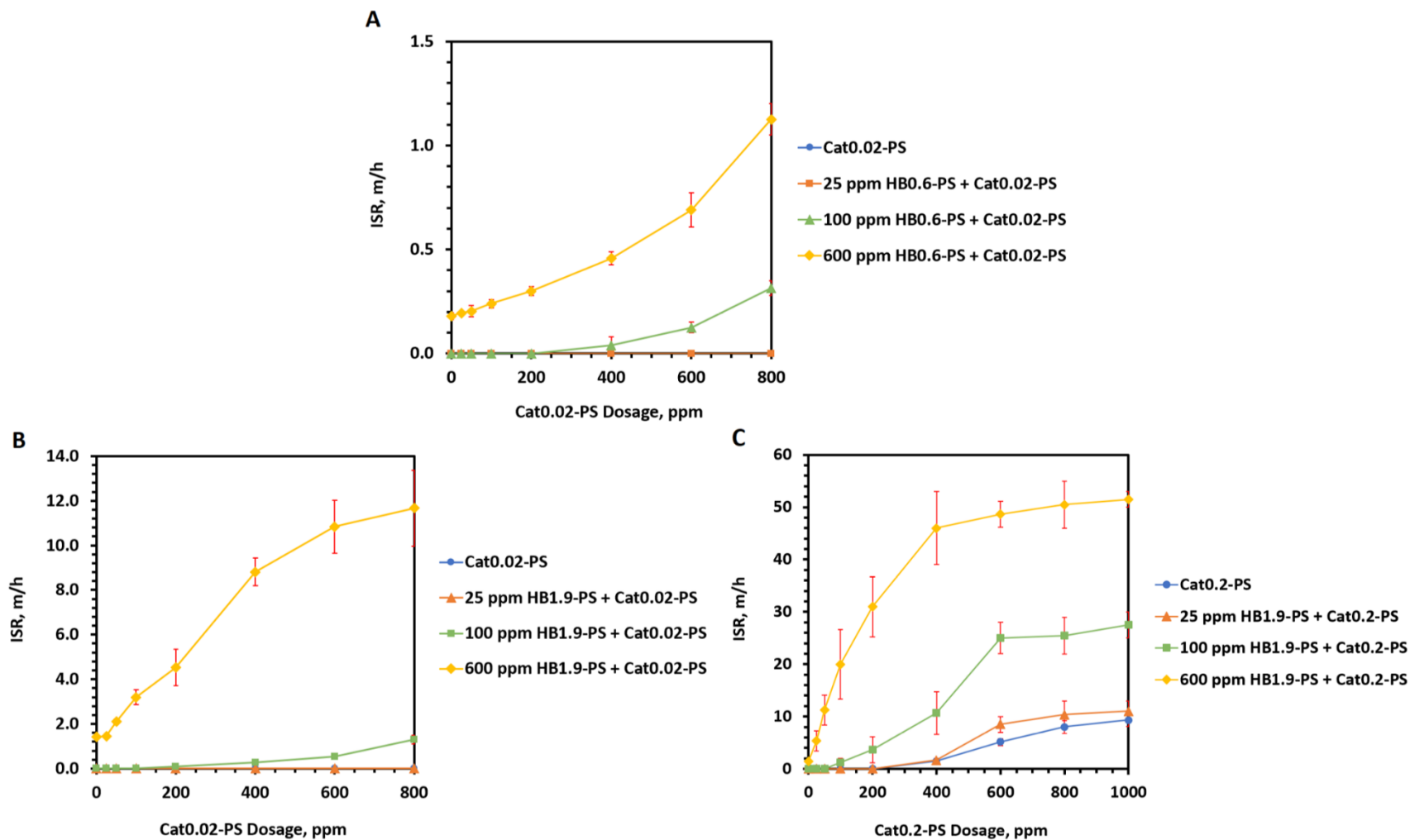


**Figure 5.16.** Initial settling rates (ISR) of the flocculation of 10 wt % MFT using flocculant pairs consisting of HB0.6-PS and Cat0.02-PS (A), HB1.9-PS and Cat0.02-PS (B), and HB1.9-PS and Cat0.2-PS (C) at 50 °C. Dosage was reported on the dry/slurry basis.

Cat0.2-PS was able to flocculate 10 wt % MFT starting from a dose of 400 ppm and reached the highest ISR of 9.3 m/h at a dose of 1000 ppm (Fig. 5.16C). The dual flocculant system consisting of 25 ppm of HB1.9-PS and Cat0.2-PS resulted in ISR values that were marginally higher than when using Cat0.2-PS alone. When the dose of HB1.9-PS increased to 100 ppm, significantly higher setting rates were obtained and the ISR values plateaued at a dose of 600 ppm of Cat0.2-PS. Further increasing the dose of HB1.9-PS to 600 ppm led to a remarkable increase in ISR values and the ISR reached a plateau at 400 ppm of Cat0.2-PS. An exceptionally high ISR at 46 m/h was achieved when using a combination of 600 ppm of HB1.9-PS and 400 ppm of Cat0.2-PS. For comparison, flocculating 10 wt % MFT with HB1.9-PS or Cat0.2-PS alone was inefficient due to their low ISR values (i.e. 1.4 m/h with the use of 600 ppm of HB1.9-PS and 1.7 m/h with 400 ppm of Cat0.2-PS). Additionally, the single flocculant systems at a dose of 1000 ppm also resulted in significantly slower settling rates, at 2.5 m/h for HB1.9-PS and at 9.3 m/h for Cat0.2-PS, than the dual flocculant system at a combined dose of 1000 ppm did. The dual flocculant systems greatly outperformed the single flocculants in terms of their settling rates.

### **5.3.10.2 Water Recovery**

When using Cat0.02-PS alone or a combination of 25 ppm of HB0.6-PS and Cat0.02-PS, no recoverable water was obtained. Poor WR, at below 60 %, was obtained with the use of 100 ppm of HB0.6-PS and a high dose of Cat0.02-PS (Fig. 5.17A). The WR improved slightly with the increasing dose of HB0.6-PS but overall, the dual flocculant pair consisting of HB0.6-PS and Cat0.02-PS yielded poor WR.

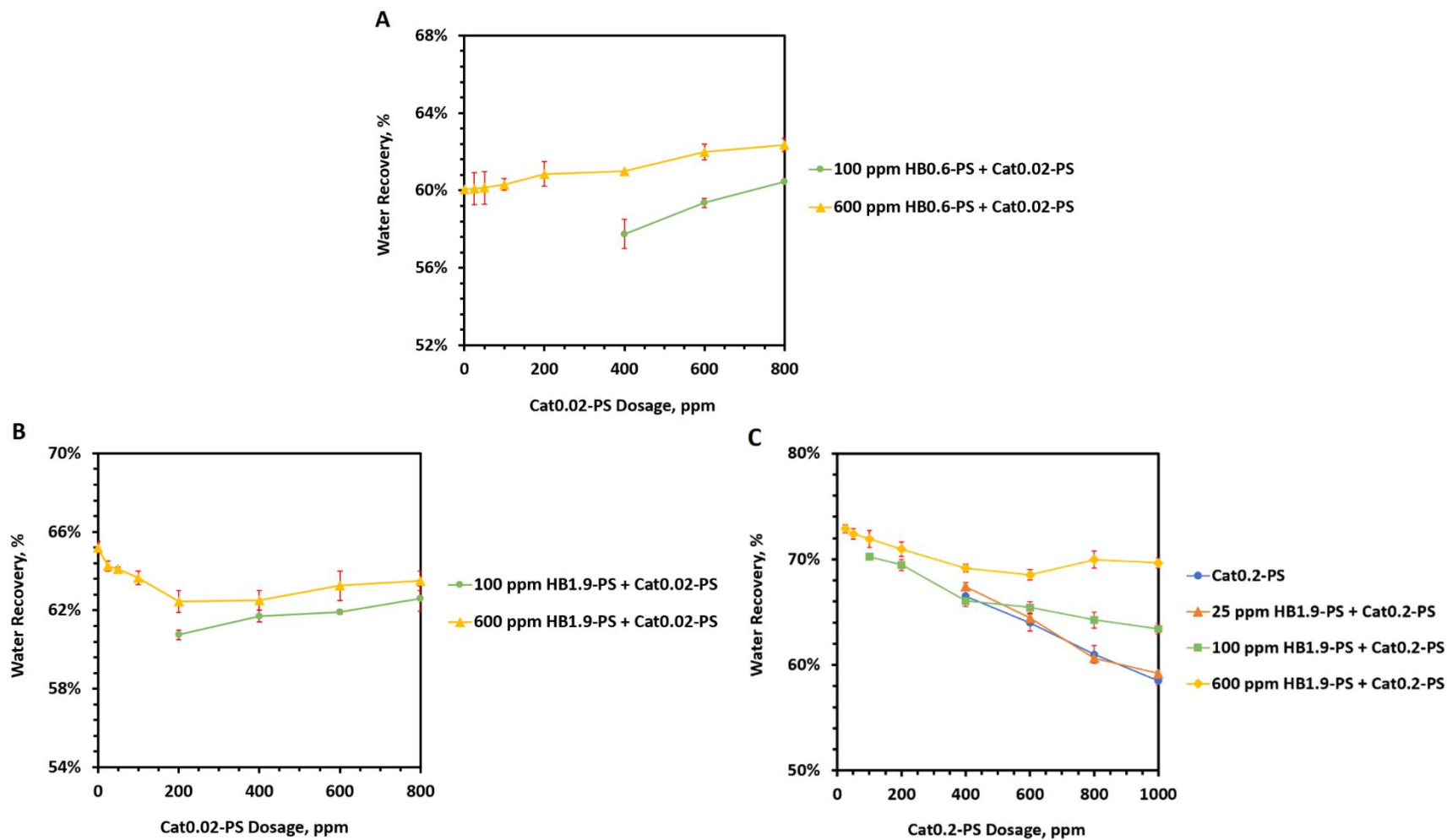


**Figure 5.17.** Water recovery of the flocculation of 10 wt % MFT using flocculant pairs consisting of HB0.6-PS and Cat0.02-PS (A), HB1.9-PS and Cat0.02-PS (B), and HB1.9-PS and Cat0.2-PS (C) at 50 °C. Dosage was reported on the dry/slurry basis.

Similar to HB0.6-PS at 25 ppm, the use of 25 ppm of HB1.9-PS and Cat0.02-PS with a dose up to 800 ppm failed to recover water from 10 wt % MFT as the HB1.9-PS at 25 ppm could still be well hydrated and the hydrophobic interactions may not be in place due to an inadequate amount of HB1.9-PS in the MFT mixture. The thermoresponsivity of the HB1.9-PS could exert a more profound effect on WR only when the polymer was used at a higher dose. With the use of 100 ppm of HB1.9-PS, a WR of higher than 60 % was obtained (Fig. 5.17B). Further increasing the dose of HB1.9-PS to 600 ppm improved the WR and the highest WR was 64 % with the use of 25 ppm of Cat0.02-PS.

Both the single flocculant system, Cat0.2-PS, and the dual flocculant system, 25 ppm of HB1.9-PS and Cat0.2-PS, started to recover water with a turbidity lower than 1000 NTU at a dose of 400 ppm and their WR decreased rapidly with the increasing dose of Cat0.2-PS (Fig. 5.17C). A higher dose of Cat0.2-PS could cause stronger electrostatic repulsions and higher water retention within the flocs. However, the electrostatic repulsions might be partially overcome by more effective bridging due to the thermoresponsive HB1.9-PS when used at higher doses. This was supported by the observation that the WR values were generally higher with the use of 100 ppm of HB1.9-PS and much higher at a dose of 600 ppm compared to at 25 ppm (Fig. 5.17C). The highest WR (73 %) was achieved with the use of 600 ppm of HB1.9-PS and 25 ppm of Cat0.2-PS, and the WR values were close to 70 % even after a high dose of Cat0.2-PS was added. For comparison, 1000 ppm of HB1.9-PS yielded a WR of 66 % and 1000 ppm of Cat0.2-PS gave a WR of only 59 %. Overall, the flocculant pair consisting of HB1.9-PS and Cat0.2-PS significantly improved the WR of the flocculation of 10 wt % MFT.

### 5.3.10.3 Supernatant Turbidity

The supernatants produced by Cat0.02-PS alone or a combination of 25 ppm of HB0.6-PS and Cat0.02-PS were extremely turbid with ST values much higher than 1000 NTU. Starting from a dose of 400 ppm, Cat0.02-PS together with 100 ppm of HB0.6-PS produced supernatants that were still quite turbid (Fig. 5.18A), and the ST decreased greatly with the increasing dose of Cat0.02-PS as more suspended solids could be removed by the cationic polymers. The use of 600 ppm of HB0.6-PS also produced turbid supernatants when used in a flocculant pair with Cat0.02-PS at a dose below 100 ppm, while the ST was improved to around 100 NTU when a higher dose of Cat0.02-PS was used (Fig. 5.18A). When the HB0.6-PS was placed with HB1.9-PS, supernatants with a turbidity of approximately 50 NTU were obtained at high Cat0.02-PS doses (Fig. 5.18B).

For the setting tests using Cat0.2-PS alone or a dual flocculant pair consisting of 25 or 100 ppm of HB1.9-PS and Cat0.2-PS, ST values decreased sharply from about 1000 NTU to under 30 NTU with the increasing dose of Cat0.2-PS (Fig. 5.18C). Compared to Cat0.02-PS, Cat0.2-PS was better at removing the suspended particles due to its higher charge density. The cleanest supernatant, with an ST of 16 NTU, was produced by the use of the dual flocculant pair containing 600 ppm of HB1.9-PS and 400 ppm of Cat0.2-PS. For comparison, flocculation using 600 ppm of HB1.9-PS yielded an ST of 110 NTU and 400 ppm of Cat0.2-PS yielded an ST of 829 NTU. Overall, the water recovered by the dual polymer flocculants was considerably cleaner than that by the single polymer flocculants.



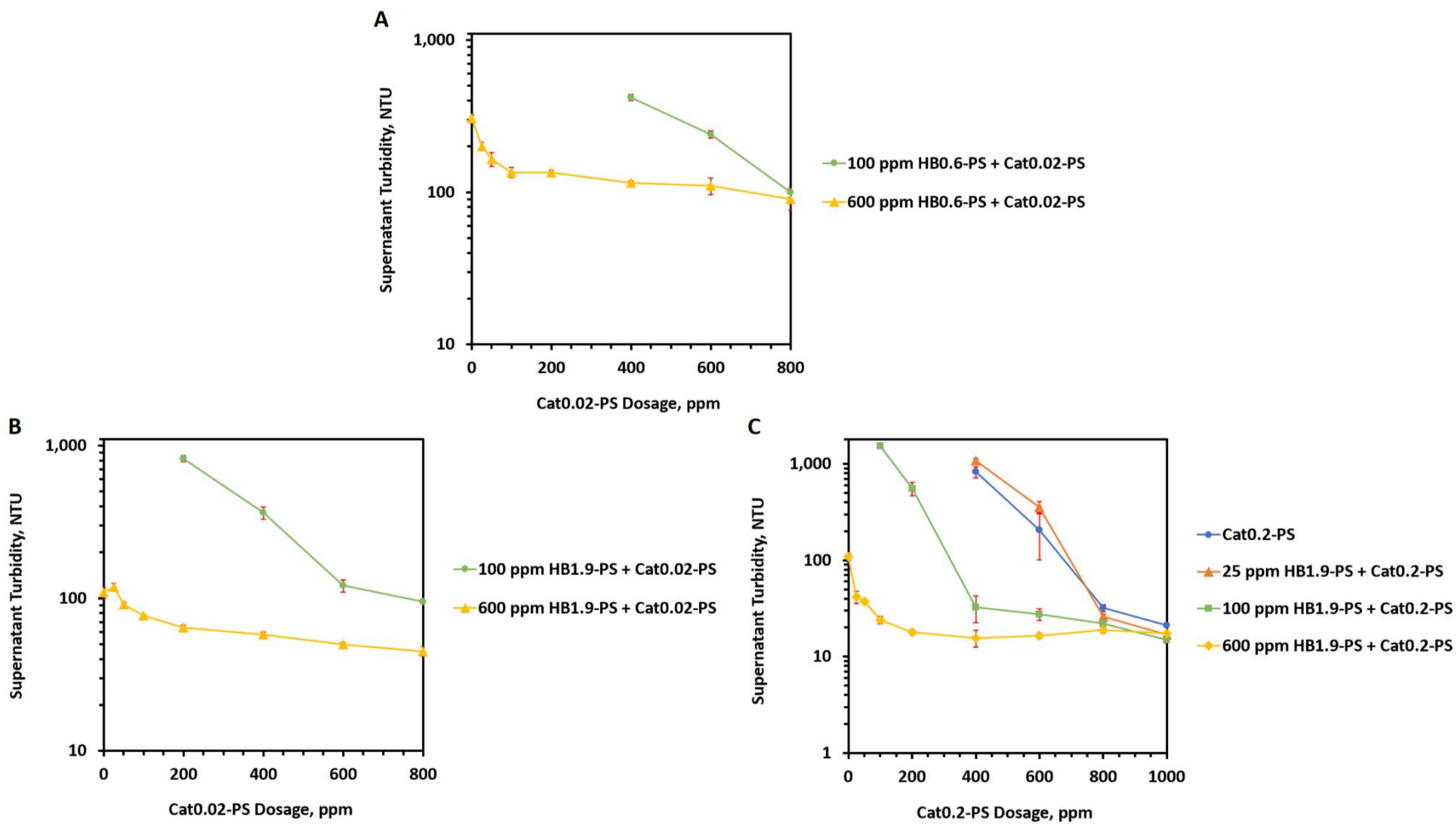


**Figure 5.18.** Supernatant turbidity of the flocculation of 10 wt % MFT using flocculant pairs consisting of HB0.6-PS and Cat0.02-PS (A), HB1.9-PS and Cat0.02-PS (B), and HB1.9-PS and Cat0.2-PS (C) at 50 °C. Dosage was reported on the dry/slurry basis.

#### 5.3.10.4 Sediment Solids Content

The sediments still retained a significant amount of water after flocculating with the polymer pair, HB0.6-PS and Cat0.02-PS. Flocculation could become more effective if a higher dose of HB0.6-PS was added to facilitate floc formation. This was supported by the observation that 600 ppm of HB0.6-PS produced a denser sediment with an SSC of about 26 wt % compared to 100 ppm (Fig. 5.19A). Moreover, replacing the HB0.6-PS with HB1.9-PS generally improved the SSC and the highest SSC (about 27.5 wt %) was obtained when using 600 ppm of the HB1.9-PS and Cat0.2-PS at a low dose (Fig. 5.19B). HB1.9-PS may assist in keeping water out of the flocs as the polymer becomes more hydrophobic above its LCST. This was more noticeable for the flocculation with the polymer pair, HB1.9-PS and Cat0.2-PS. Flocculating with a high dose of Cat0.2-PS may produce sediments that contain a significant amount of water, which was supported by the observation that the SSC decreased from 28.9 wt % to 23.2 wt % as the dose of Cat0.2-PS increased from 400 ppm to 1000 ppm (Fig. 5.19C). Fortunately, this adverse effect on SSC was greatly mitigated by the thermoresponsive feature of HB1.9-PS. With the addition of 600 ppm of HB1.9-PS, the SSC stayed above 31 wt % even at a high dose of Cat0.2-PS. The highest SSC was 35.6 wt %, which was a result of flocculating with 600 ppm of HB1.9-PS and 25 ppm of Cat0.2-PS. The highest SSC values obtained by using HB1.9-PS or Cat0.2-PS alone were 29.1 wt % and 28.9 wt %, respectively. The dual polymer system was again far superior to the one with a single polymer for the settling of 10 wt % MFT.

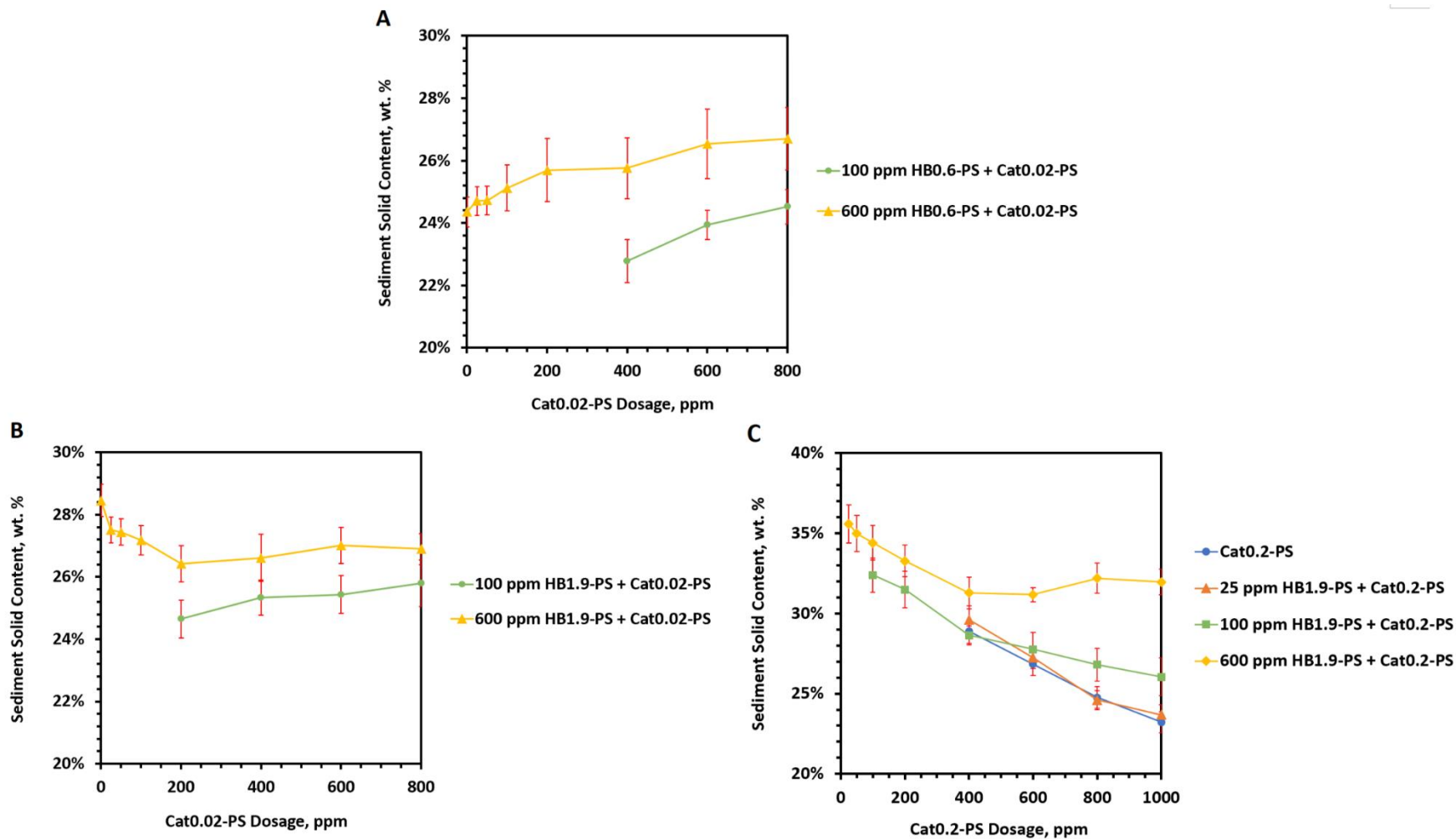


**Figure 5.19.** Sediment solids content of the flocculation of 10 wt % MFT using flocculant pairs consisting of HB0.6-PS and Cat0.02-PS (A), HB1.9-PS and Cat0.02-PS (B), and HB1.9-PS and Cat0.2-PS (C) at 50 °C. Dosage was reported on the dry/slurry basis.

### 5.3.11 Effect of Settling Temperatures on the Dual Polymer Flocculation

Flocculation tests of 10 wt % MFT were conducted at two different temperatures, 23 °C and 50 °C, with the use of a polymer pair consisting of 600 ppm of HB1.9-PS and Cat0.2-PS at various doses. At 23 °C, HB1.9-PS is well hydrated in a dispersion as its LCST is not reached. However, at 50 °C, which is above the LCST, HB1.9-PS becomes more dehydrated and hydrophobic. Here we report the differences in the flocculation performance of the settling tests conducted at 23 °C and 50 °C.

At both settling temperatures, the ISR values reached a plateau when 400 ppm of Cat0.2-PS was used (Fig. 5.20A). However, the ISR obtained by the 50 °C flocculation was almost two folds higher than that flocculating at 23 °C. This was likely due to the increase in hydrophobic interactions between the HB1.9-PS bound flocs above the LCST, which could lead to the formation of larger flocs, hence, a higher ISR. At 23 °C, WR decreased with the increasing dose of Cat0.2-PS while at 50 °C, the WR decreased at low doses of Cat0.2-PS but stayed relatively constant beyond 200 ppm of Cat0.2-PS (Fig. 5.20B). The WR values were considerably higher for the settling tests conducted at 50 °C. A similar trend was also observed for the SSC values of the settling tests conducted at these temperatures (Fig. 5.20D). We speculate that the reason behind the differences in the WR and SSC values to be that the sediments could be more dehydrated at 50 °C due to the thermoresponsive HB1.9-PS. The settling temperature did not make a big difference in ST (Fig. 5.20C).

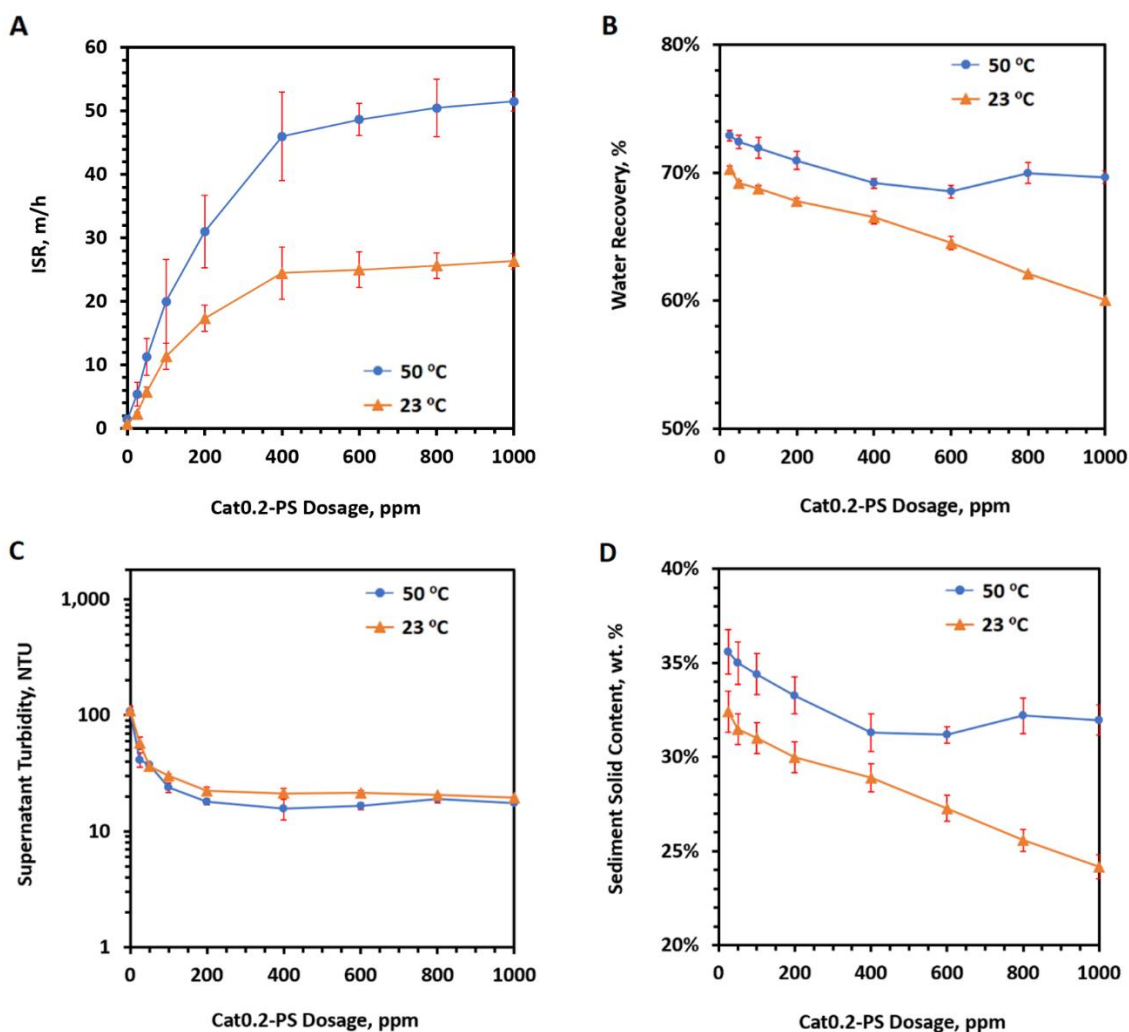


**Figure 5.20.** The effect of the settling temperatures on the performance regarding initial settling rate (ISR, **A**), water recovery (**B**), supernatant turbidity (**C**), and sediment solids content (**D**) when flocculating 10 wt % MFT with a dual polymer pair consisting of 600 ppm of HB1.9-PS and Cat0.2-PS at various doses from 0 to 1000 ppm (dry/slurry).

### 5.3.12 Comparison with other Polymers used to Flocculate 10 wt % MFT

Various polymers were employed to flocculate 10 wt % MFT in the literature and their performance was summarized in Table 5.3. Among the different flocculants, Magnafloc 1011, which is a high molecular weight anionic PAM with 27 % charge density, demonstrated the

fastest settling with an ISR of 8.8 m/h when 100 ppm of the polymer was used (Table 5.3, entry 1).<sup>122</sup> Both the thermoresponsive polymer, PNIPAM, and its cationic derivative, poly(AEMA-*st*-NIPAM), exhibited relatively high WR values at a dose of 1000 ppm (Table 5.3, entries 3 and 6).<sup>11</sup> The PAM-based cationic polymer, poly(AM-*st*-DADMAC), produced the most clarified supernatant, however, the flocculation was extremely slow (Table 5.3, entry 4).<sup>11</sup> The highest WR, at 66 %, and a relatively clean supernatant, with a turbidity of about 95 NTU, were obtained after the flocculation using a dual polymer flocculant consisting of 500 ppm of PNIPAM and 500 ppm of poly(AM-*st*-DADMAC) (Table 5.3, entry 5).<sup>11</sup> The same polymer pair was also reported to have the highest SSC at 33 wt %.<sup>11</sup> Flocculant dose reported in the literature can range from 75 to 1500 ppm depending on the type of polymer. We have demonstrated that a number of polymer pairs exhibited good performance in the flocculation of 10 wt % MFT in this chapter. As an example, the polymer pair which contained 600 ppm of HB1.9-PS and 100 ppm of Cat0.2-PS compared favorably in most aspects with those reported in the literature (Table 5.3, entry 9).

**Table 5.3.** A summary of performance of various polymers used to flocculate 10 wt % MFT.

	Flocculant	Functionality	MW, kDa	Dosage <sup>a</sup> , ppm	ISR, m/h	WR, %	ST, NTU	SSC, wt %	Ref.
1	Magnafloc 1011	anionic	17500	100	8.8	n.a.	162	30	122
2	Al-PAM	cationic	2000	75	6.2	n.a.	156	29	122
3	PNIPAM	thermoreponsive	324	1000	3.6	64	420	31	11
4	poly(AM- <i>st</i> -DADMAC)	cationic	n.a.	1000	0.08	22	80	17	11
5	1:1 mixture of PNIPAM and poly(AM- <i>st</i> -DADMAC)	thermoreponsive, cationic	n.a.	1000	4.5	66	95	33	11
6	poly(AEMA- <i>st</i> -NIPAM)	thermoreponsive, cationic	961	1000	4.8	64	180	30	11
7	poly(NIPAM-MATMAC-BAAM)	thermoreponsive, cationic, hydrophobic	n.a.	500	7.0	n.a.	n.a.	n.a.	142
8	poly(PLA <sub>4</sub> ChMA)	degradable, cationic	n.a.	1500	n.a.	n.a.	n.a.	33 <sup>b</sup>	174
9	a dual polymer flocculant of HB1.9-PS and Cat0.2-PS	thermoreponsive, cationic	n.a.	700 <sup>c</sup>	20	72	24	34.4	n.a.

<sup>a</sup> Polymer doses are expressed with reference to total MFT mass.

<sup>b</sup> Sediment was kept at 50 °C for 5 days prior to the SSC measurements.<sup>174</sup>

<sup>c</sup> A combined dose of 600 ppm HB1.9-PS and 100 ppm of Cat0.2-PS.

### 5.3.13 Conclusion of Dual Polymer Flocculation for 10 wt % MFT

The potato starch-based flocculant pairs performed better than the ones derived from corn starch. The dual flocculant system consisting of HB1.9-PS and Cat0.2-PS was in all aspects superior to the individual flocculants when used separately. Thermoresponsivity is absolutely required for optimal results in that the dual flocculant system was considerably more effective in most respects at settling temperatures above the LCST of HB1.9-PS than below.

Among all results obtained from the flocculation of 10 wt % MFT using a dual flocculant system, the highest ISR (52 m/h) was achieved by the use of 600 ppm of HB1.9-PS and 1000 ppm of Cat0.2-PS while a supernatant, which had the lowest turbidity of 16 NTU, was obtained by the flocculation using 600 ppm of HB1.9-PS and 400 ppm of Cat0.2-PS.

Additionally, a combination of 600 ppm of HB1.9-PS and 25 ppm of Cat0.2-PS produced the highest WR (73 %) and SSC (35.6 wt %). To achieve a reasonable performance with the least possible amount of flocculants, the polymer pair containing 600 ppm of HB1.9-PS and 100 ppm of Cat0.2-PS was one of the best candidates for the flocculation of 10 wt % MFT (ISR: 20 m/h, WR: 72 %, ST: 24 NTU and SSC: 34.4 wt %).



## Chapter 6

# Preparation and Characterization of Hydrophobically Modified Thermoresponsive Starch

### 6.1 Introduction

In the past decade, many efforts have been directed towards the development of more biocompatible and biodegradable thermoresponsive polymers (TRPs) derived from biopolymers such as cellulose,<sup>55,63,69,163,175</sup> and starch.<sup>22,24–26,72</sup> In 2012, Ju and coworkers reported the synthesis of thermoresponsive 2-hydroxy-3-butoxypropyl (HBP) or 2-hydroxy-3-isopropoxypropyl (HIP) starch by reacting cooked starch with butyl- or isopropyl glycidyl ether under basic conditions and showed that their LCSTs could be adjusted from 4.5–32.5 °C or 28–69 °C by varying their respective molar substitution of the HBP or HIP groups.<sup>25,26</sup> In 2017, Jong and Ju reported the synthesis of a TRP by hydrophobic modification of hydroxyethyl starch, a non-thermoresponsive polymer, with 2-propynylglycidyl ether and yielded thermoresponsive starch with the LCSTs ranging from 31 °C to 48 °C.<sup>22</sup>

Very recently, we reported the synthesis of thermoresponsive starch nanoparticles (SNPs) by reacting SNPs with simple alkene oxides such as butene oxide and found that the hydroxybutyl SNPs (HB-SNPs) with molar substitution (MS) higher than 1.3 exhibited an LCST of 52 °C and an increase in the MS to 1.9 decreased the LCST to 33 °C.<sup>72</sup> Reaction efficiency was between 31 % and 52 %. Adjusting the concentration of a polymer dispersion was one way to tune the LCST of the HB-SNPs in that the LCST decreases with the increasing concentration. The addition of salts and alcohols also greatly affected the LCST. Sodium

sulphate, a kosmotropic salt, was shown to drastically decrease the LCST of an HB-SNP from 60 °C without salt to 25 °C in a 0.3 M sodium sulphate solution. A substantial increase in particle size (hydrodynamic diameter,  $D_h$ ) was observed by dynamic light scattering (DLS) when the dispersion temperature was above the LCST of the HB-SNP indicating the formation of large insoluble aggregates. Oligomerized substituents on the hydroxyl groups of the starch backbone was found to contain up to five hydroxybutyl groups by analyzing the acid-hydrolyzed thermoresponsive HB-SNP by high resolution positive electrospray ionization mass spectrometry (HR+ESIMS) while the substituents of the non-thermoresponsive HB-SNP were determined to contain up to three hydroxybutyl groups.<sup>154</sup>

Other than varying molar substitution and polymer and salt concentrations, another effective way to manipulate the LCST of a TRP is via the hydrophobic modification of the polymer. Substituting a second hydrophobic ethyl group onto the amide nitrogen atom of poly(*N*-ethylacrylamide), with an LCST of 74 °C,<sup>32</sup> yielded poly(*N,N*-diethylacrylamide) of which the LCST was significantly reduced to 32 °C.<sup>47</sup> Moreover, substituting poly(*N*-methylacrylamide), which was not thermoresponsive, a second alkyl group, ethyl or propyl, yielded poly(*N,N*-dialkylacrylamide)s with an LCST of 60 °C,<sup>49</sup> and 15 °C respectively.<sup>48</sup> This demonstrates that the addition of a more hydrophobic substituent causes a larger decrease in the LCST compared to a less hydrophobic substituent. Preliminary studies showed that hydrophobically modified SNPs could be obtained by reacting SNPs with styrene oxide under basic conditions.<sup>154</sup> In this chapter, we report the synthesis and characterization of hydrophobically modified thermoresponsive SNPs obtained from hydroxybutylation of SNPs and hydrophobic modification by styrene oxide.

## **6.2 Materials and Methods**

### **6.2.1 Materials**

Starch nanoparticles were provided by EcoSynthetix Inc. (Burlington, Ontario, Canada). The SNPs contain approximately 8 % water by weight. 1,2-Butene oxide and styrene oxide were obtained from Sigma-Aldrich Co. (USA). Other reagents and solvents were commercially available and used without further purification unless stated otherwise.

### **6.2.2 Preparation of Hydrophobic Thermoresponsive SNPs**

Hydrophobic thermoresponsive SNPs were synthesized in three slightly different ways: firstly, thermoresponsive or non-thermoresponsive HB-SNPs were modified with styrene oxide; secondly, SNPs were modified with the simultaneous addition of butene oxide and styrene oxide; thirdly, SNPs were modified with styrene oxide followed by the subsequent addition of butene oxide without purification between the two reactions. The reaction conditions with butene oxide were mostly identical to that with styrene oxide. Briefly, SNP (or HB-SNP, 1 g) was dispersed in deionized water to make a 25 wt % dispersion. 10 M NaOH was added dropwise to the dispersion with vigorous stirring to give a pH of 13. Styrene oxide was added alone or simultaneously with butene oxide to the mixture and stirred vigorously at 40 °C for 24 h. For the reaction when styrene oxide was added alone, the pH of the reaction mixture was adjusted by the addition of 10 M NaOH to a pH of 13 and butene oxide was added to react for another 24 h at 40 °C under stirring. The mixture was cooled to room temperature (rt) then neutralized by the dropwise addition of 1 M HCl with vigorous stirring. The neutralized mixture was subjected to dialysis against deionized water for 2 days using a dialysis

bag with molecular weight cut-off ( $MW_{\text{cutoff}}$ ) of 1 kD. A minimum of 5 water replacements were performed over the course of 2 days to give an overall dilution ratio of approximately  $1:10^{10}$ . The dialyzed product was lyophilized for at least 3 days to yield a white powder.

### 6.2.3 Determination of Molar Substitution

The molar substitution (MS) was determined using  $^1\text{H-NMR}$  spectroscopy on a Bruker Avance 500 NMR spectrophotometer. The hydrophobic thermoresponsive starch (10 mg) was dispersed in deuterium oxide ( $\text{D}_2\text{O}$ , 600  $\mu\text{L}$ ) for 16 h at 4  $^\circ\text{C}$  then allowed to warm to rt before obtaining the spectra. The MS of hydroxybutyl (HB) groups ( $\text{MS}_{\text{HB}}$ ) was defined as the molar ratio of the HB substituents to the anhydroglucose units (AGUs) of the SNPs. The  $\text{MS}_{\text{HB}}$  was calculated using Eq. 6.1:

$$\text{MS}_{\text{HB}} = \frac{I_{\text{CH}_3}/3}{I_{\text{H}_a}}$$

#### Equation 6.1

where  $I_{\text{CH}_3}$  is the integral value for the signal of the methyl protons of HB groups at 0.70-1.05 ppm and  $I_{\text{H}_a}$  is the integral value for the anomeric proton ( $\text{H}_a$ ) at 5.20-5.85 ppm. The MS of the phenyl hydroxyethyl (PHE) groups ( $\text{MS}_{\text{PHE}}$ ) resulting from the styrene oxide modification was defined as the molar ratio of the PHE substituents to AGU and was calculated using Eq. 6.2:

$$\text{MS}_{\text{PHE}} = \frac{I_{\text{phenyl-H}}/5}{I_{\text{H}_a}}$$

#### Equation 6.2

where  $I_{\text{phenyl-H}}$  is the integral value for the phenyl proton peak at 7.20-7.60 ppm. The reaction efficiency (RE) is calculated by dividing the MS by the mole equivalent of reagents used to obtain such MS.

#### **6.2.4 Determination of the LCST by Light Transmittance**

Light transmittance values were determined using a Cary 4000 Bio UV-Visible spectrophotometer equipped with a multi-cuvette holder and a temperature controller. The hydrophobic thermoresponsive SNPs were dispersed in deionized water to a concentration of 10 g/L, unless otherwise stated, for 16 h at 4 °C before the light transmittance studies were conducted. The temperature of the dispersion was measured by a temperature probe in a reference cell. The transmittance was recorded at a wavelength of 500 nm with a heating rate of 1 °C/min. The polymer dispersions were equilibrated for at least 5 minutes at 10 °C in the multi-cuvette holder before commencing the measurements. Absorbance data points were taken every 0.25 °C and recorded up to 80 °C. The absorbance data was converted to transmittance. All transmittance data was normalized by the maximum transmittance and plotted against dispersion temperature to give a transmittance curve. The LCST is defined as the temperature at the inflection point of the transmittance curve of a 10 g/L polymer dispersion.

#### **6.2.5 DLS Measurements**

The hydrophobic thermoresponsive starch was dispersed in deionized water to a concentration of 3 g/L. The dispersions were stirred for 2 h at 4 °C and left undisturbed for 16 h at 4 °C. The dynamic light scattering (DLS) measurements were performed at 15 °C and 70 °C using the Zetasizer Nano (Malvern Instruments, Worcestershire, UK). The dispersions were equilibrated for 5 minutes at each temperature settings before starting the measurements.

## 6.3 Results and Discussion

### 6.3.1 Preparation of Hydrophobic Thermoresponsive SNPs

The preparation of hydrophobic thermoresponsive SNPs was initially performed using the thermoresponsive HB-SNP with an  $MS_{HB}$  of 1.28 (HB1.28-SNP, LCST = 55 °C) and the non-thermoresponsive HB0.68-SNP as starting materials to react with styrene oxide in aq. base (Fig. 6.1). The results are shown in Table 6.1.

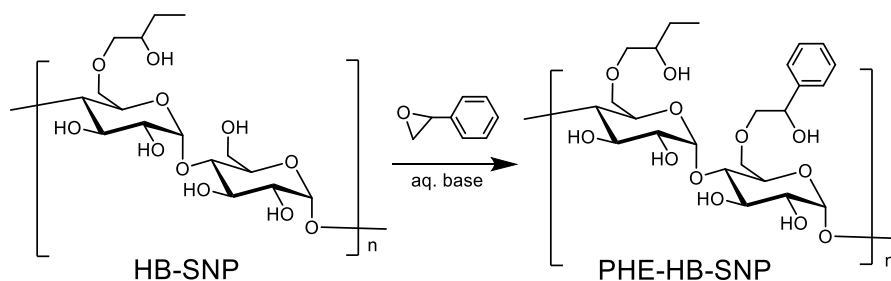


**Figure 6.1.** Preparation of PHE-HB-SNP. Substitution is shown only at O-6 while in fact substitution can occur at O-2, O-3 and O-6.

**Table 6.1.** The molar substitution (MS), reaction efficiency (RE) and LCSTs of PHE-HB-SNPs obtained from modifying the HB-SNPs with styrene oxide.

Entry	Starting Material	$MS_{HB}$	SO:AGU <sup>a</sup>	$MS_{PHE}$	RE	LCST (°C) <sup>b</sup>
1	HB0.68-SNP	0.68	0.5	0.27	54 %	23
2	HB1.28-SNP	1.28	0.2	0.12	60 %	34
3	HB1.28-SNP	1.28	0.5	0.20	40 %	26
4	HB1.28-SNP	1.28	1	0.26	26 %	23

<sup>a</sup> SO:AGU is the molar ratio of styrene oxide to anhydroglucose unit.

<sup>b</sup> LCST is defined as the temperature at the inflection point of the transmittance curve of a 10 g/L polymer dispersion.

A typical <sup>1</sup>H-NMR spectrum for the phenylhydroxyethyl hydroxybutyl SNP (PHE-HB-SNP) is shown in Figure 6.2, along with the spectra of unmodified SNP, HB-SNP and PHE-

SNP for comparison. The success of hydroxybutyl modification could be identified by the appearance of the methyl and methylene peaks at 1.1-0.8 and 1.7-1.3 ppm (Fig. 6.2B) and the incorporation of the phenylhydroxyethyl groups was confirmed by the peak corresponding to the phenyl protons at 7.6-7.2 ppm (Fig. 6.2C).<sup>154</sup> Similarly, the NMR spectrum of PHE-HB-SNP which showed both sets of peaks would confirm that both HB and PHE groups were successfully incorporated (Fig. 6.2A).

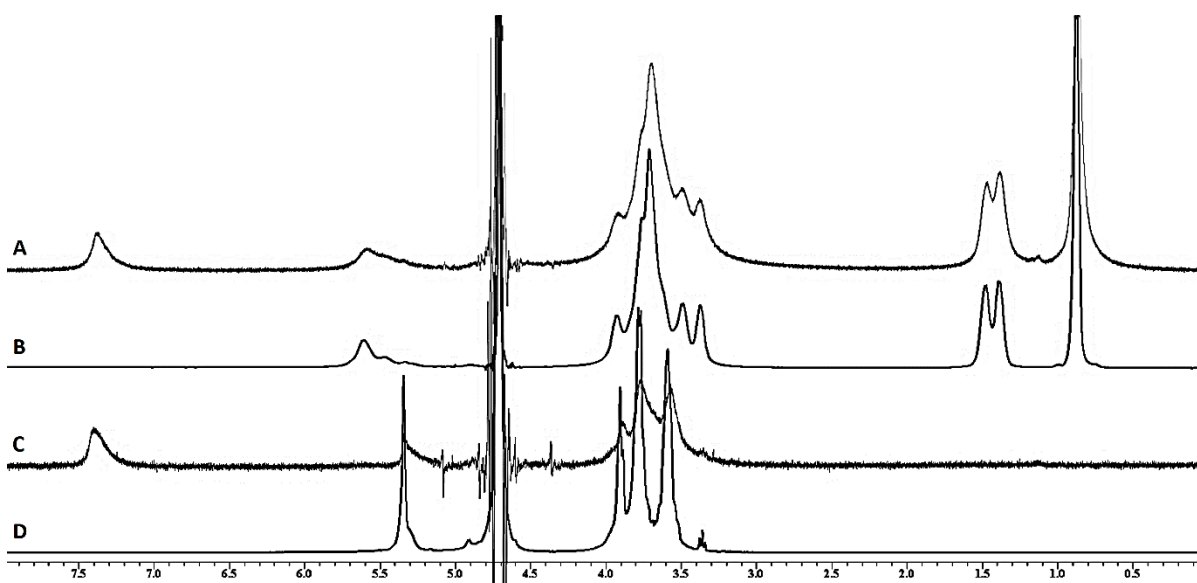


**Figure 6.2.** <sup>1</sup>H-NMR spectral comparison for PHE-HB-SNP (A), HB-SNP (B), PHE-SNP (C), and unmodified SNP (D).

PHE-HB-SNPs are found to have remarkably low LCSTs when compared to the HB-SNPs. For example, the reaction using HB0.68-SNP as starting material and 0.5 mole equivalent of styrene oxide yielded PHE0.27-HB0.68-SNP with an LCST of 23 °C (Table 6.1 entry 1). It is important to note that the HB0.68-SNP prior to the hydrophobic modification are not thermoresponsive. For PHE0.27-HB0.68-SNP, an LCST of 23 °C was achieved by reacting SNPs with only 1 mole equivalent of butene oxide (to give an  $MS_{HB}$  of 0.68) and 0.5 mole

equivalent of styrene oxide (to give an  $MS_{PHE}$  of 0.27); without the hydrophobic modification, a considerably greater amount of butene oxide (6 mole equivalent) was required to produce HB1.9-SNP with an LCST of 32 °C.<sup>72</sup> For reactions using HB1.28-SNP (LCST = 55 °C) as starting materials, the addition of a small amount of PHE groups substantially lowered the LCST of the resultant PHE-HB1.28-SNPs. For instance, the product with an  $MS_{PHE}$  of 0.12 had an LCST of 34 °C (Table 6.1, entry 2), which was an impressive 21 °C decrease from the LCST before the hydrophobic modification. Moreover, further increase in  $MS_{PHE}$  decreased the LCSTs of the hydrophobic thermoresponsive SNPs. An increase of  $MS_{PHE}$  from 0.12 to 0.26 decreased the LCST from 34 to 23 °C (Table 6.1, entries 2 and 4). Interestingly, PHE0.26-HB1.28-SNP had the same LCST as PHE0.27-HB0.68-SNP (Table 6.1, entries 1 and 4), which suggested that the PHE groups were more effective in lowering the LCST than the HB groups and the increase in  $MS_{HB}$  above 0.68 had a negligible effect on the LCST. Similar findings can be obtained when comparing the transmittance curves of these hydrophobic thermoresponsive SNPs (Figure 6.3).



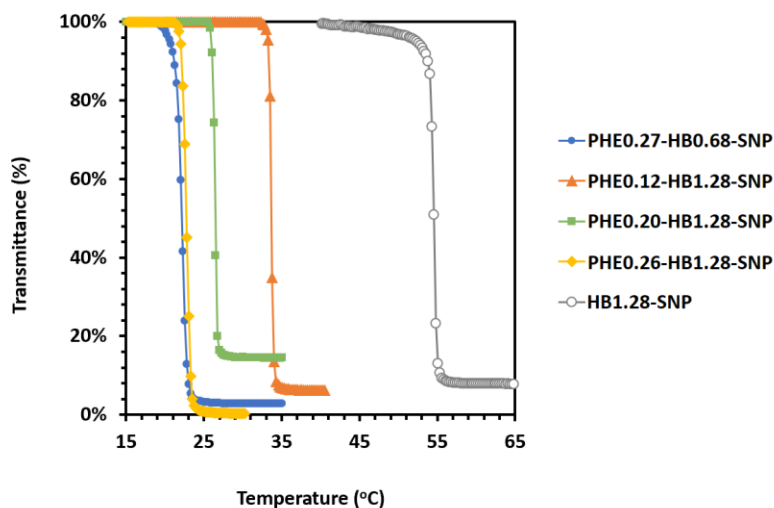


**Figure 6.3.** Light transmittance measurements of various aqueous PHE-HB-SNP dispersions and an HB1.28-SNP dispersion for comparison.

Hydrophobic modification on the HB-SNPs using styrene oxide is an effective method to manipulate their LCSTs; however, the hydrophobic modification still required to be optimized to achieve a higher reaction efficiency. The reaction efficiency of the hydrophobic modification decreased with increasing mole equivalent of styrene oxide used in the reactions (Table 6.1, entries 2-4). Moreover, the reaction efficiency also decreased significantly with the increasing  $MS_{HB}$  of the starting HB-SNPs (Table 6.1, entries 1 and 3). The decrease in reaction efficiency is possibly due to the decrease in active reaction sites, which were a result of being pre-occupied by more HB groups. Intuitively, a strategy to improve the reaction efficiency of the hydrophobic modification is to use the unmodified SNPs as the starting material such that there will be no pre-occupied reaction sites prior to the modification. More specifically, there are two options regarding how styrene oxide is introduced to the reaction: firstly, styrene oxide is added alone to complete the hydrophobic modification before the hydroxybutylation reaction

commences; secondly, styrene oxide is added simultaneously with butene oxide such that the hydrophobic modification and the hydroxybutylation occur at the same time.

### **6.3.1.1 PHE-HB-SNPs by Hydrophobic Modification prior to Hydroxybutylation**

From the preceding section, it appears that the reaction efficiency of the styrene oxide reaction greatly depended on the availability of the reaction sites on AGUs. In this section, we prepared PHE-HB-SNPs by reacting SNPs with 0.3-0.4 mole equivalent of styrene oxide alone at 40 °C and pH of 13 for 24 h prior to the addition of 0.1-1 mole equivalent of butene oxide to react for another 24 h and their results are summarized in Table 6.2. The reaction efficiency of the hydrophobic modification ( $RE_{HM}$ ) fluctuated to some extent (average  $RE_{HM} = 80 \pm 5 \%$ ) but there was no discernable trend between  $RE_{HM}$  and the amount of butene oxide used (Table 6.2). This was intuitive as the hydroxybutylation reaction occurred after the hydrophobic modification. Interestingly, the reaction efficiency of the hydroxybutylation reaction ( $RE_{HB}$ ) increased with the increasing amount of styrene oxide added in that the  $RE_{HB}$  increased from an average of  $65 \pm 4 \%$  to  $77 \pm 3 \%$  when the mole equivalent of styrene oxide increased from 0.30 to 0.40 (Table 6.2). The reason to the increase in  $RE_{HB}$  due to the amount of styrene oxide (hence,  $MS_{PHE}$ ) is not yet well understood. We speculate that butene oxide may react with the PHE substituted AGUs more preferably than the unsubstituted AGUs.

**Table 6.2.** The molar substitution (MS), reaction efficiency (RE) and LCSTs of PHE-HB-SNPs obtained from SNPs subjected to hydrophobic modification prior to hydroxybutylation.

Entry	BO:AGU <sup>a</sup>	MS <sub>HB</sub>	RE <sub>HB</sub> <sup>b</sup>	SO:AGU <sup>a</sup>	MS <sub>PHE</sub>	RE <sub>HM</sub> <sup>b</sup>	LCST (°C) <sup>c</sup>
1	0.1	0.06	60%	0.3	0.25	83%	n.a.
2	0.2	0.13	65%	0.3	0.23	78%	n.a.
3	0.3	0.21	70%	0.3	0.22	73%	n.a.
4	0.4	0.26	65%	0.3	0.21	71%	n.a.
5	0.1	0.07	70%	0.35	0.26	75%	n.a.
6	0.2	0.16	80%	0.35	0.30	86%	n.a.
7	0.4	0.31	78%	0.35	0.30	84%	n.a.
8	0.5	0.36	72%	0.35	0.28	79%	66
9	0.6	0.40	67%	0.35	0.31	89%	53
10	0.8	0.57	71%	0.35	0.27	76%	45
11	1	0.72	71%	0.35	0.27	78%	43
12	0.1	0.08	80%	0.4	0.33	82%	38
13	0.2	0.16	80%	0.4	0.33	82%	39
14	0.3	0.22	73%	0.4	0.30	74%	46
15	0.4	0.30	75%	0.4	0.35	87%	34

<sup>a</sup> BO:AGU or SO:AGU is the molar ratio of butene oxide or styrene oxide to anhydroglucose unit.

<sup>b</sup> RE<sub>HB</sub> and RE<sub>HM</sub> represent the respective reaction efficiencies of the hydroxybutylation and hydrophobic modification.

<sup>c</sup> LCST is defined as the temperature at the inflection point of the transmittance curve of a 10 g/L polymer dispersion.

Without the addition of HB groups, PHE-SNPs were not thermoresponsive.<sup>154</sup> At a low MS<sub>HB</sub> and at a low MS<sub>PHE</sub>, the PHE-HB-SNPs were not thermoresponsive either (Table 6.2, entries 1 and 5). However, at a relatively high MS<sub>PHE</sub>, the addition of only a small amount of HB groups was enough to produce thermoresponsive SNPs (Table 6.2, entry 12). We speculate that HB groups on PHE-HB-SNPs could stabilize the polymers due to the surrounding hydration shells of the HB groups at a low dispersion temperature. The HB groups may be responsible for an increase in dispersibility of PHE-HB-SNPs below their LCSTs. This was supported by the observation that the majority of the PHE-HB-SNP dispersions showed higher

transmittance values at 15 °C compared to the dispersion of PHE-SNP with the same  $MS_{PHE}$  (Fig. 6.4). At a higher temperature, as the hydration shells surrounding HB groups get disrupted and if the polymer was hydrophobic enough (i.e. high  $MS_{PHE}$ ), the PHE-HB-SNPs could no longer be stabilized in a dispersion and the dispersibility of the polymers would decrease drastically resulting in a decrease in the transmittance of the dispersion, hence, exhibiting an LCST.

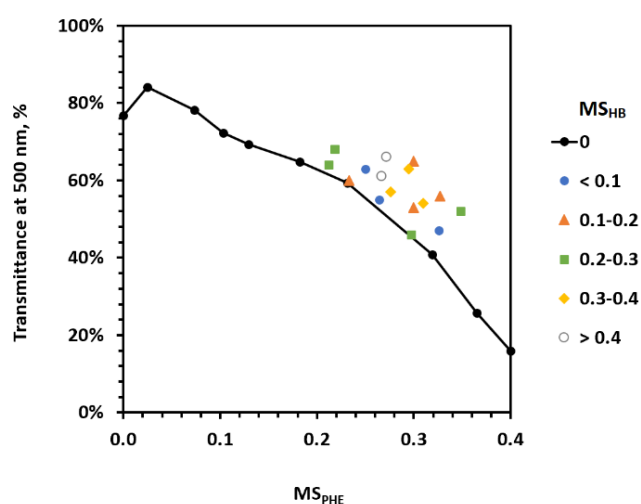


**Figure 6.4.** Transmittance plot of 10 g/L PHE-HB-SNP dispersions with different  $MS_{PHE}$  and  $MS_{HB}$ . Transmittance values were measured at a wavelength of 500 nm at 15 °C.

Interestingly, the PHE0.27-HB0.72-SNP obtained by SNPs that were subjected to hydrophobic modification prior to hydroxybutylation exhibited an LCST of 43 °C (Table 6.2, entry 11), and this LCST is significantly higher than that of the PHE0.27-HB0.68-SNP (23°C) which was prepared by hydrophobic modification of HB0.68-SNP (Table 6.1, entry 1), despite having the same  $MS_{PHE}$  and only a small difference in  $MS_{HB}$ . It is clear that the change in reaction protocols greatly affected the LCSTs of the corresponding products.

### 6.3.1.2 Effect of Reaction Protocols on the LCSTs of PHE-HB-SNPs

In the previous section, we have established that the reaction protocols had a significant effect on the LCSTs of PHE-HB-SNPs. This section mainly investigates the effect of different protocols on reaction efficiency and thermoresponsivity of PHE-HB-SNPs. A set of reactions were carried out to produce PHE-HB-SNPs with similar MS values in three slightly different reaction protocols: firstly, SNPs were subjected to hydrophobic modification by styrene oxide prior to hydroxybutylation without purification between the reactions; secondly, SNPs were subjected to reactions in the reverse order and thirdly, the SNPs reacted with styrene oxide and butene oxide simultaneously. Table 6.3 shows the results from these reactions.

**Table 6.3.** Results of SNPs reacting with styrene oxide (SO) and butene oxide (BO) in different protocols.

Entry	Reaction Protocol	MS <sub>PHE</sub>	MS <sub>HB</sub>	RE <sub>PHE</sub> <sup>a</sup>	RE <sub>HB</sub> <sup>a</sup>	LCST (°C) <sup>c</sup>
1	SO→BO <sup>b</sup>	0.31	0.30	79%	65%	41
2	BO→SO <sup>b</sup>	0.31	0.30	74%	75%	31
3	BO+SO <sup>b</sup>	0.31	0.30	75%	74%	31

<sup>a</sup> RE<sub>HB</sub> and RE<sub>HM</sub> represent the respective reaction efficiencies of the hydroxybutylation and hydrophobic modification.

<sup>b</sup> SO→BO, BO→SO and BO+SO represent that the SNPs were subjected to hydrophobic modification prior to hydroxybutylation, subjected to the reactions in the reverse order and to the reactions simultaneously, respectively.

<sup>c</sup> LCST is defined as the temperature at the inflection point of the transmittance curve of a 10 g/L polymer dispersion.

The MS<sub>PHE</sub> and MS<sub>HB</sub> of the PHE-HB-SNPs resulted from the three protocols were the same while their LCSTs were quite different in that the PHE0.31-HB0.30-SNP produced by the hydrophobic modification of the SNPs prior to hydroxybutylation (SO→BO) exhibited a significantly lower LCST than the products by the other two protocols (Table 6.3). Transmittance curves for the PHE0.31-HB0.30-SNPs can be found in Figure 6.5A. At a

concentration of 3 g/L, the SO→BO sample did not form aggregates even at a temperature as high as 70 °C while the other two samples formed aggregates above their LCSTs, indicated by the results from DLS studies (Fig. 6.5B). The reason to the differences between the SO→BO samples and the other two samples is unclear but we speculate that when the PHE groups were substituted onto the SNP backbone, hydrophobic micro-domains due to the hydrophobic interactions could be created and upon the addition of the HB groups, a steric shell consisting of the less hydrophobic HB groups may form at the outer layer of the polymer preventing the association of a PHE-rich hydrophobic micro-domain to another. In other words, the HB groups at the outer layer of the SNPs could provide steric stability that impedes the intermolecular hydrophobic interaction of the PHE groups leading to slower intermolecular aggregation and higher LCST. To prevent the formation of the HB shell, reaction protocols in which hydroxybutylation was performed prior to hydrophobic modification (BO→SO) or both reactions performed simultaneously (BO+SO) should be employed. Additionally, the fact that the BO+SO protocol required 24 h while the BO→SO required two times the reaction time has prompted us to prepare PHE-HB-SNPs using the BO+SO protocol hereafter.

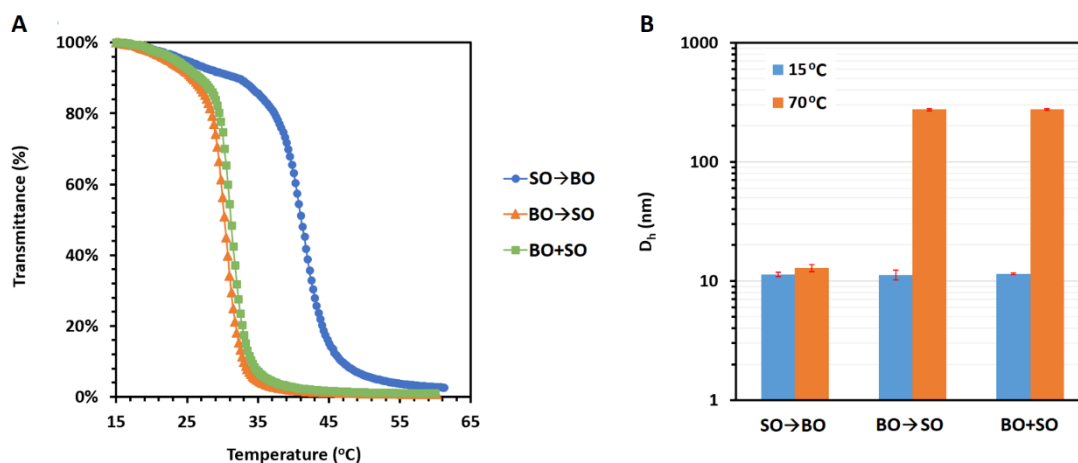


**Figure 6.5.** Transmittance curves (**A**) and hydrodynamic diameters ( $D_h$ , **B**) of PHE0.31-HB0.30-SNPs prepared in different reaction protocols. Light transmittance measurements were conducted at 10 g/L. DLS measurements were conducted at 15 °C and 70 °C with 3 g/L dispersions. SO→BO, BO→SO, and BO+SO represent that the SNPs were subjected to hydrophobic modification prior to hydroxybutylation, the reactions in the reverse order, and the reactions occurred simultaneously, respectively.

### 6.3.1.3 Simultaneous Hydroxybutylation and Hydrophobic Modification of SNPs

A general reaction scheme for the preparation of PHE-HB-SNPs by simultaneous hydroxybutylation and hydrophobic modification is shown in Figure 6.6. The reaction proceeded with the addition of butene oxide and styrene oxide at the same time to react with SNPs for 24 h at pH of 13 and at 40 °C and the results are summarized in Table 6.4.

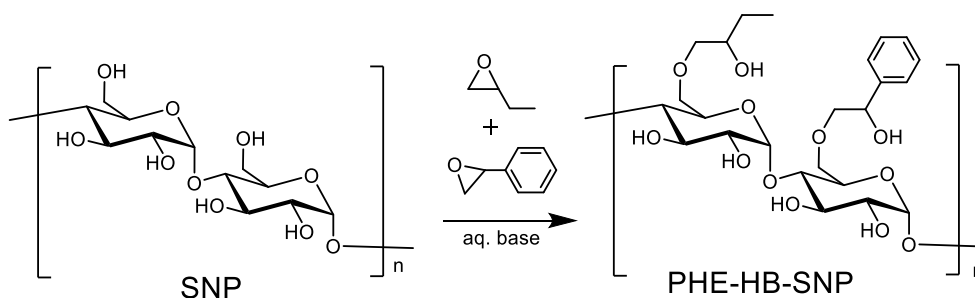


**Figure 6.6.** Preparation of PHE-HB-SNP using the BO+SO protocol. Substitution is shown only at O-6 while in fact substitution can occur at O-2, O-3 and O-6.

**Table 6.4.** The molar substitution (MS), reaction efficiency (RE), and LCSTs of PHE-HB-SNPs obtained by modifying SNPs with butene oxide (BO) and styrene oxide (SO) simultaneously.

Entry	BO:AGU <sup>a</sup>	MS <sub>HB</sub>	RE <sub>HB</sub> <sup>b</sup>	SO:AGU <sup>a</sup>	MS <sub>PHE</sub>	RE <sub>HM</sub> <sup>b</sup>	LCST (°C) <sup>c</sup>
1	0.5	0.26	52%	0.19	0.12	63%	n.a.
2	1	0.5	50%	0.19	0.12	63%	n.a.
3	1.5	0.82	55%	0.19	0.12	63%	62
4	2	0.98	49%	0.19	0.1	53%	54
5	0.5	0.36	72%	0.26	0.18	69%	n.a.
6	1	0.5	50%	0.26	0.18	69%	77.5
7	1.5	0.82	55%	0.26	0.16	62%	52.5
8	2	1.12	56%	0.26	0.16	62%	44
9	0.1	0.06	60%	0.32	0.24	75%	n.a.
10	0.2	0.14	70%	0.32	0.24	75%	n.a.
11	0.3	0.2	67%	0.32	0.24	75%	n.a.
12	0.4	0.24	60%	0.32	0.24	75%	n.a.
13	0.5	0.3	60%	0.32	0.24	75%	78
14	1	0.62	62%	0.32	0.22	69%	53
15	1.5	0.96	64%	0.32	0.18	56%	42.5
16	2	1.08	54%	0.32	0.18	56%	41
17	0.1	0.08	80%	0.39	0.32	82%	n.a.
18	0.2	0.16	80%	0.39	0.3	77%	53.5
19	0.3	0.24	80%	0.39	0.28	72%	53.5
20	0.4	0.32	80%	0.39	0.28	72%	47
21	0.5	0.42	84%	0.39	0.3	77%	46.5
22	1	0.76	76%	0.39	0.26	67%	39
23	1.5	1.08	72%	0.39	0.22	56%	36.5
24	2	1.42	71%	0.39	0.22	56%	34
25	0.1	0.08	80%	0.45	0.36	79%	16
26	0.2	0.16	80%	0.45	0.34	76%	19
27	0.3	0.26	87%	0.45	0.34	76%	25
28	0.4	0.3	75%	0.45	0.34	76%	23
29	0.5	0.42	84%	0.45	0.34	75%	24.5
30	1	0.76	76%	0.45	0.3	67%	30
31	1.5	1.2	80%	0.45	0.26	58%	31
32	2	1.64	82%	0.45	0.22	49%	30



<sup>a</sup> BO:AGU or SO:AGU is the molar ratio of butene oxide or styrene oxide to anhydroglucose unit.

<sup>b</sup> RE<sub>HB</sub> and RE<sub>HM</sub> represent the respective reaction efficiencies of the hydroxybutylation and hydrophobic modification.

<sup>c</sup> LCST is defined as the temperature at the inflection point of the transmittance curve of a 10 g/L polymer dispersion.

Interestingly, the reaction efficiency of the hydroxybutylation reaction (RE<sub>HB</sub>) improved significantly in presence of styrene oxide. We have reported previously that the RE<sub>HB</sub> was relatively poor (usually below 50 %),<sup>72</sup> while a RE<sub>HB</sub> as high as 87 % was achieved when reacting together with 0.45 mole equivalent of styrene oxide (Table 6.4, entry 27). Moreover, one would think that the RE<sub>HB</sub> should decrease when butene oxide and styrene oxide were reacting with the SNPs simultaneously due to the competing reactions of the more reactive styrene oxide but we found that the RE<sub>HB</sub> generally increased with the increasing mole equivalent of styrene oxide added in the reaction (Fig. 6.7). The exact reason behind the improvement in RE<sub>HB</sub> due to the presence of styrene oxide is not yet well understood. A possible explanation is that the HB groups could preferably react with the OH groups on PHE substituents. In other words, the total available sites of reaction may not decrease with the incorporation of the PHE groups and the PHE groups could provide more favorable substitution sites for hydroxybutylation compared to the native OH groups on AGUs. Another possible reason is that the incorporation of PHE groups increased the hydrophobicity of the SNPs which could enhance the interaction between the SNPs and the unreacted butene oxide and may improve the hydroxybutylation reaction.

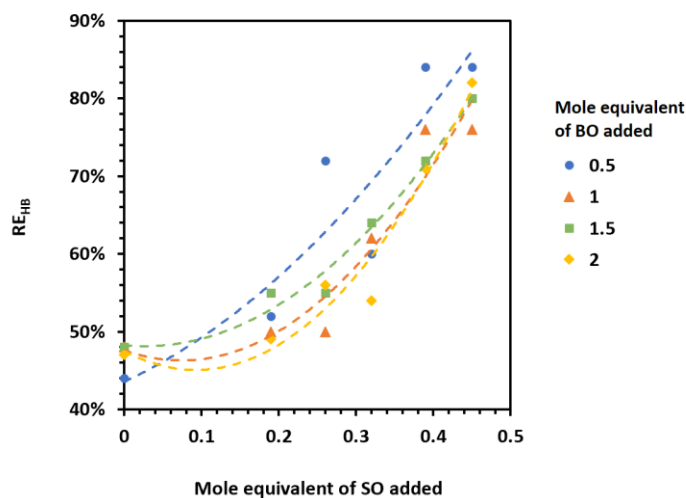


**Figure 6.7.** Correlation between the reaction efficiency of hydroxybutylation ( $RE_{HB}$ ) and the amount styrene oxide (SO) added in the reactions. The dotted lines are binominal fitted trendlines provided for visual guidance only.

### 6.3.2 Thermoresponsive Properties of PHE-HB-SNPs

#### 6.3.2.1 Effect of MS on the Thermoresponsivity of PHE-HB-SNPs

The effect of MS on the LCST of PHE-HB-SNPs was investigated by light transmittance studies. As there are two distinctive substituents on the PHE-HB-SNPs, the effect of  $MS_{PHE}$  was investigated using PHE-HB-SNPs with the same  $MS_{HB}$  and similarly, the effect of  $MS_{HB}$  was evaluated using PHE-HB-SNPs with an identical  $MS_{PHE}$ .

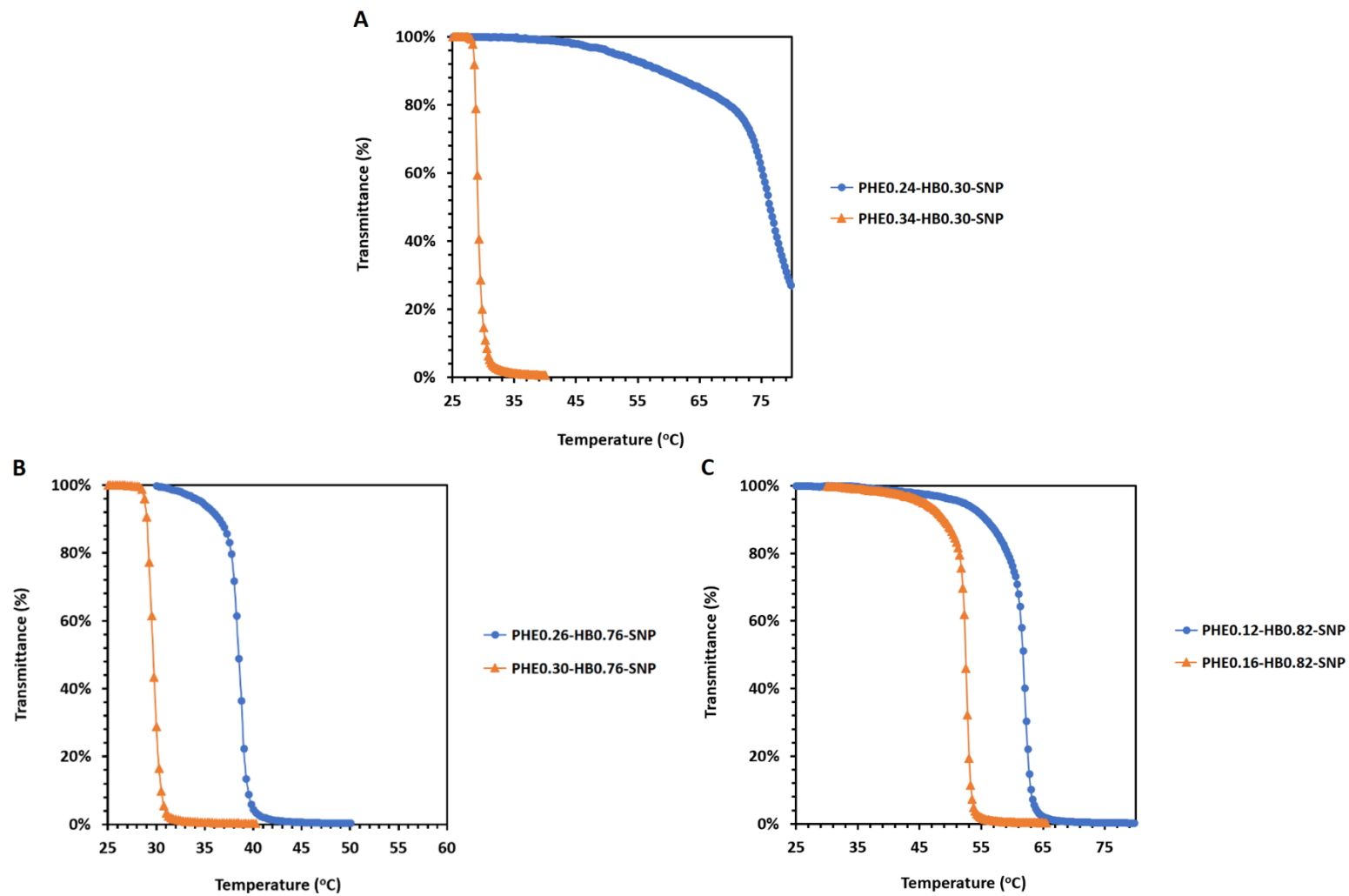


**Figure 6.8.** Comparison of transmittance curves between PHE-HB-SNPs with different  $MS_{PHE}$  but the same  $MS_{HB}$ : 0.30 (**A**), 0.76 (**B**) and 0.82 (**C**). Light transmittance measurements were conducted at 10 g/L.

The transmittance curve of PHE0.24-HB0.30-SNP exhibited a very shallow transition starting from 40 °C and the curve became significantly steeper from 70 °C, while the transmittance curve of PHE0.34-HB0.30-SNP exhibited a very steep transition at about 27 °C (Fig. 6.8A). It was quite impressive that the substantial differences in the transmittance curves and in their LCSTs were only due to a small difference in their  $MS_{PHE}$ . A similar trend was observed for the PHE-HB-SNP pairs with the same  $MS_{HB}$  but slightly different  $MS_{PHE}$  (Fig. 6.8B and C). Higher  $MS_{PHE}$  resulted in a substantially lower LCST and faster thermo-transition due to the highly hydrophobic PHE groups which could greatly facilitate hydrophobic interactions and can be easily destabilized in a dispersion via intermolecular aggregation.

The effect of  $MS_{HB}$  on the LCST was investigated by the comparison with PHE-HB-SNPs of the same  $MS_{PHE}$ . The transmittance curve of PHE0.18-HB0.50-SNP was very shallow while that of PHE0.18-HB0.96-SNP was extremely sharp indicating that the increase in  $MS_{HB}$  promoted a faster thermo-transition (Fig. 6.9A). Similar findings can be deduced from the transmittance curves of PHE-HB-SNPs with the same  $MS_{PHE}$  (0.22 and 0.30) but different  $MS_{HB}$  (Fig. 6.9B and C). Overall, increase in  $MS_{HB}$  decreased the LCST substantially, though the effect of HB substituents on the LCST was less pronounced than the more hydrophobic PHE substituents.

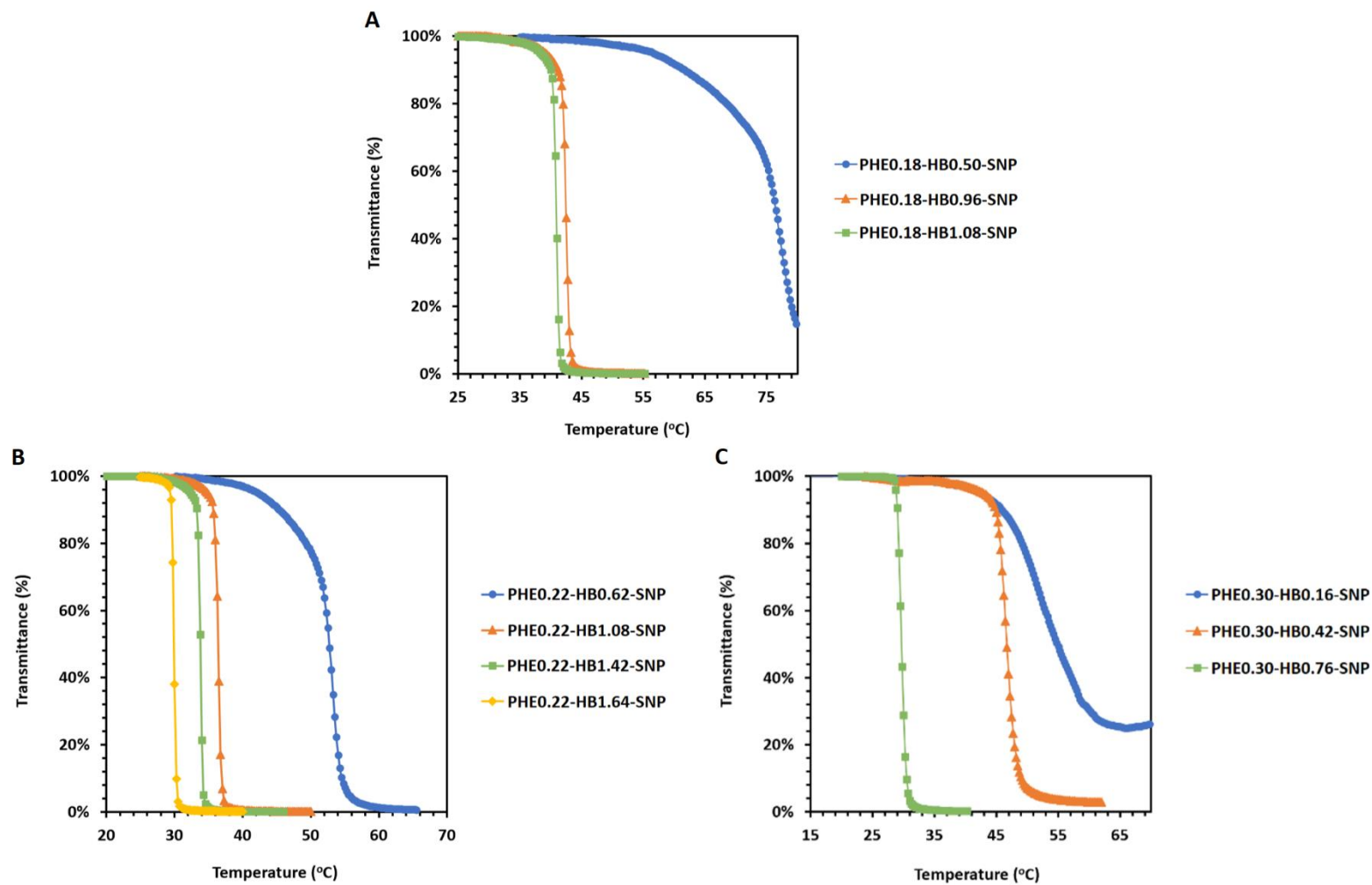


**Figure 6.9.** Comparison of transmittance curves between PHE-HB-SNPs with different  $MS_{PHE}$  but identical  $MS_{PHE}$ : 0.18 (**A**), 0.22 (**B**) and 0.3 (**C**). Light transmittance measurements were conducted at 10 g/L.

With a sufficiently high  $MS_{PHE}$ , only a small amount of HB groups on the PHE0.36-HB0.08-SNP was required to achieve an exceptionally low LCST of 16 °C (Table 6.4, entry 25). Previous studies on PHE-SNPs have shown that the PHE-SNPs did not exhibit thermoresponsivity.<sup>154</sup> The addition of a small amount of HB groups is absolutely essential for PHE-HB-SNPs to obtain thermoresponsivity but the addition of a large amount is unnecessary given that the  $MS_{PHE}$  is sufficiently high. Earlier in this chapter, we have established that the HB substituents improved the dispersibility of PHE-HB-SNPs below their LCSTs (Fig. 6.4). The dispersibility would drastically decrease if the HB substituents became dehydrated due to the increase in dispersion temperature which could no longer stabilize the PHE-HB-SNPs and consequently, the polymer precipitate out of the dispersion. Hence, we suspect that a low LCST can be achieved when the PHE-HB-SNP is highly hydrophobic (i.e. high  $MS_{PHE}$ ) and is stabilized by a minimal amount of HB groups below its LCST.

### **6.3.2.2 Effect of Concentration on the LCST of PHE-HB-SNP**

Concentration of a PHE-HB-SNP dispersion greatly affect the LCST. The concentration effect on the LCST of a TRP has been extensively studied in the literature.<sup>25,43,61,72</sup> Two samples, PHE0.28-HB0.36-SNP and PHE0.27-HB0.72-SNP, were selected to perform the concentration studies and their transmittance curves at varying concentrations in a range from 1 to 50 g/L were shown in Figure 6.10. The PHE0.28-HB0.36-SNP did not exhibit thermoresponsivity at 1 g/L and became thermoresponsive as the concentration increased (Fig. 6.10A). A relatively sharp transmittance curve was obtained at 10 g/L and a further increase in the concentration resulted in a slower thermo-transition. Similarly, the PHE0.27-HB0.72-SNP had a fast thermo-transition at 10 g/L while the

transmittance curves were less steep at higher or lower concentrations (Fig. 6.10B). At low concentrations, a higher temperature was required for the PHE-HB-SNPs to form large aggregates whereas at high concentrations, the increase in the viscosity of the dispersion may hinder the aggregation of the polymers, hence, a higher temperature was also needed for the precipitation of polymer to occur.

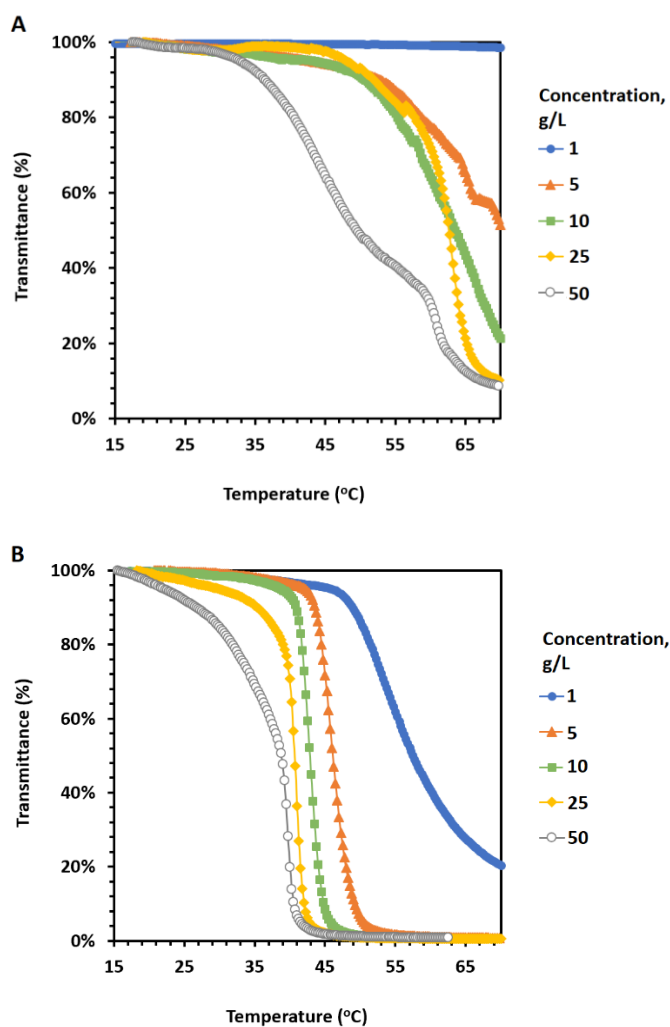


**Figure 6.10.** Transmittance curves of PHE0.28-HB0.36-SNP (A) and PHE0.27-HB0.72-SNP (B) dispersions in varying concentrations in a range of 1-50 g/L.

### 6.3.2.3 Effect of pH on the LCST of PHE-HB-SNP

The effect of pH on the LCST was studied using a 10 g/L PHE0.30-HB0.42-SNP dispersion at pH ranging from 1 to 12. The pH of the polymer dispersion was adjusted by either 1 M HCl or 1 M NaOH with a pH meter prior to the transmittance measurements. At low pH, the transition curves were steep, on the contrary, the transition curves became considerably shallower as the pH increased (Fig. 6.11A). The LCST of PHE0.30-HB0.42-SNP became greater than 70 °C at pH 12. The pH somehow had a great effect on the formation of aggregates in a dispersion in that higher pH may result in slower aggregation and a higher LCST. The pH effect on thermoresponsivity of a thermoresponsive HB-SNP (HB1.74-SNP) was negligible (Fig. 6.11B), hence, the PHE groups are likely responsible for the effect of pH on the thermoresponsivity of PHE-HB-SNPs.



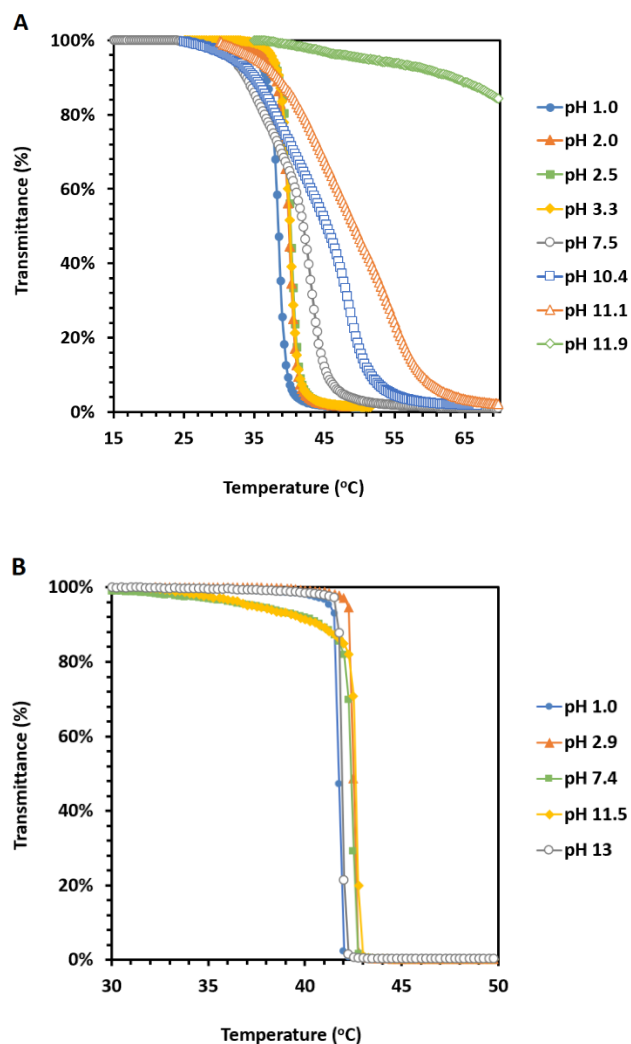


**Figure 6.11.** Transmittance curves for 10 g/L dispersions of PHE0.30-HB0.42-SNP (**A**) and HB1.74-SNP (**B**) at low to high pH.

## 6.4 Conclusion

The preparation of hydrophobically modified thermoresponsive SNPs was successful. The LCSTs of PHE-HB-SNPs can be adjusted in a range of 16 to 78 °C by varying the composition of the PHE and HB substituents. The reaction efficiency of the hydroxybutylation reaction greatly improved in the presence of styrene oxide or PHE groups on the SNPs. A small

increase in the  $MS_{PHE}$  of PHE-HB-SNP could result in a substantial decrease in its LCST and the effect of the PHE groups on manipulating the LCST was much greater than the HB groups. The HB groups were absolutely required for the thermoresponsivity of PHE-HB-SNPs and a minimal amount of HB groups, which was just enough to stabilize PHE-HB-SNP below its LCST, was optimal for achieving a low LCST.

## Chapter 7

### Extraction of Bitumen from Oil Sands using Modified Starch

#### Nanoparticles

##### 7.1 Introduction

As mentioned in Chapter 1, oil sands ores near the surface are amenable for surface mining and water-based extraction to recover bitumen. Surface mining involves a water-based extraction process in that the oil sands deposit is mined and broken down in a processing plant where water is added to make an oil sands slurry followed by aeration and finally a gravity separation process to remove water and solids to yield a bitumen-rich froth. For high-quality oil sands ores (known as good processing ores) which contain high bitumen content and very low fine content the bitumen recovery for commercial operations is usually over 90 %. Bitumen recovery is usually much lower when dealing with poor processing ores which have a high fines content and a high amount of divalent cations.<sup>176</sup> Fine (< 44  $\mu\text{m}$ ) and clay (< 2  $\mu\text{m}$ ) solids are the most troublesome component in oil sands ores that are detrimental to the water-based oil sands extractions.<sup>75</sup> Depending on the fine content in oil sands ores, the bitumen recovery can range from 30 % to 90 % and the recovery increases with the decreasing fine content.<sup>176</sup> Clay particles can deposit onto bitumen droplets via bridging by divalent cations to form a hydrophilic layer on the bitumen droplets known as slime coating which can greatly hinder bitumen-air bubbles attachment.<sup>93-96</sup> Moreover, oil sands ores when aged can become poor processing ores.<sup>176,177</sup> It has been proposed that there is a thin film of water located between bitumen and sand grains or fine solids in fresh ores, which facilitates the

liberation of bitumen when mixing with hot water.<sup>178</sup> However, for aged ores, the water film may be lost due to evaporation, leading to direct attachment of bitumen to fine solids, hence, poor bitumen liberation.<sup>177</sup> Sanford reported a significant reduction of bitumen recovery from 72 % to 33 % after the oil sands ores were aged at ambient temperature for two months.<sup>176</sup>

Generally, two main strategies can be found in the literature that aiming to improve the processability of poor processing ores: one strategy is to lower bitumen viscosity by the addition of solvents such as naphtha, kerosene, toluene, etc.; and another approach is to reduce bitumen-solids interfacial attraction by chemical additives such as surfactants and polymers that favor the polymer-clay interaction and attract divalent cations. In 2012, Hooshiar et al. used a solvent mixture containing toluene and heptane (70/30 v/v) to extract bitumen from poor processing ores and achieved a recovery of as high as 70 %.<sup>102</sup> Harjai and coworkers reported that the use of 10 wt % of kerosene (on the basis of bitumen weight) in an aqueous and solvent hybrid extraction process and resulted in an increase of bitumen recovery from 80 % to 99 % for good processing ores and from about 30 % to 70 % for poor processing ores.<sup>105</sup> More recently, Wang et al. have screened a series of solvents and found that *o*-xylene, toluene, methyl ethyl ketone, chloroform and trichloroethylene resulted in good bitumen recovery (as high as 75 %) when 2 mL of the solvents per gram of oil sands were used.<sup>106</sup>

In 2005, Li et al. employed a partially hydrolyzed anionic polyacrylamide (PAM) to extract bitumen from poor processing ores. The use of the anionic PAM at a dose of 30 ppm achieved an optimal recovery of 80 % from 60 % without any polymer.<sup>107</sup> At this dose, it was also shown that bitumen-clay adhesion was at its lowest level. Shortly after, the same group of researchers reported the extraction of poor processing ores by a combination of 5 ppm

Al(OH)<sub>3</sub>-PAM and 15 ppm anionic PAM to achieve an optimal recovery of 86 %.<sup>108</sup> The study of polymer additives to affect the bitumen-clay interactions has been extended to thermoresponsive polymers. In 2011, Long and coworkers have used a thermoresponsive polymer, PNIPAM ( $M_n = 3.2$  million Da, LCST = 32 °C), in bitumen extraction of poor processing oil sands ores and showed that the extraction with 400 ppm of PNIPAM at 40 °C achieved a recovery of close to 70 % which was significantly higher than the extractions conducted at room temperature, however, with the addition of the polymer, the froth quality was deteriorated.<sup>109</sup>

In 2015, Yang and Duhamel reported the use of a thermoresponsive copolymer of poly(ethylene glycol) (PEG) and poly(2-(2-methoxyethoxy) ethyl methacrylate) (PMEO<sub>2</sub>MA) as surfactants in an aqueous and solvent hybrid extraction process for good processing ores.<sup>10</sup> The copolymer has an LCST of 35 °C and above its LCST, the copolymer has been shown to form monodisperse micelles which are stable in an aqueous dispersion, unlike in the case of other thermoresponsive polymers such as PNIPAM which becomes insoluble above its LCST. The polymer micelles were suggested to be assisting the transfer of the solvents from the upper layer of the aqueous slurry to the bottom of the extraction vessel during the extraction process in a shaker at 50 °C and subsequently, solvating the bitumen and shuttling it through the aqueous phase back to the top layer leading to the formation of bitumen-rich froth (Fig. 7.1). Furthermore, upon the cooling of the aqueous slurry to room temperature (below the LCST), the copolymer become more soluble, leading to micelle deformation and the release of the bitumen/solvent droplets which eventually accumulate on the top layer. In their study, with the use of 1 g/L of the copolymer (with respects to the oil sands-water slurry volume) and 65 mg

of toluene, a recovery close to 100 % was achieved when the extraction was conducted in a shaker at 50 °C for 24 h. The copolymer-containing tailings can be recycled up to five times while still maintaining close to 100 % recovery.<sup>10</sup> In 2018, Zhang in the same research group has reported that the use of a copolymer of PMEO<sub>2</sub>MA and starch nanoparticles (PMEO<sub>2</sub>MA-SNP, LCST = ~32 °C) at 1 g/L and 200 mg of toluene was able to successfully extract bitumen from poor processing ores with a recovery of 80 % when the extraction was conducted in a shaker for 24 h at 45 °C.<sup>179</sup> It has been shown that only the thermoresponsive polymer which can form colloiddally stable micelles above its LCST could improve the bitumen recovery, while those ones that form insoluble aggregates above the LCST impaired the ability to extract bitumen.

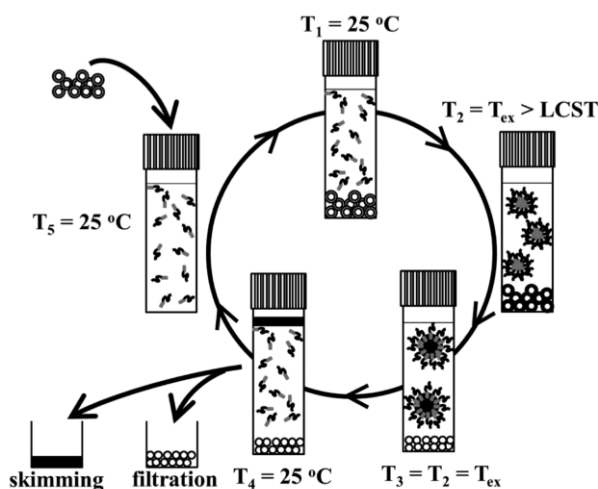


**Figure 7.1.** Schematic representation of oil recovery procedures using the thermoresponsive block copolymer PEG-*b*-PMEO<sub>2</sub>MA. This picture was adapted from Yang and Duhamel with permission.<sup>10</sup>

From the preceding chapters, cationic starch, cationic hydrophobic starch and cationic thermoresponsive starch have shown to be interacting with clay particles in mature fine

tailings, hence, it is reasonable to suggest that these cationic starches will attract clay particles in a water-oil sands slurry during the extraction and reduce the bitumen-clay interaction. Moreover, in Chapter 4, we have shown that cationic-hydroxybutylated (Cat-HB) thermoresponsive starch forms stable mesoglobules above its LCST, which should increase the bitumen-solvent interaction during an aqueous-solvent hybrid extraction and enhance bitumen liberation. The Cat-HB thermoresponsive starch may also improve bitumen flotation when the mesoglobules deform below the LCST and induce the release of bitumen-saturated solvent droplets that are previously stabilized by the mesoglobules above the LCST. In this chapter, we investigate the effectiveness of cationic starch, cationic hydrophobic starch and thermoresponsive Cat-HB starch as polymer aids in an aqueous-solvent hybrid extraction process to extract bitumen from poor processing ores and aged oil sands ores with toluene as the solvent.

## **7.2 Materials and Methods**

### **7.2.1 Materials**

Starch nanoparticles (SNPs) were obtained from EcoSynthetix Inc. (Burlington, Ontario, Canada). *N*-(3-chloro-2-hydroxypropyl) trimethyl ammonium chloride (CHPTAC) (60 wt % solution in H<sub>2</sub>O), 1,2-butene oxide and styrene oxide were obtained from Sigma-Aldrich Co. (USA). Oil sands ores were obtained from Alberta Innovate Technology Futures Sample Bank and were determined to contain approximately 10.5 wt % of bitumen and 2 wt % of fine solids by Soxhlet extraction.<sup>179</sup> Other reagents and solvents were commercially available and used without further purification unless stated otherwise.

## 7.2.2 Preparation of Modified Starch Nanoparticles

Cationic SNP (Cat-SNP) was prepared as described in Section 3.2.2. Two types of cationic thermoresponsive SNPs were prepared: cationic hydroxybutyl SNP (Cat-HB-SNP) and cationic phenylhydroxyethyl hydroxybutyl SNP (Cat-PHE-HB-SNP). The Cat-HB-SNP was prepared as described in Section 4.2.2. The cationic hydrophobic SNP, cationic phenyl hydroxyethyl SNP (Cat-PHE-SNP), was synthesized in a similar way as the Cat-HB-SNP in that the hydroxyalkylating agent, butene oxide, was replaced by styrene oxide.

The preparation of the Cat-PHE-HB-SNP began with making a 25 wt % dispersion of SNP (1 g) with deionized water. To the dispersion, 10 M NaOH was added dropwise with vigorous stirring to give a pH of 13. Butene oxide and styrene oxide were added to the mixture simultaneously and stirred vigorously at 40 °C for 24 h. The pH of the reaction mixture was again adjusted by the addition of 10 M NaOH to a pH of 13 and CHPTAC was then added to the mixture which was stirred vigorously at 50 °C for 18 h. The mixture was cooled to room temperature (rt) then neutralized by the dropwise addition of 1 M HCl with vigorous stirring. The neutralized mixture was subjected to dialysis against deionized water for 2 days using a dialysis bag with molecular weight cut-off ( $MW_{\text{cutoff}}$ ) of 1 kD. A minimum of 5 water replacements were performed over the course of 2 days to give an overall dilution ratio of approximately 1:10<sup>10</sup>. The dialyzed Cat-PHE-HB-SNP was lyophilized for at least 3 days to yield a white powder.



### 7.2.3 Light Transmittance Studies

Light transmittance values were determined using a Cary 4000 Bio UV-Visible spectrophotometer equipped with a multi-cuvette holder and a temperature controller. The Cat-HB-SNP and Cat-PHE-HB-SNP were dispersed in deionized water to a concentration of 1 g/L for 16 h at 4 °C before transmittance measurements. The temperature of the dispersion was measured by placing a temperature probe in a reference cell. The transmittance was recorded at 500 nm with a heating rate of 1 °C/min. A pre-determined amount of 6 M NaCl solution was added to the dispersion if required. The polymer dispersion was equilibrated for at least 5 minutes at 5 °C in the multi-cuvette holder before the measurements commenced. Absorbance data points were taken every 1 °C and recorded up to 45 °C. The LCST is defined as the temperature at the inflection point of the transmittance curve at 1 g/L.

### 7.2.4 Bitumen Extraction Tests

Polymer was dispersed in deionized water to make a stock solution with a concentration of 1 g/L unless stated otherwise. Oil sands ores (1 g) were weighed into a 20 mL scintillation vial with cap. 15 mL of the polymer dispersion was added to the scintillation vial followed by the addition of 50 mg of toluene unless stated otherwise. The vial was secured on a rotator in an oven and the extraction took place at 45 °C with a rotating speed of 90 rpm for 24 h. Subsequently, the vial was removed from the oven and left to stand undisturbed on a laboratory bench at rt for 16 h before froth collection commenced. The extraction mixture separated into three layers: bitumen-rich froth (top layer), tailings (middle layer), sands (bottom layer). The froth layer was diluted by toluene and the bitumen saturated toluene was collected into a

container labelled as “extracted bitumen”. The middle layer was removed by pipetting to a separatory funnel and bitumen emulsion in the aqueous phase was extracted by toluene into a container labelled “bitumen in tailings”. Residual bitumen in sands after the initial extraction was extracted by tetrahydrofuran (THF) into a container labelled as “unextracted bitumen”. Toluene and THF were evaporated by injecting a stream of air into the containers for 16 h and further dried in a vacuum oven for 16 h at 70 °C. The weight of bitumen in each of the containers was obtained and used for the calculation of bitumen recovery (Eq. 7.1). All extraction tests were performed at least three times to obtain representative results.

**Equation 7.1**

$$\text{Bitumen Recovery} = \frac{\text{Extracted Bitumen} \times 100 \%}{(\text{Extracted Bitumen} + \text{Bitumen in Tailings} + \text{Unextracted Bitumen})}$$

## 7.3 Results and Discussion

### 7.3.1 The Stabilization of Thermoresponsive SNPs

HB-SNPs with a molar substitution of HB groups of 1.9 (HB1.9-SNP) had an LCST of 31.5 °C, which was defined as the temperature at the inflection point of its transmittance curve. HB1.9-SNP becomes completely dehydrated and hydrophobic and forms insoluble aggregates above its LCST as evidenced by the reduction in the transmittance of the polymer dispersion to close to 0 % above the LCST (Fig. 7.2). Cat-HB1.9-SNP with an MS of 0.013 (Cat0.013-HB1.9-SNP) showed improved stability above its LCST which was indicated by the transmittance values (~ 30 %) of the polymer dispersion at temperatures above the LCST (Fig. 7.2). Further increase in the MS of cationic groups increased the stability of the corresponding Cat-HB1.9-SNPs above their LCSTs. Cat0.036-HB1.9-SNP had an LCST of about 32 °C and

an approximately 10 % reduction in transmittance values above the LCST (Fig. 7.2). The thermoresponsive properties of Cat0.036-HB1.9-SNP are similar to those of the block copolymer, PEG-*b*-PMEO<sub>2</sub>MA, used by Yang and Duhamel in their bitumen extraction studies.<sup>10</sup>

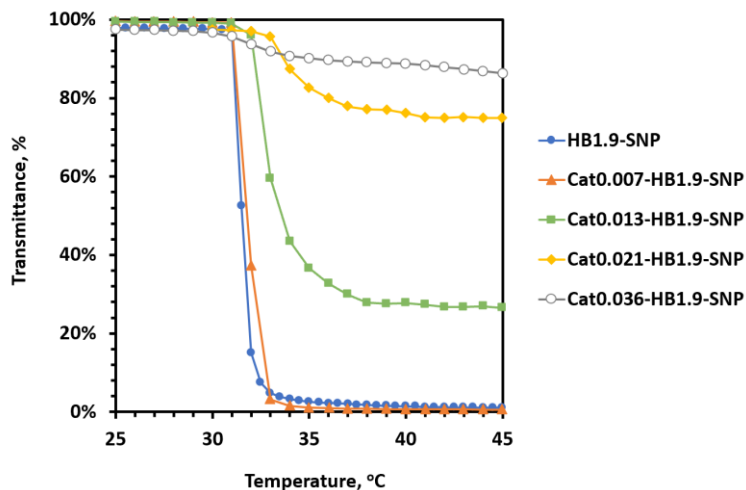


**Figure 7.2.** Transmittance curves of the 1 g/L dispersions of Cat-HB1.9-SNP with MS of cationic groups ranging from 0 to 0.036.

### 7.3.2 Bitumen Extraction Tests on Fresh Oil Sands Ores

Bitumen extraction tests were initially conducted with the oil sands ores as received. No bitumen was recovered when the extraction was conducted with the addition of deionized water only at an extraction temperature of 45 °C. This was expected as poor processing ores generally result in a poor bitumen recovery.<sup>176,177</sup> The bitumen recovery of the extractions with 50 mg of toluene but without any polymers was about 30 %. The bitumen recovery did not improve when using 50 mg of toluene and unmodified SNP at a concentration of 1 g/L.

### 7.3.2.1 Extraction using Cat-HB1.9-SNP

As the Cat-HB1.9-SNPs with MS values higher than 0.013 showed an improvement in stability in an aqueous dispersion above their LCSTs, bitumen extraction tests using the Cat-HB1.9-SNPs along with 50 mg of toluene were conducted at 45 °C and the results were shown in Figure 7.3.

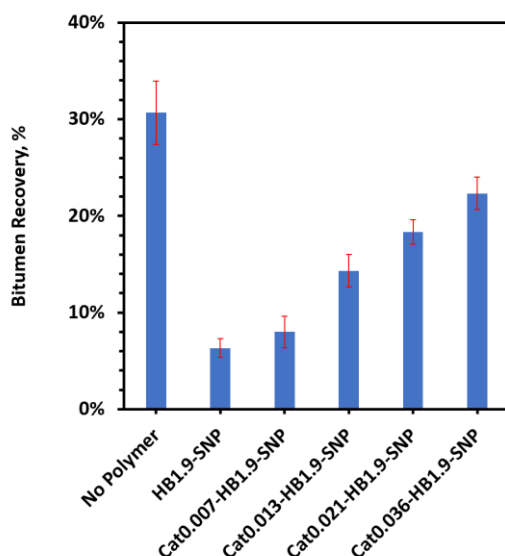


**Figure 7.3.** Bitumen recovery of extractions of fresh oil sands ores using Cat-HB1.9-SNPs with MS of cationic groups ranging from 0 to 0.036 along with 50 mg of toluene.

The Cat-HB1.9-SNPs were generally better than HB1.9-SNP and the bitumen recovery increased with the increasing MS of the cationic groups. However, even at an MS of 0.036, the Cat0.036-HB1.9-SNP did not improve the bitumen recovery compared to the extractions without polymer. The results suggested that the polymer failed to maintain its stability at the extraction temperature (45 °C) in the oil sands/water slurry. Though the light transmittance studies showed the colloidal stability of the Cat0.036-HB1.9-SNP above its LCST when the polymer was dispersed in deionized water, the Cat0.036-HB1.9-SNP may not be stable in the

oil sands/water slurry during the extraction due to the naturally occurring salts in the oil sands ores. The water within the oil sands may contain salts with a concentration similar to that of a NaCl solution in a concentration range between 30 and 100 mM.<sup>77</sup> Additionally, it is widely accepted that the type of salts and salt concentration in a polymer dispersion greatly affect the thermoresponsive behaviors of thermoresponsive polymers.<sup>25,62,72</sup> We have previously shown that the LCST of HB1.2-SNP decreased from 60 to 47 °C with the increasing of NaCl concentration from 0 to 0.5 M in a 10 g/L polymer dispersion.<sup>72</sup> Kosmotropic salts such as NaCl contain anions that can strongly interact with water molecules, hence, disrupting the hydrogen bonds that enable the thermoresponsive polymers to stay solvated.

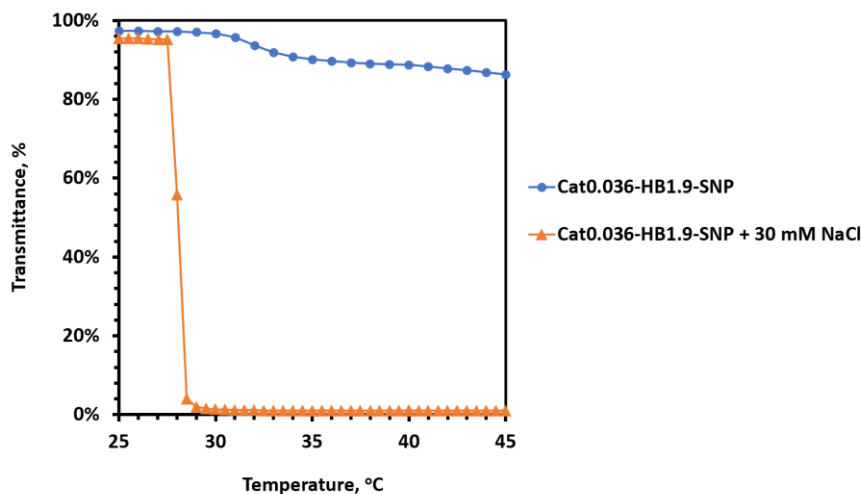


**Figure 7.4.** Transmittance curves of Cat0.036-HB1.9-SNP in a 1 g/L aqueous dispersion with no salts or with NaCl at a concentration of 30 mM.

A light transmittance study was conducted with the addition of saturated NaCl solution to the 1 g/L Cat0.036-HB1.9-SNP dispersion to give a NaCl concentration of 30 mM. Not surprisingly, the LCST of the polymer decreased from 32 °C to 28 °C (Fig. 7.4), and the dispersion transmittance values above the LCST decreased to close to 0 % indicating the

formation of insoluble aggregates which could explain the poor bitumen recovery. Moreover, as the polymers became hydrophobic, they may attach to the bitumen due to hydrophobic interactions and forming aggregates (or flocs) with clay particles. As a result, the polymer/bitumen/clay aggregates may settle to the bottom of the scintillation vial during the flotation process and preventing the bitumen to float to the top of the aqueous layer. This was evidenced by a picture of the extraction mixture taken after the extraction in oven using Cat0.036-HB1.9-SNP and allowed for phase separation for 16 h at rt and a layer of black sediments accumulated on top of the sands at the bottom of the vial was very noticeable (see Fig. E1 in Appendix E). Overall, the Cat-HB1.9-SNPs with MS values up to 0.036 were not a good candidate for polymer additives in the bitumen extraction tests because the polymers were unstable above their LCSTs in a salt containing dispersion.

### **7.3.2.2 Extraction using Cat-PHE-HB-SNP**

We demonstrated in Chapter 6 that SNPs modified with butene oxide and styrene oxide can yield thermoresponsive SNPs. One such polymer is PHE0.38-HB0.4-SNP with MS of phenylhydroxyethyl groups of 0.38 and hydroxybutyl groups of 0.4. The PHE0.38-HB0.4-SNP had an LCST of 13 °C and it was unstable above its LCST at a concentration of 1 g/L indicated by the low transmittance of the dispersion (Fig. 7.6). Upon the substitution of cationic groups with MS ranging from 0.014 to 0.036 (Fig. 7.5), the Cat-PHE0.38-HB0.4-SNPs did not exhibit an LCST up to 45 °C (Fig. 7.6). The effect of the addition of cationic groups on the thermoresponsive behaviors was much more pronounced for the Cat-PHE0.38-HB0.4-SNPs

compared to the Cat-HB1.9-SNPs. This suggested that the Cat-PHE0.38-HB0.4-SNPs were very stable at 45 °C when dispersed in deionized water and with no salts.

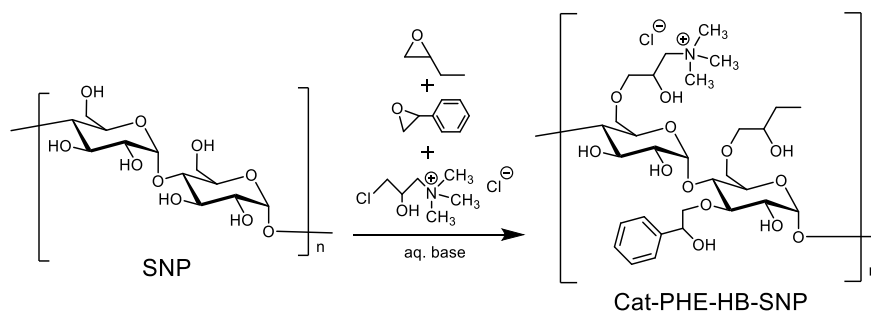


**Figure 7.5.** Preparation of Cat-PHE-HB-SNP. Substitution can occur at O-2, O-3 and O-6.

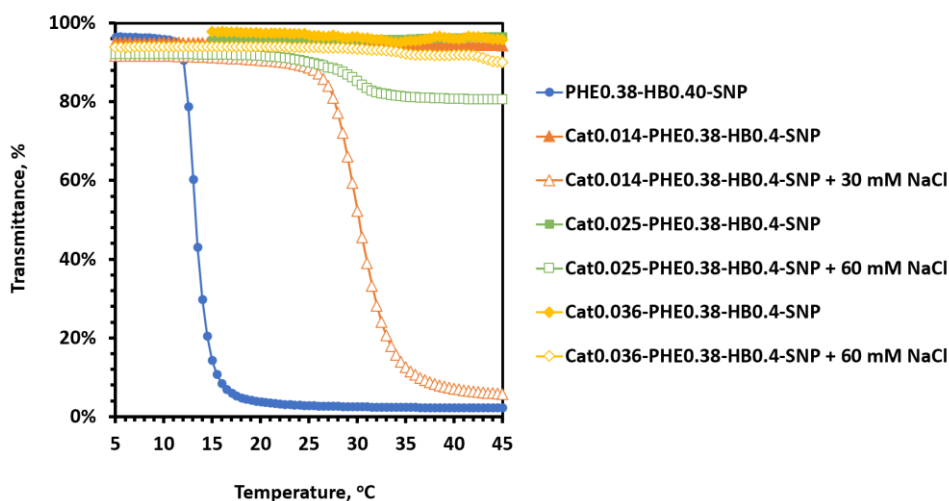


**Figure 7.6.** Transmittance curves of Cat-PHE0.38-HB0.4-SNPs in a 1 g/L aqueous dispersion with no salts or with NaCl at a concentration of 30 or 60 mM.

When NaCl was added to the dispersions of Cat-PHE0.38-HB0.4-SNPs, the NaCl disrupted the stability of the polymers. With 30 mM of NaCl, the Cat0.014-PHE0.38-HB0.4-SNP exhibited an LCST at 30 °C but it formed unstable aggregates above the LCST indicated by the low transmittance values at temperatures higher than its LCST (Fig. 7.6). With 60 mM of NaCl, the Cat0.036-PHE0.38-HB0.4-SNP was very stable, but it did not exhibit an LCST,

while the Cat0.025-PHE0.38-HB0.4-SNP exhibited an LCST at approximately 31 °C and a transmittance reduction of about 10 % above its LCST. Dynamic light scattering (DLS) studies showed that the hydrodynamic diameters ( $D_h$ ) of the Cat0.025-PHE0.38-HB0.4-SNP increased from 15 to 79 nm when the dispersion temperature increased from 15 °C to 45 °C and the dispersion was at a concentration of 1 g/L and with 60 mM of NaCl. In a salt containing dispersion, the Cat0.025-PHE0.38-HB0.4-SNP not only exhibited an LCST but also formed relatively stable mesoglobules above its LCST, which could be a good candidate as polymer aids for the bitumen extraction.

Extraction tests were performed using Cat-PHE0.38-HB0.4-SNPs with MS of cationic groups ranging from 0 to 0.23 and their results were compared to those of the cationic SNPs (Cat-SNPs) and the cationic hydrophobically modified SNPs (Cat-PHE0.38-SNP). When the MS of cationic groups was low ( $<0.02$ ), the Cat-PHE0.38-HB0.4-SNPs yielded very low bitumen recovery (Fig. 7.7) because such polymers were unstable at the extraction temperature of 45 °C. When the MS of cationic groups increased to 0.025, the Cat0.025-PHE0.38-HB0.4-SNP significantly improved the extraction and an optimal bitumen recovery of 86 % was obtained (Fig. 7.7). As mentioned in the paragraph above, the Cat0.025-PHE0.38-HB0.4-SNP could form mesoglobules that were quite stable in a salt containing dispersion at temperatures that were higher than the LCST of the polymer, which was similar to the thermoresponsive behaviors of PEG-*b*-PMEO<sub>2</sub>MA reported by Yang and Duhamel.<sup>10</sup> The mesoglobules could improve bitumen liberation by shuttling the solvent, toluene, through the aqueous phase to reach the oil sands ores and solvate the bitumen that adheres to the ores. Furthermore, the deformation of mesoglobules, when the slurry temperature was cooled to below the LCST,



could induce the release of the bitumen saturated toluene which eventually accumulated on top of the aqueous phase to be collected as froth (see Fig. E2 in Appendix E).

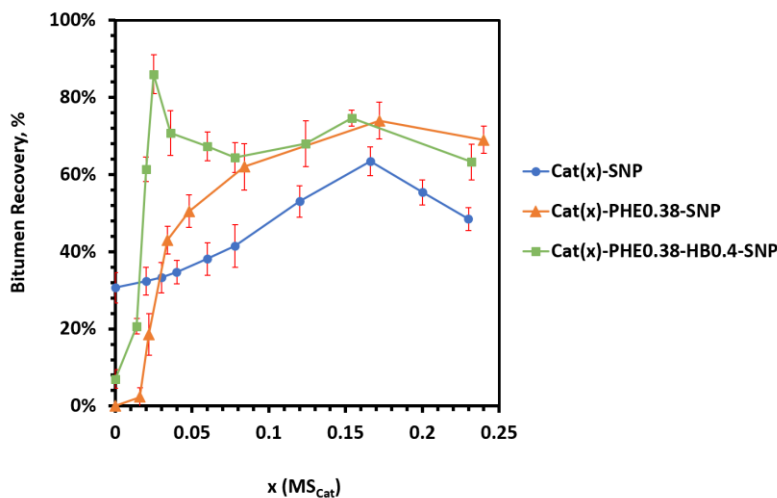


**Figure 7.7.** Bitumen recovery of extractions of fresh oil sands ores using 50 mg of toluene and 1 g/L of Cat-SNPs, Cat-PHE0.38-SNPs and Cat-PHE0.38-HB0.4-SNPs with varying MS of cationic groups.

Further increase in the MS of cationic groups to 0.036 or above resulted in over-stabilizing the polymers, which failed to exhibit an LCST up to 45 °C, in a dispersion with 60 mM of NaCl. Thus, a decrease in bitumen recovery was observed when using the Cat-PHE0.38-HB0.4-SNP with an MS of 0.036 or higher (Fig. 7.7). However, a second maximum, at 75 %, was obtained with the use of Cat0.16-PHE0.38-HB0.4-SNP. It could be reasonable to attribute this improvement in bitumen recovery to the polymer-clay interactions due to electrostatic attraction between the positively charged polymers and the negatively charged clay particles. Hence, the bitumen-clay interactions could be at the minimum. The bitumen-clay interaction was studied by Li et al. who used atomic force microscopy (AFM) to measure the adhesion force between bitumen and clay, and found that the bitumen recovery was

optimized at where the bitumen-clay adhesion was at the lowest with the addition of anionic PAM at its optimal dose during their extraction process.<sup>107</sup>

Cat-SNPs with MS values ranging from 0 to 0.23 were also examined as polymer aids in the extraction tests and the results are shown in Figure 7.7. The bitumen recovery increased with the increasing MS of cationic groups and the maximum recovery, 63 %, was reached at an MS of 0.17. The maximum recovery achieved by Cat0.17-SNP was significantly lower than that by Cat0.16-PHE0.38-HB0.4-SNP despite the fact that the MS of the cationic groups was similar. This is possibly due to the fact that the Cat0.16-PHE0.38-HB0.4-SNP was hydrophobically modified and contained the hydrophobic PHE groups. Thus, it is of interest to investigate the effect of the PHE groups on bitumen recovery.

The cationic hydrophobic SNPs, Cat-PHE0.38-SNPs with varying MS from 0 to 0.24, were also examined as polymer aids for bitumen extraction. At an MS of 0.022 or lower, the Cat-PHE0.38-SNPs produced very low bitumen recovery due to the low dispersibility of the highly hydrophobic polymer in water (Fig. 7.7). As the MS of cationic groups increased, the Cat-PHE0.38-SNPs could become more dispersible which could enhance their ability to attract clay particles and lower the bitumen-clay interaction. The bitumen recovery reached a maximum at 74 % with the use of the Cat0.17-PHE0.38-SNPs and a further increase in the MS of cationic groups resulted in a slight decrease in bitumen recovery from its maximum (Fig. 7.7). The bitumen recovery obtained from the extractions using the Cat-PHE0.38-SNP with an MS of 0.034 or higher was noticeably higher than that using the Cat-SNP with the same MS. The Cat-PHE0.38-SNPs are amphiphilic polymers containing the hydrophobic PHE substituents and the hydrophilic cationic groups and hydroxyl groups on the starch backbone.

The amphiphilic nature of the Cat-PHE0.38-SNPs makes it an interfacially active polymeric surfactant which may be effective in reducing the bitumen saturated toluene-water interfacial tension and causing the demulsification of the bitumen saturated toluene-in-water emulsions in tailings and the water-in-bitumen saturated toluene emulsions in froth.

Poor processing ores often generate small bitumen droplets that are quite stable in the tailings producing bitumen-in-water emulsions which impede the attachment of air bubbles leading to low bitumen recovery.<sup>180</sup> The addition of a demulsifier should mitigate this problem as the demulsifier could act as bridges to aggregate the small bitumen droplets and enhance the coalescence of the bitumen droplets to form larger droplets and consequently, improving the bitumen aeration. We conducted bitumen extraction tests using either Cat0.17-SNP or Cat0.17-PHE0.38-SNP at 1 g/L together with 50 mg of toluene and the bitumen froth was collected (the “extracted bitumen”) at 10 min, 30 min, 1 h, 2 h, 5 h, 24 h, and 48 h after the extraction mixture was removed from the oven and left to stand undisturbed on a laboratory bench. At the same time, the tailings were extracted by toluene and the remaining bitumen in the sands was extracted by THF and the bitumen obtained after solvent evaporation was considered to be the “bitumen in tailings” and the “unextracted bitumen”, respectively. For both the Cat0.17-SNP and the Cat0.17-PHE0.38-SNP, the amount of “unextracted bitumen” (or the residual bitumen in sands after the extraction) increased slightly initially and remained relatively constant in the course of the 48 h (Fig. 7.8A and B), indicating a negligible amount of bitumen depositing to the sands at the bottom. For the Cat0.17-SNP, the rate of decrease of the “bitumen in tailings” or the rate of increase in the “extracted bitumen” was significantly slower compared to those of the Cat0.17-PHE0.38-SNP. The amount of “extracted bitumen”

did not reach a plateau until 24 h for the Cat0.17-SNP (Fig. 7.8A) while a plateau was reached after 5 h for the Cat0.17-PHE0.38-SNP (Fig. 7.8B). Moreover, after 24 h, the amount of “bitumen in tailings” for the Cat0.17-SNP was more than 2-fold higher than that for the Cat0.17-PHE0.38-SNP, indicating that the Cat0.17-SNP was not effective in demulsifying the toluene diluted bitumen-in-water emulsions. These observations supported that the Cat0.17-PHE0.38-SNP could act as a demulsifier to induce the coalescence of the toluene diluted bitumen in the extraction mixture and enhance bitumen aeration and flotation during the extraction process while the Cat0.17-SNP could not.

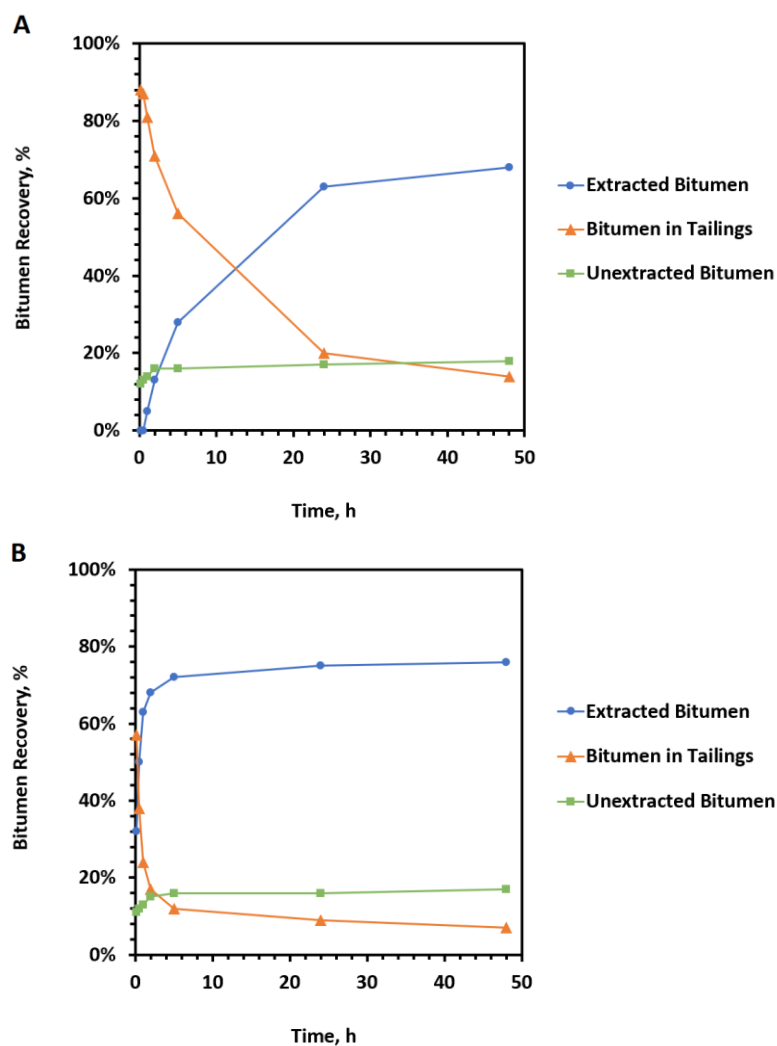


**Figure 7.8.** A plot of the amount of bitumen obtained from the top layer (“extracted bitumen”), the middle layer (“bitumen in tailings”) and the residual bitumen in the sands at the bottom (“unextracted bitumen”) versus time for the phase separation of the extraction mixture after rotating at 45 °C in an oven. The extraction tests were conducted with fresh oil sands ores using the Cat0.17-SNP (**A**) and the Cat0.17-PHE0.38-SNP (**B**) at 1 g/L along with 50 mg of toluene.

A similar biopolymer-based interfacially active surfactant, ethyl cellulose, was reported to be an effective demulsifier for water-in-solvent diluted bitumen emulsions by Feng et al.<sup>181</sup> and by Lin et al.<sup>110</sup> Cat-PHE0.38-SNPs share some similarity to the ethyl cellulose in that they are both amphiphilic biopolymers with hydrophobic substituents and hydrophilic

hydroxyl groups in their backbones. Hence, the Cat-PHE0.38-SNPs should destabilize the water droplets in the bitumen froth (water-in-toluene diluted bitumen emulsions) in a way similar to the ethyl cellulose. It is widely accepted that the water droplets are strongly stabilized by native surfactants, such as asphaltenes and clays, which are released during the extraction.<sup>182</sup> Without the addition of the demulsifier, the water droplets would remain stable in the bitumen froth and deteriorating the froth quality. Moreover, the addition of the demulsifier should also increase the hydrophilicity of the surface of sand grains by displacing bitumen and other hydrophobic compounds from the sand grains.<sup>183</sup> The chance of the sand grains carrying over to the bitumen froth would decrease with the increasing hydrophilicity of the sand grains, which could be beneficial for the bitumen froth quality.<sup>110</sup> Figure 7.9 illustrated the phase separation of the bitumen extraction mixtures given by the Cat0.17-PHE0.38-SNP (Fig. 7.9A) and the Cat0.17-SNP (Fig. 7.9B) after sitting undisturbed on a bench for 24 h. The darker band on top of the aqueous phase produced by the Cat0.17-PHE0.38-SNP could be more or less indicative of higher quality bitumen froth which contained less emulsified water or suspended solids. Similarly, the Cat-PHE0.38-HB0.4-SNPs with MS higher than 0.06, though they were no longer thermoresponsive, would be a good demulsifier, which was supported by the observation that the Cat-PHE0.38-HB0.4-SNPs exhibited almost identical bitumen recovery as the Cat-PHE0.38-SNPs at MS of cationic groups ranging from 0.08 to 0.24 (Fig. 7.7).

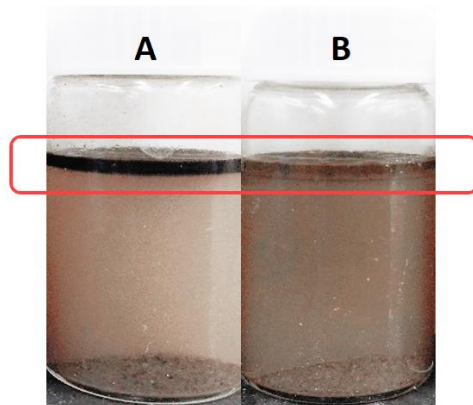


**Figure 7.9.** Pictures of bitumen extraction mixtures taken after 24 h of phase separation for the Cat0.17-PHE0.38-SNP (A) and the Cat0.17-SNP (B). The dark band on top of the aqueous phase is corresponding to the froth consisting mainly of the toluene diluted bitumen.

### 7.3.3 Bitumen Extraction Tests on Aged Oil Sands Ores

The bitumen extractions of the aged oil sands ores, which were stored in a plastic container for eight months at room temperature, showed unsatisfactory results using Cat-PHE0.38-HB0.4-SNP with an MS of 0.025 or 0.036. The Cat0.025-PHE0.38-HB0.4-SNP had a bitumen recovery of 86 % on fresh oil sands ores while the polymer completely failed to recover any bitumen on the aged oil sands ores. Bitumen recovery would be drastically decreased if the oil sands ores were aged,<sup>105,176,177,184,185</sup> and a reduction in the bitumen recovery from 72 % to 33 % was reported by Sanford after the oil sands ores were aged at room temperature for about two months.<sup>176</sup> Wallwork and coworkers have attributed the decrease in bitumen recovery of aged oil sands ores to a reduction in the hydrophilicity of the surface of sand grains and fine solids due to the evaporation of the moisture of the ores and bitumen liberation becomes considerably more difficult with the decreasing hydrophilicity of the solids.<sup>177</sup> Moreover, Wallace et al. have shown that the aged oil sands ores contained

significantly more inorganic salts such as sulphate.<sup>96</sup> The increase in the amount of inorganic salts in the aged ores was detrimental to the bitumen extraction using the cationic thermoresponsive SNPs such as Cat0.025-PHE0.38-HB0.4-SNP because the salts would destabilize the polymer drastically.

Cat-SNPs with varying MS were capable of extracting bitumen from the aged oil sands ores though there were slight differences in extraction efficiencies between the aged and fresh oil sands. For the aged ores, the bitumen recovery plateaued at an MS of 0.17, while the maximum recovery was reached at this MS for the fresh ores (Fig. 7.10). Moreover, the bitumen recovery decreased from 63 % to 51 % when the extractions were conducted using the aged oil sands ores and Cat0.17-SNP. The bitumen extraction of the aged oil sands was more difficult which was consistent with other extraction results reported in the literature.<sup>105,176,177,184,185</sup> For aged oil sands ores, increasing the MS of cationic groups on the Cat-SNPs from 0.17 to 0.9 did not seem to affect the bitumen recovery (Fig. 7.10). The reasons for this observation are not yet well understood. It could be due to the increase in the amount of anionic species in the aged oil sands ores that interact with the Cat-SNPs with a high MS, hence, the cationic groups were not overdosed even though the MS was high.



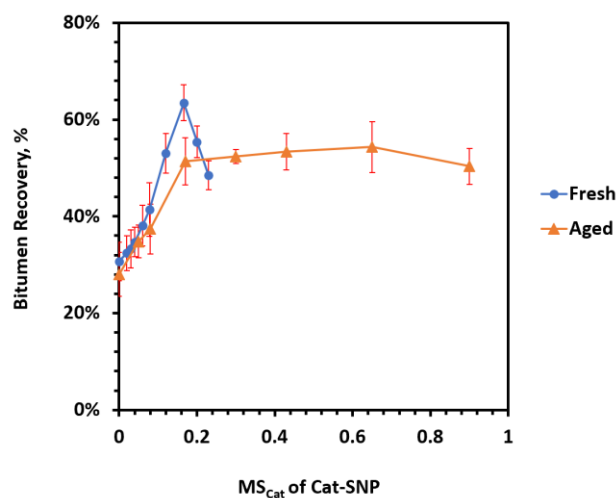


**Figure 7.10.** Bitumen recovery of extractions of fresh or aged oil sands ores using 50 mg of toluene and 1 g/L of Cat-SNPs with varying MS of cationic groups.

Cat-PHE-SNP has been demonstrated to be a good demulsifier for the bitumen extractions of the fresh oil sands ores in the previous section. Here we investigate the effectiveness of the Cat-PHE-SNP as a demulsifier for the bitumen extractions of the aged oil sands ores. Extraction tests were conducted using Cat0.17-PHE-SNPs, with MS ranging from 0 to 0.54 for the PHE groups, at a concentration of 1 g/L and with the addition of 50 mg of toluene. Bitumen recovery increased with the increasing MS of the PHE groups and the maximum recovery (81 %) was obtained when using Cat0.17-PHE0.38-SNP (Fig. 7.11A). The maximum recovery from the aged ores was marginally better than the maximum recovery from the fresh oil sands (74 %) which may imply that the bitumen extraction with the Cat0.17-PHE0.38-SNP was not affected by the aging of the ores. This is possible because of the use of a solvent, toluene, during the extraction in that the solvent could assist in bitumen liberation from the sand grains and the negative impact of aging on the bitumen recovery could be greatly mitigated. Lin and coworkers reported that the use of cyclohexane as the solvent in a pilot-

scale aqueous and solvent hybrid extraction process significantly improved bitumen recovery from the aged oil sands ores.<sup>186</sup> Further increase in the MS of PHE groups increased the hydrophobicity of the polymer, and a decrease in the bitumen recovery was observed (Fig. 7.11A). The polymer with an exceedingly high hydrophobicity could re-stabilize bitumen droplets in the aqueous extraction slurry, leading to a reduction in the bitumen recovery.

Optimization studies using Cat0.17-SNPs and Cat0.17-PHE0.38-SNPs were conducted by varying the toluene dose, the extraction temperature and the polymer concentration. Bitumen recovery increased with increasing dose of toluene added in the extractions regardless of the polymers (Fig. 7.11B). This makes sense as the toluene could reduce the viscosity of bitumen and increase the mobility of the bitumen leading to better bitumen liberation.<sup>187</sup> Additionally, the reduction in bitumen viscosity due to the addition of toluene could decrease the mobility of oil sands surfactants in the bitumen-water interfaces that stabilize the bitumen droplets,<sup>110</sup> and increase the chance of the coalescence of the bitumen droplets, hence, improving bitumen flotation. Bitumen recovery was significantly higher for the extractions using the Cat0.17-HB0.38-SNP compared to the Cat0.17-SNP (Fig. 7.11B) across the toluene doses examined, which supported that the Cat0.17-HB0.38-SNP was a better demulsifier.

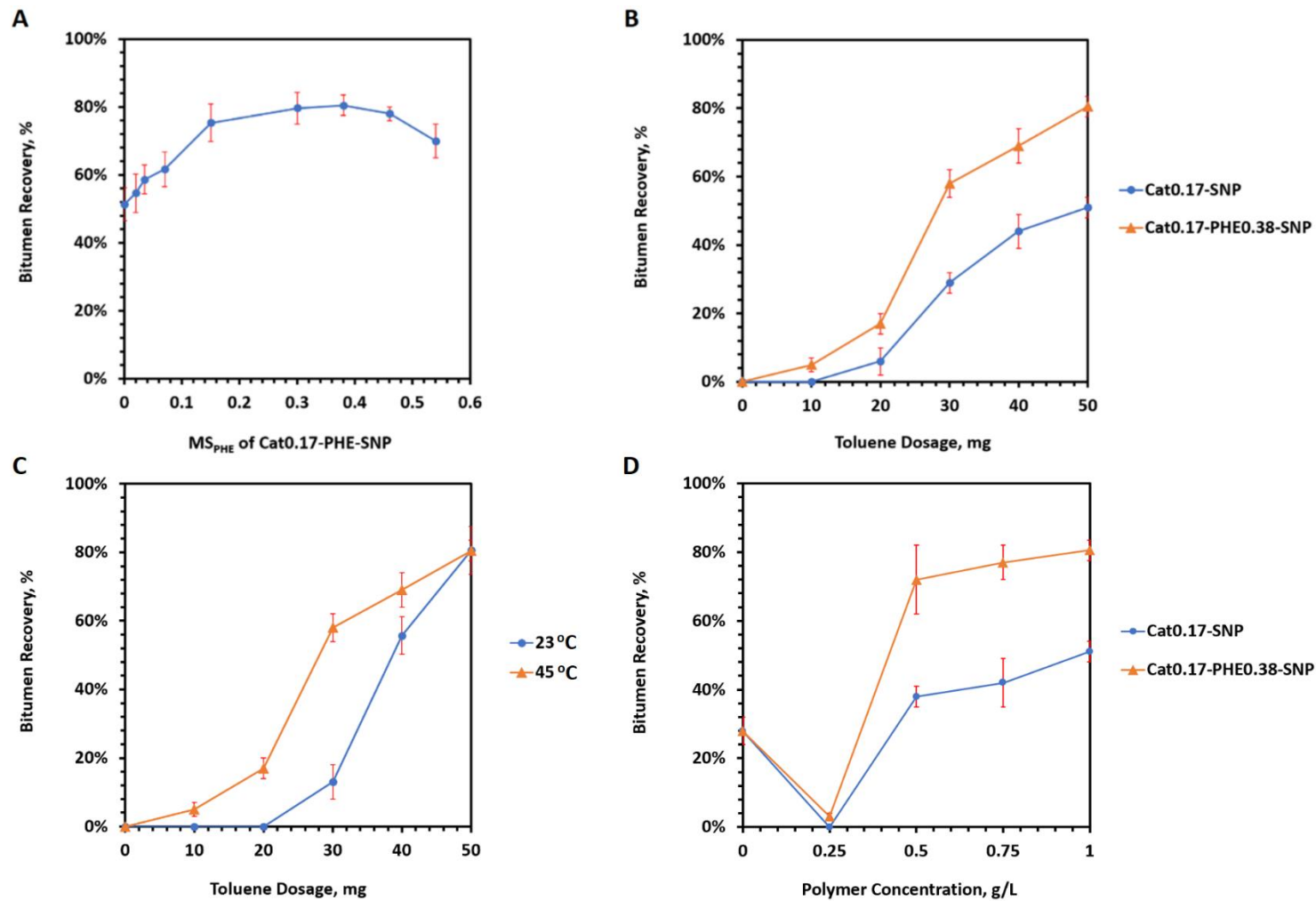


**Figure 7.11.** Optimization of the  $MS_{PHE}$  values of Cat0.17-PHE-SNP in the extractions of the aged oil sands ores were performed (A). The effect of toluene dose (B), extraction temperature (C) and polymer concentration (D) were shown for the extractions of the aged ores using Cat0.17-PHE0.38-SNP at 1 g/L and 50 mg of toluene.

Bitumen recovery for the extractions conducted at 45 °C was significantly better than that at 23 °C at 40 mg of toluene or below, and at a dose of 50 mg, the extraction temperatures had a negligible effect on the bitumen recovery (Fig.7.11C).

The effect of polymer concentration on bitumen recovery was examined by varying the concentrations from 0 to 1 g/L in the extraction mixture. At 0.25 g/L, both the Cat0.17-SNP and the Cat0.17-PHE0.38-SNP failed to recover any bitumen (Fig. 7.11D), and the extraction mixture contained very little suspended solids or emulsified bitumen (see Fig. E3 in Appendix E). These observations suggested that the cationic polymers could act as flocculants for the extraction mixture at this concentration in that the suspended solids could be flocculated together with the bitumen droplets due to charge neutralization by the cationic polymers. The bitumen-containing flocs would settle to the bottom of the vial and consequently, bitumen recovery was greatly hindered. When the polymer concentration was increased to 0.5 g/L or above, the cationic polymers could no longer flocculate the extraction mixture, but they could still strongly interact with clay and fine particles during the extraction and weaken the bitumen-clay interactions. Hence, an improvement in bitumen recovery was observed at a concentration of 0.5 g/L or above (Fig. 7.11D). Moreover, the Cat0.17-PHE0.38-SNP yielded a much higher bitumen recovery than the Cat017-SNP did, which again supported that the Cat0.17-PHE0.38-SNP could act as a better demulsifier.

The ability of recycling the polymer containing tailings for subsequent rounds of bitumen extraction from the aged oil sands ores were examined using the Cat0.17-PHE0.38-SNP starting with a concentration of 1 g/L. 15 mL of the tailings containing the polymers from the previous extraction mixture were used in the next round of bitumen extraction. A relatively

good bitumen recovery was obtained up to the third extraction cycle and the extraction efficiency decreased drastically starting from the 4<sup>th</sup> extraction cycle (Fig. 7.12). As the bitumen recovery decreased drastically when the polymer concentration was below 0.5 g/L (Fig. 7.11D), it suggested a slightly over 50 % loss of the polymers after three extraction cycles which represented an approximately 25 % loss of the polymers for each cycle, and in other words, about 75 % of the polymers can be recycled for the subsequent extractions.

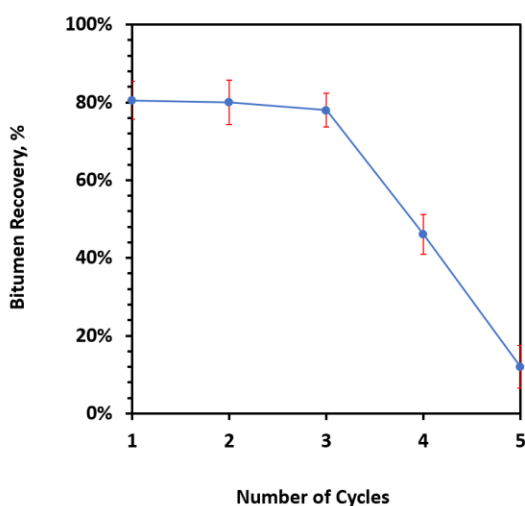


**Figure 7.12.** Bitumen recovery versus the number of extraction cycles. The extractions started with Cat0.17-PHE0.38-SNP at 1 g/L for the first extraction cycle and 50 mg of toluene for each cycle.

## 7.4 Conclusion

Thermoresponsive SNPs were successfully stabilized by the substitution of a small amount of cationic groups. These cationic thermoresponsive SNPs were shown to form relatively stable mesoglobules when the dispersion temperature was higher than their LCSTs. The Cat-HB1.9-SNPs were stable in deionized water above their LCSTs, but they formed insoluble aggregates above the LCSTs in the presence of salts. The Cat-HB1.9-SNPs failed to

improve bitumen recovery for the extractions with fresh oil sands ores. The Cat-PHE0.38-HB0.4-SNPs with low MS of cationic groups were thermoresponsive in the presence of salts and the Cat0.025-PHE0.38-HB0.4-SNP exhibited an LCST of 32 °C and mesoglobules with a  $D_h$  of 89 nm were formed in a 1 g/L dispersion with 60 mM of NaCl. Using the Cat0.025-PHE0.38-HB0.4-SNP at 1 g/L was able to recover about 86 % of the bitumen from the fresh oil sands ores when the extractions were conducted at 45 °C. Both the Cat-PHE0.38-HB0.4-SNPs and the Cat-PHE0.38-SNPs were shown to be a good demulsifier for the bitumen extractions when their MS of cationic groups were higher than 0.03 and the optimal MS was 0.17.

The use of the cationic thermoresponsive SNPs failed to recover any bitumen from the aged oil sands ores possibly due to the increase in the release of salts from the aged ores. The bitumen extraction of the aged ores was demonstrated to be more difficult than the fresh ones. The Cat0.17-PHE0.38-SNP produced good bitumen recovery (81 %) when used at a concentration of 1 g/L together with 50 mg of toluene to extract bitumen from the aged ores. The Cat0.17-PHE0.38-SNP showed good demulsification ability for the bitumen extractions from aged ores. Bitumen recovery was greatly reduced when the flocculation of the suspended solids occurred during the extraction. The polymer concentration for the bitumen extractions should be higher than that at which the cationic polymer could induce flocculation. The Cat0.17-PHE0.38-SNP resulted in a satisfactory bitumen recovery even for three consecutive extraction cycles starting with 1 g/L and approximately 25 % of polymers was lost after each extraction.

## Chapter 8

### Summary and Future Directions

#### 8.1 Summary

Hydroxybutyl corn starch (HB-CS) and hydroxybutyl potato starch (HB-PS) were shown to be capable of flocculating mature fine tailings (MFT) with solids content up to 10 wt %. The thermoresponsivity of these hydroxybutyl starches was absolutely required for their optimal flocculation performance in that they were considerably more effective in several respects when the settling tests were conducted at temperatures above their LCSTs than below. At least in terms of initial settling rates (ISRs), the HB-PS was considerably better than the HB-CS due to its higher molecular weight and the naturally occurring phosphates in potato starch.

Cationic corn starch (Cat-CS) and cationic potato starch (Cat-PS) flocculated 2 wt % MFT and showed very high ISRs and low supernatant turbidity (ST). The water recovery (WR) and sediment solids content (SSC) were unsatisfactory due to the high hydrophilicity of the cationic starches. Cat0.2-PS successfully flocculated 10 wt % MFT with an ISR slightly above 9 m/h but the WR and SSC were again unsatisfactory.

Cationic thermoresponsive corn starch and potato starch were prepared successfully and used in the flocculation of MFT. The cationic thermoresponsive starches performed better than the cationic starches in regard to ST and they performed better than the thermoresponsive

starches in terms of ISR and ST. However, WR and SSC resulted from the use of the cationic thermoresponsive starches as flocculants were still not satisfactory.

A dual polymer flocculation system consisting of hydroxybutyl starch and cationic starch was shown to be very capable of flocculating MFT. The dual polymer flocculants were in all aspects superior to the individual flocculants when used separately. The use of thermoresponsive starch in a dual polymer flocculation system definitely improved its flocculation performance. An ISR as high as 52 m/h and a ST as low as 16 NTU was achieved with the use of a dual polymer flocculant consisting of HB-PS and Cat-PS to flocculate 10 wt % MFT.

Hydrophobically modified thermoresponsive starch nanoparticles (SNPs) were successfully synthesized by modifying the SNPs with both styrene oxide and butene oxide under basic conditions. The modification resulted in the incorporation of phenylhydroxyethyl (PHE) and hydroxybutyl (HB) substituents on the SNPs and yielded PHE-HB-SNPs with the LCSTs in a range of 16 to 78 °C depending on the composition of the substituents. The reaction efficiency of the hydroxybutylation reaction on hydrophobically modified SNPs greatly improved over that of the reaction on the unmodified SNPs. A small increase in the molar substitution (MS) of the PHE groups ( $MS_{\text{PHE}}$ ) had a drastic effect on the LCST of PHE-HB-SNP. Though the increase in the MS of the HB groups ( $MS_{\text{HB}}$ ) had a lesser effect of the LCST of PHE-HB-SNP compared to  $MS_{\text{PHE}}$ , the HB groups were absolutely required for the PHE-HB-SNP to exhibit an LCST. The lowest LCST could be achieved when the PHE-HB-SNP was highly hydrophobic due to a high  $MS_{\text{PHE}}$  but still had a good water dispersibility below its LCST due to a sufficient amount of HB groups.



Thermoresponsive SNPs and hydrophobically modified thermoresponsive SNPs would form insoluble aggregates above their LCSTs but they could be stabilized after the incorporation of a small amount of cationic groups which provided electrostatic stabilization. The presence of salts destabilized the thermoresponsive polymer dispersions, but the stabilization provided by the cationic groups of cationic PHE-HB-SNPs (Cat-PHE-HB-SNPs) was able to overcome the destabilizing effect due to salts. Cat0.025-PHE0.38-HB0.4-SNP exhibited an LCST of 32 °C in a 1 g/L dispersion with 60 mM of NaCl. The use of the Cat0.025-PHE0.38-HB0.4-SNP at 1 g/L was able to recover about 86 % of bitumen from fresh oil sands ores when the extractions were conducted at 45 °C with 50 mg of toluene. At an MS of cationic groups higher than 0.03, the Cat-PHE0.38-HB0.4-SNPs were no longer thermoresponsive in the extraction mixture, but they were shown to have a good demulsifying ability which could facilitate the formation of bitumen-rich froth. The bitumen extraction of the aged ores was more difficult compared the fresh ones. The Cat0.025-PHE0.38-HB0.4-SNP, which gave a high bitumen recovery for the fresh ores, failed to recover any bitumen from the aged ores. On the other hand, Cat0.17-PHE0.38-SNP, an interfacially active polymer with hydrophobic PHE groups and hydrophilic cationic and hydroxyl groups, had a good bitumen recovery (81 %) for the extraction of bitumen from the aged ores due to its good demulsification ability. Starting with a 1 g/L dispersion, the Cat0.17-PHE0.38-SNP showed a satisfactory bitumen recovery even after three consecutive extraction cycles.

## 8.2 Future Directions

### 8.2.1 Flocculation of Oil Sands MFT

Optimization of the flocculation process could be done to further improve the flocculation performance. A study on the effect of different types of water, such as deionized water, tap water and oil sands process water, to be used to make the dilutions of the original MFT could be conducted. Mechanical mixing speed and duration during the flocculation process could be optimized for a better performance. Settling vessels with different diameter and column length could also be tested to investigate their effects on the flocculation performance.

Carboxymethyl starch (CMS), an anionic starch-based polymer, has been shown to be capable of flocculating a 5 wt % kaolin suspension and 5.5 wt % oil sands tailings from flotation overflow,<sup>153</sup> however, there has not been any reports on the use of CMS in the flocculation of MFT. Anionic CMS could be used in a dual polymer flocculation system along with the cationic starches presented in this thesis and it would be interesting to compare the performance of this dual polymer flocculant to those consisting of a thermoresponsive starch and a cationic starch reported in Chapter 5.

Floc size could be an important parameter to be studied to provide insights to a flocculation process. Senaputra et al. described a method to use focused beam reflectance measurement (FBRM) for monitoring flocculation processes,<sup>188</sup> and this method has been used by others who studied the flocculation of MFT by polymeric flocculants.<sup>127,152,174,189,190</sup> FBRM can give real-time evolution of floc size in MFT and reveal the change in floc size before and

after the addition of a flocculant which could be useful for the analysis of the performance of such flocculant. It would be useful to obtain floc sizes for the settling tests using the starch-based flocculants reported in this thesis.

Flocculation of MFT often serves as the first step towards the consolidation and dewatering of MFT. Secondary consolidation and dewatering technologies, such as centrifugation,<sup>136</sup> filtration,<sup>122</sup> thin lift deposition,<sup>191</sup> and freeze-thaw drying,<sup>192</sup> are required to achieve higher solids content and water recovery. It would be interesting to investigate the improvement on the consolidation and dewatering of MFT when a secondary technology is applied to the flocculant-treated MFT in this thesis. A proposed method for MFT treatment is shown in Figure 8.1. Diluted MFT (~10 wt % solids) can be flocculated by a dual polymer flocculant consisting of 600 ppm of HB1.9-PS and 100 ppm of Cat0.2-PS to yield sediments (~34 wt % solids) that could be centrifuged or filtered to produce sediments with a much higher solids content. Water recovered from the flocculation process and from centrifugation or filtration can be recycled and used to make the MFT dilution for the subsequent flocculation process.

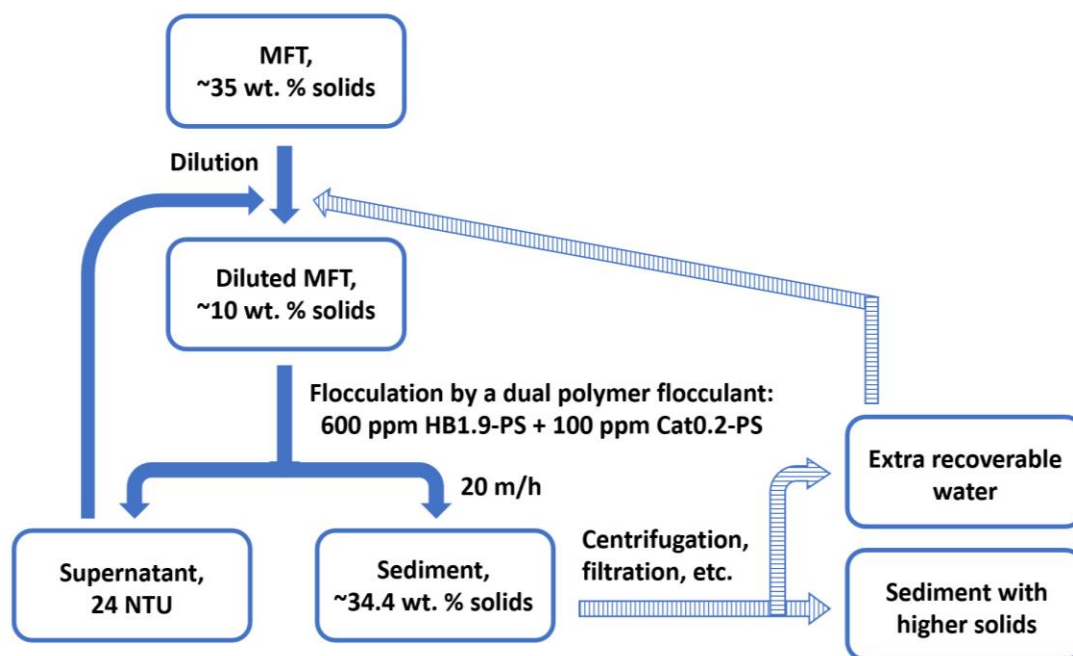


**Figure 8.1.** Schematic flow diagram of a proposed method for improving the consolidation and dewatering of MFT. A dual polymer flocculant consisting of 600 ppm of HB1.9-PS and 100 ppm of Cat0.2-PS is used as an example.

### 8.2.2 Extraction of Bitumen from Oil Sands

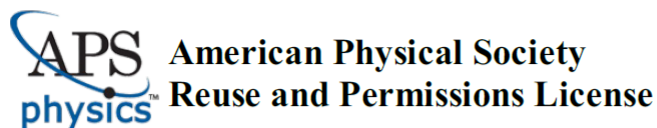
To elucidate the effect of the addition of a polymer in a water/oil sands slurry during a bitumen extraction, atomic force microscopy (AFM) could be used to study the change in colloidal interactions between bitumen and clays in the slurry due to the presence of the polymer. As it has been well documented in the literature that bitumen recovery is negatively influenced by strong bitumen-clay interactions in the extraction slurry,<sup>76,92,109</sup> studying the effect of the starch-based polymers presented in this thesis on bitumen-clay interactions during the extractions would be of interest.

We have established in Chapter 7 that both the cationic thermoresponsive SNPs and the cationic hydrophobically modified SNPs are potentially good polymeric aids for the

extraction of bitumen from oil sands. The starch-based polymers which exhibited a good bitumen recovery in our extraction experiments could be tested in a laboratory hydrotransport extraction system (LHES) as described by Long and coworkers to better mimic the conditions of full scale bitumen extraction operations in the oil sands industry.<sup>109</sup>

# Copyright Permissions

Permission for Figure 1.2:



15-Jul-2020

This license agreement between the American Physical Society ("APS") and bo zheng ("You") consists of your license details and the terms and conditions provided by the American Physical Society and SciPris.

## Licensed Content Information

**License Number:** RNP/20/JUL/028377  
**License date:** 15-Jul-2020  
**DOI:** 10.1103/PhysRevLett.80.4092  
**Title:** Globule-to-Coil Transition of a Single Homopolymer Chain in Solution  
**Author:** Chi Wu and Xiaohui Wang  
**Publication:** Physical Review Letters  
**Publisher:** American Physical Society  
**Cost:** USD \$ 0.00

## Request Details

**Does your reuse require significant modifications:** No  
**Specify intended distribution locations:** Canada  
**Reuse Category:** Reuse in a thesis/dissertation  
**Requestor Type:** Student  
**Items for Reuse:** Figures/Tables  
**Number of Figure/Tables:** 2  
**Figure/Tables Details:** Figure 1 and Figure 3  
**Format for Reuse:** Electronic

## Information about New Publication:

**University/Publisher:** University of Waterloo  
**Title of dissertation/thesis:** Starch-based Polymers as Flocculants of Oil Sands Mature Fine Tailings and for Extraction of Bitumen from Oil Sands  
**Author(s):** bowei zheng  
**Expected completion date:** Sep. 2020

## License Requestor Information

**Name:** bo zheng  
**Affiliation:** Individual  
**Email Id:** hahbowen@gmail.com  
**Country:** Canada

Permission for Figure 1.3 and Figure 1.4:

ELSEVIER LICENSE  
TERMS AND CONDITIONS

Jul 15, 2020

This Agreement between university of waterloo -- bo zheng ("You") and Elsevier ("Elsevier") consists of your license details and the terms and conditions provided by Elsevier and Copyright Clearance Center.

License Number: 4870520821088

License date: Jul 15, 2020

Licensed Content Publisher: Elsevier

Licensed Content Publication: Progress in Polymer Science

Licensed Content Title: Stimuli-responsive polymers and their bioconjugates

Licensed Content Author: Eun Seok Gil, Samuel M. Hudson

Licensed Content Date: Dec 1, 2004

Licensed Content Volume: 29

Licensed Content Issue: 12

Licensed Content Pages: 50

Start Page: 1173

End Page: 1222

Type of Use: reuse in a thesis/dissertation: Portion figures/tables/illustrations

Number of figures/tables/illustrations: 2

Format: electronic

Are you the author of this Elsevier article? No

Will you be translating? No

Title: Starch-based Polymers as Flocculants of Oil Sands Mature Fine Tailings and for Extraction of Bitumen from Oil Sands

Institution name: university of waterloo

Expected presentation date: Sep 2020

Portions: Figure 7, Figure 9

Requestor Location: university of waterloo

200 University Ave. West, Waterloo

waterloo, ON N2L 3G1

Canada

Attn: university of waterloo

Publisher Tax ID GB 494 6272 12

Total 0.00 USD

Permission for Figure 1.6A:

**SPRINGER NATURE LICENSE**

**TERMS AND CONDITIONS**

Jul 15, 2020

This Agreement between univeristy of waterloo -- bo zheng ("You") and Springer Nature ("Springer Nature") consists of your license details and the terms and conditions provided by Springer Nature and Copyright Clearance Center.

License Number: 4870521150701

License date: Jul 15, 2020

Licensed Content Publisher: Springer Nature

Licensed Content Publication: Colloid and Polymer Science

Licensed Content Title: The collapse transition of poly(styrene-b-(N-isopropylacrylamide)) diblock copolymers in aqueous solution and in thin films

Licensed Content Author: K. Troll et al

Licensed Content Date: May 30, 2008

Type of Use: Thesis/Dissertation

Requestor type: academic/university or research institute

Format: electronic

Portion: figures/tables/illustrations

Number of figures/tables/illustrations: 1

Will you be translating? no

Circulation/distribution: 1 - 29

Author of this Springer Nature content: no

Title: Starch-based Polymers as Flocculants of Oil Sands Mature Fine Tailings and for Extraction of Bitumen from Oil Sands

Institution name: university of waterloo

Expected presentation date: Sep 2020

Portions: figure 6

Requestor Location: university of waterloo

200 University Ave. West, Waterloo

waterloo, ON N2L 3G1

Canada

Attn: university of waterloo

Total 0.00 USD



## Permission for Figure 1.6B and Figure 7.1:



RightsLink®



Home



Help



Email Support



bo zheng ▾

### Extraction of Oil from Oil Sands Using Thermoresponsive Polymeric Surfactants



Author: Bingqing Yang, Jean Duhamel

Publication: Applied Materials

Publisher: American Chemical Society

Date: Mar 1, 2015

Copyright © 2015, American Chemical Society

#### PERMISSION/LICENSE IS GRANTED FOR YOUR ORDER AT NO CHARGE

This type of permission/license, instead of the standard Terms & Conditions, is sent to you because no fee is being charged for your order. Please note the following:

- Permission is granted for your request in both print and electronic formats, and translations.
  - If figures and/or tables were requested, they may be adapted or used in part.
  - Please print this page for your records and send a copy of it to your publisher/graduate school.
  - Appropriate credit for the requested material should be given as follows: "Reprinted (adapted) with permission from (COMPLETE REFERENCE CITATION). Copyright (YEAR) American Chemical Society." Insert appropriate information in place of the capitalized words.
  - One-time permission is granted only for the use specified in your request. No additional uses are granted (such as derivative works or other editions). For any other uses, please submit a new request.
- If credit is given to another source for the material you requested, permission must be obtained from that source.

[BACK](#)

[CLOSE WINDOW](#)

## Permission for Figure 1.7:



RightsLink®



Home



Help



Email Support



bo zheng ▾



### End Group Effect on the Thermal Response of Narrow-Disperse Poly(N-isopropylacrylamide) Prepared by Atom Transfer Radical Polymerization

**Author:** Yan Xia, Nicholas A. D. Burke, Harald D. H. Stöver

**Publication:** Macromolecules

**Publisher:** American Chemical Society

**Date:** Mar 1, 2006

*Copyright © 2006, American Chemical Society*

#### PERMISSION/LICENSE IS GRANTED FOR YOUR ORDER AT NO CHARGE

This type of permission/license, instead of the standard Terms & Conditions, is sent to you because no fee is being charged for your order. Please note the following:

- Permission is granted for your request in both print and electronic formats, and translations.
  - If figures and/or tables were requested, they may be adapted or used in part.
  - Please print this page for your records and send a copy of it to your publisher/graduate school.
  - Appropriate credit for the requested material should be given as follows: "Reprinted (adapted) with permission from (COMPLETE REFERENCE CITATION). Copyright (YEAR) American Chemical Society." Insert appropriate information in place of the capitalized words.
  - One-time permission is granted only for the use specified in your request. No additional uses are granted (such as derivative works or other editions). For any other uses, please submit a new request.
- If credit is given to another source for the material you requested, permission must be obtained from that source.

[BACK](#)

[CLOSE WINDOW](#)

Permission for Figure 1.8:

ELSEVIER LICENSE  
TERMS AND CONDITIONS

Jul 15, 2020

This Agreement between univeristy of waterloo -- bo zheng ("You") and Elsevier ("Elsevier") consists of your license details and the terms and conditions provided by Elsevier and Copyright Clearance Center.

License Number: 4870530198820

License date: Jul 15, 2020

Licensed Content Publisher: Elsevier

Licensed Content Publication: International Journal of Pharmaceutics

Licensed Content Title: Effect of some physiological and non-physiological compounds on the phase transition temperature of thermoresponsive polymers intended for oral controlled drug delivery

Licensed Content Author: Frederic Eeckman, Karim Amighi, André J. Moës

Licensed Content Date: Jul 17, 2001

Licensed Content Volume: 222

Licensed Content Issue: 2

Licensed Content Pages: 12

Start Page: 259

End Page: 270

Type of Use: reuse in a thesis/dissertation

Portion: figures/tables/illustrations

Number of figures/tables/illustrations: 1

Format: electronic

Are you the author of this Elsevier article? No

Will you be translating? No

Title: Starch-based Polymers as Flocculants of Oil Sands Mature Fine Tailings and for Extraction of Bitumen from Oil Sands

Institution name: university of waterloo

Expected presentation date: Sep 2020

Portions: Figure 3

Requestor Location: university of waterloo

200 University Ave. West, Waterloo

waterloo, ON N2L 3G1

Canada

Attn: university of waterloo

Publisher Tax ID GB 494 6272 12

Total 0.00 USD

## Permission for Figure 1.12:



**Anna Giove** <anna.giove@oilsandsmagazine.com>

2020/7/16 上午 11:00

Hi Bo,

Yes, you may use the figures as required for your thesis.

Thanks for your email. Hope you have a great day.

Anna

Anna M. Giove, P.Eng.

EDITOR | OIL SANDS MAGAZINE

SOCIAL [linkedin.com/in/annagiove](https://www.linkedin.com/in/annagiove)

WEBSITE [www.oilsandsmagazine.com](http://www.oilsandsmagazine.com)

**Name:** bo zheng

**Position Held:**

**Company:** university of waterloo

**Link:**

**Message:** To whom it may concern,

I am writing to ask for a permission to use one of your figures on the website below in my PhD thesis if possible. Please let me know. Thank you in advance.

<https://www.oilsandsmagazine.com/technical/mining>

Best regards,

Bo

Permission for Figure 1.13:

JOHN WILEY AND SONS LICENSE  
TERMS AND CONDITIONS

Jul 15, 2020

This Agreement between university of waterloo -- bo zheng ("You") and John Wiley and Sons ("John Wiley and Sons") consists of your license details and the terms and conditions provided by John Wiley and Sons and Copyright Clearance Center.

License Number: 4870530860915

License date: Jul 15, 2020

Licensed Content Publisher: John Wiley and Sons

Licensed Content Publication: Canadian Journal of Chemical Engineering

Licensed Content Title: Microscopic structure of athabasca oil sand

Licensed Content Author: Koichi Takamura

Licensed Content Date: Mar 26, 2009

Licensed Content Volume: 60

Licensed Content Issue: 4

Licensed Content Pages: 8

Type of use: Dissertation/Thesis

Requestor type: University/Academic

Format: Electronic

Portion: Figure/table

Number of figures/tables: 1

Will you be translating? No

Title: Starch-based Polymers as Flocculants of Oil Sands Mature Fine Tailings and for Extraction of Bitumen from Oil Sands

Institution name: university of waterloo

Expected presentation date: Sep 2020

Portions: figure 10

Requestor Location: university of waterloo

200 University Ave. West, Waterloo

waterloo, ON N2L 3G1

Canada

Attn: university of waterloo

Publisher Tax ID EU826007151

Total 0.00 USD

Permission for Figure 1.14:

JOHN WILEY AND SONS LICENSE  
TERMS AND CONDITIONS

Jul 15, 2020

This Agreement between univeristy of waterloo -- bo zheng ("You") and John Wiley and Sons ("John Wiley and Sons") consists of your license details and the terms and conditions provided by John Wiley and Sons and Copyright Clearance Center.

License Number: 4870530976391

License date: Jul 15, 2020

Licensed Content Publisher: John Wiley and Sons

Licensed Content Publication: Canadian Journal of Chemical Engineering

Licensed Content Title: Understanding Water-Based Bitumen Extraction from Athabasca Oil Sands

Licensed Content Author: Hassan Hamza, Jan Czarnecki, Zhenghe Xu, et al

Licensed Content Date: May 19, 2008

Licensed Content Volume: 82

Licensed Content Issue: 4

Licensed Content Pages: 27

Type of use: Dissertation/Thesis

Requestor type: University/Academic

Format: Electronic

Portion: Figure/table

Number of figures/tables: 1

Will you be translating? No

Title: Starch-based Polymers as Flocculants of Oil Sands Mature Fine Tailings and for Extraction of Bitumen from Oil Sands

Institution name: university of waterloo

Expected presentation date: Sep 2020

Portions: figure 5

Requestor Location: university of waterloo

200 University Ave. West, Waterloo

waterloo, ON N2L 3G1

Canada

Attn: university of waterloo

Publisher Tax ID EU826007151

Total 0.00 USD

Permission for Figure 1.15:

JOHN WILEY AND SONS LICENSE  
TERMS AND CONDITIONS

Jul 15, 2020

This Agreement between univeristy of waterloo -- bo zheng ("You") and John Wiley and Sons ("John Wiley and Sons") consists of your license details and the terms and conditions provided by John Wiley and Sons and Copyright Clearance Center.

License Number: 4870531088812

License date: Jul 15, 2020

Licensed Content Publisher: John Wiley and Sons

Licensed Content Publication: Canadian Journal of Chemical Engineering

Licensed Content Title: Effect of Operating Temperature on Water-Based Oil Sands Processing

Licensed Content Author: Jacob H. Masliyah, Zhenghe Xu, Jaroslaw Drelich, et al

Licensed Content Date: May 19, 2008

Licensed Content Volume: 85

Licensed Content Issue: 5

Licensed Content Pages: 13

Type of use: Dissertation/Thesis

Requestor type: University/Academic

Format: Electronic

Portion: Figure/table

Number of figures/tables: 1

Will you be translating? No

Title: Starch-based Polymers as Flocculants of Oil Sands Mature Fine Tailings and for Extraction of Bitumen from Oil Sands

Institution name: university of waterloo

Expected presentation date: Sep 2020

Portions: figure 3

Requestor Location: university of waterloo

200 University Ave. West, Waterloo

waterloo, ON N2L 3G1

Canada

Attn: university of waterloo

Publisher Tax ID EU826007151

Total 0.00 USD

Permission for Figure 1.16:

JOHN WILEY AND SONS LICENSE  
TERMS AND CONDITIONS

Jul 15, 2020

This Agreement between univeristy of waterloo -- bo zheng ("You") and John Wiley and Sons ("John Wiley and Sons") consists of your license details and the terms and conditions provided by John Wiley and Sons and Copyright Clearance Center.

License Number: 4870531194061

License date: Jul 15, 2020

Licensed Content Publisher: John Wiley and Sons

Licensed Content Publication: Canadian Journal of Chemical Engineering

Licensed Content Title: Processibility of Athabasca Oil Sand Using a Laboratory Hydro transport Extraction System (LHES)

Licensed Content Author: Jacob Masliyah, Zhenghe Xu, Vince Wallwork

Licensed Content Date: May 19, 2008

Licensed Content Volume: 82

Licensed Content Issue: 4

Licensed Content Pages: 9

Type of use: Dissertation/Thesis

Requestor type: University/Academic

Format: Electronic

Portion: Figure/table

Number of figures/tables: 1

Will you be translating? No

Title: Starch-based Polymers as Flocculants of Oil Sands Mature Fine Tailings and for Extraction of Bitumen from Oil Sands

Institution name: university of waterloo

Expected presentation date: Sep 2020

Portions: figure 9

Requestor Location: university of waterloo

200 University Ave. West, Waterloo

waterloo, ON N2L 3G1

Canada

Attn: university of waterloo

Publisher Tax ID EU826007151

Total 0.00 USD




Permission for Figure 1.17:




RightsLink®

 Home


 Help

 Email Support

 bo zheng ▾

**A PHYSICAL CHEMICAL EXPLANATION FOR DETERIORATION IN THE HOT WATER PROCESSABILITY OF ATHABASCA OIL SAND DUE TO AGING**

Author: Dean Wallace, , Deborah Henry, et al

 Publication: Petroleum Science and Technology

Publisher: Taylor & Francis

Date: Jan 1, 1989

*Rights managed by Taylor & Francis*



**Thesis/Dissertation Reuse Request**

Taylor & Francis is pleased to offer reuses of its content for a thesis or dissertation free of charge contingent on resubmission of permission request if work is published.

BACK

CLOSE

## Permission for Figure 1.18:

HomeHelpEmail Supportbo zheng ▾

---

**Solvent Extraction of Bitumen from Oil Sands**

**Author:** Tong Wang, Chao Zhang, Ruiyu Zhao, et al  
**Publication:** Energy & Fuels  
**Publisher:** American Chemical Society  
**Date:** Apr 1, 2014

*Copyright © 2014, American Chemical Society*

**PERMISSION/LICENSE IS GRANTED FOR YOUR ORDER AT NO CHARGE**

This type of permission/license, instead of the standard Terms & Conditions, is sent to you because no fee is being charged for your order. Please note the following:

- Permission is granted for your request in both print and electronic formats, and translations.
- If figures and/or tables were requested, they may be adapted or used in part.
- Please print this page for your records and send a copy of it to your publisher/graduate school.
- Appropriate credit for the requested material should be given as follows: "Reprinted (adapted) with permission from (COMPLETE REFERENCE CITATION). Copyright (YEAR) American Chemical Society." Insert appropriate information in place of the capitalized words.
- One-time permission is granted only for the use specified in your request. No additional uses are granted (such as derivative works or other editions). For any other uses, please submit a new request.

If credit is given to another source for the material you requested, permission must be obtained from that source.

[BACK](#) [CLOSE WINDOW](#)

Permission for Figure 1.19:

JOHN WILEY AND SONS LICENSE  
TERMS AND CONDITIONS

Jul 15, 2020

This Agreement between university of waterloo -- bo zheng ("You") and John Wiley and Sons ("John Wiley and Sons") consists of your license details and the terms and conditions provided by John Wiley and Sons and Copyright Clearance Center.

License Number: 4870531476767

License date: Jul 15, 2020

Licensed Content Publisher: John Wiley and Sons

Licensed Content Publication: Canadian Journal of Chemical Engineering

Licensed Content Title: Water-soluble polymers for oil sands tailing treatment: A Review

Licensed Content Author: João B. P. Soares, Diógenes R. L. Vedoy

Licensed Content Date: Mar 19, 2015

Licensed Content Volume: 93

Licensed Content Issue: 5

Licensed Content Pages: 17

Type of use: Dissertation/Thesis

Requestor type: University/Academic

Format: Electronic

Portion: Figure/table

Number of figures/tables: 1

Will you be translating? No

Title: Starch-based Polymers as Flocculants of Oil Sands Mature Fine Tailings and for Extraction of Bitumen from Oil Sands

Institution name: university of waterloo

Expected presentation date: Sep 2020

Portions: figure 1

Requestor Location: university of waterloo

200 University Ave. West, Waterloo

waterloo, ON N2L 3G1

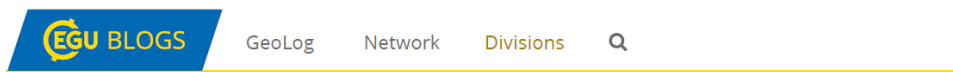
Canada

Attn: university of waterloo

Publisher Tax ID EU826007151

Total 0.00 USD

## Permission for Figure 1.20:



[EGU Blogs](#) » [Divisions](#) » [Soil System Sciences](#) » [Copyright](#)

# Copyright

## Licensing and Attribution

Unless otherwise indicated, the content on this blog is licensed under the [Creative Commons Attribution 4.0 international licence \(CC BY 4.0\)](#). This means that:

- Copyright on any article is retained by the author(s) for the post. The name of a post author is specified in the by-line or, if no by-line exists, at the end of the post under "author".
- Any third party can use the article freely as long as its original authors and citation details are identified. This includes a link to the post if used in an online publication, or citing [blogs.egu.eu](#) for print materials, together with the author's name.

Note that this licence applies to the text on the blog. While some images are licensed under Creative Commons, others have been reproduced with permission from the author. Please check the original source for information on how they are licensed before using them.

To summarise, this licence means anyone is free

- **to Share** — to copy, distribute and transmit the work
- **to Remix** — to adapt the work

Under the following conditions:

Permission for Figure 1.22:



*Council*

**Charles P. France**  
*President*  
University of Texas Health Science  
Center

**Margaret E. Gnegy**  
*President-Elect*  
University of Michigan Medical  
School

**Wayne L. Backes**  
*Past President*  
Louisiana State University Health  
Sciences Center

**Mary-Ann Bjornsti**  
*Secretary/Treasurer*  
University of Alabama, Birmingham

**Carol L. Beck**  
*Secretary/Treasurer-Elect*  
Thomas Jefferson University

**Jin Zhang**  
*Past Secretary/Treasurer*  
University of California, San Diego

**Kathryn A. Cunningham**  
*Councilor*  
University of Texas Medical  
Branch

**Namandjé N. Bumpus**  
*Councilor*  
Johns Hopkins University School  
of Medicine

**Randy A. Hall**  
*Councilor*  
Emory University School of  
Medicine

**Emily E. Scott**  
*Chair, Board of Publications  
Trustees*  
University of Michigan

**Catherine M. Davis**  
*FASEB Board Representative*  
Johns Hopkins University School  
of Medicine

**Michael W. Wood**  
*Chair, Program Committee*  
Neupham LLC

**Judith A. Siuciak**  
*Executive Officer*

July 16, 2020

Bo Zheng  
Chemistry  
University of Waterloo  
200 University Ave, West  
Waterloo, ON  
Canada

Email: bowen.zheng1990@hotmail.com

Dear Bo Zheng:

This is to grant you permission to include the following figure in your thesis titled "Starch-based Polymers as Flocculants of Oil Sands Mature Fine Tailings and for Extraction of Bitumen from Oil Seeds" for the University of Waterloo:

Figure 3 from P Yingchoncharoen, DS Kalinowski, and DR Richardson (2016) Lipid-Based Drug Delivery Systems in Cancer Therapy: What Is Available and What Is Yet to Come, *Pharmacol Rev*, 68(3): 701-787; DOI: <https://doi.org/10.1124/pr.115.012070>

Permission to reproduce the figure is granted for one-time use in any format or medium including print and electronic. The authors and the source of the materials must be cited in full, including the article title, journal title, volume, year, and page numbers.

Sincerely yours,

Richard Dodenhoff  
Journals Director

Transforming Discoveries into Therapies  
ASPET · 1801 Rockville Pike, Suite 210 · Rockville, MD 20852 · Office: 301-634-7060 · [aspet.org](http://aspet.org)



Permission for Figure 1.23:

ELSEVIER LICENSE  
TERMS AND CONDITIONS

Jul 15, 2020

This Agreement between university of waterloo -- bo zheng ("You") and Elsevier ("Elsevier") consists of your license details and the terms and conditions provided by Elsevier and Copyright Clearance Center.

License Number: 4870540938597

License date: Jul 15, 2020

Licensed Content Publisher: Elsevier

Licensed Content Publication: Elsevier Books

Licensed Content Title: Science and Technology of Concrete Admixtures

Licensed Content Author: G. Gelardi, R.J. Flatt

Licensed Content Date: Jan 1, 2016

Licensed Content Pages: 22

Start Page: 257

End Page: 278

Type of Use: reuse in a thesis/dissertation

Portion: figures/tables/illustrations

Number of figures/tables/illustrations: 1

Format: electronic

Are you the author of this Elsevier chapter? No

Will you be translating? No

Title: Starch-based Polymers as Flocculants of Oil Sands Mature Fine Tailings and for Extraction of Bitumen from Oil Sands

Institution name: university of waterloo

Expected presentation date: Sep 2020

Portions: figure 4

Requestor Location: university of waterloo

200 University Ave. West, Waterloo

waterloo, ON N2L 3G1

Canada

Attn: university of waterloo

Publisher Tax ID GB 494 6272 12

Total 0.00 USD

## Bibliography

- (1) Srinivasa, S.; Flury, C.; Afacan, A.; Masliyah, J.; Xu, Z. Study of Bitumen Liberation from Oil Sands Ores by Online Visualization. *Energy and Fuels* **2012**, *26*, 2883–2890.
- (2) Vedoy, D. R. L.; Soares, J. B. P. Water-Soluble Polymers for Oil Sands Tailing Treatment: A Review. *Can. J. Chem. Eng.* **2015**, *93*, 888–904.
- (3) Lavigne, M. D.; Pennadam, S. S.; Ellis, J.; Yates, L. L.; Alexander, C.; Górecki, D. C. Enhanced Gene Expression through Temperature Profile-Induced Variations in Molecular Architecture of Thermoresponsive Polymer Vectors. *J. Gene Med.* **2007**, *9*, 44–54.
- (4) Chung, J. E.; Yokoyama, M.; Yamato, M.; Aoyagi, T.; Sakurai, Y.; Okano, T. Thermo-Responsive Drug Delivery from Polymeric Micelles Constructed Using Block Copolymers of Poly(N-Isopropylacrylamide) and Poly(Butylmethacrylate). *J. Control. Release* **1999**, *62*, 115–127.
- (5) De Las Heras Alarcón, C.; Pennadam, S.; Alexander, C. Stimuli Responsive Polymers for Biomedical Applications. *Chem. Soc. Rev.* **2005**, *34*, 276–285.
- (6) Nitschke, M.; Gramm, S.; Götze, T.; Valtink, M.; Drichel, J.; Voit, B.; Engelmann, K.; Werner, C. Thermo-Responsive Poly(NiPAAm-Co-DEGMA) Substrates for Gentle Harvest of Human Corneal Endothelial Cell Sheets. *J. Biomed. Mater. Res. - Part A* **2007**, *80*, 1003–1010.
- (7) Hatakeyama, H.; Kikuchi, A.; Yamato, M.; Okano, T. Patterned Biofunctional Designs of Thermoresponsive Surfaces for Spatiotemporally Controlled Cell Adhesion, Growth, and Thermally Induced Detachment. *Biomaterials* **2007**, *28*, 3632–3643.
- (8) Lokuge, I.; Wang, X.; Bohn, P. W. Temperature-Controlled Flow Switching in Nanocapillary Array Membranes Mediated by Poly(N-Isopropylacrylamide) Polymer Brushes Grafted by Atom Transfer Radical Polymerization. *Langmuir* **2007**, *23*, 305–311.
- (9) Rotzetter, A. C. C.; Schumacher, C. M.; Bubenhofer, S. B.; Grass, R. N.; Gerber, L. C.; Zeltner, M.; Stark, W. J. Thermoresponsive Polymer Induced Sweating Surfaces as an Efficient Way to Passively Cool Buildings. *Adv. Mater.* **2012**, *24*, 5352–5356.
- (10) Yang, B.; Duhamel, J. Extraction of Oil from Oil Sands Using Thermoresponsive Polymeric Surfactants. *ACS Appl. Mater. Interfaces* **2015**, *7*, 5879–5889.
- (11) Zhang, D.; Thundat, T.; Narain, R. Flocculation and Dewatering of Mature Fine Tailings Using Temperature-Responsive Cationic Polymers. *Langmuir* **2017**, *33*, 5900–5909.

- (12) Li, H.; Long, J.; Xu, Z.; Masliyah, J. H. Flocculation of Kaolinite Clay Suspensions Using a Temperature-Sensitive Polymer. *AIChE J.* **2007**, *53*, 479–488.
- (13) Wang, Y.; Kotsuchibashi, Y.; Liu, Y.; Narain, R. Temperature-Responsive Hyperbranched Amine-Based Polymers for Solid-Liquid Separation. *Langmuir* **2014**, *30*, 2360–2368.
- (14) O’Shea, J. P.; Qiao, G. G.; Franks, G. V. Solid-Liquid Separations with a Temperature-Responsive Polymeric Flocculant: Effect of Temperature and Molecular Weight on Polymer Adsorption and Deposition. *J. Colloid Interface Sci.* **2010**, *348*, 9–23.
- (15) O’Shea, J. P.; Qiao, G. G.; Franks, G. V. Temperature-Responsive Solid-Liquid Separations with Charged Block-Copolymers of Poly(N-Isopropyl Acryamide). *Langmuir* **2012**, *28*, 905–913.
- (16) Gumfekar, S. P.; Soares, J. B. P. A Novel Hydrophobically-Modified Polyelectrolyte for Enhanced Dewatering of Clay Suspension. *Chemosphere* **2018**, *194*, 422–431.
- (17) Wu, C.; Wang, X. Globule-to-Coil Transition of a Single Homopolymer Chain in Solution. *Phys. Rev. Lett.* **1998**, *80*, 4092.
- (18) Idziak, I.; Avoce, D.; Lessard, D.; Gravel, D.; Zhu, X. X. Thermosensitivity of Aqueous Solutions of Poly(N,N-Diethylacrylamide). *Macromolecules* **1999**, *32*, 1260–1263.
- (19) Meeussen, F.; Nies, E.; Berghmans, H.; Verbrugghe, S.; Goethals, E.; Du Prez, F. Phase Behaviour of Poly(N-Vinyl Caprolactam) in Water. *Polymer (Guildf)*. **2000**, *41*, 8597–8602.
- (20) Lutz, J. F.; Hoth, A. Preparation of Ideal PEG Analogues with a Tunable Thermosensitivity by Controlled Radical Copolymerization of 2-(2-Methoxyethoxy)Ethyl Methacrylate and Oligo(Ethylene Glycol) Methacrylate. *Macromolecules* **2006**, *39*, 893–896.
- (21) Chevillard, C.; Axelos, M. A. V. Phase Separation of Aqueous Solution of Methylcellulose. *Colloid Polym. Sci.* **1997**, *275*, 537–545.
- (22) Jong, K.; Ju, B. Thermo-Responsive Behavior of Propynyl-Containing Hydroxyethyl Starch. *Colloid Polym. Sci.* **2017**, *295*, 307–315.
- (23) Yuan, X.; Ju, B.; Zhang, S. Novel PH- and Temperature-Responsive Polymer: Tertiary Amine Starch Ether. *Carbohydr. Polym.* **2014**, *114*, 530–536.
- (24) Ju, B.; Zhang, C.; Zhang, S. Thermoresponsive Starch Derivates with Widely Tuned



LCSTs by Introducing Short Oligo(Ethylene Glycol) Spacers. *Carbohydr. Polym.* **2014**, *108*, 307–312.

- (25) Ju, B.; Cao, S.; Zhang, S. Effect of Additives on the Cloud Point Temperature of 2-Hydroxy-3- Isopropoxypropyl Starch Solutions. *J. Phys. Chem. B* **2013**, *117*, 11830–11835.
- (26) Ju, B.; Yan, D.; Zhang, S. Micelles Self-Assembled from Thermoresponsive 2-Hydroxy-3-Butoxypropyl Starches for Drug Delivery. *Carbohydr. Polym.* **2012**, *87*, 1404–1409.
- (27) Gandhi, A.; Paul, A.; Sen, S. O.; Sen, K. K. Studies on Thermoresponsive Polymers: Phase Behaviour, Drug Delivery and Biomedical Applications. *Asian J. Pharm. Sci.* **2015**, *10*, 99–107.
- (28) Gil, E. S.; Hudson, S. M. Stimuli-Reponsive Polymers and Their Bioconjugates. *Prog. Polym. Sci.* **2004**, *29*, 1173–1222.
- (29) Némethy, G.; Scheeaga, H. A. Structure of Water and Hydrophobic Bonding in Proteins. I. A Model for the Thermodynamic Properties of Liquid Water. *J. Chem. Phys.* **1962**, *36*, 3382–3400.
- (30) Southall, N. T.; Dill, K. A.; Haymet, a D. J. A View of the Hydrophobic Effect. *J. Phys. Chem.* **2002**, *106*, 521–533.
- (31) Heskins, M.; Guillet, J. E. Solution Properties of Poly(N-Isopropylacrylamide). *J. Macromol. Sci. Part A - Chem.* **1968**, *2*, 1441–1455.
- (32) Taylor, L. D.; Cerankowski, L. D. Preparation of Films Exhibiting a Balanced Solutions-A Study of Lower Consolute Behavior. *J. Polym. Sci.* **1975**, *13*, 2551–2570.
- (33) Cheng, H.; Xie, S.; Zhou, Y.; Huang, W.; Yan, D.; Yang, J.; Ji, B. Effect of Degree of Branching on the Thermoresponsive Phase Transition Behaviors of Hyperbranched Multiarm Copolymers: Comparison of Systems with Lcst Transition Based on Coil-to-Globule Transition or Hydrophilic-Hydrophobic Balance. *J. Phys. Chem. B* **2010**, *114*, 6291–6299.
- (34) Alexandridis, P.; Alan Hatton, T. Poly(Ethylene Oxide)Poly(Propylene Oxide)Poly(Ethylene Oxide) Block Copolymer Surfactants in Aqueous Solutions and at Interfaces: Thermodynamics, Structure, Dynamics, and Modeling. *Colloids Surfaces A Physicochem. Eng. Asp.* **1995**, *96*, 1–46.
- (35) Dimitrov, I.; Trzebicka, B.; Müller, A. H. E.; Dworak, A.; Tsvetanov, C. B. Thermosensitive Water-Soluble Copolymers with Doubly Responsive Reversibly Interacting Entities. *Prog. Polym. Sci.* **2007**, *32*, 1275–1343.

- (36) Aseyev, V.; Tenhu, H.; Winnik, F. M. Non-Ionic Thermoresponsive Polymers in Water. *Adv. Polym. Sci.* **2011**, *242*, 29–89.
- (37) Wang, X.; Qiu, X.; Wu, C. Comparison of the Coil-to-Globule and the Globule-to-Coil Transitions of a Single Poly(N-Isopropylacrylamide) Homopolymer Chain in Water. *Macromolecules* **1998**, *31*, 2972–2976.
- (38) Troll, K.; Kulkarni, A.; Wang, W.; Darko, C.; Bivigou Koumba, A. M.; Laschewsky, A.; Müller-Buschbaum, P.; Papadakis, C. M. The Collapse Transition of Poly(Styrene-*b*-(N-Isopropyl Acrylamide)) Diblock Copolymers in Aqueous Solution and in Thin Films. *Colloid Polym. Sci.* **2008**, *286*, 1079–1092.
- (39) Kubota, K.; Fujishige, S.; Ando, I. Single-Chain Transition of Poly(N-Isopropylacrylamide) in Water. *J. Phys. Chem.* **1990**, *94*, 5154–5158.
- (40) Maeda, Y.; Nakamura, T.; Ikeda, I. Changes in the Hydration States of Poly(N-n-Propylmethacrylamide) and Poly(N-Isopropylmethacrylamide) during Their Phase Transitions in Water Observed by FTIR Spectroscopy. *Macromolecules* **2001**, *34*, 8246–8251.
- (41) Ito, D.; Kubota, K. Thermal Response of Poly(N-n-Propylacrylamide). *Polym. J.* **1999**, *31*, 254–257.
- (42) Maeda, T.; Kanda, T.; Yonekura, Y.; Yamamoto, K.; Aoyagi, T. Hydroxylated Poly(N-Isopropylacrylamide) as Functional Thermoresponsive Materials. *Biomacromolecules* **2006**, *7*, 545–549.
- (43) Uğuzdoğan, E.; Çamli, T.; Kabasakal, O. S.; Patir, S.; Öztürk, E.; Denkbaş, E. B.; Tuncel, A. A New Temperature-Sensitive Polymer: Poly(Ethoxypropylacrylamide). *Eur. Polym. J.* **2005**, *41*, 2142–2149.
- (44) Aoki, T.; Muramatsu, M.; Torii, T.; Sanui, K.; Ogata, N. Thermosensitive Phase Transition of an Optically Active Polymer in Aqueous Milieu [2]. *Macromolecules* **2001**, *34*, 3118–3119.
- (45) Maeda, Y.; Sakamoto, J.; Wang, S. Y.; Mizuno, Y. Lower Critical Solution Temperature Behavior of Poly(n-(2-Ethoxyethyl) Acrylamide) as Compared with Poly(N-Isopropylacrylamide). *J. Phys. Chem. B* **2009**, *113*, 12456–12461.
- (46) Uğuzdoğan, E.; Kabasakal, O. S. Synthesis and Characterization of Thermally-Sensitive Polymer: Poly(Aminomethoxypropylacrylamide). *Colloids Surfaces A Physicochem. Eng. Asp.* **2010**, *368*, 129–136.
- (47) Liu, H. Y.; Zhu, X. X. Lower Critical Solution Temperatures of N-Substituted Acrylamide Copolymers in Aqueous Solutions. *Polymer (Guildf)*. **1999**, *40*, 6985–

6990.

- (48) Fischer, F.; Zufferey, D.; Tahoces, R. Lower Critical Solution Temperature in Superheated Water: The Highest in the Poly(N,N-Dialkylacrylamide) Series. *Polym. Int.* **2011**, *60*, 1259–1262.
- (49) Xu, J.; Jiang, X.; Liu, S. Synthesis of Low-Polydispersity Poly(N-Ethylmethacrylamide) by Controlled Radical Polymerizations and Their Thermal Phase Transition Behavior. *J. Polym. Sci. Part A Polym. Chem.* **2008**, *46*, 60–69.
- (50) Maeda, Y.; Nakamura, T.; Ikeda, I. Changes in the Hydration States of Poly(N-Alkylacrylamide)s during Their Phase Transitions in Water Observed by FTIR Spectroscopy. *Macromolecules* **2001**, *34*, 1391–1399.
- (51) Djokpé, E.; Vogt, W. N-Isopropylacrylamide and N-Isopropylmethacrylamide: Cloud Points of Mixtures and Copolymers. *Macromol. Chem. Phys.* **2001**, *202*, 750–757.
- (52) Ishizone, T.; Seki, A.; Hagiwara, M.; Han, S.; Yokoyama, H.; Oyane, A.; Deffieux, A.; Carlotti, S. Anionic Polymerizations of Oligo(Ethylene Glycol) Alkyl Ether Methacrylates: Effect of Side Chain Length and  $\omega$ -Alkyl Group of Side Chain on Cloud Point in Water. *Macromolecules* **2008**, *41*, 2963–2967.
- (53) Han, S.; Hagiwara, M.; Ishizone, T. Synthesis of Thermally Sensitive Water-Soluble Polymethacrylates by Living Anionic Polymerizations of Oligo(Ethylene Glycol) Methyl Ether Methacrylates. *Macromolecules* **2003**, *36*, 8312–8319.
- (54) Chen, Y.; Sone, M.; Fuchise, K.; Sakai, R.; Kakuchi, R.; Duan, Q.; Sun, J.; Narumi, A.; Satoh, T.; Kakuchi, T. Structural Effect of a Series of Block Copolymers Consisting of Poly(N-Isopropylacrylamide) and Poly(N-Hydroxyethylacrylamide) on Thermoresponsive Behavior. *React. Funct. Polym.* **2009**, *69*, 463–469.  
<https://doi.org/10.1016/j.reactfunctpolym.2008.12.016>.
- (55) Yang, L. li; Zhang, J. ming; He, J. song; Zhang, J.; Gan, Z. hua. Synthesis and Characterization of Temperature-Sensitive Cellulose-Graft-Poly(N-Isopropylacrylamide) Copolymers. *Chinese J. Polym. Sci. (English Ed.)* **2015**, *33*, 1640–1649.
- (56) Saeki, S.; Kuwahara, N.; Nakata, M.; Kaneko, M. Upper and Lower Critical Solution Temperatures in Poly (Ethylene Glycol) Solutions. *Polymer (Guildf.)* **1976**, *17*, 685–689.
- (57) Yue, G.; Cui, Q.; Zhang, Y.; Wang, E.; Wu, F. Thermo-Responsive Block Copolymers Based on Linear-Type Poly(Ethylene Glycol): Tunable LCST within the Physiological Range. *Chinese J. Polym. Sci. (English Ed.)* **2012**, *30*, 770–776.

- (58) Furyk, S.; Zhang, Y.; Ortiz-Acosta, D.; Cremer, P. S.; Bergbreiter, D. E. Effects of End Group Polarity and Molecular Weight on the Lower Critical Solution Temperature of Poly(N-Isopropylacrylamide). *J. Polym. Sci. Part A Polym. Chem.* **2006**, *44*, 1492–1501.
- (59) Xia, Y.; Yin, X.; Burke, N. A. D.; Stöver, H. D. H. Thermal Response of Narrow-Disperse Poly(N-Isopropylacrylamide) Prepared by Atom Transfer Radical Polymerization. *Macromolecules* **2005**, *38*, 5937–5943.
- (60) Xia, Y.; Burke, N. A. D.; Stöver, H. D. H. End Group Effect on the Thermal Response of Narrow-Disperse Poly(N-Isopropylacrylamide) Prepared by Atom Transfer Radical Polymerization. *Macromolecules* **2006**, *39*, 2275–2283.
- (61) Chen, S.; Wang, K.; Zhang, W. A New Thermoresponsive Polymer of Poly(N-Acryloylsarcosine Methyl Ester) with a Tunable LCST. *Polym. Chem.* **2017**, *8*, 3090–3101.
- (62) Eeckman, F.; Amighi, K.; Moës, A. J. Effect of Some Physiological and Non-Physiological Compounds on the Phase Transition Temperature of Thermoresponsive Polymers Intended for Oral Controlled-Drug Delivery. *Int. J. Pharm.* **2001**, *222*, 259–270.
- (63) Harsh, D. C.; Gehrke, S. H. Controlling the Swelling Characteristics of Temperature-Sensitive Cellulose Ether Hydrogels. *J. Control. Release* **1991**, *17*, 175–185.
- (64) Clasen, C.; Kulicke, W. M. Determination of Viscoelastic and Rheo-Optical Material Functions of Water-Soluble Cellulose Derivatives. *Prog. Polym. Sci.* **2001**, *26*, 1839–1919.
- (65) Pásztor, E.; Makó, Á.; Csóka, G.; Fenyvesi, Z.; Benko, R.; Prosszer, M.; Marton, S.; Antal, I.; Klebovich, I. New Formulation of in Situ Gelling Metolose-Based Liquid Suppository. *Drug Dev. Ind. Pharm.* **2011**, *37*, 1–7.
- (66) Kapsabelis, S.; Prestidge, C. A. Adsorption of Ethyl(Hydroxyethyl)Cellulose onto Silica Particles: The Role of Surface Chemistry and Temperature. *J. Colloid Interface Sci.* **2000**, *228*, 297–305.
- (67) Csóka, G.; Gelencsér, A.; Makó, A.; Marton, S.; Zelkó, R.; Klebovich, I.; Antal, I. Potential Application of Metolose® in a Thermoresponsive Transdermal Therapeutic System. *Int. J. Pharm.* **2007**, *338*, 15–20.
- (68) Sarkar, N. Thermal Gelation Properties of Methyl and Hydroxypropyl Methylcellulose. *J. Appl. Polym. Sci.* **1979**, *24*, 1073–1087.
- (69) Kunugi, S.; Yoshida, D.; Kiminami, H. Effects of Pressure on the Behavior of

- (Hydroxypropyl)Cellulose in Aqueous Solution. *Colloid Polym. Sci.* **2001**, *279*, 1139–1143.
- (70) Touitou, E.; Donbrow, M. Influence of Additives on (Hydroxyethyl) Methylcellulose Properties: Relation between Gelation Temperature Change, Compressed Matrix Integrity and Drug Release Profile. *Int. J. Pharm.* **1982**, *11*, 131–148.
- (71) Pérez, S.; Bertoft, E. The Molecular Structures of Starch Components and Their Contribution to the Architecture of Starch Granules: A Comprehensive Review. *Starch/Staerke* **2010**, *62*, 389–420.
- (72) Zheng, B.; Karski, M.; Taylor, S. D. Thermoresponsive Hydroxybutylated Starch Nanoparticles. *Carbohydr. Polym.* **2019**, *209*, 145–151.
- (73) Butler, R. M. Steam-Assisted Gravity Drainage: Concept, Development, Performance and Future. *J. Can. Pet. Technol.* **1994**, *33*, 44–50.
- (74) Bao, Y.; Wang, J.; Gates, I. D. On the Physics of Cyclic Steam Stimulation. *Energy* **2016**, *115*, 969–985.
- (75) Clark, K. A.; Pasternack, D. S. Hot Water Separation of Bitumen from Alberta Bituminous Sand. *Ind. Eng. Chem.* **1932**, *24*, 1410–1416.
- (76) Liu, J.; Xu, Z.; Masliyah, J. Interaction Forces in Bitumen Extraction from Oil Sands. *J. Colloid Interface Sci.* **2005**, *287*, 507–520.
- (77) Takamura, K. Microscopic Structure of Athabasca Oil Sand. *Can. J. Chem. Eng.* **1982**, *60*, 538–545.
- (78) Mossop, G. D. Geology of the Athabasca Oil Sands. *Science (80- )*. **1980**, *207*, 145–152.
- (79) Takamura, K.; Chow, R. S. A Mechanism for Initiation of Bitumen Displacement from Oil Sand. *J. Can. Pet. Technol.* **1983**, *22*, 22–30.
- (80) Masliyah, J.; Zhou, Z. J.; Xu, Z.; Czarnecki, J.; Hamza, H. Understanding Water-Based Bitumen Extraction from Athabasca Oil Sands. *Can. J. Chem. Eng.* **2008**, *82*, 628–654.
- (81) Romanova, U. G.; Valinasab, M.; Stasiuk, E. N.; Yarranton, H. W.; Schramm, L. L.; Shelfantook, W. E. The Effect of Oil Sands Bitumen Extraction Conditions on Froth Treatment Performance. *J. Can. Pet. Technol.* **2006**, *45*, 36–45.
- (82) Long, J.; Drelich, J.; Xu, Z.; Masliyah, J. H. Effect of Operating Temperature on Water-Based Oil Sands Processing. *Can. J. Chem. Eng.* **2008**, *85*, 726–738.

- (83) Zhou, Z.; Kasongo, T.; Xu, Z.; Masliyah, J. Assessment of Bitumen Recovery from the Athabasca Oil Sands Using a Laboratory Denver Flotation Cell. *Can. J. Chem. Eng.* **2008**, *82*, 696–703.
- (84) Wallwork, V.; Xu, Z.; Masliyah, J. Processibility of Athabasca Oil Sand Using a Laboratory Hydro Transport Extraction System (LHES). *Can. J. Chem. Eng.* **2008**, *82*, 687–695.
- (85) Flynn, Morris Bara, Barry Czarnecki, Jan Masliyah, J. An Investigation of the Effect of Air Injection during Oil Sand Conditioning. *Can. J. Chem. Eng.* **2001**, *79*, 468–470.
- (86) Sanders, R. S.; Schaan, J.; McKibben, M. M. Oil Sand Slurry Conditioning Tests in a 100 Mm Pipeline Loop. *Can. J. Chem. Eng.* **2007**, *85*, 756–764.
- (87) Gu, G.; Sanders, R. S.; Nandakumar, K.; Xu, Z.; Masliyah, J. H. A Novel Experimental Technique to Study Single Bubble-Bitumen Attachment in Flotation. *Int. J. Miner. Process.* **2004**, *74*, 15–29.
- (88) Malysa, K.; Ng, S.; Czarnecki, J.; Masliyah, J. A Method of Visualization and Characterization of Aggregate Flow inside a Separation Vessel, Part 2. Composition of the Bitumen-Air Aggregates. *Int. J. Miner. Process.* **1999**, *55*, 171–188.
- (89) Wang, N.; Mikula, R. J. Small Scale Simulation of Pipeline or Stirred Tank Conditioning of Oil Sands: Temperature and Mechanical Energy. *J. Can. Pet. Technol.* **2002**, *41*, 8–10.
- (90) Ren, S.; Dang-Vu, T.; Zhao, H.; Long, J.; Xu, Z.; Masliyah, J. Effect of Weathering on Surface Characteristics of Solids and Bitumen from Oil Sands. *Energy and Fuels* **2009**, *23*, 334–341.
- (91) Ren, S.; Zhao, H.; Dang-Vu, T.; Xu, Z.; Masliyah, J. H. Effect of Weathering on Oil Sands Processability. *Can. J. Chem. Eng.* **2009**, *87*, 879–886.
- (92) Ren, S.; Zhao, H.; Long, J.; Xu, Z.; Masliyah, J. Understanding Weathering of Oil Sands Ores by Atomic Force Microscopy. *AIChE J.* **2009**, *55*, 3277–3285.
- (93) Liu, J.; Xu, Z.; Masliyah, J. Role of Fine Clays in Bitumen Extraction from Oil Sands. *AIChE J.* **2004**, *50*, 1917–1927.
- (94) Moran, K.; Masliyah, J.; Yeung, A. Factors Affecting the Aeration of Small Bitumen Droplets. *Can. J. Chem. Eng.* **2000**, *78*, 625–634.
- (95) Gu, G.; Xu, Z.; Nandakumar, K.; Masliyah, J. Effects of Physical Environment on Induction Time of Air-Bitumen Attachment. *Int. J. Miner. Process.* **2003**, *69*, 235–250.

- (96) Wallace, D.; Henry, D.; Takamura, K. A Physical Chemical Explanation for Deterioration in the Hot Water Processability of Athabasca Oil Sand Due to Aging. *Fuel Sci. Technol. Int.* **1989**, *7*, 699–725.
- (97) Flury, C.; Afacan, A.; Tamiz Bakhtiari, M.; Sjoblom, J.; Xu, Z. Effect of Caustic Type on Bitumen Extraction from Canadian Oil Sands. *Energy and Fuels* **2014**, *28*, 431–438.
- (98) Ozum, B. Method for Extraction of Bitumen from Oil Sands Using Lime. US 7.931,800 B2, 2011.
- (99) Li, H.; Zhou, Z. A.; Xu, Z.; Masliyah, J. H. Role of Acidified Sodium Silicate in Low Temperature Bitumen Extraction from Poor-Processing Oil Sand Ores. *Ind. Eng. Chem. Res.* **2005**, *44*, 4753–4761.
- (100) Sury, K. N. Low Temperature Bitumen Recovery Process. US4946597A, 1990.
- (101) Allcock, G.; Siy, R.; Spence, J.; Sury, K. Cold Dense Slurrying Process for Extracting Bitumen from Oil Sand. US6007708A, 1999.
- (102) Hooshiar, A.; Uhlik, P.; Liu, Q.; Etsell, T. H.; Ivey, D. G. Clay Minerals in Nonaqueous Extraction of Bitumen from Alberta Oil Sands: Part 1. Nonaqueous Extraction Procedure. *Fuel Process. Technol.* **2012**, *94*, 80–85.
- (103) Li, X.; He, L.; Wu, G.; Sun, W.; Li, H.; Sui, H. Operational Parameters, Evaluation Methods, and Fundamental Mechanisms: Aspects of Nonaqueous Extraction of Bitumen from Oil Sands. *Energy and Fuels* **2012**, *26*, 3553–3563.
- (104) Yang, H.; Wang, Y.; Ding, M.; Hu, B.; Ren, S. Water-Assisted Solvent Extraction of Bitumen from Oil Sands. *Ind. Eng. Chem. Res.* **2012**, *51*, 3032–3038.
- (105) Harjai, S. K.; Flury, C.; Masliyah, J.; Drelich, J.; Xu, Z. Robust Aqueous-Nonaqueous Hybrid Process for Bitumen Extraction from Mineable Athabasca Oil Sands. *Energy and Fuels* **2012**, *26*, 2920–2927.
- (106) Wang, T.; Zhang, C.; Zhao, R.; Zhu, C.; Yang, C.; Liu, C. Solvent Extraction of Bitumen from Oil Sands. *Energy and Fuels* **2014**, *28*, 2297–2304.
- (107) Li, H.; Long, J.; Xu, Z.; Masliyah, J. H. Synergetic Role of Polymer Flocculant in Low-Temperature Bitumen Extraction and Tailings Treatment. *Energy and Fuels* **2005**, *19*, 936–943.
- (108) Li, H.; Long, J.; Xu, Z.; Masliyah, J. H. Novel Polymer Aids for Low-Grade Oil Sand Ore Processing. *Can. J. Chem. Eng.* **2008**, *86*, 168–176.

- (109) Long, J.; Li, H.; Xu, Z.; Masliyah, J. H. Improving Oil Sands Processability Using a Temperature-Sensitive Polymer. *Energy and Fuels* **2011**, *25*, 701–707.
- (110) Lin, F.; He, L.; Hou, J.; Masliyah, J.; Xu, Z. Role of Ethyl Cellulose in Bitumen Extraction from Oil Sands Ores Using an Aqueous-Nonaqueous Hybrid Process. *Energy and Fuels* **2016**, *30*, 121–129.
- (111) Botha, L.; Soares, J. B. P. The Influence of Tailings Composition on Flocculation. *Can. J. Chem. Eng.* **2015**, *93*, 1514–1523.
- (112) Chalaturnyk, R. J.; Scott, J. D.; Özüm, B. Management of Oil Sands Tailings. *Pet. Sci. Technol.* **2002**, *20*, 1025–1046.
- (113) Yingchoncharoen, P.; Kalinowski, D. S.; Richardson, D. R. Lipid-Based Drug Delivery Systems in Cancer Therapy: What Is Available and What Is yet to Come. *Pharmacol. Rev.* **2016**, *68*, 701–787.
- (114) Gelardi, G.; Flatt, R. J. Working Mechanisms of Water Reducers and Superplasticizers. In *Science and Technology of Concrete Admixtures*; Woodhead Publishing, 2016; pp 257–278.
- (115) Tridib, T.; Bhudeb R., D. Flocculation : A New Way to Treat the Waste Water. *J. Phys. Sci.* **2006**, *10*, 93–127.
- (116) Griot, O.; Kitchener, J. A. “Ageing” of Silica Suspensions in Water and Its Influence on Flocculation by Polyacrylamide. *Nature* **1963**, *200*, 1004–1005.
- (117) Cymerman, G.; Kwong, T.; Lord, E.; Hamza, H.; Xu, Y. Thickening and disposal of fine tails from oil sand processing.
- (118) Sworska, A.; Laskowski, J. S.; Cymerman, G. Flocculation of the Syncrude Fine Tailings Part I. Effect of PH, Polymer Dosage and Mg<sup>2+</sup> and Ca<sup>2+</sup> Cations. *Int. J. Miner. Process.* **2000**, *60*, 143–152.
- (119) Long, J.; Li, H.; Xu, Z.; Masliyah, J. H. Role of Colloidal Interactions in Oil Sand Tailings Treatment. *AIChE J.* **2006**, *52*, 371–383.
- (120) Sworska, A.; Laskowski, J. S.; Cymerman, G. Flocculation of the Syncrude Fine Tailings Part II. Effect of Hydrodynamic Conditions. *Int. J. Miner. Process.* **2000**, *60*, 153–161.
- (121) Li, H.; Long, J.; Xu, Z.; Masliyah, J. H. Effect of Molecular Weight and Charge Density on the Performance of Polyacrylamide in Low-Grade Oil Sand Ore Processing. *Can. J. Chem. Eng.* **2008**, *86*, 177–185.



- (122) Alamgir, A.; Harbottle, D.; Masliyah, J.; Xu, Z. Al-PAM Assisted Filtration System for Abatement of Mature Fine Tailings. *Chem. Eng. Sci.* **2012**, *80*, 91–99.
- (123) Strandman, S.; Vachon, R.; Dini, M.; Giasson, S.; Zhu, X. X. Polyacrylamides Revisited: Flocculation of Kaolin Suspensions and Mature Fine Tailings. *Can. J. Chem. Eng.* **2018**, *96*, 20–26.
- (124) Zhou, Y.; Gan, Y.; Wanless, E. J.; Jameson, G. J.; Franks, G. V. Interaction Forces between Silica Surfaces in Aqueous Solutions of Cationic Polymeric Flocculants: Effect of Polymer Chargen. *Langmuir* **2008**, *24*, 10920–10928.
- (125) Zhou, Y.; Franks, G. V. Flocculation Mechanism Induced by Cationic Polymers Investigated by Light Scattering. *Langmuir* **2006**, *22*, 6775–6786.
- (126) Wang, L. J.; Wang, J. P.; Zhang, S. J.; Chen, Y. Z.; Yuan, S. J.; Sheng, G. P.; Yu, H. Q. A Water-Soluble Cationic Flocculant Synthesized by Dispersion Polymerization in Aqueous Salts Solution. *Sep. Purif. Technol.* **2009**, *67*, 331–335.
- (127) Wang, C.; Han, C.; Lin, Z.; Masliyah, J.; Liu, Q.; Xu, Z. Role of Preconditioning Cationic Zetag Flocculant in Enhancing Mature Fine Tailings Flocculation. *Energy and Fuels* **2016**, *30*, 5223–5231.
- (128) Vajihinejad, V.; Guillermo, R.; Soares, J. B. P. Dewatering Oil Sands Mature Fine Tailings (MFTs) with Poly(Acrylamide-Co-Diallyldimethylammonium Chloride): Effect of Average Molecular Weight and Copolymer Composition. *Ind. Eng. Chem. Res.* **2017**, *56*, 1256–1266.
- (129) Yang, W. Y.; Qian, J. W.; Shen, Z. Q. A Novel Flocculant of Al(OH)<sub>3</sub>-Polyacrylamide Ionic Hybrid. *J. Colloid Interface Sci.* **2004**, *273*, 400–405.
- (130) Sun, W.; Long, J.; Xu, Z.; Masliyah, J. H. Study of Al(OH)<sub>3</sub>-Polyacrylamide-Induced Pelleting Flocculation by Single Molecule Force Spectroscopy. *Langmuir* **2008**, *24*, 14015–14021.
- (131) Wang, X. W.; Feng, X.; Xu, Z.; Masliyah, J. H. Polymer Aids for Settling and Filtration of Oil Sands Tailings. *Can. J. Chem. Eng.* **2010**, *88*, 403–410.
- (132) Lee, K. E.; Teng, T. T.; Morad, N.; Poh, B. T.; Hong, Y. F. Flocculation of Kaolin in Water Using Novel Calcium Chloride-Polyacrylamide (CaCl<sub>2</sub>-PAM) Hybrid Polymer. *Sep. Purif. Technol.* **2010**, *75*, 346–351.
- (133) Lee, K. E.; Teng, T. T.; Morad, N.; Poh, B. T.; Mahalingam, M. Flocculation Activity of Novel Ferric Chloride-Polyacrylamide (FeCl<sub>3</sub>-PAM) Hybrid Polymer. *Desalination* **2011**, *266*, 108–113.

- (134) Shang, H.; Liu, J.; Zheng, Y.; Wang, L. Synthesis, Characterization, and Flocculation Properties of Poly(Acrylamide-Methacryloxyethyltrimethyl Ammonium Chloride-Methacryloxypropyltrimethoxy Silane). *J. Appl. Polym. Sci.* **2009**, *111*, 1594–1599.
- (135) Reis, L. G.; Oliveira, R. S.; Palhares, T. N.; Spinelli, L. S.; Lucas, E. F.; Vedoy, D. R. L.; Asare, E.; Soares, J. B. P. Using Acrylamide/Propylene Oxide Copolymers to Dewater and Densify Mature Fine Tailings. *Miner. Eng.* **2016**, *95*, 29–39.
- (136) Hripko, R.; Vajihinejad, V.; LopesMotta, F.; Soares, J. B. P. Enhanced Flocculation of Oil Sands Mature Fine Tailings Using Hydrophobically Modified Polyacrylamide Copolymers. *Glob. Challenges* **2018**, *2*, 170135.
- (137) Bazoubandi, B.; Soares, J. B. P. Amylopectin-Graft-Polyacrylamide for the Flocculation and Dewatering of Oil Sands Tailings. *Miner. Eng.* **2020**, *148*, 106196.
- (138) Li, H.; O’Shea, J. P.; Franks, G. V. Effect of Molecular Weight of Poly(n-Isopropyl Acrylamide) Temperature-Sensitive Flocculants on Dewatering. *AIChE J.* **2009**, *55*, 2070–2080.
- (139) Li, H.; Zhou, J.; Chow, R.; Adegoroye, A.; Najafi, A. S. Enhancing Treatment and Geotechnical Stability of Oil Sands Fine Tailings Using Thermo-Sensitive Poly(n-Isopropyl Acrylamide). *Can. J. Chem. Eng.* **2015**, *93*, 1780–1786.
- (140) Zhang, H.; Jiang, J.; Shang, S.; Song, Z.; Song, J. Novel, Rosin-Based, Hydrophobically Modified Cationic Polyacrylamide for Kaolin Suspension Flocculation. *J. Appl. Polym. Sci.* **2018**, *135*, 46637.
- (141) Lu, H.; Wang, Y.; Li, L.; Kotsuchibashi, Y.; Narain, R.; Zeng, H. Temperature- and PH-Responsive Benzoboroxole-Based Polymers for Flocculation and Enhanced Dewatering of Fine Particle Suspensions. *ACS Appl. Mater. Interfaces* **2015**, *7*, 27176–27187.
- (142) Gumfekar, S. P.; Soares, J. B. P. Polymer Reaction Engineering Tools to Design Multifunctional Polymer Flocculants. *Chemosphere* **2018**, *210*, 156–165.
- (143) Loerke, R.; Tan, X.; Liu, Q. Dewatering of Oil Sands Mature Fine Tailings by Dual Polymer Flocculation and Pressure Plate Filtration. *Energy and Fuels* **2017**, *31*, 6986–6995.
- (144) Lu, Q.; Yan, B.; Xie, L.; Huang, J.; Liu, Y.; Zeng, H. A Two-Step Flocculation Process on Oil Sands Tailings Treatment Using Oppositely Charged Polymer Flocculants. *Sci. Total Environ.* **2016**, *565*, 369–375.
- (145) Ghimici, L.; Nichifor, M. Flocculation Properties of Some Cationic Polysaccharides. *J. Macromol. Sci. Part B Phys.* **2009**, *48*, 106–113.

- (146) Wang, J. P.; Yuan, S. J.; Wang, Y.; Yu, H. Q. Synthesis, Characterization and Application of a Novel Starch-Based Flocculant with High Flocculation and Dewatering Properties. *Water Res.* **2013**, *47*, 2643–2648.
- (147) Lu, Y.; Shang, Y.; Huang, X.; Chen, A.; Yang, Z.; Jiang, Y.; Cai, J.; Gu, W.; Qian, X.; Yang, H.; Cheng, R. Preparation of Strong Cationic Chitosan- Graft -Polyacrylamide Flocculants and Their Flocculating Properties. *Ind. Eng. Chem. Res.* **2011**, *50*, 7141–7149.
- (148) Molatlhegi, O.; Alagha, L. Adsorption Characteristics of Chitosan Grafted Copolymer on Kaolin. *Appl. Clay Sci.* **2017**, *150*, 342–353.
- (149) Woodrow, J. E.; Seiber, J. N.; Miller, G. C. Acrylamide Release Resulting from Sunlight Irradiation of Aqueous Polyacrylamide/Iron Mixtures. *J. Agric. Food Chem.* **2008**, *56*, 2773–2779.
- (150) Levitt, D. B.; Pope, G. A.; Jouenne, S. Chemical Degradation of Polyacrylamide Polymers under Alkaline Conditions. *SPE Reserv. Eval. Eng.* **2011**, *14*, 281–286.
- (151) Bolto, B.; Gregory, J. Organic Polyelectrolytes in Water Treatment. *Water Res.* **2007**, *41*, 2301–2324.
- (152) Pennetta De Oliveira, L.; Gumfekar, S. P.; Lopes Motta, F.; Soares, J. B. P. Dewatering of Oil Sands Tailings with Novel Chitosan-Based Flocculants. *Energy and Fuels* **2018**, *32*, 5271–5278.
- (153) Zhao, N.; Al Bitar, H.; Zhu, Y.; Xu, Y.; Shi, Z. Flocculation Performance of Anionic Starch in Oil Sand Tailings. *Water Sci. Technol.* **2018**, *78*, 1268–1275.
- (154) Zheng, B. Synthesis and Characterization of Thermoresponsive Starch Nanoparticles, University of Waterloo, 2016.
- (155) Wu, C.; Li, W.; Zhu, X. X. Viscoelastic Effect on the Formation of Mesoglobular Phase in Dilute Solutions. *Macromolecules* **2004**, *37*, 4989–4992.
- (156) Kasemsuwan, T.; Jane, J. L. Quantitative Method for the Survey of Starch Phosphate Derivatives and Starch Phospholipids by <sup>31</sup>P Nuclear Magnetic Resonance Spectroscopy. *Cereal Chem.* **1996**, *73*, 702–707.
- (157) Lim, S.; Seib, P. A. Location of Phosphate-Esters in a Wheat-Starch Phosphate by <sup>31</sup>P-Nuclear Magnetic-Resonance Spectroscopy. *Cereal Chem.* **1993**, *70*, 145–145.
- (158) Ji, Y.; Lu, Q.; Liu, Q.; Zeng, H. Effect of Solution Salinity on Settling of Mineral Tailings by Polymer Flocculants. *Colloids Surfaces A Physicochem. Eng. Asp.* **2013**, *430*, 29–38.

- (159) Schwarz, S.; Jaeger, W.; Paulke, B. R.; Bratskaya, S.; Smolka, N.; Bohrisch, J. Cationic Flocculants Carrying Hydrophobic Functionalities: Applications for Solid/Liquid Separation. *J. Phys. Chem. B* **2007**, *111*, 8649–8654.
- (160) Burdukova, E.; Ishida, N.; Shaddick, T.; Franks, G. V. The Size of Particle Aggregates Produced by Flocculation with PNIPAM, as a Function of Temperature. *J. Colloid Interface Sci.* **2011**, *354*, 82–88.
- (161) Ng, W. S.; Connal, L. A.; Forbes, E.; Franks, G. V. A Review of Temperature-Responsive Polymers as Novel Reagents for Solid-Liquid Separation and Froth Flotation of Minerals. *Miner. Eng.* **2018**, *123*, 144–159.
- (162) Krentz, D. O.; Lohmann, C.; Schwarz, S.; Bratskaya, S.; Liebert, T.; Laube, J.; Heinze, T.; Kulicke, W. M. Properties and Flocculation Efficiency of Highly Cationized Starch Derivatives. *Starch/Staerke* **2006**, *58*, 161–169.
- (163) Singh, R. P.; Tripathy, T.; Karmakar, G. P.; Rath, S. K.; Karmakar, N. C.; Pandey, S. R.; Kannan, K.; Jain, S. K.; Lan, N. T. Novel Biodegradable Flocculants Based on Polysaccharides. *Curr. Sci.* **2000**, *78*, 798–803.
- (164) Yuan, B.; Shang, Y.; Lu, Y.; Qin, Z.; Jiang, Y.; Chen, A.; Qian, X.; Wang, G.; Yang, H.; Cheng, R. The Flocculating Properties of Chitosan-Graft-Polyacrylamide Flocculants (I) - Effect of the Grafting Ratio. *J. Appl. Polym. Sci.* **2010**, *117*, 1876–1882.
- (165) Pal, S.; Mal, D.; Singh, R. P. Cationic Starch: An Effective Flocculating Agent. *Carbohydr. Polym.* **2005**, *59*, 417–423.
- (166) Chen, Y.; Liu, S.; Wang, G. A Kinetic Investigation of Cationic Starch Adsorption and Flocculation in Kaolin Suspension. *Chem. Eng. J.* **2007**, *133*, 325–333.
- (167) Chen, Y.; Liu, S.; Wang, G. Flocculation Properties and Adsorption Kinetics of Cationic Starches in Kaolin Suspensions. *J. Appl. Polym. Sci.* **2007**, *105*, 2841–2849.
- (168) Bratskaya, S.; Schwarz, S.; Liebert, T.; Heinze, T. Starch Derivatives of High Degree of Functionalization: 10. Flocculation of Kaolin Dispersions. *Colloids Surfaces A Physicochem. Eng. Asp.* **2005**, *254*, 75–80.
- (169) Sableviciene, D.; Klimaviciute, R.; Bendoraitiene, J.; Zemaitaitis, A. Flocculation Properties of High-Substituted Cationic Starches. *Colloids Surfaces A Physicochem. Eng. Asp.* **2005**, *259*, 23–30.
- (170) Heinze, T.; Haack, V.; Rensing, S. Starch Derivatives of High Degree of Functionalization. 7. Preparation of Cationic 2-Hydroxypropyltrimethylammonium Chloride Starches. *Starch/Staerke* **2004**, *56*, 288–296.

- (171) Blennow, A.; Bay-Smidt, A. M.; Leonhardt, P.; Bandsholm, O.; Madsen, M. H. Starch Paste Stickiness Is a Relevant Native Starch Selection Criterion for Wet-End Paper Manufacturing. *Starch/Staerke* **2003**, *55*, 381–389.
- (172) Blennow, A.; Bay-Smidt, A. M.; Olsen, C. E.; Møller, B. L. The Distribution of Covalently Bound Phosphate in the Starch Granule in Relation to Starch Crystallinity. *Int. J. Biol. Macromol.* **2000**, *27*, 211–218.
- (173) Zhu, Y.; Tan, X.; Liu, Q. Dual Polymer Flocculants for Mature Fine Tailings Dewatering. *Can. J. Chem. Eng.* **2017**, *95*, 3–10.
- (174) Younes, G. R.; Proper, A. R.; Rooney, T. R.; Hutchinson, R. A.; Gumfekar, S. P.; Soares, J. B. P. Structure Modifications of Hydrolytically-Degradable Polymer Flocculant for Improved Water Recovery from Mature Fine Tailings. *Ind. Eng. Chem. Res.* **2018**, *57*, 10809–10822.
- (175) Jain, S.; Sandhu, P. S.; Malvi, R.; Gupta, B. Cellulose Derivatives as Thermoresponsive Polymer: An Overview. *J. Appl. Pharm. Sci.* **2013**, *3*, 139–144.
- (176) Sanford, E. C. Processibility of Athabasca Oil Sand: Interrelationship between Oil Sand Fine Solids, Process Aids, Mechanical Energy and Oil Sand Age after Mining. *Can. J. Chem. Eng.* **1983**, *61*, 554–567.
- (177) Wallwork, V.; Xu, Z.; Masliyah, J. Bitumen Recovery with Oily Air Bubbles. *Can. J. Chem. Eng.* **2008**, *81*, 993–997.
- (178) Czarnecki, J.; Radoev, B.; Schramm, L. L.; Slavchev, R. On the Nature of Athabasca Oil Sands. *Adv. Colloid Interface Sci.* **2005**, *114*, 53–60.
- (179) Zhang, Q. Thermoresponsive Starch Nanoparticles for Use in the Extraction of Oil from Oil Sands, University of Waterloo, 2018.
- (180) Wu, X.; Czarnecki, J.; Hamza, N.; Masliyah, J. Interaction Forces between Bitumen Droplets in Water. *Langmuir* **1999**, *15*, 5244–5250.
- (181) Feng, X.; Wang, S.; Hou, J.; Wang, L.; Cepuch, C.; Masliyah, J.; Xu, Z. Effect of Hydroxyl Content and Molecular Weight of Biodegradable Ethylcellulose on Demulsification of Water-in-Diluted Bitumen Emulsions. *Ind. Eng. Chem. Res.* **2011**, *50*, 6347–6354.
- (182) Rao, F.; Liu, Q. Froth Treatment in Athabasca Oil Sands Bitumen Recovery Process: A Review. *Energy and Fuels* **2013**, *27*, 7199–7207.
- (183) Wang, S.; Segin, N.; Wang, K.; Masliyah, J. H.; Xu, Z. Wettability Control Mechanism of Highly Contaminated Hydrophilic Silica/Alumina Surfaces by Ethyl

- Cellulose. *J. Phys. Chem. C* **2011**, *115*, 10576–10587.
- (184) Liu, J.; Xu, Z.; Masliyah, J. Processability of Oil Sand Ores in Alberta. *Energy and Fuels* **2005**, *19*, 2056–2063.
- (185) Wang, L.; Dang-Vu, T.; Xu, Z.; Masliyah, J. H. Use of Short-Chain Amine in Processing of Weathered/Oxidized Oil Sands Ores. *Energy and Fuels* **2010**, *24*, 3581–3588.
- (186) Lin, F.; Xu, Y.; Nelson, R. Pilot Evaluation of an Aqueous/Nonaqueous Hybrid Bitumen Extraction Process for Mineable Oil Sands. *Miner. Eng.* **2019**, *131*, 241–248.
- (187) Quraishi, S.; Bussmann, M.; Acosta, E. Capillary Curves for Ex-Situ Washing of Oil-Coated Particles. *J. Surfactants Deterg.* **2015**, *18*, 811–823.
- (188) Senaputra, A.; Jones, F.; Fawell, P. D.; Smith, P. G. Focused Beam Reflectance Measurement for Monitoring the Extent and Efficiency of Flocculation in Mineral Systems. *AIChE J.* **2014**, *60*, 251–265.
- (189) Botha, L.; Davey, S.; Nguyen, B.; Swarnakar, A. K.; Rivard, E.; Soares, J. B. P. Flocculation of Oil Sands Tailings by Hyperbranched Functionalized Polyethylenes (HBfPE). *Miner. Eng.* **2017**, *108*, 71–82.
- (190) Vajihinejad, V.; Soares, J. B. P. Monitoring Polymer Flocculation in Oil Sands Tailings: A Population Balance Model Approach. *Chem. Eng. J.* **2018**, *346*, 447–457.
- (191) Wilson, G.; Kabwe, L.; Donahue, R.; Lahaie, R. Field Performance of In-Line Flocculated Fluid Fine Tailings Using Thin Lift Deposition. In *Proceedings of the Sixth International Conference on Mine Closure*; Australian Centre for Geomechanics, 2011; pp 473–481.
- (192) Farkish, A.; Fall, M. Rapid Dewatering of Oil Sand Mature Fine Tailings Using Super Absorbent Polymer (SAP). *Miner. Eng.* **2013**, *50*, 38–47.

# Appendices

## Appendix A

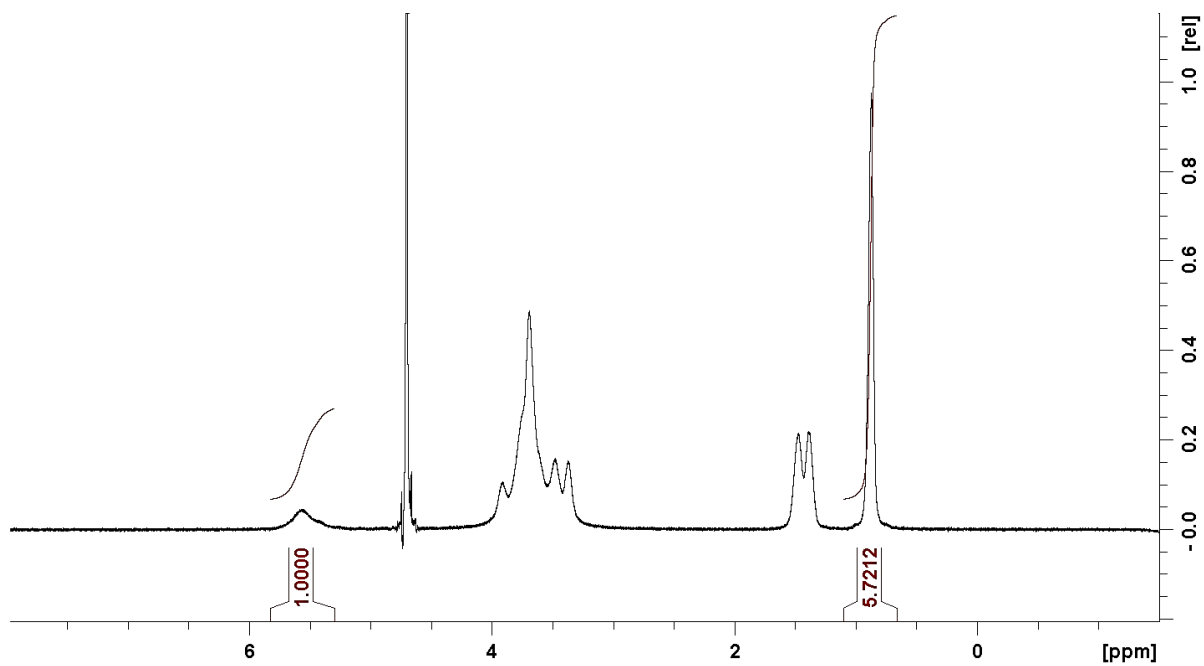


**Figure A1.**  $^1\text{H}$  NMR spectrum of HB1.9-CS in  $\text{D}_2\text{O}$ .

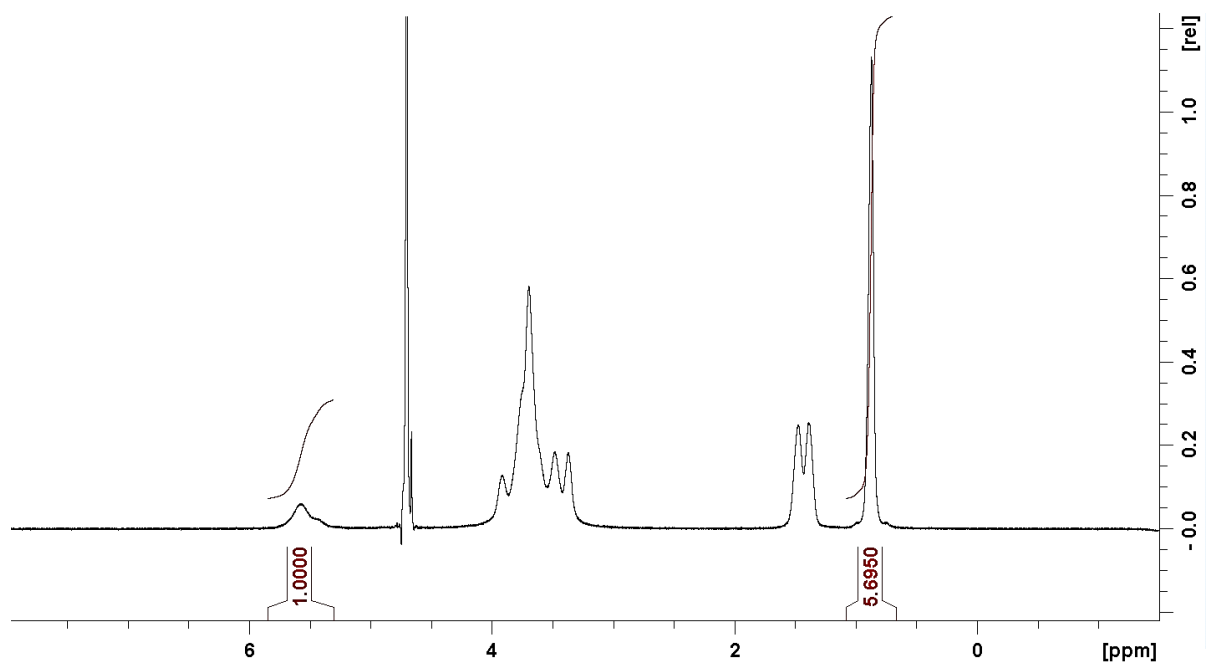


**Figure A2.**  $^1\text{H}$  NMR spectrum of HB1.9-PS in  $\text{D}_2\text{O}$ .

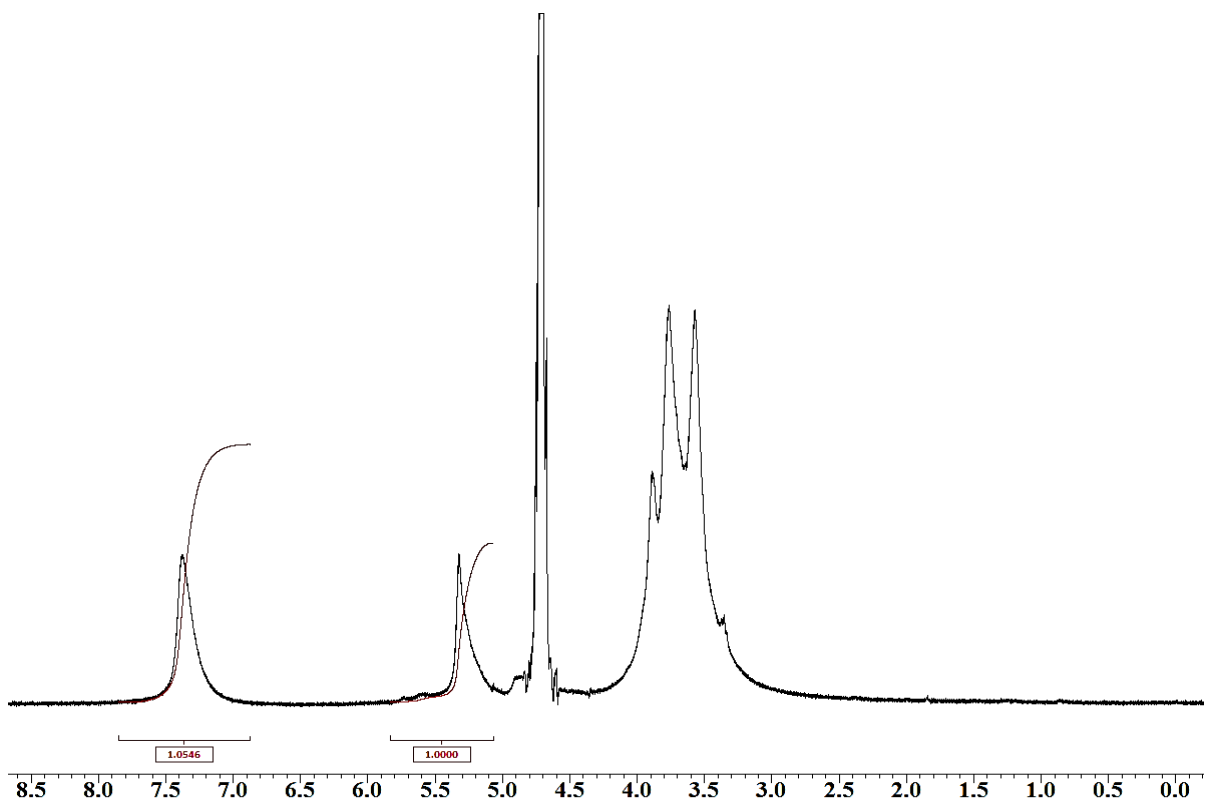


**Figure A3.**  $^1\text{H}$  NMR spectrum of PHE0.2-PS in  $\text{D}_2\text{O}$ .



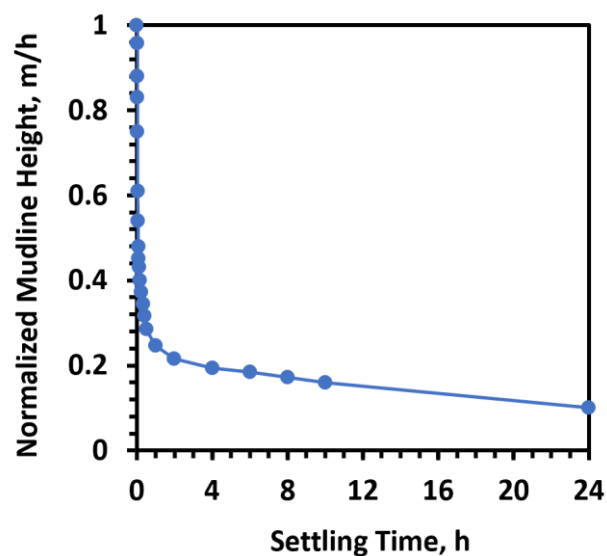


**Figure A4.** Normalized mudline height as a function of settling time plot for the settling test using 600 ppm HB2.3-CS at 50 °C.

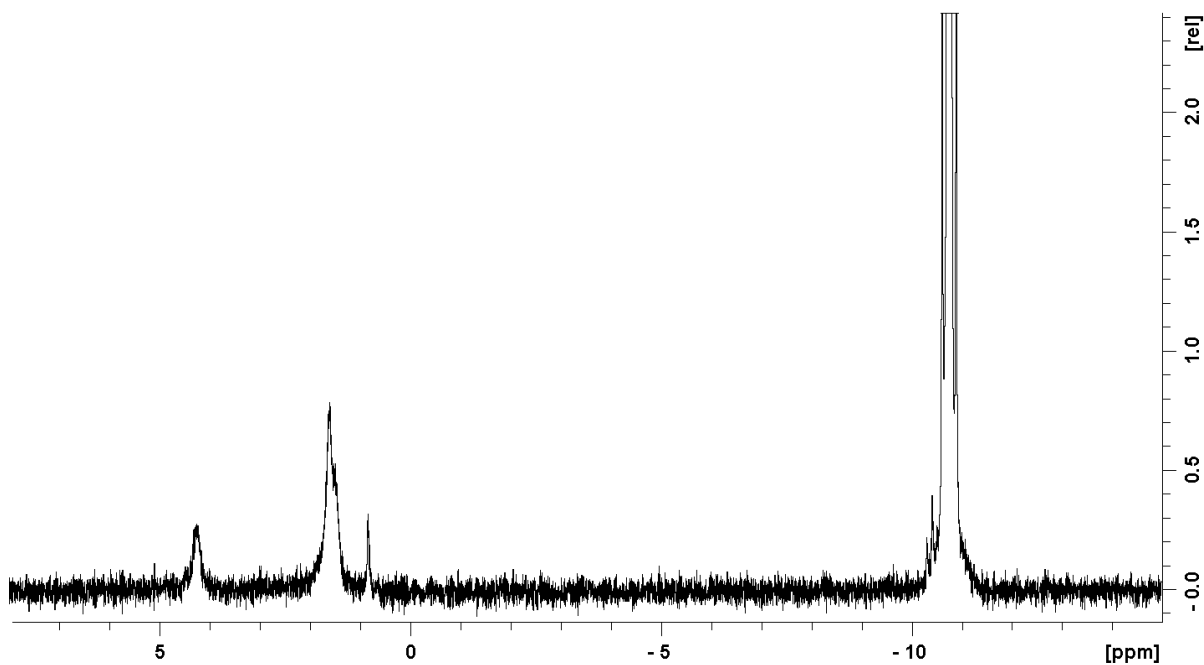


**Figure A5.**  $^{31}\text{P}$ -NMR spectrum of  $\alpha$ -limited potato starch in a solvent mixture of 45 % DMSO- $\text{d}_6$  and 55 %  $\text{D}_2\text{O}$  with nicotinamide adenine dinucleotide (NAD) as an internal standard.

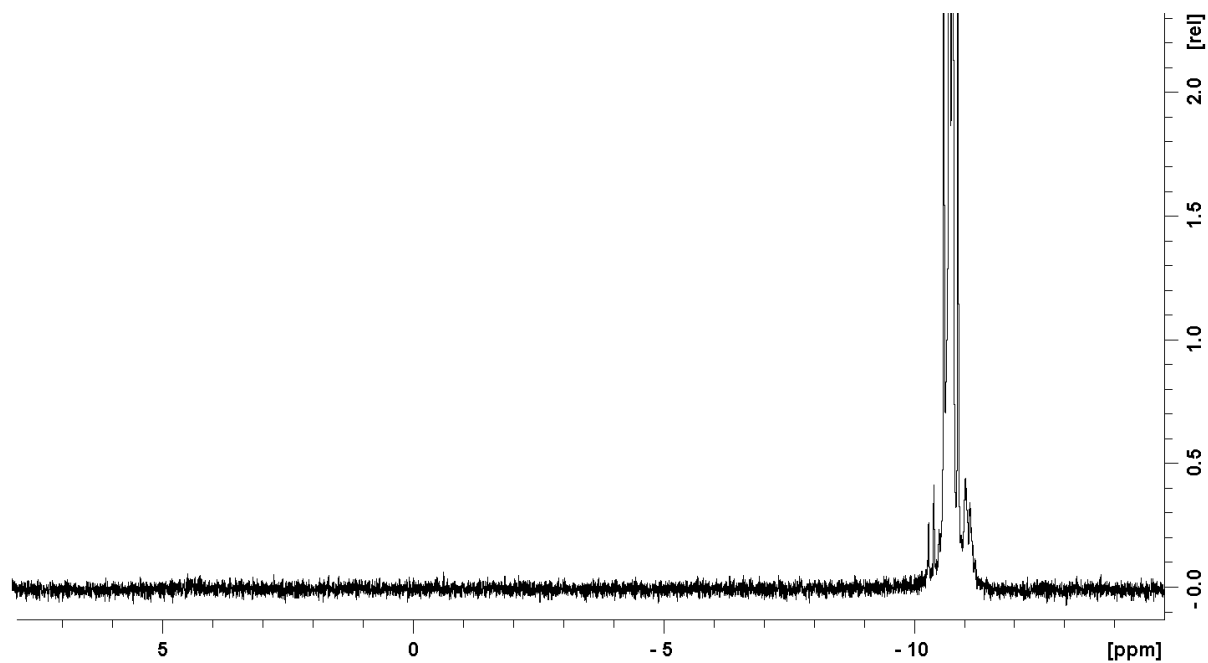


**Figure A6.** <sup>31</sup>P-NMR spectrum of  $\alpha$ -limited corn starch in a solvent mixture of 45 % DMSO- $d_6$  and 55 % D<sub>2</sub>O with NAD as an internal standard.

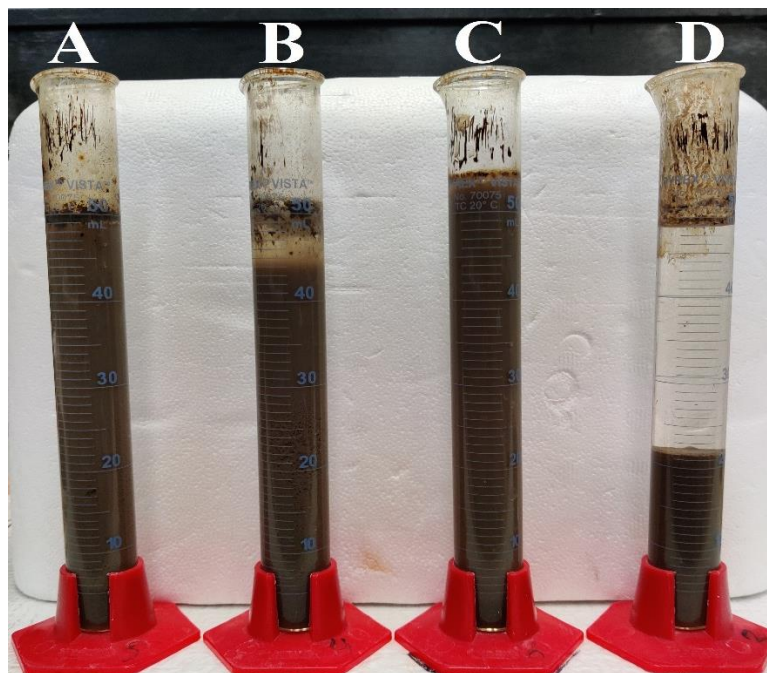


**Figure A7.** Settling tests using 50 ppm (A), 100 ppm (B) and 1000 ppm (C) Magnafloc 1011, and 1000 ppm HB1.9-PS (D). The picture was taken after a settling time of 24 h.

## Appendix B

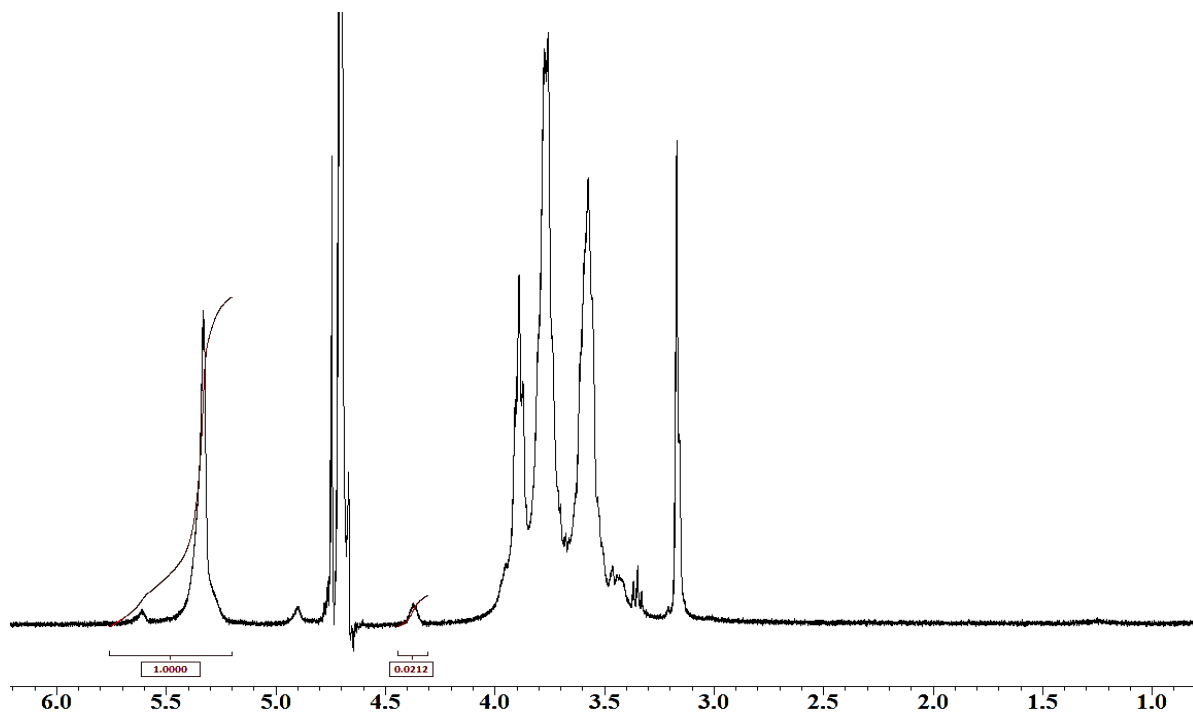


**Figure B1.** <sup>1</sup>H NMR spectrum of Cat0.02-CS in D<sub>2</sub>O.

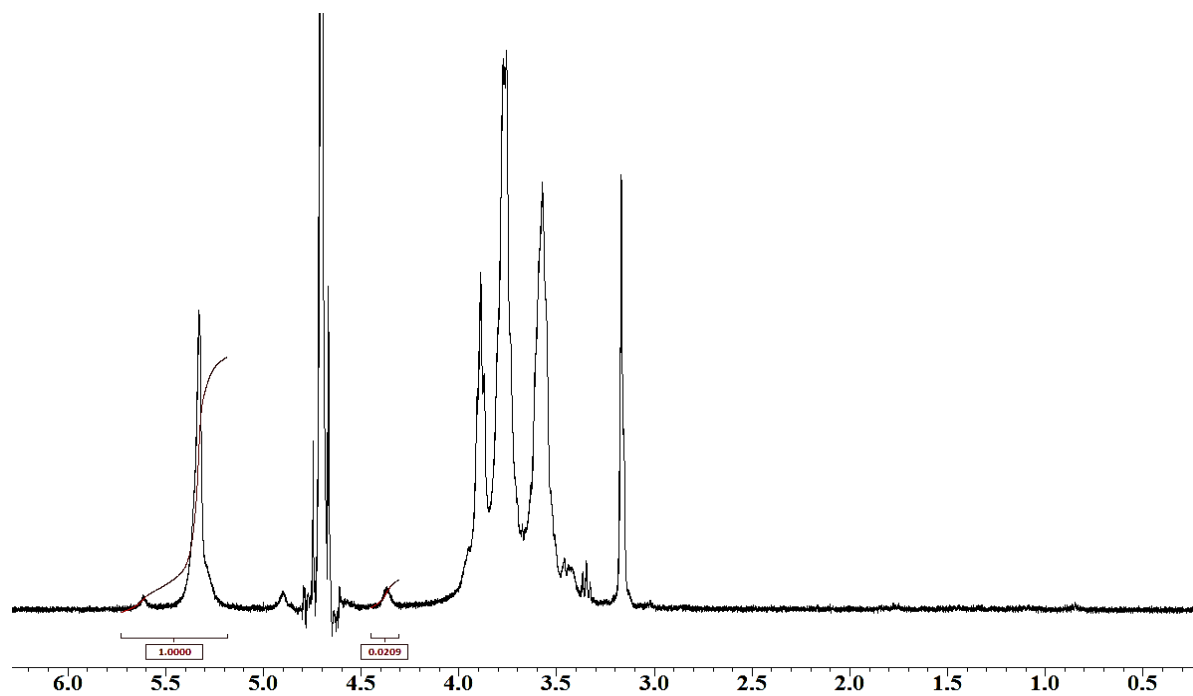


**Figure B2.** <sup>1</sup>H NMR spectrum of Cat0.02-PS in D<sub>2</sub>O.

**Table B1.** Conversion between polymer doses based on dry polymer/MFT slurry (dry/slurry) and dry polymer/dry MFT solids (dry/dry).

<b>2 wt %</b>		<b>10 wt %</b>	
<b>Dry/slurry , ppm</b>	<b>Dry/dry, ppm</b>	<b>Dry/slurry , ppm</b>	<b>Dry/dry, ppm</b>
1000	50000	1000	10000
800	40000	800	8000
600	30000	600	6000
400	20000	400	4000
200	10000	200	2000
100	5000	100	1000
50	2500	50	500
25	1250	25	250

## Appendix C

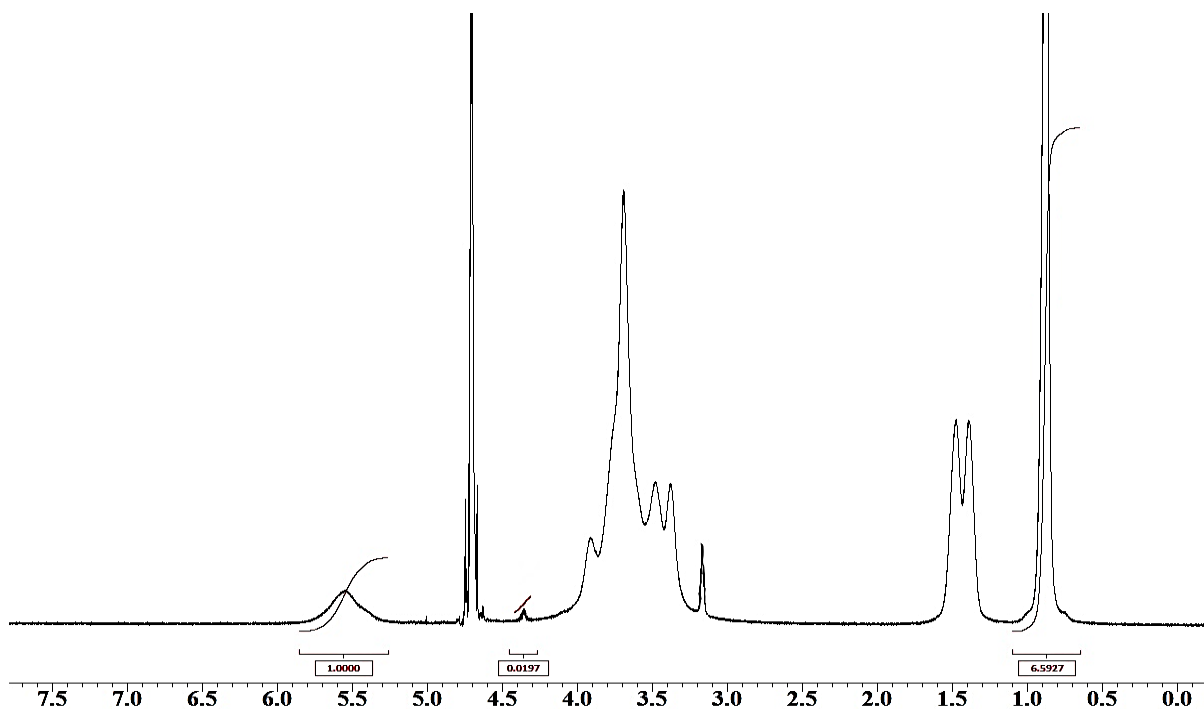


**Figure C1.**  $^1\text{H}$  NMR spectrum of Cat0.02-HB2.2-CS in  $\text{D}_2\text{O}$ .

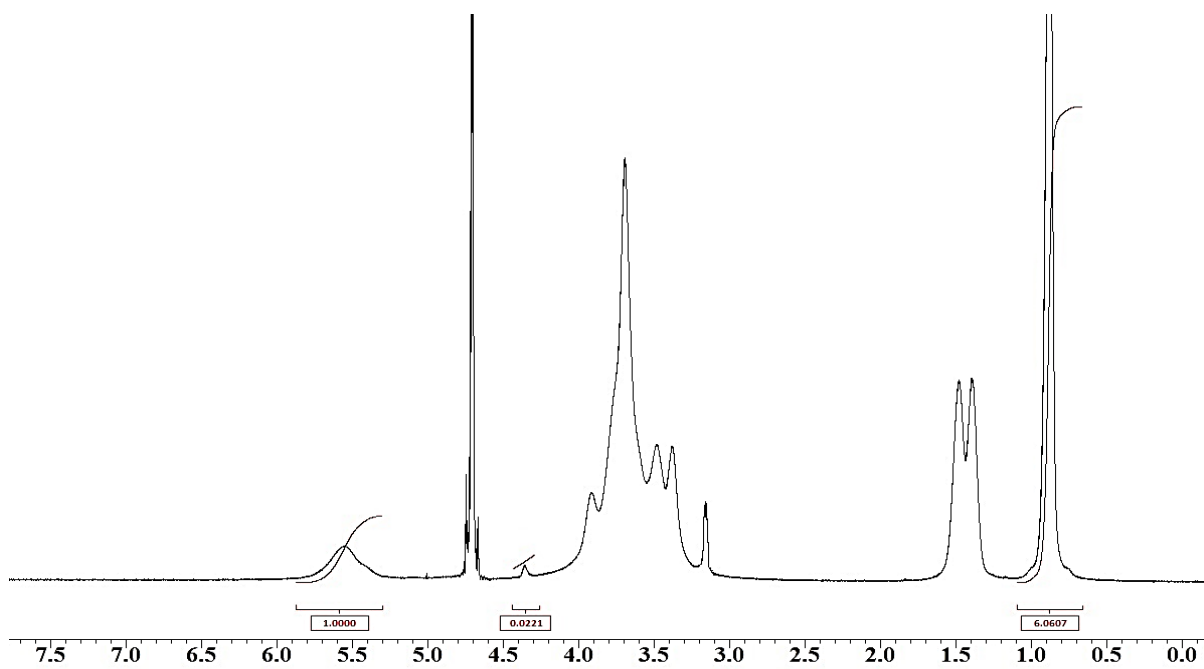


**Figure C2.**  $^1\text{H}$  NMR spectrum of Cat0.02-HB2.0-PS in  $\text{D}_2\text{O}$ .

## Appendix D

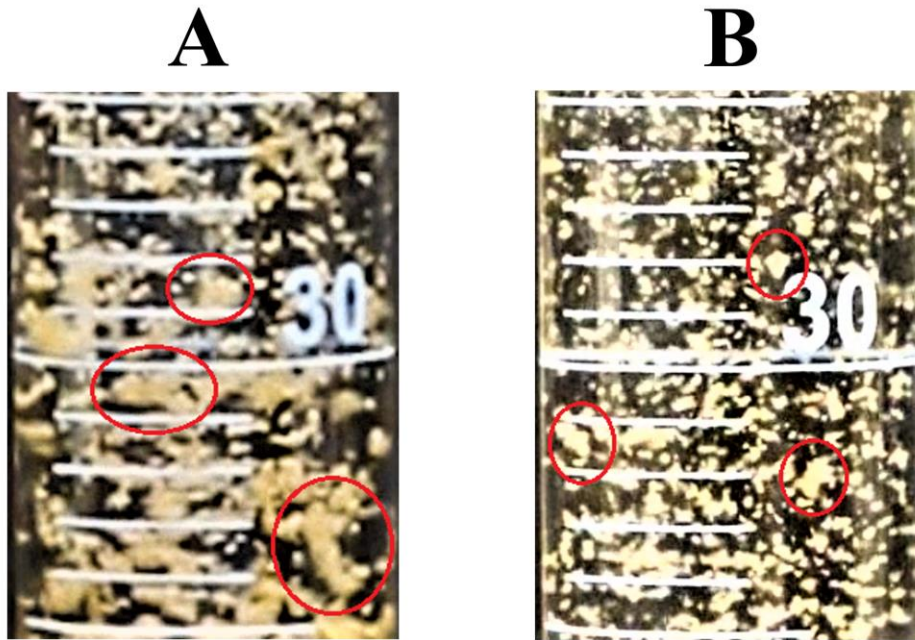


**Figure D1.** Pictures taken during the settling tests using a flocculant pair of 25 ppm HB0.6-CS and 600 ppm Cat0.02-CS (A) and Cat0.02-CS alone (B). Red circles are used to guide the eye to the flocs.

## Appendix E



**Figure E1.** A picture of the extraction mixture using fresh oil sands ores and 1 g/L of Cat0.036-HB1.9-SNP after phase separation for 16 h at rt. At the bottom, the layer of black sediment on top of sands was very noticeable.



**Figure E2.** A picture of the extraction mixture using fresh oil sands ores and 1 g/L of Cat0.025-PHE0.38-HB0.4-SNP after phase separation for 16 h at rt. Bitumen froth is the dark layer consisting mostly of bitumen on top of the aqueous phase.



**Figure E3.** A picture of the extraction mixture using the aged oil sands ores and 0.25 g/L of Cat0.17-PHE0.38-SNP after phase separation for 16 h at rt. The supernatant was mostly free of suspended particles and emulsified bitumen droplets.